FUNDAMENTAL CHARACTERIZATION OF NEW ZEALAND BITUMINOUS COAL FOR PREDICTION OF CARBONIZATION BEHAVIOUR - WITH SPECIAL EMPHASIS ON FLUOROMETRIC ANALYSIS

A THESIS

SUBMITTED FOR THE DEGREE

OF

DOCTOR OF PHILOSOPHY IN GEOLOGY

IN THE

UNIVERSITY OF CANTERBURY

BY

JEFFREY C. QUICK

UNIVERSITY OF CANTERBURY

1992

CONTENTS

LIST OF FIGURES

LIST OF TABLES

LIST OF PLATES

ABSTRACT

This study identifies properties of New Zealand bituminous coals that can be used to predict carbonization behaviour. 165 bituminous coal specimens (most between 0.5 and 1.3% Romax) were examined. Analytical methods include proximate and ultimate analysis, sulphur forms, CO2, ash composition, Gieseler fluidity, Rock Eval pyrolysis, maceral composition, safranin O staining, vitrinite reflectance, oxidative etching, fluorometric analysis, and microscopic examination of carbonized coal specimens.

Gieseler fluid temperature range, Rock Eval S1 & S2, volatile matter yield, and the optical texture of carbonized coals can be predicted where both vitrinite reflectance and mean vitrinite-inertinite fluorescence intensity are used as regression variables. The results suggest that the combined use of reflectance analysis and fluorometric analysis is useful for fundamental characterization of New Zealand bituminous coals to predict carbonization behaviour.

Fluorometric analysis also provides a way to identify perhydrous vitrinite and a quantitative method to correct for "suppressed" vitrinite reflectance is presented and explained.

Fluorometric analysis is sufficiently well developed for routine use and is convenient where an inert gas flow over the specimen is maintained during analysis. The results of this study suggest that reproducible results are possible where similar standards and wavelengths are used. Agreement on standard instrumental conditions that can be achieved with existing microscopes is suggested to realize the maximum value of the technique.

ACKNOWLEDGEMENTS

This thesis is dedicated to Dr. William A. Kneller who first told me about coal and inspired a persistent enthusiasm for the subject.

The study was made possible by funding from the New Zealand Ministry of Energy (now Energy and Resources Section, Ministry of Commerce). Pike River and Upper Waimangaroa samples and analyses were obtained through a joint Canterbury Coal Research Group / Energy and Resources Section (Ministry of Commerce) / Foundation for Research Science and Technology, drilling and analytical program. Coal Corporation of New Zealand and Greymouth Coal Limited kindly provided samples and data used in the course of this study. I also thank the Coal Research Association of New Zealand (CRANZ) for samples and analyses accomplished under the capable supervision of Grant Murray who graciously accommodated me in his home while I worked at CRANZ. David Glick at the Energy and Fuels Research Center (E&FRC) answered many requests for information and provided the foil laminate bags used in this study. Dr. Alan Davis (Director, E&FRC) kindly granted permission to use selected data from the Penn State Coal Data Base. Determination of ash oxide composition was undertaken by Steve Brown, Rose Fitzgerald, and Todd Warner.

I am especially grateful to Dr. Jane Newman for her tireless efforts to secure funding for the project and for critically reviewing the entire manuscript under a demanding schedule. David Bell provided useful comment on the bulk of the thesis. I thank Dr. Pat Suggate for thoughtful comment on early drafts of chapter 2 and Dr. Nigel Newman for specific commentary on mineral matter in coal and for insight into the interpretation of ash composition data. Dr. Tim Moore and Dr. Joan Esterle showed me how to etch coal and and reminded me that coal is derived from plants.

Dr. Dave Craw (Geology Dept. University of Otago) graciously loaned the dry microscope objective used in this study. Arthur Nicholas made components for the nitrogen gas delivery system used for fluorometric analysis. Dr. Nigel Newman wrote the computer software used for petrographic data acquisition. The photographic skills of Albert Downing are also gratefully acknowledged.

Finally, I acknowledge the constant support of my wife, Beth, who listened.

CHAPTER ONE
INTRODUCTION

This thesis is directed towards fundamental characterization of New Zealand bituminous coal for evaluation of industrial carbonization behaviour. To realize the maximum value of a resource requires that the nature of the resource be understood. This knowledge is of scientific interest but, by itself, has little practical value unless coupled with an understanding of how it can be used to predict industrial behaviour. Thus this thesis sets out to define the fundamental characteristics of New Zealand bituminous coal and then demonstrate, by correlation with empirical tests, how these characteristics influence carbonization behaviour. This approach was advocated by Neavel (1986) in a plenary speech to the International Coal Science Conference; many of the ideas expressed in this chapter find their origin in Dr. Neavel's persuasive text.

To achieve the objective of this study several questions need to be answered. What are the fundamental properties of New Zealand bituminous coal? What test parameters can be used to measure these properties? How do these properties correlate with empirical measures of carbonization behaviour? The approach used in this thesis to answer these questions recognizes the geological origin of coal and emphasises microscopic techniques for measurement of coal properties.

1.1 FUNDAMENTAL PROPERTIES OF COAL

1.1.1 Definition of Fundamental Properties

Identification of fundamental coal properties requires a clear definition of the term 'fundamental'. The following example illustrates the difficulty of this task. McCartney and Teichmüller (1972, p.64) consider vitrinite reflectance to be a "fundamental physical property whose determination can be reasonably divorced from empirical factors". Conversely, Murchison (1978, p.425) points out that "reflectance is not a fundamental property of organic matter" since it depends on a complex relationship between the material's refractive index and absorption

index. These optical parameters are respectively controlled by the aromatic stacking order and the diameter of the aromatic layers. Furthermore, the molecular structure of coal cannot be directly measured. These observations illustrate some conceptual and practical difficulties of defining what constitutes a fundamental property. Nevertheless, for the purpose of this thesis, fundamental properties are defined as those measurable qualities that can be universally used to predict industrial performance. The proposed definition is specific to the technological objective of the thesis. This is an important qualification. For example, if the study were directed towards an understanding of molecular structure then the refractive index and absorption index of vitrinite are clearly more fundamental optical parameters than reflectance since they relate more directly to molecular structural parameters. Likewise, if the objective was to understand of paleoenvironments then determination of palynomorph assemblages rather than liptinite content might be appropriate.

1.1.2 Identification of Fundamental Properties

Although fundamental properties are defined (in this study) as those coal properties that can be universally used to predict industrial behaviour this definition does not identify what those properties are since the actual industrial behaviour(s) of every coal cannot be known. The approach advocated in this thesis to help recognize fundamental properties is that such properties can be attributed to universally shared geological processes. What are these processes and how are they expressed as coal properties? All coals originate as an accumulation of plant debris where mineral influx is restricted. Plants produce a limited number of organic constituents, primarily lignin and cellulose. The wet, acidic, and nutrient poor character of mires restricts botanic diversity and biological degradation of the plant debris. Upon burial both temperature and pressure increase and drive the coalification processes that homogenize the organic matter; substances condense and evolve in accordance with physical laws at predictable stages. Inorganic constituents may be added, transformed or lost from the coal before, during and after coalification. After coalification coal seams

may be uplifted and change upon interaction with the biosphere either in the seam or outcrop; such changes are inevitable upon mining. Thus all coals form in response to universally shared processes that vary within naturally constrained limits. These processes are described on the simplest level as peatification, coalification, mineralisation, and weathering and are conceptually expressed as coal type, rank, grade, and weathering.

It is important to note that coal rank, type, grade, and weathering are concepts, not properties. For example, the literature is replete with diagrams that show how some behaviour of coal varies with "coal rank", where rank is indicated by a measured value such as vitrinite reflectance. In these instances, what is meant (but rarely stated) is that coal rank is expressed as vitrinite reflectance since this property is known to vary largely as a consequence of coalification. In this thesis measured properties that vary largely in response to a single geological processes are called parameters. Depending on the process, these properties are expressed as coal rank, type, grade, and weathering parameters. Since fundamental properties allow prediction of industrial behaviour of all coals the identification of fundamental properties according to universally shared geological factors is suggested.

Fundamental characterization should allow prediction of multiple industrial uses for all coals regardless of origin. In this thesis only carbonization behaviour is specifically targeted and only New Zealand bituminous rank coals are evaluated. For this reason it is impossible to know with certainty if the identified properties will allow prediction of other industrial behaviours or if relationships established between New Zealand coal properties and carbonization behaviour will hold for other coals. Despite these limitations it is possible to evaluate the suitability of specific properties for fundamental characterization. Such an evaluation can be accomplished in several ways as discussed below.

Published correlations of coal properties with utilization behaviour that work well for coals for which they were designed sometimes fail to accurately predict industrial behaviour of other coals. The reason for this failure can be

attributed to provincial differences between coals from different regions. This realization does not answer the question of what these differences are, and how they can be measured. However, where such failures are noted they provide clues that help identify properties that are not recognized or accounted for in the predictive method.

Fundamental characterization should allow prediction of industrial behaviour by multiple regression techniques (Neavel 1986). The use of multiple regression methods recognises that more than one property may be required to accurately predict a given industrial behaviour. For the resulting equation to be universally applicable, it must be derived from a balanced data set that encompasses the whole range of coal variability. Indeed where regression techniques are applied to provincial suites of coal statistically significant correlations but entirely erroneous relationships are sometimes found. Because this study is narrowly restricted to New Zealand bituminous rank coals this possibility cannot be entirely discounted. However, where appropriate New Zealand coal data are available, it is possible to evaluate selected properties in the context of published equations developed from other more extensive data sets. Likewise, predictive equations derived from data obtained in this study can be validated where appropriate data from more variable data sets are accurately predicted by the equation.

1.2 MEASUREMENT OF COAL PROPERTIES

Coal properties can be measured at the megascopic, microscopic, molecular and elemental levels. In this study microscopic characterization methods are emphasized due to the belief that the heterogeneity of coal is best exposed at the microscopic level of analysis and because the reflected light microscopy has proven commercial value for prediction of coking behaviour. Other characterization techniques are also used since they provide information that cannot be obtained with microscopic methods. This information not only augments the microscopic data but also enables interpretation of these data.

Nomination of fundamental properties according to rank, type, grade, and weathering parameters implies that certain coal properties can be attributed to a specific geological process. Two major problems associated with measurement of such parameters are addressed. First, it is recognized that any single measured property will vary in response to more than one geological processes. For example, although carbon content varies in response to coalification it can also vary, to a lesser degree, due to peatification, mineralisation, and weathering. The second problem relates to the recognition of multiple mechanisms that drive a single geological process. For example, both moisture content and vitrinite reflectance are rank parameters but vary in response to different coalification processes (i.e., pressure and temperature). The importance of these complications and strategies used to minimize their effect are discussed in Chapter 2.

1.3 EMPIRICAL TESTING OF CARBONIZATION BEHAVIOUR

Two different approaches are used in this thesis to assess carbonization behaviour. Since carbonization is a pyrolysis process directed towards production of a solid carbon product, conventional analyses based on pyrolysis are used as measures of carbonization behaviour. The second approach involves microscopic analysis of the carbon forms present in semicokes produced upon pyrolysis. This dual approach recognizes that all carbonization processes share a pyrolysis step, and assumes that the quality of the resulting carbon product is expressed at the microscopic level of examination. It is also assumed that the results of these bench scale tests have general relevance to diverse industrial carbonization processes.

This study does not address some economically important aspects of industrial carbonization such as the behaviour of coal blends, the effect of variation in process conditions, and methods for accurate industrially significant evaluation of carbon product quality. These topics are best studied by commercial performance testing in an industrial setting whereas this study is limited to bench scale tests. Nonetheless, where selected properties can be correlated with laboratory pyrolysis behaviour and resulting microscopic carbon

forms, the results are relevant to guide selection of coal feedstocks for commercial performance testing.

1.4 SUMMARY

Fundamental properties of coal are defined here as those properties that can be universally used to predict industrial behaviour. Rank type grade and weathering parameters are suggested to be likely candidates for selection of fundamental coal properties. Despite acknowledged limitations fundamental properties of coal are suggested to be identified where these selected coal properties can be used to predict carbonization behaviour. Carbonization behaviour is evaluated using laboratory scale tests as analogs of industrial behaviour. Measurement of coal properties by microscopic techniques augmented by conventional whole coal analyses is advocated.

CHAPTER TWO
COAL RANK, TYPE, GRADE, AND WEATHERING - A REVIEW

2.1 INTRODUCTION

Coal rank and type are qualities of the organic fraction of coal whereas coal grade refers to the inorganic fraction. Weathering results from interaction with both the atmosphere and near surface groundwater and may alter both organic and inorganic constituents. Conceptually, coal rank is the result of geological processes that occur after burial of the coal-forming peat. Coal type is the outcome of the botanic composition of the peat, including biological and chemical modification of the organic matter during peat accumulation and prior to significant burial. Coal grade is a consequence of the accumulation of inorganics in the coal-forming mire and later epigenetic emplacement or transformation of inorganic constituents. Weathering may occur in the subsurface and outcrop, or during beneficiation, stockpile storage and transport.

One goal of this chapter is to demonstrate that rank, type, grade and weathering are not objective properties of coal. Nonetheless, assessment of coal rank, type, grade, and weathering is routinely accomplished for both geological and industrial purposes. These assessments are possible because certain measured properties vary largely in response to a single geological process. These properties are called parameters in this thesis. However, no rank, type, grade, or weathering parameter is completely immune to the perturbing effect of other geological processes. Consequently, for valid appraisal of a single parameter the effect of these other geological processes on the parameter of interest must be considered. For example, to be useful for rank assessment many rank parameters are calculated to a mineral free basis. Likewise, weathering is generally acknowledged as a valid reason to reject many analyses for assessment of rank. The complex interaction of peatification, coalification, mineralisation and weathering on a single measured parameter often obscures the significance of any single coal property. However even where it is possible to isolate a single parameter by accounting for the perturbing effects of the remaining geological

processes (peatification, coalification mineralisation or weathering) the measured parameter can not uniquely define the process of interest. This is because peatification, coalification, mineralisation and weathering are not single mechanisms but are each the sum of multiple causative factors. This chapter sets out to discuss those factors that constrain evaluation of rank, type, grade and weathering and some parameters through which they are expressed.

2.2 COAL RANK

Commenting on the definition of coal rank, Carpenter (1989 p.14) states: "The rank of a coal is the degree or stage a coal has reached during its coalification, ... That is rank is a qualitative description of the coalification sequence. It is not an objective property ...". One reason why rank is not a precisely measurable property of coal is that the advance of coal rank is governed by a variety of processes. These processes include the rise of pressure and temperature with increasing depth of burial that occurs over variable amounts of time. The progressive, and irreversible advance of coal rank with increasing depth of burial is called coalification. Since more than one process is operative during coalification it is not surprising that no single property can provide a universal measure of coal rank. Indeed the idea of "physical" and "chemical" coalification was advanced by Dulhunty (1954) to differentiate the respective effects of pressure and temperature on the advance of coal rank.

Precise expression of coal rank is also hindered by the effects of inorganic composition, maceral content and weathering on a measured rank parameter. Accordingly, various methods are used to correct rank parameters to inorganic-free basis and to overcome the perturbing effect of maceral composition and degree of weathering. In recognition of the imprecision of methods used to assess mineral and maceral composition as well as the lack of any recognized standard method to assess weathering it is not surprising that these perturbing effects cannot be completely eliminated. Even vitrinite reflectance, which is relatively free of distortion arising from inorganic content and weathering, has been shown to be influenced by variation of coal type (Newman and Newman, 1982). Thus the

precision of any rank assessment is limited by our inability to completely eliminate the perturbing effect of type, grade and weathering on a single rank parameter.

2.2.1 Pressure

Dulhunty (1954) identified compressional force and temperature as the primary factors that control the respective advance of physical and chemical rank. Importantly, Dulhunty recognized that variation of hydrostatic pressure (which opposes lithostatic pressure) precludes any simple relationship between burial depth and compressive force. Indeed, the retarding effect of high hydrostatic pressure on the physical compaction of coal was demonstrated in the laboratory by Cecil *et al.*, (1979a). Their observations confirm that the compression of coal is due to the relative difference between lithostatic and hydrostatic pressure. Consequently, a precise relationship between burial depth and the physical rank of coal is not possible.

Beside limiting the compressive force acting on a coal seam, hydrostatic pressure may also influence the advance of chemical rank. McTavish (1978) speculated that anomalous (low) vitrinite reflectance observed in an oil well resulted from overpressuring (hydrostatic pressure = lithostatic pressure). Overpressuring was thought to have inhibited chemical changes since high pressure would favour the solid reactants over the gaseous coalification products (LeChatlier's principle). Cecil *et al.*, (1979a) experimentally confirmed the retardation of chemical changes during coalification due to overpressuring. They simulated burial of a low-ash *taxodium* peat under normal and overpressured conditions (hydrostatic pressure = 8,960 and 20,700 kPa respectively). Cecil and his co-workers observed a 25% reduction of evolved CH_4 and CO_2 at the higher hydrostatic pressure. Horvath (1983) also experimentally confirmed the retardation of coalification due to overpressuring as measured by vitrinite reflectance.

The effect of pressure is greatest during the early stages of coalification. Elimination of water from peat, lignite and subbituminous coals due to increasing

compressional force has led to the use of moisture content (either directly or indirectly) to assess rank through the early stages of coalification (Alpern *et al.*, 1989, AS-2096, ASTM-D388). Figure 2.1a shows how the ASTM rank parameter (Btu/lb moist, mmf) used up to the medium volatile bituminous (mvb) stage of coalification parallels the moisture content of the coal.

There are two different reasons for the close linear relationship between moisture and moist, mmf calorific value. In large part the relationship can be explained as a dilution effect since water does not contribute to the calorific value of coal. However as shown in Figure 2.1b, at about 25% moisture the dry, mmf calorific value also begins to increase with decreasing moisture content. This gradual transition corresponds to the beginning of the subbituminous B (subB) stage of coalification. At subB rank, the elimination of moisture ceases to be primarily due to physical expulsion and water bound to carboxyl groups and carboxylate salts is increasingly lost as a result of thermal decarboxylation. Of the 6,800 BTU/lb (moist, mmf) increase from the middle of the subB rank stage up to mvb rank an increase of about 3,000 Btu/lb is due to chemical changes (section 2.2.2) and the remainder due to loss of moisture.

2.2.2 Temperature

The occurrence of contact metamorphosed anthracite next to an igneous dyke that bisects a lignite in the Canterbury district, South Island New Zealand, attests to the importance of temperature in the coalification process (Suggate, 1959). Normally, coalification proceeds at lower temperatures that gradually increase with depth of burial. Because of the possible retarding effect of high hydrostatic pressure and the possible influence of the duration of heating (section 2.2.3), precise, universally applicable rank-temperature scales are not possible. Nonetheless a general correlation between rank and temperature for bituminous coals is shown in Table 2.1. The correlation between random reflectance and ASTM rank shown in Table 2.1 was modified after Davis (1984). The maximum paleo-temperatures shown in the table were calculated from random vitrinite

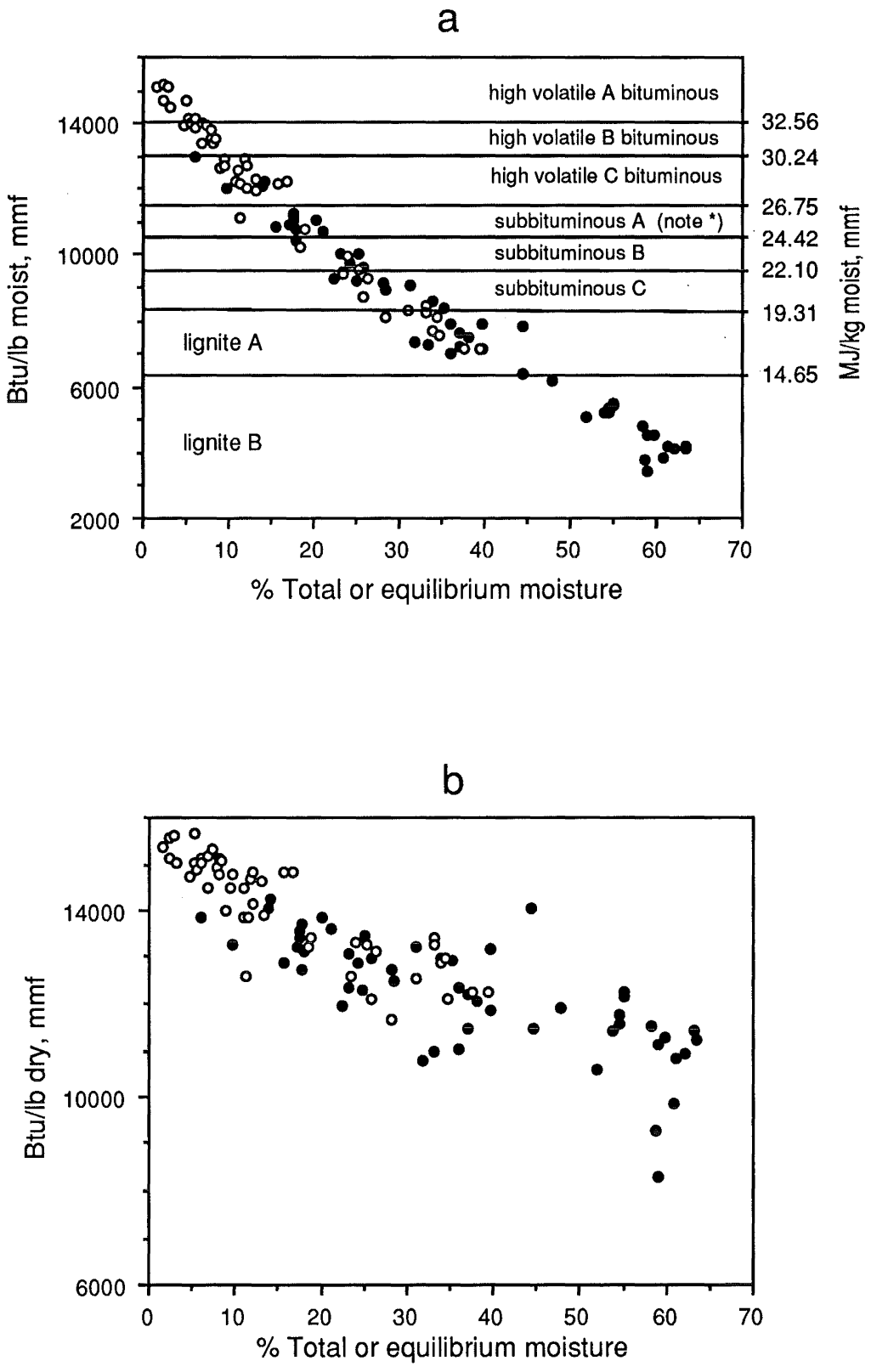

Figure 2.1 a) Moisture vs moist,mmf Btu/lb and b) Moisture vs dmmf Btu/lb for coals less than mvb rank (note * classify as high volatile C bituminous if agglomerating). Key: (•) "total moisture" Ode and Gibson, 1960; (o) "equilibrium moisture" unpublished data courtesy of the Penn State Coal Data Base.

reflectance values using an equation reported by Barker and Pawlewicz (1986, addendum) as:

$$\ln(Rm) = .0096(T_{max}) - 1.4 \qquad \text{(eq. 2.1)}$$

where Rm = random reflectance of vitrinite, and T_{max} = maximum burial temperature. Barker and Pawlewicz obtained this equation based on a major axis regression (variation of both X and Y variable minimized) from over six hundred published data points from 35 boreholes in different sedimentary sequences. Equation 2.1 replaces that originally printed in their manuscript which was based on a least squares regression (X assumed to be precisely known, variation of Y minimized) of T_{max} vs Rm for which they obtained a coefficient of determination (r^2) of 0.7. The acknowledged imprecision of the equation was suggested to be due to difficulties obtaining accurate maximum paleo-temperatures as well as variation of vitrinite populations. Different hydrostatic pressure regimes may also have contributed to the observed scatter of their data.

TABLE 2.1

APPROXIMATE RANK - MAXIMUM PALEO-TEMPERATURE CORRELATION

ASTM Rank Code	Range Random Reflectance	Range Maximum Paleo-temperature
subA/hvCb	0.44 - 0.54	61 - 81 °C
hvBb	0.54 - 0.67	81 - 104 °C
hvAb	0.67 - 1.04	104 - 150 °C
mvb	1.04 - 1.42	150 - 182 °C
lvb	1.42 - 1.93	182 - 215 °C

ASTM rank-reflectance correlation modified after Davis (1984) according to $Ro_{random} = Ro_{maximum}/1.06$; Reflectance - Maximum Paleo-temperature correlation after Barker and Pawlewicz (1986).

As mentioned in section 2.2.1, thermal decarboxylation, which begins prior to the bituminous stage of coalification, results in an increase of about 3,000 dmmf Btu/lb up to mvb rank (see Figure 2.1b). This net loss of oxygen occurs during processes called diagenetic gelification or vitrinisation. Table 2.2 shows how the organic elements in coal contribute to the heat of combustion. Loss of oxygen directly increases specific energy, especially because the remaining C, H, N, and S proportionally increase as oxygen is lost from the coal.

TABLE 2.2

COMPILATION OF COEFFICIENTS FOR VARIABLES IN FORMULAE USED TO CALCULATE SPECIFIC ENERGY (BTU/LB) FROM COAL COMPOSITION

Reference	Carbon	Hydrogen	Oxygen	Nitrogen	Sulphur	Ash*
1.	145.9	569.6	-53.89		43.08	-6.30
2.	145.6	568.6	-51.44		48.30	-2.45
3.	146.6	568.8	-51.53	29.40		-6.58
4.	153.8	488.3	-36.3	25.5	48.10	-418.7 (intercept)
5.	145.0	610.0	-65.0			
6.	144.54	610.2	-62.46		40.5	
7.	145.44	620.28	-77.54		40.5	
8.	151.2	499.77	-47.7	27.0	45.0	

References cited: 1&2. Neavel *et al.*, 1986, Fuel 65:310; 3. Mason and Gandhi, 1983, Fuel Process. Technol., 7:11; 4. Loyd and Davenport, 1980, J. Chem Ed., 57:55; 5. Given, pers. comm in Neavel *et al.*, 1986; 6. Mott -Spooner formulae, 7. Dulong formulae, and 8. Boie formulae, all in Francis, 1961, Coal, Edward Arnold , Ltd., London, p. 363

(from Neavel, *et al.*, 1986, * note; where ash is listed variables are on a dry basis, where ash is not listed variables are on a dry, mmf basis)

Thermally induced loss of hydrogen rich constituents becomes increasingly important above high volatile A bituminous (hvAb) rank. Consequently there is a slight decrease in the calorific value of coal due to the loss of hydrogen as rank progresses into the low volatile stage of coalification. Important thermally induced changes to coal properties also occur before significant loss of potentially volatile constituents. At the beginning of the bituminous stage of coalification a profound change in the character of coal occurs. This has been called the "first coalification jump" and marks the maximum rate of generation of constituents soluble in organic solvents. It is the generation of these petroleum-like substances in coal (bituminisation), which begins during the subbituminous B (subB) stage of coalification, that is largely responsible for the thermoplastic properties of coal (Teichmüller, 1974). Unlike dispersed organic matter, which is often surrounded by hydrophilic clay minerals, migration of these newly generated bitumens out of the coal seam is hindered by the hydrophobic, micro-porous character of coal. A good analogy is provided by Illing (1933) who showed that oils are preferentially passed through water wet sand but retained on oil wet sand. With a further rise in rank these bitumens thermally disproportionate into gaseous products and condensed insoluble constituents. The loss of these bitumens begins during the mvb stage of coalification (near 87% carbon) and

corresponds to the second coalification jump. The culmination of this process is marked by the loss of thermoplastic properties at the end of the bituminous stage of coalification. A more comprehensive discussion of these processes is provided by Teichmüller and Teichmüller (1982).

Although typical geothermal gradients are reported as 3 to 4 °C/100m (Teichmüller and Teichmüller, 1982b) gradients can vary widely between (and within) basins and even within a single drillhole. Other than regional basement heat flow, factors that control geothermal gradients include: proximity to igneous intrusives, thermal conductivity of lithologies (Jones *et al.*, 1972) and the pressure regime (Law *et al.*, 1989, Hunt, 1979 p.339).

The extent of chemical changes due to geothermal heating has been called "chemical rank" (Dulhunty, 1954, Suggate, 1974). Since the geothermal gradient varies from basin to basin there is no universal scale of burial depth with chemical rank.

2.2.3 Time

In the 1970's methods to evaluate thermal history were advanced which incorporated the duration of heating as an important factor in the coalification process. These methods predict that equivalent maturation can result from either brief heating at a relatively high temperature or prolonged heating at a lower temperature. Veto and Dovenyi (1986) examined four different published methods and found that the calculated vitrinite reflectance varied from 1.0% up to 1.75% reflectance for the same hypothetical burial history depending upon which method was used. Although the lack of agreement of these different methods is grounds to question their precision, it does not invalidate the concept of time as an important factor during coalification. Because the thermal history of a basin cannot be known with certainty it is difficult to evaluate the relative merit of specific methods.

Most time - temperature models to explain coalification are based on the idea that coalification processes can be adequately described by the Arrhenius equation,

$$K = A^{(-E/RT)} \qquad \text{(eq. 2.2)}$$

where K is the rate constant, A is the frequency factor, E is the activation energy, R is the gas constant, and T is temperature (Kelvin). Further, nearly all methods assume a single or single distribution of activation energies to describe the coalification process. Although this approach may be useful if only the generation of hydrocarbons is of interest, it is of limited value to evaluate coalification where multiple chemical processes must be considered. More useful is the approach outlined by Burnham and Sweeney (1989) who proposed a kinetic model for the coalification of vitrinite based on a distribution of activation energies for four independent parallel reactions (viz. elimination of water, carbon dioxide, higher hydrocarbons, and methane). Substitution of Burnham and Sweeney's empirically derived kinetic constants for each of these parallel reactions into equation 2.2 shows that at a particular temperature the relative rates of generation are, $H_2O > CO_2 > CH_n > CH_4$. Since abundant generation of H_2O and CO_2 occur prior to catagenetic generation of higher hydrocarbons (bitumen) and methane it can be concluded that time is less important during the early stages of coalification than at later stages.

Barker and Pawlewicz (1986) argue that the duration of heating has little effect on coalification and that vitrinite reflectance is a useful, albeit imprecise, paleo-thermometer. They produced an empirically derived equation (eq. 2.1) that can be used to estimate the maximum burial temperature using vitrinite reflectance. Their ideas are supported by Tilley *et al.*, (1989) in a comparative study of fluid inclusion and vitrinite reflectance data, and by Connolly (1989) who found good agreement with temperatures predicted by clay mineral assemblages from 100 to 170 °C. Although the relative importance of time upon coalification has been questioned (McTavish 1978, Suggate, 1982, Barker and Pawlewicz, 1986, Barker, 1989) the importance of the concept may have little to do with the accuracy of the various time-temperature models. Indeed, in a critical review Barker (1989) agrees with the premise that time <u>is</u> a control on coalification but

goes on to argue that the quality of data necessary for time to be a useful parameter is unattainable.

2.3 MEASURES OF COAL RANK

Temperature, lithostatic and hydrostatic pressure, and time are all factors responsible for the advance of coal rank. The different geothermal gradients and hydrostatic regimes that persist through variable amounts of time and space leads to the general conclusion that every coal seam has experienced a unique coalification history. (An exception to this generalization is the special case of closely spaced seams or closely spaced samples taken within a single seam. In these instances, close proximity ensures identical coalification histories where faulting, unconformities or igneous intrusions are not present.) Thus coal rank does not provide a precise, quantitative description of the coalification history and a precise universal scale of equivalent degrees of coalification is not possible. Fortunately, the notion of a universal geological coalification sequence is generally true since the causes of coalification (lithostatic pressure, hydrostatic pressure, temperature and time) all increase with increasing burial depth and vary within naturally constrained limits. This allows general rank schemes to be established based on measured coal properties that have been shown to vary largely with depth of burial. In this thesis these properties are called rank parameters.

2.3.1 Scales of Coal Rank

Examination of the ASTM classification of coal by rank attests to the notion of multiple mechanisms responsible for the advancement of coal rank. Table 2.3 lists the limits and measured values used in the standard to classify coal according to rank. It shows that specific energy on a moist, mineral matter free basis is used to classify lignite, subbituminous and high volatile rank coals, and dry, mineral matter free fixed carbon is used to classify higher rank coals. Agglomerating properties are used to differentiate high volatile C bituminous (hvCb) and subbituminous A (subA) rank coals as well as to identify low volatile bituminous (lvb) rank coals with more than 86% fixed carbon. The use of a variety of measured properties in the standard can be attributed to the dual

influence of physical and chemical coalification processes. As discussed in section 2.2.1, the value "moist, mineral matter free specific energy" is largely a function of moisture content rather than variation of the intrinsic calorific value of the coal. Coalification through the lignite and subbituminous ranks is largely a function of the physical expulsion of moisture. As coalification continues through the subbituminous and high volatile bituminous ranks both physical and chemical coalification processes are important. Because moisture is associated with oxygen containing functional groups (especially carboxylate salts) it remains a good rank parameter up to the high volatile B bituminous (hvBb) stage of coalification. The use of fixed carbon to classify mvb and higher rank coals shows that chemical coalification processes predominate at greater burial depths.

Although the ASTM coal classification scheme accounts for both physical and chemical coalification processes, it is essentially an industrial classification. Problems arise if ASTM ranks are indiscriminately applied to sedimentary sequences to establish rank gradients. For example, lithotype samples from an unusual canneloid coal in Utah (described by Given *et al.*, 1985) vary in ASTM rank from lignite to medium volatile bituminous (data from Penn State Coal Data Base). Although some of the variation has resulted from differential weathering of the lithotypes, most is due to different group maceral abundances. In recognition of the problem, the ASTM (1987) standard classification of coals by rank states (D-388 p.225) "This classification is applicable to coals that are rich in vitrinite. Coals rich in inertinite or liptinite (exinite) do not fit into the classification..." (see also note a, Table 2.3).

Other published scales of coal rank are also based on the nature of vitrinite in coal. For example Figure 2.2 shows that the percent reflectance, volatile matter, carbon and bed moisture of vitrite can, within indicated limits, all be used to evaluate coal rank. Specifically, vitrite is a microlithotype which is recognized microscopically and defined as coal grains that contain more than 95% vitrinite. Such material may be physically separated from the coal by hand-picking vitrain bands or by gravity separation techniques. It is worth noting that Brown *et al.*,

(1964) found volatile matter determined on floated vitrinite concentrates was 2 to 5% higher than volatile matter determined on hand-picked vitrains from the same bituminous coals. Finally note that Figure 2.2 is not a classification scheme; it simply illustrates approximate correlations of rank parameters. For example, ASTM rank terms are listed in Figure 2.2 even though none of the listed rank parameters are strictly used in the ASTM classification.

Restriction of analyses to exclude liptinite and inertinite group macerals acknowledges the perturbing effect of group maceral variation on rank assessment based on whole-coal analysis. However, even where analyses are restricted to vitrite, variation within the vitrinite group of macerals can still cause difficulties. For example, using the correlation chart shown in Figure 2.2 Correa da Silva (1989) showed that the indicated rank of Brazilian vitrinite concentrates varied according to the parameter used to assess rank. She attributed this behaviour to the perhydrous composition of some Brazilian vitrinite precursors. The correlation between rank parameters shown in Figure 2.2 was suggested to be inappropriate for vitrite derived from perhydrous precursors because they follow a different coalification path than the European vitrites used to establish the correlation chart.

A clear demonstration of how compositional differences within the vitrinite group can affect rank evaluation was made by Newman and Newman (1982). They showed that the mean maximum reflectance of vitrinite rich coals from a vertical succession of 5 coal seams varied irregularly from 0.67 to 0.92% over 250 meters of depth. Furthermore, some of the lowest reflectance values occurred near the base of the sequence. Since these coals have experienced a similar burial history, with no igneous intrusions or faulting, the variation was attributed to variable vitrinite composition.

Besides the multiple causative factors responsible for the advance of coal rank, and the difficulty correcting measured values for the interfering effects of type, precise correlation of the different rank parameters as implied by Figure 2.2 may be hindered by the multitude of standard methods used to analyze coal. For

TABLE 2.3

VALUES USED FOR ASTM CLASSIFICATION OF COAL BY RANK [a]

ASTM Rank Code	Fixed Carbon Limits, Percent (Dry-Mineral-Matter-Free Basis)		Volatile Matter Limits, Percent (Dry, Mineral-Matter-Free Basis)		Gross Calorific Value Limits, Btu per pound (Moist [b], Mineral Matter Free Basis)		Agglomerating Character
	Equal or Greater Than	Less Than	Greater Than	Equal or Less Than	Equal or Greater Than	Less Than	
ma	98	...	...	2	...	...	non-
an	92	98	2	8	...	...	agglomer-
sa [c]	86	92	8	14	...		ating
lvb	78	86	14	22	...	...	commonly
mvb	69	78	22	31	...	...	agglomer-
hvAb	...	69	31	...	14,000 [d]	...	ating [e]
hvBb	...	...	...	...	13,000 [d]	14,000	
hvCb	...	...	...	...	11,500	13,000	
hvCb					10,500	11,500	agglomer-ating
subA	...	...	...	...	10,500	11,500	non-
subB	...	...	...	...	9,500	10,500	agglomer-
subC	...	...	...	...	8,300	9,500	ating
ligA	...	...	...	...	6,300	8,300	
ligB	...	...	...	...	...	6,300	

[a] This classification does not apply to certain coals rich in liptinite or inertinite.

[b] Moist refers to coal containing its natural inherent moisture but not including visible moisture on the surface of the coal.

[c] If agglomerating, classify in the lvb group of coals.

[d] Coals having 69% or more fixed carbon on the dry, mineral-matter- free basis shall be classified according to fixed carbon regardless of gross calorific value.

[e] It is recognized that there may be non-agglomerating varieties in these groups of bituminous coals and there are notable exceptions in the hvCb group.

(Adapted from, ASTM D-388)

example, Table 2.4 shows that the methods used to determine volatile matter in the ASTM classification scheme are markedly different than the methods used in the Australian, British and International standards (see section 2.8.1i for a comparison of methods to determine ash content). Further, it has been suggested that differences between sampling and sample preparation methodology specified by the various standards may be responsible for most of the variance between analytical methods (Thompson, 1986). The relative importance of specified analysis conditions (shown in Table 2.4) and specified sample preparation methodology (not shown) on the volatile matter yield is not known.

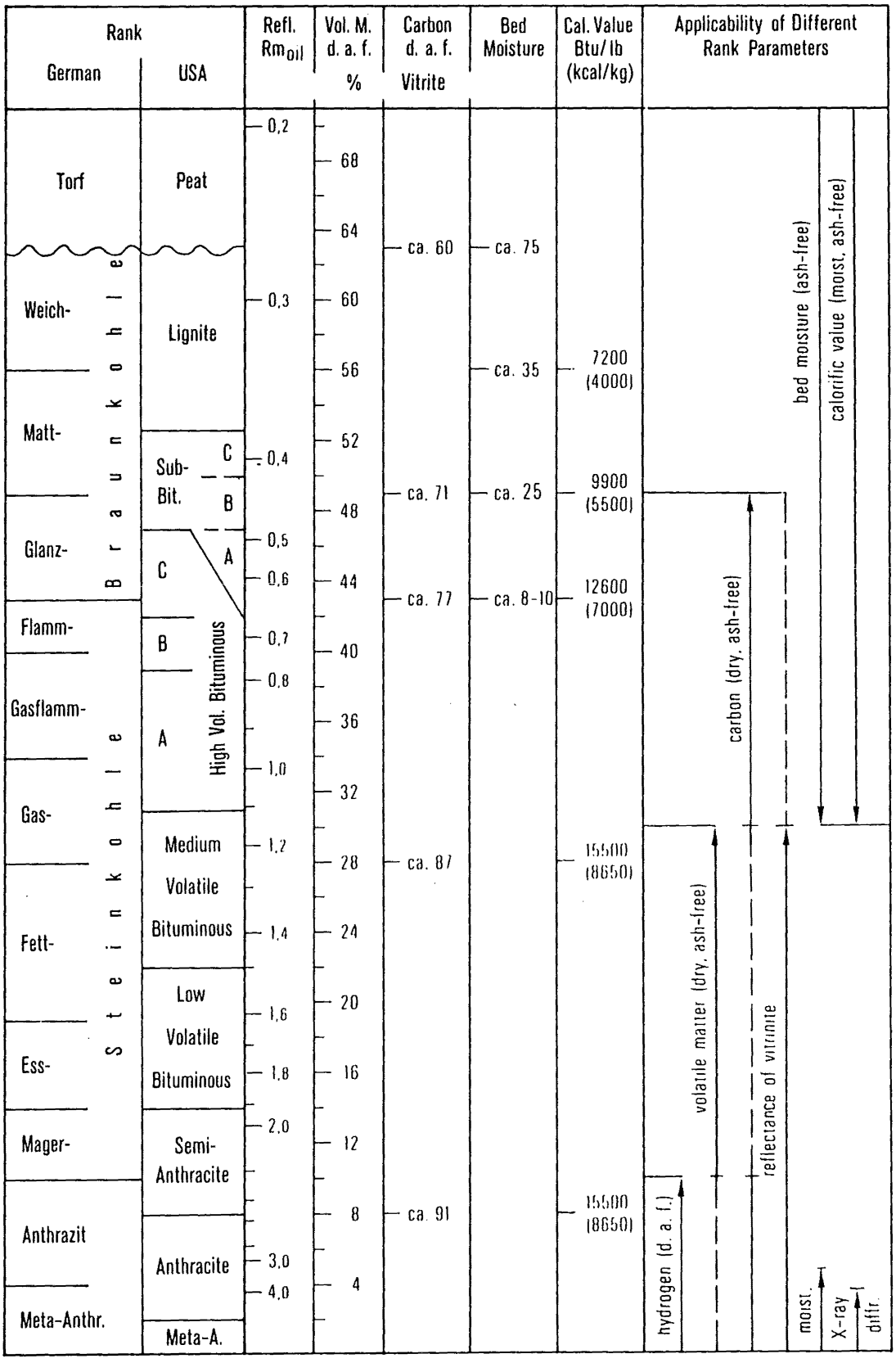

Figure 2.2 Applicability and generalized correlation of different rank parameters at different levels of coalification in relation to German (DIN) and North American (ASTM) terminology (from Teichmüller and Teichmüller, 1982).

The necessity of correcting measured rank parameters to a mineral matter free basis also hinders rank assessment. Since not all coals have similar mineral assemblages or inorganic contents no single correction formula is appropriate for all coals (N. Newman, 1988); different mineral correction formula yield different calculated values. Consequently, errors are introduced either from the use of different formulas to calculate mineral contents for similar coals or from the use of a single formula to calculate mineral contents of coals that contain substantially different kinds of minerals. Finally, the perturbing effect of weathering on coal composition also hampers assessment of coal rank. Thus assessment of rank requires an understanding of the uses and limitations of laboratory tests, as well as an awareness of the perturbing effect of coal type, grade, and weathering on the resulting measured rank parameter.

Comparisons of different coal classification systems useful to categorize coal according to rank have been made by many authors (McClung and Greer 1979, Ward 1984, Carpenter 1988, Alpern *et al.*, 1989, Loison *et al.*, 1989). Less frequent are comparisons of the different analytical methods specified by various classification systems. Both Gray (1983) and Thompson (1986) judge the relative merit of the different methods based on repeatability and reproducibility limits provided in the standards. This approach is of questionable value since these limits are based on round-robin laboratory exchanges of nationally mined or internationally traded coals. Thus the better precision of BS and AS standard methods for determination of volatile yield shown in Table 2.4 may simply be an outcome of less variability in the sets of round-robin samples used to determine repeatability and reproducibility rather than superior methodology.

2.3.2 Rank Parameters

Each rank parameter has a limited range of applicability, and a variable susceptibility to the perturbing effects of type, grade and weathering. The following sections discuss some of the more common rank parameters, their range of applicability, geological controls, and perturbing factors.

TABLE 2.4

SUMMARY OF DIFFERENT METHODS USED TO DETERMINE VOLATILE MATTER

Method	Australian		North American		British	International
	AS 2434.2-1989	AS 1038.3-1989	ASTM D3175-1982		BS1016 part 3 1973	ISO 562-1981
Applicability	low rank	high rank	sparking	non-sparking	not specified	hard coal
Furnace	Horizontal	Horizontal	Vertical	Vertical	Horizontal	Horizontal
Crucible	Silica	Silica	Platinum	Platinum	Silica	Silica
Time and Temperature	7 min at 900°C cool & combine to 1 g, then 7 min at 400°C followed by 4 min at 900°C	7 min at 900°C	slow heating to 600°C over 6 min then 6 min at 900°C	7 min at 950°C	7 min at 900°C	7 min at 900°C
Sample mass size	2 g - 212 um	1 g 212 um topsize	1 g - 250 um	1 g -250 um	1 g 200 um topsize or - 212 um	1 g - 200 um
Repeatability, volatiles =						
9%	na	0.2 (dry)	0.5 (dry)	0.5 (dry)	0.2 (air dried)	0.3 (dry)
30%	na	0.2 (dry)	na	0.5 (dry)	0.3 (air dried)	0.9 (dry)
40%	0.7 (dry)	na	0.7 (dry) subbituminous 1.0 (dry) lignite	na	0.3 (air dried)	na
Reproducibility volatiles =						
9%	na	0.5 (dry)	na	1.0 (dry)	0.5 (air dried)	0.5 (dry)
30%	na	1.0 (dry)	na	1.0 (dry)	1.0 (air dried)	1.2 (dry)
40%	2.0 (dry)	na	1.4 (dry) subbituminous 2.0 (dry) lignite	na	1.0 (air dried)	na

na: not applicable

(i) moisture

The bed moisture content of coal is an appropriate rank parameter for brown coal and continues to be useful up to about hvBb/hvAb rank. Because determination of bed moisture requires samples carefully collected from the mineface (or fresh cores) it is not widely used. Instead, the total moisture of freshly mined coal, or the equilibrium moisture is used to approximate bed moisture. The total moisture of freshly mined coal is the same as bed moisture for coal with up to 40% bed moisture (Ode and Gibson, 1960). Likewise, equilibrium moisture (moisture holding capacity at 97% rel. humidity and 30°C) is equivalent to bed moisture of subbituminous and bituminous coal (Selvig and Ode, 1953). The equilibrium moisture of lignite and brown coal is only equivalent to bed moisture if the samples are freshly mined and not dried during sample preparation.

For nearly 30 years, the phrase "air-dried" has been used in New Zealand to indicate the moisture holding capacity of coal equilibrated at 70% relative humidity and 20°C. International use of the expression "air dried" generally indicates coal dried at ambient to slightly elevated temperatures with no provisions made for humidity control. Consequently, air-dried moisture values determined in New Zealand are nearly always higher than air dried moisture values determined elsewhere. In this thesis the phrase "air-dried" is hyphenated to distinguish accepted New Zealand conditions of analysis. (i.e., "air-dried" specifies New Zealand standard conditions whereas "air dried" is used to distinguish the international sense of the phrase).

Budge (1972) compared the air-dried moisture of 10 New Zealand coals to both the moisture holding capacity at 98% relative humidity, 20°C and the total moisture of the coals. Budge's data are plotted in Figures 2.3a and 2.3b. Figure 2.3a, shows a linear relationship between moisture holding capacity and total moisture where moisture holding capacity of fresh coal is about 4% lower than the total moisture content of fresh coal. Ode and Gibson (1960) show a 1 to 1 correspondence between total moisture and equilibrium moisture. The reason

that Budge's moisture holding capacity values are consistently lower than total moisture content is probably due to the use of different analytical methods rather than differences in the character of the coals used in the two studies; Ode and Gibson followed ASTM methodology whereas Budge used an in-house method to determine moisture holding capacity. This idea is supported by data from Suggate (1974) which are plotted on Figure 2.3. Suggate's data were obtained on coals encountered in boreholes (offshore, Gippsland Basin) and provide the only direct comparison of equilibrium moisture (presumably determined according to AS-2096) and air-dried moisture ever published. Examination of Figure 2.3b shows that equilibrium moisture and air-dried moisture are similar near 6% air-dried moisture but equilibrium moisture is higher than air-dried moisture above 12% air-dried moisture.

Suggate and Lowery (1982) state that a close relationship exists between bed moisture and moisture in air-dried coal up to about 22% bed moisture or 18% moisture in air-dried coal. Suggate (1974) made a similar claim which he supported by a line drawn on a semi-log graph of air-dried moisture vs total moisture; the plot was reported (p.167) to be "derived by data on air-drying at relative humidities obtained by Suggate 1956". Since Suggate (1956a) made no direct comparison of air-dried moisture vs bed moisture, total moisture, or equilibrium moisture it is not clear how this graphic relationship was derived. Gray (1983) tested the relationship between air-dried moisture and total moisture suggested by Suggate (1974). He provides a plot of air-dried moisture vs "saturation moisture/Moisture holding capacity" for 31 coals as evidence that moisture holding capacity (MHC) can be calculated from the equation:

$$\text{MHC} = 1.13\ (\text{air-dried moisture}) \qquad \text{(eq. 2.3)}$$

for coals with less than 20% moisture holding capacity. According to equation 2.3, 20% MHC equals 17.7% air-dried moisture. Thus the relationship expressed in equation 2.3 is only valid for eight of the 31 coals examined by Gray (1983) where the predicted moisture holding capacity is less than 20%. Perhaps more importantly, Gray (1983, p.14) notes that the BS (ISO equivalent) method he used

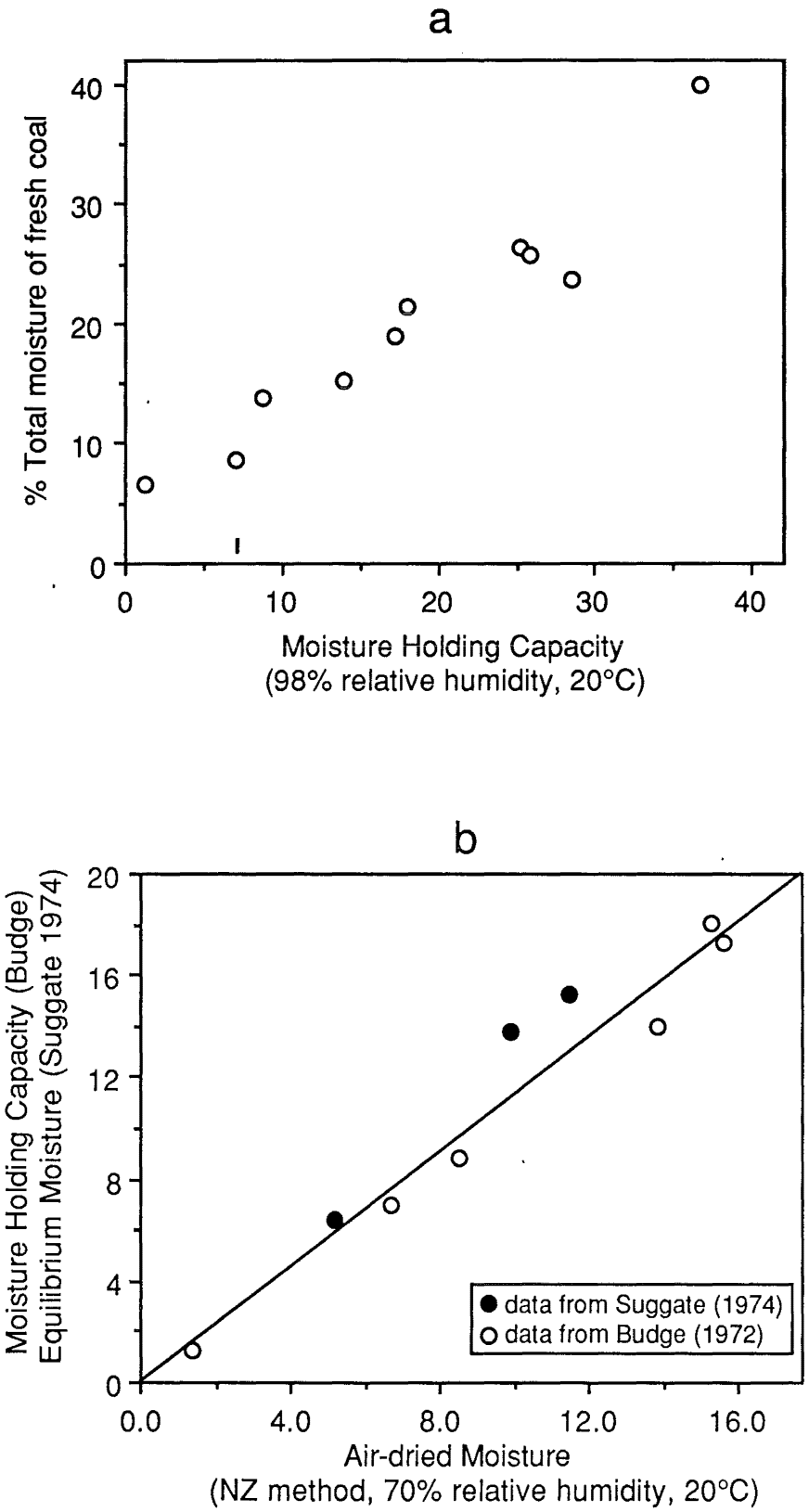

Figure 2.3 a) Total moisture of fresh coal vs Moisture holding capacity. b) Air-dried moisture vs Moisture holding capacity at two temperatures Data shown by open circles were obtained at 98% relative humidity and 20 °C (Budge, 1972) whereas data shown by closed circles were obtained at 98% relative humidity and 30 °C (Suggate, 1974).

to determine MHC is designated for hard coals (approximately bituminous rank and higher). Although equation 2.3 is based on limited data it may provide a reasonable estimation of bed moisture for the bituminous coals examined in this thesis. However, where only air-dried moisture values are known, classification of lower rank coals according to AS-2096 or ASTM-388 is not possible since bed moisture cannot be approximated by calculation based on air-dried moisture. It is also important to recognize that air-dried moisture values determined by New Zealand methodology are higher than what would be determined in laboratories overseas. The use of a unique method to determine moisture content hinders comparisons of New Zealand coals with coals overseas, and unfairly represents New Zealand coals in competitive export markets.

(ii) elemental measures

Carbon content of vitrinite has been considered a useful rank parameter for coals with carbon contents between 71 and 86% daf carbon (Figure 2.2). The increase in carbon content through this range of rank (about subB to mvb) is largely due to loss of oxygen upon diagenetic gelification (section 2.2.2). Indeed as noted by Neavel *et al.*, (1986 p.314) "what really changes in the rank sequence is oxygen content". Because the organic elements of coal also include hydrogen, sulphur and nitrogen, plots of carbon and oxygen can show considerable scatter like that observed by Neavel and his co-workers for high sulphur, Interior Basin US coals. This may be particularly significant for New Zealand coals which sometimes contain substantial amounts of organic sulphur. Thus the O/C ratio is probably a better indicator of diagenetic gelification than either carbon or oxygen content alone.

There are difficulties in the determination of precise O/C ratios. Since direct determination of oxygen content is not easily accomplished, oxygen is usually determined "by difference" where oxygen=100-(C+H+N+S) or sometimes 100-(C+H+N). Errors in determination of the constituents subtracted from 100 may be additive or partially compensating (Rees, 1966). For accurate work, carbon in carbonate minerals should be subtracted from total carbon and organic

sulphur should be determined by subtracting sulphate and pyritic sulphur from total sulphur. More difficult is the necessity of subtracting from total hydrogen the contribution from the hydration water of clay minerals. This is usually done based on an empirical factor related to ash yield. British Standard 1016 part 16 provides good methods for the correction of elemental data to a dmmf basis.

(iii) specific energy

Specific energy (or calorific value) if expressed on a moist basis is a useful rank parameter up through the high volatile stages of coalification (Figure 2.2). As discussed in sections 2.2.1 and 2.2.2, variation of moist, mmf calorific value through these ranks is largely a consequence of moisture content, rather than organic composition. However from subB through hvAb rank about half of the increase in moist, mmf calorific value is due to catagenetic loss of oxygen. Consequently, at these ranks moist, mmf calorific value is a more useful rank parameter than either moisture or dmmf specific energy alone, since moist, mmf calorific value reflects both physical and chemical coalification processes.

If expressed on a dmmf basis specific energy increases from the subB stage of coalification up to mvb rank due to the progressive loss of oxygen. Above mvb rank, dmmf calorific value decreases due to the loss of hydrogen. Because dmmf calorific value does not vary greatly below the subB stage of coalification (about 25% moisture in Figure 2.1b), and decreases above mvb rank, its range of usefulness is restricted.

Calorific value is also affected by coal type, grade and weathering. Coals with high hydrogen contents due to abundant liptinite or perhydrous vitrinite exhibit high specific energy values compared to other coals. Coals with high inertinite contents have lower specific energy values than associated coals (Strauss *et al.*, 1976). The low specific energy values associated with inertinite rich coals are a consequence of comparatively low hydrogen contents that more than compensate for the higher specific energy values that might otherwise be expected due to the relatively low oxygen contents of these coals. Thus variation of specific energy due to group maceral content is largely a consequence of

hydrogen abundance rather than oxygen or carbon content. This is not surprising in view of the relative contribution of hydrogen to specific energy (Table 2.2). The inorganic content of coal may also perturb specific energy. Consequently the ASTM rank classification requires 50 BTU for every percent of sulphur to be subtracted from the total calorific value to account for the energy released by pyrite and marcasite upon combustion. Finally, weathered coals usually have lower specific energy values than fresh coals due to loss of hydrogen and uptake of both moisture and oxygen upon weathering.

(iv) reflectance

The reflectance of vitrinite is an excellent rank parameter above mvb rank (about 1.12% R_o max) and remains useful at ranks as low as subA (Figure 2.2). The advantages of vitrinite reflectance as a rank parameter include, (1) no correction for inorganic content is required, (2) it is relatively unaffected by variation of group maceral content (with the possible exception of some coals with elevated liptinite contents, Hutton and Cook, 1980), and (3) it is the only method that can identify blends of coals of different rank. Because the analysis can be carried out on dispersed organic matter in sedimentary rocks it has become firmly established as a useful rank parameter for petroleum exploration.

It is well known that not all vitrinite macerals in a single coal will display the same reflectance due to differences in vitrinite submaceral type (Brown *et al.*, 1964). Accordingly vitrinite reflectance is sometimes measured on only one submaceral type in an effort to increase the precision of the analysis. For most bituminous coals the differences in reflectance between various vitrinite submacerals are small. Greater differences are observed in low rank coals for which measurement of selected submacerals has been advised (Goodarzi, *et al.*, 1988). However, certain coals display unusually high or low average reflectance values that cannot be accounted for by normal submaceral variation.

Low-reflecting vitrinite in a boghead-canneloid lithotype was observed by Given *et al.*, (1985). They suggested that the "influence of molecules derived from algae" was the causative factor responsible for the anomalously low reflectance

value. Similarly, Hutton and Cook (1980) attributed progressively lower reflectance values to increasing amounts of associated alginite. They explain the low vitrinite reflectance as resulting from localized diffusion of aliphatic rich compounds into the vitrinite. They attribute these compounds to alginite because both desmocollinite and band vitrinite (telocollinite) exhibit higher reflectance in algal poor lithotypes than in algal rich lithotypes. These studies support the notion of bitumen impregnation (Teichmüller, 1974, Teichmüller and Teichmüller, 1982) that posits an epigenetic incorporation of hydrogen rich material derived from liptinite macerals into associated vitrinite. Raymond and Murchison (1991) provide a well reasoned discussion in support of the bitumen impregnation mechanism.

Although the association of low reflecting vitrinite with algal rich facies is compelling evidence for bitumen impregnation, it does not prove a causal relationship. Kalkreuth (1982) noted that suppressed vitrinite reflectance was generally associated with high liptinite contents, and thus supported the idea of bitumen impregnation. Nonetheless, the occurrence of anomalously low reflecting vitrinite in several coals with low liptinite contents induced him to state (p.125) "it is hard to believe that this effect (*bitumen impregnation*) could be the only reason." Furthermore, the occurrence of low reflecting vitrinite in certain vitrinite rich New Zealand, Japanese, and Polish coals also argues against a universal bitumen impregnation mechanism (Newman and Newman, 1982, Newman, 1985, Fujii *et al.*, 1982, Fujii and Kiyo, 1985, Mastalerz, 1991). An alternate mechanism was advanced by Fermont (1988) who suggested that the occurrence of liptinitic algae "must have been accompanied by other microbiota that contributed specific biopolymers to the kerogen precursors". Like Fermont, Goodarzi *et al.*, (1988) observed that vitrinite reflectance varied with the lithologies surrounding coal. Similarly, Buiskool Toxopeus (1983) showed that vitrinite in coal exhibited higher reflectance than vitrinite dispersed in associated clays. Whereas Buiskool Toxopeus noted that the different vitrinite reflectance populations were morphologically distinct, Goodarzi *et al.*, (1988) observed this effect on a single maceral subtype. This observation led Goodarzi and his co-workers to reject the

notion that the reflectance variation had resulted from variable organic composition due to differential degradation of the organic matter at the time of deposition.

The significance of reflectance variation is of immediate concern to organic petrologists who use the technique to measure the level of maturation of organic matter dispersed in oil-prone source rocks. Vitrinite in these hydrogen rich facies exhibits lower reflectance values than equivalent rank, oxygen rich vitrinite found in most coals (Price and Barker, 1985). As with coal, two postulated origins have been suggested to explain the low reflectance of dispersed, perhydrous vitrinite namely: the bitumen impregnation concept (Walker *et al.*, 1983) and alternately, the notion that hydrogen enrichment during or shortly after deposition predetermines the subsequent expression of vitrinite reflectance (Wenger and Baker, 1987). Regardless of how some vitrinites are enriched in hydrogen, the occurrence of low reflecting vitrinite in certain atypical perhydrous coals as well as its common manifestation in liptinite rich source rocks suggests that hydrogen enrichment of vitrinite is an important causative factor responsible for low reflectance. Indeed, Shibaoka (1980) clearly showed the presence of low reflecting hydrogenation rims in vitrinite reacted with hydrogen in the laboratory.

In addition to bitumen impregnation or microbial lipid enrichment, variation of paleofloral assemblage has also been suggested to perturb the relationship between reflectance and burial depth (Newman and Newman, 1982). This conclusion is supported by the work of Lapo (1978) who observed different vitrinite compositions at equivalent levels of coalification and suggested that these differences arise, in part, from differences in botanic precursors. Expanding on earlier work Newman (1985, 1989b) suggests that the influence of the depositional environment also needs to be considered to explain variation of vitrinite composition. Newman (1985) observed that anomalously low reflectance values are found where geological evidence points to exceptionally wet, or submerged mires. In these instances, hydrogen enrichment was attributed to restricted oxygen access during peatification.

Beside perhydrous coals, certain oxygen rich coals may also exhibit anomalous vitrinite reflectance. Jones *et al.*, (1984) observed that some oxygen rich British coals often exhibit lower reflectance values than other coals with similar volatile and carbon yields. The vitrinite in these coals exhibited a patchy or mottled appearance similar to anomalously low reflecting vitrinite in certain US Interior province coals (Waddell *et al.*,1978) and some Australian coals from the Bowen Basin (Davis, 1971). Patchy vitrinite has also been observed in US interior province coals from Oklahoma (Cardott, 1987). Taylor and Lui (1987) speculated that patchy vitrinite may represent relic void spaces that were generated by biological degradation of vitrinite precursors during the peat stage of coalification. If filled with water or bitumen, these voids might lower reflectance. The idea that moisture in pore space lowers reflectance is due to work done at the Illinois State Geological Survey (Harrison, 1965, Harrison and Thomas, 1966, Thomas and Damberger, 1976). These workers showed that the reflectance of some coals increases upon drying in proportion to the moisture content of the coal. Following this idea Suggate and Lowery (1982) argue that apparent low reflectance of vitrinite can be a consequence of a relatively high geothermal gradient. They cite an example of a thermally mature coal encountered in a drillhole (Great South Basin, New Zealand) with a random reflectance of only 0.4%, and suggest that the sediment had reached the oil window at a relatively shallow depth, but high geothermal temperature. The presumed shallow burial (low lithostatic pressure) facilitated the persistence of pore hosted moisture thought to be the causative factor responsible for the anomalously low reflectance.

Does pore hosted moisture cause low reflectance? Thomas and Damberger (1976) suggested that low reflectance might be due to the low reflectance of water filled pores which upon desiccation are filled with higher reflecting air; they advanced this idea to explain the observed increase of vitrinite reflectance upon drying. Although this argument is intuitively appealing, some simple calculations suggest that it is probably wrong. For example, say the surface of a vitrinite grain reports a measured reflectance of 0.68% and that 20% of the surface is water filled pores and the remaining 80% is "solid" vitrinite (20% void space is

considered a reasonable figure for the affected hvCb coals discussed by Thomas and Damberger). If upon drying the water (Ro of water = 0.42%) is replaced by air (Ro of air = 4.23%) the measured reflectance will increase to 1.45%. The intrinsic reflectance of the "solid" vitrinite can be shown to be 0.75% which, due to the 20% surface area present as pore hosted moisture, is reduced to the measured value of 0.68%. Thus, if pore hosted moisture is the cause of diminished reflectance then the reason for the increase in reflectance upon drying cannot be due to simple replacement of water in pores with air since this would result in anomalously high reflectance. If replacement of water filled pores with air filled pores were the reason for observed increase in reflectance upon drying then the same calculations show that where only 2% of the surface is present as water filled pores the measured reflectance would be essentially the same as that of the vitrinite with no pores present (i.e., no suppressed reflectance would be observed) but would increase significantly upon drying. A more plausible explanation is that upon drying the water filled pores collapse. Thus the measured reflectance of a vitrinite with 20% of its surface covered with water filled pores would increase from 0.68% to 0.75% due to collapse of pores upon drying. This explanation is supported by the well known hysteresis upon drying; after drying coals do not regain their original moisture content (Allardice and Evans, 1978) possibly because of the collapse of affected pores. Thus water present in pores can be shown by calculation to depress reflectance but the observed increase in reflectance upon drying is more easily explained as a consequence of pore collapse, rather than replacement of pore water with air.

McTavish (1978) cited high hydrostatic pressure as a causal factor responsible for anomalously low vitrinite reflectance. McTavish noted that vitrinite encountered in overpressured zones in a number of oil wells exhibit lower reflectance values than expected based on measured formation temperatures. A significantly improved correlation between depth and reflectance was reported to be obtained by considering both pressure and temperature. Rather than invoking preservation of porosity as a causal factor to explain the lower reflectance

McTavish suggests that coalification is retarded by high hydrostatic pressure which impedes the generation of gaseous coalification products.

In a few coals, anomalously high rather than anomalously low reflectance values are observed. Some (presumably oxygen-rich) vitrinite macerals identified by Benedict *et al.*, (1968) as "pseudovitrinite" display a slightly higher reflectance than associated vitrinite, ranging from about 0.13% higher at hvBb rank to 0.03% higher at lvb rank. Kaegi (1985) found the reflectance of pseudovitrinite in some mvb rank coals was essentially the same as the rest of the vitrinite population. He further showed that most of the material identified as "pseudovitrinite" is likely to have resulted from post-coalification oxidation either in the seam or after mining. Although thermal oxidation in the laboratory leads to the development of bright oxidation rims (Prado, 1977), natural oxidation (weathering) generally results in lower reflectance values at particle edges and along cracks (Lowenhaupt and Gray, 1980). It is worth noting that low reflectance weathering rims may be restricted to bituminous rank coals; Marchioni (1983) observed increased reflectance due to weathering of subbituminous coal.

To summarize, causal factors that have been suggested to modify vitrinite reflectance include, variation of paleofloral assemblages, microbial lipid enrichment, bitumen impregnation, low lithostatic pressure, high hydrostatic pressure, and severe weathering. Causal factors to explain downhole reflectance anomalies in drillholes include many of the above mechanisms as well as transient heat transfer mechanisms associated with overpressuring (Law *et al.*, 1989), faulting (Dow, 1977), thermal conductivity of associated sediments (Jones *et al.*, 1972) and localized heating near igneous intrusions (many, reviewed by Murchison, 1991).

(v) volatile matter

With the exception of coals that contain abundant inertinite (Strauss *et al.*, 1976), volatile matter is a reasonable rank parameter where less than about 31% dmmf. It is worth noting that although dmmf volatile matter is listed in the ASTM classification as a rank parameter, adherence to the standard requires that dmmf

volatile matter be calculated from the fixed carbon content after calculation of fixed carbon to a dmmf basis. As noted by Given and Yarzab (1975) this is not a logical procedure since only the volatile matter can be rationally corrected to a dmmf basis. Below mvb rank volatile matter is relatively insensitive to rank variation because differences between (and within) the maceral groups are significant. Indeed, at these ranks volatile matter, after adjustment for rank variation and inorganic content, has been used to indicate coal type (Newman, 1985, 1987, 1989a).

The most significant advantage of the volatile matter test is that it is fast and inexpensive, a fact which likely explains its widespread use. Unfortunately, as noted by Gray *et al.*, (1978) it is one of the least reproducible properties determined on coal. The sensitivity of the test to variation in analytical conditions probably stems from the rapid heating rate used; the sample is plunged into a furnace set at about 900°C for 7 minutes. Competition between thermal decomposition and polymerization reactions are considered to control pyrolysis behaviour (Derbyshire *et al.*, 1989). Higher heating rates favour decomposition whereas slower heating rates favour polymerization. This explains why the lower heating rate used for sparking (i.e. non-agglomerating) coals in the ASTM standard yields lower volatile matter values (Rees, 1966) and why Suhr and Gong (1983) observed lower volatile matter yields at lower heating rates. Table 2.4 illustrates the similarities and differences between some standard methods used to determine volatile matter.

2.4 COAL TYPE

Suggate (1959, p.17) states that "Type depends on the nature of the vegetation and the amount of biochemical alteration of that vegetation before its burial beneath sediments". It is clear that Suggate considered coal type to be fixed upon burial of the coal-forming peat and recognized two different processes that control type variation. The first process is that of botanic input (i.e. "nature of the vegetation") and the second is biochemical alteration. Since biochemical decay can result from aerobic and anaerobic processes (faunal, fungal and

bacterial), and alteration by inorganic processes (desiccation, fire) is also possible, it follows that type variation is the result of multiple controls (nature of vegetation, redox potential, moisture, temperature, pH). Importantly, some of these processes may occur after burial.

2.4.1 Botanic Input

Coal is a product of variously altered plant remains. Consequently different types of plants can produce different types of coal. Humic coals result from preservation and burial of vascular plants whereas torbanites and bogheads develop from the preservation and burial of algae. The evolution and occasional extinction of different kinds of plants through geologic time has led to different types of coal being produced at different times in the geologic past. For example, coals formed during the Carboniferous period are rich in spores from shallow-rooted pteridophyta (spore plants) that produce large amounts of spores. At the end of the Carboniferous period the pteridophyta were gradually replaced by the pteridospermales (seed-ferns) and later gymnosperms. Consequently cannel coals are rarely found in post-Carboniferous coal measures. Permian Gondwana coals are sometimes rich in waxes and resins derived from gymnosperms but lack the abundant spores typical of Carboniferous coals (Diessel, 1984). During the late Cretaceous, modern angiosperms began to develop and together with the gymnosperms contributed to Cenozoic coals. Coniferous flora produce abundant terpene resin lumps and impregnations whereas tropical angiosperms are rich in both terpene resins and lipid resins (Teichmüller, 1989). The general succession from arborescent lycopods and pteridophytes in the Paleozoic to gymnosperms in the Mesozoic and angiosperms in the Cenozoic was interpreted by Robinson (1990) to indicate a progressively more sparing use of lignin and greater production of cellulose.

The botanic precursors to the bituminous New Zealand coals examined in this thesis are not known. However, based on this limited review it seems probable that resinous gymnosperms dominated many of the late Cretaceous

coal-forming mires, whereas tropical angiosperms were abundant in the Cenozoic mires.

2.4.2 Biochemical and Inorganic Alteration

Factors that alter the organic matter in mires prior to burial include, desiccation, fire, and ingestion by metabolism. These same mechanisms may continue after shallow burial during early diagenesis (prior to lithification). The initial changes that organic matter undergoes are profound. Rapid, early loss of cellulose and concentration of lignin was suggested by Van Krevelen (1950) based on elemental difference between fresh wood, lignin, cellulose and modern peat. Stout *et al.*, (1989) attribute the loss of these carbohydrates to hydrolysis by microbial enzymes. The idea of selective preservation of organic matter has attracted the attention of organic geochemists. Based on comparative microscopic and chemical studies of kerogens Tegelaar *et al.*, (1989) compiled a list of bio-macromolecules, their sources, and "preservation potential". They stress that the "preservation potential" is a relative concept and can be affected by other factors such as encapsulation of labile polysaccharides in recalcitrant structures such as cuticular membranes. They note that low molecular weight molecules produced from microbial degradation of parent bio-macromolecules contribute to geopolymer formation via "direct incorporation" and "natural vulcanization".

Aerobic degradation of lignin and cellulose by bacteria or fungi subtracts hydrogen (demethanation), and subsequent condensation of the humic acid products results in loss of oxygen via dehydration (Van Krevelen 1950). Migration of humic acids out of the seam is also consistent with loss of oxygen (Hatcher *et al.*, 1982). Thus aerobic degradation promotes a hydrogen-poor coal. Anaerobic degradation (putrification) is generally considered to produce a hydrogen rich coal (Teichmüller and Teichmüller 1982). However, since the ultimate product of fermentation (where secondary methanogenic bacteria are active) is gaseous methane anaerobic decomposition may diminish hydrogen in the residual peat. The production of methane from complex polymers involves an interdependent series of different bacteria. Fermentive anaerobes collectively decompose

polymers to CO_2, H_2 and water (Brock and Madigan, 1988). These bacteria thrive only where the product hydrogen is subsequently removed. Two kinds of bacteria are likely to compete for the hydrogen. Where sulphate is not available methanogens convert the hydrogen to methane gas. However, where sulphate is available, sulphate reducing bacteria successfully compete for the hydrogen and methanogenesis is inhibited.

Marine waters provide an abundant source of sulphate that is reduced by organic matter via heterotrophic anaerobic bacterial processes to yield H_2S. The higher pH of marine waters buffers the normally acidic peat water and accelerates bacterial decomposition of organic matter (Cecil *et al.*, 1979b) since bacteria favour neutral to slightly alkaline environments (Bass-Becking *et al.*, 1960). In the absence of reactive iron, hydrogen sulphide combines with organic matter. Other possible sources of organic sulphur (amino acids from plant and bacterial remains) are thought to contribute insufficient amounts of sulphur to account for observed enrichments in recent peats. In a comprehensive review of the origin of sulphur in coal Casagrande (1987, p.102) states that "organic sulphur in high sulphur coals undoubtedly originates from sulphate through hydrogen sulphide". Until recently, how hydrogen sulphide combines with organic matter in sediments was not known. Sinninghe Damste *et al.*, (1989ab) showed intermolecular and intramolecular crosslinking mechanisms involved in the fixation of H_2S to a stable organic form. Thus organic sulphur enrichment results from biogenic reduction of sulphate and subsequent abiogenic coupling of H_2S with specific organic substrates. The source of the elevated hydrogen content of coal from anaerobically decomposed peat may to be due to preservation of remnant bacterial lipids (Taylor and Lui, 1987), as well as the natural vulcanization of otherwise labile functionalized lipids such as fatty acids, steroids, isoprenoid alchohols or alkenes (Sinninghe Damste *et al.*, 1989a,b). Bacteriohopanoids (a family of terpenoids belonging to the isoprenoid group) are common constituents of bacterial lipids (Ourisson *et al.*, 1984). Fatty acids are degradation products produced from cellulose. Incorporation of sulphur into these hydrocarbons produces organic sulphur compounds that resist further bacterial degradation

and thus enrich the organic matter in hydrogen. The preservation of these otherwise labile, unsaturated lipid components results in both hydrogen and sulphur enrichment and may explain the origin of high sulphur, vitrinite rich perhydrous coals.

The idea that organic sulphur originates from sulphate via hydrogen sulphide is well supported but the timing of this enrichment is less clear. Although Casagrande (1987) has shown that virtually all of the sulphur in coal can be accounted for in the peat-forming stage, he refutes the notion that all high sulphur coals accumulated in marine conditions. He contends that ancient peats were more likely to have accumulated under freshwater conditions and were subsequently influenced by marine derived, sulphate rich groundwater to yield high sulphur coals. Geological evidence for post depositional enrichment of sulphur in some west coast South Island New Zealand coals has been presented by Suggate (1959) and Newman (1986, 1991).

2.5 MEASURES OF COAL TYPE

Since a variety of factors have been shown to control coal type, it follows that no single property can measure the whole range of type variation. For example, Newman (1986, 1987) found two different type parameters (tissue preservation index and rank-corrected volatile matter) necessary to deduce the depositional setting of some coals in the Upper Waimangaroa valley, Buller coalfield, New Zealand. Thus, like coal rank, appropriate measurement of coal type depends upon both the nature of the coal and the purpose of the study.

In the international literature the phrase "coal type" is synonymous with maceral content. Within New Zealand coal type has a broader meaning and can be evaluated at the bulk, megascopic, microscopic, molecular and elemental level. Bulk properties are measures that are based on analyses of the whole coal. Megascopic properties are visually apparent whereas microscopic properties require magnification. Molecular properties are based on the molecular components liberated by either solvent extraction or pyrolysis techniques. Although useful, molecular indicators of coal type are not considered in this

thesis. Elemental properties include whole-coal determinations of C H N O and S contained in the organic fraction of coal.

2.5.1 Bulk Properties

Bulk properties include moisture, specific energy, and volatile matter. Although moisture and specific energy are influenced by type variation they are predominantly rank parameters. Above hvAb rank, volatile matter is widely regarded as a good rank parameter for vitrinite rich coals; at lower ranks it is strongly influenced by type variation.

Historically, determination of volatile matter has played an important role in the analysis and classification of New Zealand coal according to both type and rank (Suggate 1959). In view of the importance and use of volatile matter as a type parameter in New Zealand it is discussed in the following section. Since the determination of volatile matter is a pyrolysis technique the use of Rock-Eval pyrolysis to characterize type variation is also discussed.

(i) volatile matter

The use of volatile matter as a measure of rank is discussed in section 2.3.2(v). Table 2.4 lists different standard analytical conditions used to measure volatile matter in coal. The influence of weathering on volatile matter is discussed in section 2.10.4(iv).

Newman (1987) quantified type variation with the parameter ΔVM which is determined by subtracting the expected "average type" volatile matter from the measured volatile matter. The average type volatile matter is found by using relationships established between volatile matter and air-dried moisture. She later suggested that a better estimate (applicable over a wider range of rank) of average type volatile matter for a given coal is obtained where a modified "Suggate rank" method is used (Newman, 1989a).

(ii) Rock-Eval pyrolysis

Rock-Eval pyrolysis was developed to evaluate dispersed organic matter to provide petroleum geologists with a rapid assessment of the quantity, quality and

maturity of dispersed organic matter encountered in exploration drillholes. The method has been widely accepted as a routine screening tool in the petroleum industry and various Rock-Eval pyroanalyzers are commercially available (Peters, 1986). Although Rock-Eval pyrolysis has been applied to coal (Teichmüller and Durand, 1983) it is not commercially used for coal analysis.

The method requires up to 100 mg of sample which is heated in a stream of helium at 300 °C for 3 to 4 minutes then heated at 25 °C/minute up to 550 °C. A flame ionization detector is used to measure various hydrocarbons (HC) in the pyrolyzate; the resulting data are expressed as mg HC/gram of sample.

The hydrocarbon fraction distilled at 300 °C (S_1) is considered to be free hydrocarbon and is diminished upon extraction of the sample with organic solvents. Hydrocarbons evolved above 300 °C (S_2) are considered to represent the potential yield if maturation were to continue. Unlike S_1, S_2 is relatively unaffected by solvent extraction of the sample. The CO_2 evolved up to 390 °C (S_3) is recorded separately. Like volatile matter, S_1, S_2, and S_3 decline with increasing inorganic content. Consequently, these measures are often expressed as mg/g total organic carbon. Rock-Eval pyrolysis also reports the temperature at which the maximum amount of S_2 pyrolysis products are generated (Tmax). Table 2.5 provides a summary of Rock-Eval parameters.

2.5.2 Megascopic Indicators Of Coal Type

Coal seams can be classified as humic or sapropelic based on visually observed fracture and lustre in hand specimen; most economic coal is humic. Sapropelic coals can be further differentiated as cannel (spore-rich) or boghead (algal-rich) although microscopic examination is required for positive identification. Humic coals are often banded and various, more or less horizontally continuous lithotypes (vitrain, clarain, durain and fusain) can sometimes be observed in the seam. The usefulness of these type distinctions has

TABLE 2.5
ROCK EVAL PARAMETERS

PARAMETER	UNITS	USE
S_1 (free hydrocarbons)	$\frac{\text{mg HC (300°C)}}{\text{g sample}}$	varies with both rank and type
S_2 (potential yield)	$\frac{\text{mg HC (300-550°C)}}{\text{g sample}}$	varies primarily with type
S_3 (non-hydrocarbon CO_2)	$\frac{\text{mg } CO_2 \text{ (300-390°C)}}{\text{g sample}}$	varies primarily with rank
HI (hydrogen index)	$\frac{S_2}{\text{g TOC}}$	a type parameter
OI (oxygen index)	$\frac{S_3}{\text{g TOC}}$	a rank parameter
PI production index	$\frac{S_1}{(S_1+S_2)}$	a rank parameter
S_2/S_3 ratio	$\frac{S_2}{S_3}$	a type parameter
Tmax	°C	a rank parameter

recently been questioned (Ting, 1988). Nonetheless, within a single mine the abundance of individual lithotypes may have industrial significance (Hower and Lineberry, 1988). However, significant petrographic variation of megascopically uniform lithotypes (Esterle and Ferm 1986, Hower *et al.*, 1988) suggests that detailed analyses of lithotypes are required to reliably predict industrial behaviour.

In many New Zealand coals, vertical and lateral compositional variation through a coal seam are not expressed by lithotype variation; many coals appear remarkably homogeneous at the mineface. This may explain why Suggate's 1959 classification scheme for New Zealand coals was based on elemental (H and C) data obtained from overseas lithotypes (appendix D). Nonetheless, serial ply samples taken vertically through a seam frequently exhibit differences in organic composition, even in the absence of obvious lithotype variation (Newman 1985).

2.5.3 Microscopic Indicators of Coal Type

(i) macerals

Examination of coal through the microscope readily reveals that coal is composed of a variety of intimately associated constituents which are called macerals. Three groups of macerals, vitrinite, inertinite and liptinite, are recognized. The abundant vitrinite group macerals are rich in oxygen, and are largely derived from lignin or cellulose degradation products. Inertinite group macerals are rich in carbon and are the product of variously oxidized or charred plant tissue. Liptinite group macerals are rich in hydrogen and are derived from spores, resins, algae, and protective waxy plant tissues. Alpern *et al.*, (1989) proposed a classification of coal according to type based on the proportions of these maceral groups. Vitric coal contains more than 60% vitrinite. Inertic coal contains less than 60% vitrinite and more inertinite than liptinite. Liptic coals are those with less than 60% vitrinite and more liptinite than inertinite. According to this classification nearly all New Zealand coals would be classified as vitric type.

There are two possible nomenclatures for the identification of macerals. Petrographic nomenclatures are based on pure observation or form, whereas petrologic nomenclatures are largely the domain of the theoretical and are based on ideas or concepts related to the genesis of coal. Potonie (1954) clearly laid out the differences between the systems and suggests (p.9) "To avoid confusion we should not engage in coal petrology and petrography at the same time." Potonie adds that petrologic definitions of macerals are not suited for industrial use since these change by virtue of our constantly evolving conceptions.

It is sometimes assumed that macerals with uniform shape, reflectivity and texture, have similar chemical compositions, and thus should behave the same way in technological processes. However, visibly similar macerals may be composed of distinctly different chemical structures. Although each maceral group (hydrogen-rich liptinite, carbon-rich inertinite and oxygen-rich vitrinite) is chemically distinct, it is not entirely uniform. Indeed, each group of macerals is in turn made up of a variety of macerals and submacerals which may be further

differentiated as maceral varieties. In practice the identification of macerals is subjective and based on form, (petrographic features), inferred botanical affinity (petrologic concepts) and other criteria that have little to do with chemical composition (Neavel, 1986). The tendency to regard optically similar macerals and submacerals as chemically identical entities is likely a consequence of the geological training of most coal petrographers. Geological definitions of coal usually begin by defining coal as a "rock". Some examples include "Coal is a readily combustible rock..." (Schopf, 1956) and "a combustible sedimentary rock ..." (ICCP, 1963). Since rocks are composed of minerals that posses generally well defined crystalline structures, the analogous idea that macerals should possess a regular organic composition is perhaps understandable. However, the organic nature of macerals precludes a comparatively limited number of known structures (about 3,000 naturally occurring minerals) and allows potentially millions of different organic structures. Nevertheless, as discussed by Neavel (1986 p.1635), the reason that maceral analysis "works as well as it does" to predict industrial behaviour is because there is a relatively narrow compositional range of substances that have identical reflectances. This is because the depositional setting of coal-forming peats restricts botanical diversity and limits the subsequent decomposition of the dead plant material. Eventual coalification of the peat further homogenizes the organic matter. Indeed, the tremendous morphological diversity of lignite is no longer evident by the bituminous stage of coalification and is nearly lost by the time the anthracite stage of coalification is reached.

The notion that optically similar macerals may possess different chemical compositions is supported by the limitation of petrographic methods to predict the coking behaviour of coal. For example, the Shapiro-Gray method of coke strength prediction was developed based on observed relationships between coke quality and coal composition for Carboniferous age coals from the eastern United States. The method works well for the coals for which it was developed, but fails if applied to western Canadian or Australian coals, largely because the inertinite in these coals is more reactive than inertinite in Carboniferous age coals (Nandi and

Montgomery, 1975, Diessel, 1983). Differences between vitrinites may also hinder the application of petrographic methods to predict coke quality. Creaney *et al.*, (1980) attributed the anomalous coking behaviour of an Australian coal (Wolgan seam, Sydney basin) to the presence of exceptionally reactive vitrinite. Similarly, Benedict *et al.*, (1968) found it necessary to distinguish pseudovitrinite (a non-reactive variety of telocollinite) to accurately predict the coking behaviour of certain Carboniferous age coals from the eastern US.

(ii) chemical etching

The vitrinite rich character of New Zealand coals suggests that coal type might be expressed in the variation of vitrinite group macerals and submacerals. However as noted by Taylor (1991) it is not always possible to distinguish vitrinite submacerals; this is particularly true for many bituminous New Zealand coals. Etching the polished specimen surface can be used to reveal differences within the vitrinite group. Newman (1988) was the first to show that chemical etching of the polished surface of New Zealand coal allows better differentiation of vitrinite group macerals and submacerals than possible with conventional incident light examination under oil immersion.

(iii) fluorescence microscopy

Fluorescence techniques to characterize coal have been continually evolving for the last 40 years (Diessel, 1990) and quantitative fluorescence measurements have been made for more than 25 years (Van Gijzel, 1979). Relatively recent advances in analytical technique have made possible the quantitative measurement of fluorescent vitrinite (Teichmüller, 1982b) and inertinite (Diessel, 1985). Due to the better recognition of liptinite group macerals using fluorescence techniques, many petrographers now conduct standard maceral analyses using both conventional white light and fluorescence techniques (Davis, 1987).

Although spectral measurements of liptinite group macerals have been used as maturity parameters for petroleum exploration the low amounts of liptinite in most coals has limited the value of the technique for industrial

characterization of coal. However the development of fluorescence techniques to induce measurable fluorescence of more abundant vitrinite and inertinite group macerals has led to renewed interest in the use of fluorescence microscopy for characterization of coal (Creaney *et al.*, 1980, Teichmüller, 1982b, Wolf *et al.*, 1983, Brown *et al.*, 1985, Diessel, 1985, Diessel and McHugh, 1986, Diessel and Wolff Fischer ,1986, 1987, Lin *et al.*, 1986, 1987, Quick *et al.*, 1988, Sasaki *et al.*, 1990, Davis *et al.*, 1991, Mitchell *et al.*, 1991, McHugh *et al.*, 1991, Kalkreuth *et al.*, 1991, Quick and Moore, 1991). Indeed, since the introduction of efficient longer wave excitation filters to the study of coal macerals (Diessel, 1985) measurement of fluorescence intensity of vitrinite and inertinite has rapidly developed and the technique is commonly referred to as fluorometric analysis.

Fluorometric analysis reports the mean fluorescence intensity of vitrinite and/or inertinite macerals. Units of fluorescence intensity are usually reported relative to a uranyl glass standard. The mean is calculated from 50 or more measurements on a maceral population which can be presented as a frequency histogram. In general inertinite group macerals exhibit lower fluorescence intensities than vitrinite group macerals. Within the vitrinite group telocollinite displays slightly lower mean fluorescence intensity than the more variable and positively skewed desmocollinite population (McHugh *et al.*, 1991). The mean intensities of all three maceral groups show a progressive increase and subsequent decline as rank advances through the bituminous stages of coalification.

In addition to being influenced by coal rank the fluorescence intensity of vitrinite and inertinite macerals is lowered by weathering in the seam (McHugh *et al.*, 1991) and stockpile (Quick and Moore, 1991), as well as low-level laboratory oxidation that occurs as a result of sample storage (McHugh 1986, Quick *et al.*, 1989, Mitchell *et al.*, 1991). The use of fluorometric analysis to detect weathering is discussed in section 2.10.1.

Fluorescence intensity is also controlled by the depositional environment and conditions of peatification (Sasaki *et al.*, 1990). It has been shown that

within the bituminous ranks marine influenced coals display markedly higher vitrinite fluorescence intensities than equivalent rank coals devoid of a marine influence (Diessel and Wolff-Fischer, 1989). Quick and Moore (1991) have shown significant isorank variation of vitrinite/inertinite fluorescence intensity through a cored Brunner coal seam from the Pike River coalfield. Thus, fluorescence intensity of maceral populations can be used as a measure of coal type.

The dependence of fluorescence intensity of vitrinite and inertinite maceral populations on coal rank, type, and degree of weathering may appear to limit the usefulness of the technique. In fact, these three factors also largely control the thermoplastic or carbonization behaviour of coal. Indeed, the striking parallelism between fluorescence response and coking behaviour has been a major reason for the continued development of the technique.

2.5.4 Elemental Indicators Of Coal Type

Van Krevelen (1950) showed how the atomic H/C - O/C diagram can be used to explain peatification and coalification processes and to graphically illustrate the effect of these processes. This graphic method to demonstrate rank and type variation (sometimes referred to as a "Van Krevelen diagram") has been widely adopted. Figure 2.4 shows how an H/C - O/C diagram reveals relative positions of some botanic precursors of coal and clearly shows the dramatic chemical changes that occur in the coal-forming paleo-mire.

Like all whole-coal or bulk chemical analyses the use of elemental data to evaluate coal type requires relatively pure maceral concentrates for useful interpretation. Cook (1975 p.63) explains: " ... it is impossible to make more than very approximate inferences concerning type from chemical or proximate analyses since coal contains three major phases, exinite, vitrinite and inertinite". Since most New Zealand coals lack appreciable liptinite and inertinite they can be usefully examined by whole-coal analyses, but comparison with liptic or inertic coals is difficult with these methods.

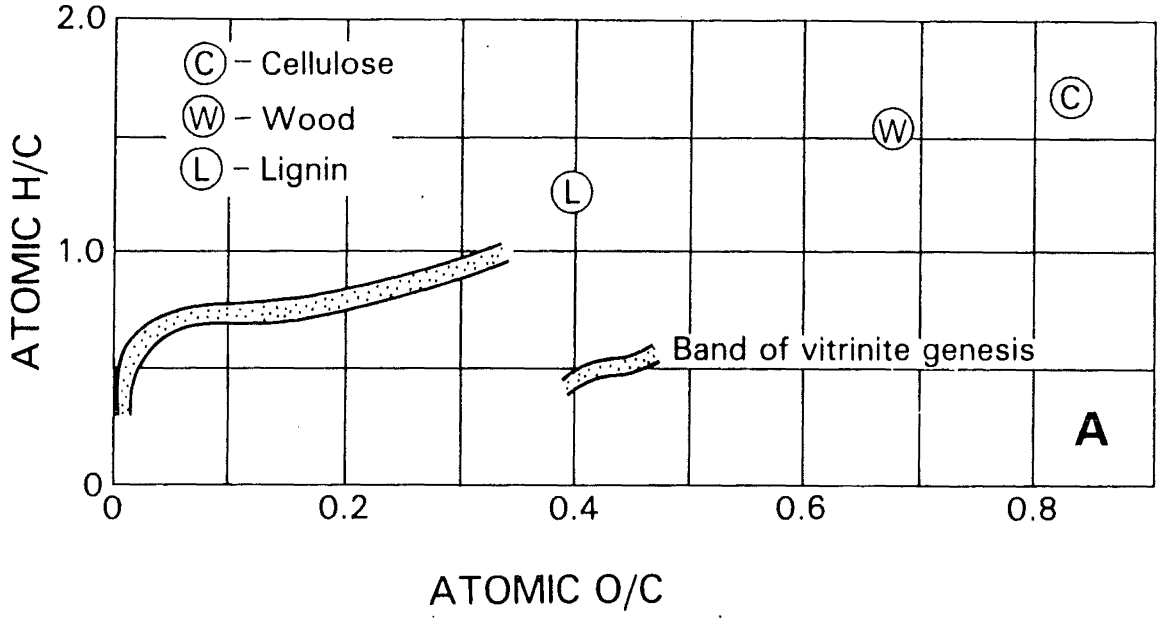

Figure 2.4 Van Krevelen diagram showing peatification and coalification processes, from Suggate, (1990) after Van Krevelen (1961).

2.6 COAL GRADE

The term grade, as used in this thesis, refers to the inorganic constituents of coal, that are largely present as discrete minerals, organically associated humates and carboxylates, and dissolved species in pore waters. In this thesis these constituents are collectively referred to as mineral matter. Mineral matter can be considered in terms of its distribution, origin, and type.

2.6.1 The Mode of Occurrence and Origin of Mineral Matter in Coal

Mineral matter may be physically present in coal as disseminated microscopic or submicroscopic grains, partings, nodules, fissure fillings, or various inorganic/organic admixtures. In addition, mining practices may introduce significant amounts of country rock into run of mine coal. Adventitious minerals are those easily liberated by crushing and removed by beneficiation. The more intimately mixed or disseminated mineral matter is called inherent. Some descriptive terms applied to mineral matter found in coal are included in Table 2.6. It is worth noting that these descriptive terms are empirically defined. For example, the amount of adventitious or inherent mineral matter in a coal depends, in part, on the particle size to which a coal is crushed. Nonetheless, if standard conditions are specified the amount of inherent mineral matter may be

precisely estimated. For example, the weight percent ash of a -60 mesh, 1.4 gravity float fraction can be measured with precision.

In contrast to descriptive terms used to describe the mode of mineral matter occurrence in coal, terms used to describe the origin of mineral matter can be conceptually defined. Unfortunately, the actual process of mineral formation or time of emplacement cannot be known with certainty. Consequently new terms are introduced and the definition of existing terms changes as our ideas regarding the genesis of mineral matter in coal continuously evolve. Table 2.6 lists a few of the genetic terms that have been used to describe the origin of mineral matter in coal. It should be noted that these terms are not necessarily mutually exclusive and that different authors may have different conceptual definitions for any given term. For the purpose of this thesis five groups of genetic terms are shown.

Minerals may also be distinguished according to their time of origin, i.e., syngenetic or epigenetic, or their mode of accumulation, i.e., allochthonous, autochthonous, or diagenetic. Syngenetic minerals accumulate early prior to burial of the peat. Some examples include detrital contributions such as fluvial splays and eolian tonsteins, neoformed sulphides from sulphate reducing bacteria, and diagenetic minerals such as kaolinite derived from detrital illite. Epigenetic minerals accumulate after burial of the coal-forming peat. Some examples include carbonate and sulphide minerals that accumulate in fissures and cleat, and diagenetic products. Epigenetic minerals also form from the alteration of pre-existing minerals such as illite derived from kaolinite. The foregoing discussion is based on more extensive essays by Renton and Cecil (1979), Mackowsky (1982), Ward (1986), Falcon and Synman (1987) and N. Newman (1988).

TABLE 2.6
TERMS USED TO DESCRIBE
THE ORIGIN AND MODE OF MINERAL MATTER IN COAL

Genetic Terms

Allochthonous
- allogenic
- attrital
- clastic
- detrital
- mechanical inheritance
- sedimented

Autochthonous
- authigenic
- biogenic
- neoformed
- precipitated
- vegetable ash

Diagenetic
- alteration
- transformation

Syngenetic
- synsedimentary

Epigenetic
- post cleat
- post depositional

Descriptive Terms

Inherent
- disseminated
- intrinsic

Adventitious
- segregated
- liberated
- extraneous

Because the accumulation and alteration of mineral matter is a continuous process the differentiation of syngenetic and epigenetic minerals is often difficult. The problem differentiating syngenetic and epigenetic minerals is perhaps best illustrated by Querol *et al.*, (1989) who defined five temporal stages for iron sulphide formation but acknowledged overlap between these stages. Thus the differentiation of syngenetic and epigenetic is probably overly simplistic. Ward (1986, p.97) defines two additional temporal stages of mineral formation; early diagenetic minerals form "shortly after burial by more peat or other sediment" and late diagenetic minerals form due to "processes associated with deeper burial and rank advance."

2.7. MINERALS FOUND IN COAL

Mackowsky (1982) lists 45 minerals found in coal. Only a few of these minerals, however, are abundant in coal. Clays, quartz, carbonates, sulphides and sulphates comprise the bulk of the inorganic matter in most bituminous

coals. Ion-exchangeable cations can account for a significant proportion of the total inorganic matter in lower rank coals. Table 2.7 lists the relative abundance of some minerals identified in coals from the west coast, South Island, New Zealand. Although not listed in Table 2.7 expandable clays and sulphate minerals have also been identified in these coals.

2.7.1 Clay Minerals

Clays are a major inorganic constituent of coals. Four groups of clay minerals are often recognized: kaolinite, illite, the expandable clays, and chlorite. Unlike other discrete minerals found in coal, clays do not always closely correspond to stoichiometric formulae. Suhr and Gong (1983, p.31) state:

> Thus, where quartz and calcite can only mean SiO_2 and $CaCO_3$, "montmorillonite" (smectites) can mean a wide range of chemical formulae depending whether it is montmorillonite proper, beidillite, nontronite, etc. Although the various "montmorillonites" (smectites), "illites," etc. show gross physical and chemical properties (e.g., swelling, cation exchange), the crystallographic differences due to composition and the variance in the degrees of crystallinity preclude any simple forms of quantitative analyses.

Berry and Mason (1959) list three factors that determine the nature of a clay, namely: the parent material (provenance), the physicochemical environment of decomposition (climate and transport), and the environment of deposition and diagenesis. The relative importance of these three processes to the distribution of clay minerals in coal has not been established. Accordingly, there are different opinions concerning the origin of clay minerals in coal. Many coal scientists agree that clays have a predominantly detrital origin whereas others argue for a primarily neoformed origin. Both origins are important. Indeed, Mackowsky (1982) notes that clay minerals in coal may be either neoformed or detrital but adds (p.158) "... as to their genesis we are much more in the dark than in the case of any other minerals". In an important but controversial paper Renton and Cecil (1979) argue that most clays are neoformed rather than detrital. Although their idea that most mineral matter in coal is not detrital has not been widely accepted, a significant contribution of neoformed clays is generally acknowledged.

TABLE 2.7

RELATIVE ABUNDANCE OF MINERALS IDENTIFIED IN COALS FROM THE WEST COAST, SOUTH ISLAND, NEW ZEALAND

Mineral	Paparoa coal measures	Brunner coal measures
clay minerals		
kaolinite	abundant,	abundant
illite	common	common
chlorite	trace	trace
quartz	abundant	abundant, locally variable
sulphides	trace	common, locally abundant
carbonates		
siderite	abundant	usually absent, locally abundant
calcite	trace	locally abundant
dolomite/ankerite	trace	minor, locally abundant
aragonite	absent	minor
dawsonite	absent	absent, locally minor
other minerals		
rutile	minor	trace
crandallite	minor	trace
apatite	absent	trace
boehmite	trace	minor

(adapted from N. Newman 1988)

(i) kaolinite

Renton and Cecil (1979) propose that most syngenetic kaolinite is neoformed rather than detrital. In support of this idea, they cite abundant inorganic material in plants, as well as an observation made by Staub and Cohen (1979) that detrital clays flocculate at the edge of a swamp margins. Finkelman (1980) also concluded that syngenetic kaolinite is authigenic because of its common appearance in maceral pores and disseminated in vitrinite. Ward (1978) came to the same conclusion based on the widespread occurrence of well crystallized kaolinite in many Australian coals.

Transformation of existing silicate minerals is another possible origin of kaolinite. The occurrence of kaolinitic tonsteins (Spears and Kanaris-Sotiriou, 1979) as well as the apparent alteration of expandable clays present in underclays (Staub and Cohen, 1978) clearly illustrate the propensity of silicate minerals to alter to kaolinite in the coal forming environment. Rimmer and Davis (1984)

suggested that the observed relative enrichment of kaolinite in the lower Kittanning coal at the edges of the basin resulted from more acidic conditions which favoured the alteration of existing clays to kaolinite, preservation of detrital kaolinite, and neoformation of kaolinite.

The occurrence of kaolinite as a cleat filling (Harris *et al.*, 1980, N. Newman, 1988) indicates that kaolinite may also have an epigenetic origin. Ward (1978) suggests that remobilization of existing kaolinite is a possible origin of kaolinite in cleat. Beginning in the low volatile stage of coalification, kaolinite alters to illite/muscovite or chlorite if sufficient cations are available (K or Mg+Fe respectively) (Kisch, 1968).

(ii) illite

In a study of the Upper Freeport seam in western Pennsylvania, Cecil *et al.*, (1979c) found that the illite/kaolinite ratio increases with increasing Ca, ash, and pyritic sulphur content of the coal. They concluded that illite is enriched in coals deposited in marine influenced conditions. Renton and Cecil (1979) contend that most syngenetic illite is neoformed (rather than detrital), and is preferentially formed in more alkaline, marine influenced conditions. The presence of high temperature polytypes of illite in Lower Kittanning seam samples from Pennsylvania and Ohio led Davis *et al.*, (1984) to conclude that some syngenetic illite is detrital. N. Newman (1988) regarded illite in coals from the west coast South Island New Zealand as a detrital mineral.

(iii) expandable clays

Expandable clays such as montmorillonite are rarely found in coal. Where present, they cause slimes and dewatering problems at coal preparation plants and if found in roof rocks or mine floors, they cause rock falls and heaving (Mackowsky, 1982). Staub and Cohen (1978) observed that montmorillonite rich underclays appeared to rapidly alter to kaolinitic clays in a modern peat forming environment. Detrital montmorillonite in crevasse splays (eroded from nearby salt marsh clays) were shown to alter to kaolinite due to intensive leaching. Because of the instability of expandable clays in freshwater fluvial systems, a significant

detrital origin is doubtful. Abundant montmorillonite is more likely to be neoformed from the alteration of volcanic ashfalls. Triplehorn and Bohor (1986) suggest that either smectite or kaolinite are formed from the alteration of volcanic ashfalls. Ultimately these pyroclastic sediments will alter to kaolinite but an intermediate stage consisting of smectites may precede kaolinite formation.

2.7.2 Quartz

Mackowsky (1982 p.168) lists two origins for quartz in coal, detrital quartz and authigenic quartz which "formed more recently from solution". Renton *et al.*, (1980) observed that modern plants contain sufficient silica to account for the amount of quartz in most coals and concluded that most quartz is derived from inorganic materials present in plants from which the coal was derived. Ruppert *et al.*, (1987) used cathodoluminescence to examine quartz grains in the Upper Freeport coal of Western Pennsylvania and distinguished both luminescent and non-luminescent grains. Based on inferred paleo-environments they suggested that the luminescent quartz grains were primarily detrital whereas the non-luminescent grains were authigenic. Based on petrographic observations N. Newman (1988) regarded quartz in west coast South Island coals to be primarily detrital.

2.7.3 Sulphides

The major sulphide minerals found in coal are pyrite and, less commonly, marcasite. In a study of selected coals from Pennsylvania, Reidenouer *et al.*, (1967) concluded that variation of the total sulphur is largely the result of the distribution of pyritic sulphur. In a comprehensive study of 1,847 coal samples from West Virginia, King and Renton (1979) came to the same conclusion. As shown in Figure 2.5 this is not true for coals from the west coast, South Island, New Zealand. Total sulphur variation of these coals is largely a result of variation of organic sulphur.

The bulk of the pyrite in most coals is thought to be syngenetic, forming prior to compaction of the peat. Casagrande *et al.*, (1977) found that marine

influenced peats in Florida exhibit pyrite contents similar to those of marine influenced coals in the Illinois basin.

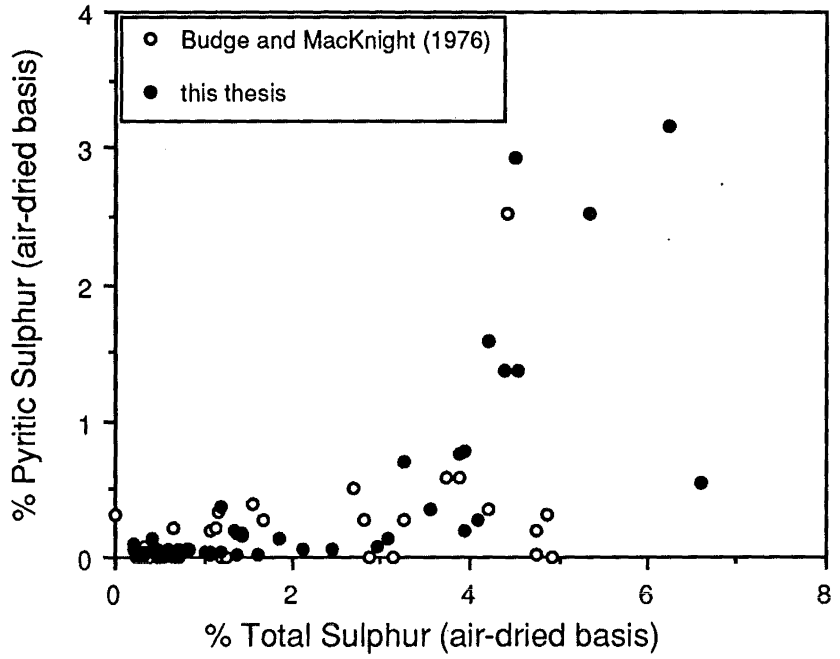

Figure 2.5 Scatterplot of total sulphur vs pyritic sulphur of coals from the west coast, South Island, New Zealand. Data from run of mine samples Budge and MacKnight (1976) and varied samples (this thesis).

Epigenetic sulphide minerals are often found as cleat fillings. Unlike syngenetic or early diagenetic forms of sulphide that require bacterial generation of H_2S, epigenetic sulphides in coal are thought to form due to poorly characterized chemical processes.

The role of sulphate reducing bacteria in the genesis of pyrite in coal is well established (Williams and Keith, 1963, Reidenouer *et al.*, 1967, Casagrande *et al.*, 1977, Cecil *et al.*, 1979b, Renton and Cecil, 1980). The genesis of syngenetic pyrite in coal requires anaerobic bacterial reduction of sulphate to sulphide which then combines with ferrous iron to form iron monosulphides (i.e., mackinawite and greigite) and finally pyrite. Berner (1984) states that the availability of sulphate, organic matter, and reactive iron, are the principal factors that control the formation of pyrite. The abundant organic matter which characterizes coal rules out organic content as a limiting factor to explain the distribution of pyrite in coal. In addition to the availability of sulphate and iron, Cecil *et al.*, (1979b, p.238) list the pH of the coal-forming mire as an important control on the distribution of pyrite in coal. They contend that acidic conditions inhibit both the

activity of sulphate reducing bacteria and the reduction of ferric iron to ferrous iron. Conversely, a higher pH encourages bacterial activity as well as the formation of ferrous iron and thus promotes the fixation of sulphur (from bacterially generated H_2S) as sulphide minerals. In the absence of reducible iron, H_2S is thought to combine with unsaturated labile aliphatics resulting in an enrichment of organic sulphur (Sinninghe Damste *et al.*, 1989a). Thus the factor limiting pyrite formation in many low ash, high sulphur New Zealand coals is probably the lack of iron.

Reidenouer *et al.*, (1967) concluded that paleo-topography controlled the availability of ferrous iron (associated with detrital minerals), and consequently the local distribution of pyritic sulphur. Williams and Keith (1963) have related regional variation of sulphur content to the availability of sulphate ions. Williams and Keith (p.727) state;

> "Thus the invasion of the coal swamp by marine waters and consequent increased availability of sulfate ion probably was a causative factor in controlling regional sulfur variation in the Lower Kittanning coal."

It should be pointed out that the concepts of "marine" and "freshwater" as used in many papers are relative and perhaps misleading. Renton *et al.*, (1980) illustrated that any significant marine influence within a mire would result in rapid degradation of the organic matter precluding the formation of coal. For this reason (and others) Renton and Cecil (1980) contend that the distribution and quantity of sulphur in coal is controlled primarily by the pH of the peat forming environment.

The presence of marcasite at the erosional surface of some Tertiary, Victorian brown coals was explained by Edwards and Baker (1951) as an indicator of acidic (freshwater) conditions. The sulphur was thought to be partly sourced in the coal itself. They contend that sulphate reducing bacteria can thrive in acidic conditions. If this is true then the limiting factor for sulphide enrichment is the availability of sulphate (and iron) rather than the pH of the coal forming mire.

2.7.4 Carbonates

Mackowsky (1982 p.164) states that "next to clay minerals the most frequent group of minerals are the carbonates". Renton, (1982) states that carbonate minerals in coal are predominantly formed from dissolved CO_2 in pore waters combining with cations such as calcium. The CO_2 is a product of the decomposition of carboxyl groups and at least some of the cations originate from related decomposition of carboxylate salts. Thus organic carbon in carboxyl groups is suggested to become inorganic carbonate.

Kemezys and Taylor (1964) found abundant siderite only in seams overlain by lacustrian rather than marine rocks. They further noted that siderite and pyrite do not usually occur together in significant amounts. Renton (1982 p.301) further explained that:

> "Siderite forms as the favored iron mineral in those environments where the availability of reducible sulfate ion is low. Inasmuch as the waters of marine and most freshwater alkaline environments contain appreciable sulfate ion, the appearance of siderite in coal would indicate an acid freshwater environment of peat accumulation."

Although the occurrence of siderite is widely considered to be certain evidence of the absence of marine influence, Pye *et al.*, (1989) observed siderite concretions forming in modern marine influenced marsh and coastal sediments. They explain that in this instance methanic iron reduction exceeded sulphate reduction due to a lack of suitable organic nutrients to support the sulphate reducing bacteria. Thus it is a lack of H_2S rather than sulphate ion which favours siderite formation. Nonetheless, the abundant organic matter that characterize coal forming environments rules out restricted availability of organic nutrients as a control on the growth of sulphate reducing bacteria. Consequently, the occurrence of siderite in coal is still good evidence of a strictly freshwater depositional environment.

Rare occurrences of both siderite and sulphide enrichment result from syngenetic (or early diagenetic) formation of siderite followed by emplacement of sulphide (Kemezys and Taylor, 1964) or transformation of siderite to sulphide (N.

Newman 1988). In these instances sulphide can be observed under the microscope to either dissect or encircle siderite.

Carbonates are rare in coals that contain appreciable acid form carboxyl groups (Brown coals) since the acidic nature of these groups in presence of water causes decomposition of carbonate minerals. However, carbonates present in intraseam partings have been observed in some lignites from Thailand (Ward, 1991). The persistence of carbonates in this instance was attributed to an unusually high pH of interstitial waters. Apparently, carboxyl groups are present in the salt form which effectively neutralizes their ability to dissolve carbonate.

Although rare, the presence of syngenetic dolomite is considered to document marine invasions of the paleo-mire (Mackowsky, 1982).

2.7.5 Sulphates

Calcium sulphate (gypsum) and iron sulphates (szomolnokite, jarosite) are secondary minerals that originate from sulphides, sulphides and carbonates, or sulphides and clays. Although rare in fresh coal, sulphates are often found in coals that have weathered or deteriorated due to laboratory storage. Hydrated forms of szomolnokite (primarily melanterite or rozenite) occur as white fibrous crystal growths on the surface of oxidized coal. Jarosite and other sulphates containing hydroxyl are generally yellow. The importance of microbial processes in the oxidation of pyrite to various sulphates was discussed by Nordstrom (1982) who provides a comprehensive review of the mechanisms of sulphide oxidation. Nordstrom emphasises the importance of *T ferrooxidans* that generate ferric iron to directly oxidize pyrite in an acid environment. Table 2.8 lists some sulphate minerals that have been identified in coal.

The list of sulphates shown in Table 2.8 is not comprehensive. Zodrow and McCandlish (1978) have also found pickeringite, aluminocopiapite, and halotrichite in outcrop samples and state (p.22) "many esoteric sulphates await discovery". The variety of sulphates found in coal results from the ease of cationic substitution as well as the variable hydration states of these minerals.

TABLE 2.8

SULPHATE MINERALS FOUND IN COAL

Calcium Sulphates	
gypsum	$CaSO_4 \cdot 2 H_2O$
bassinite	$CaSO_4 \cdot 0.5 H_2O$
Iron Sulphates	
szomolnokite	$FeSO_4 \cdot H_2O$
fibroferrite	$FeSO_4 \cdot 5 H_2O$
rozenite	$FeSO_4 \cdot 4 H_2O$
melanterite	$FeSO_4 \cdot 7 H_2O$
coquimbite	$Fe(SO_4)_3 \cdot 9 H_2O$
roemerite	$FeSO_4Fe(SO_4)_3 \cdot 12 H_2O$
Iron Sulphates Containing Hydroxyl	
jarosite	$KFe_3(SO_4)_3(OH)_6$
Al-substituted	$K(Fe,Al)_3(SO4)_2(OH)_6$
natrojarosite	$NaFe_3(SO_4)_2(OH)_6$
sideronatrite	$Na_2Fe(SO_4)_2(OH) \cdot 3 H_2O$
carphosiderite	$(H_3O)Fe_3(SO_4)_2(OH)_6$

References: Huggins *et al.*, 1983; Gluskoter, 1975; Zodrow and McCandlish, 1978

In a study of three bituminous coals, Huggins *et al.*, (1983) found szomolnokite to be the initial oxidation product of pyrite in both weathered and stored coal samples. Gypsum was absent in the weathered coals but did form during laboratory storage where carbonate and sulphide minerals were in intimate contact. In severely weathered coals the iron sulphates were rare; they apparently are transient transformation products and rapidly alter to goethite. Sulphates that formed due to laboratory storage were more persistent. The high solubility of ferrous sulphate minerals in water may explain their absence in severely weathered coal samples. For example, a variety of different sulphates co-existing in outcrop were later found by Zodrow and McCandlish (1978) to be absent. They noted (p.21), "heavy rains have since obliterated these samples". Likewise, the typical absence of sulphate in severely weathered New Zealand coals, especially in areas of frequent and heavy rainfall such as the west coast of the South Island, is also thought to have resulted from dissolution of sulphate minerals (N. Newman 1988). Unlike soluble ferrous sulphates, ferric sulphates such as jarosite are more persistent in the natural environment (Huggins and Huffman, 1989). Huggins *et al.*, (1983) suggested that sulphide weathering in the

presence of potassium (from illite) facilitates jarosite formation, whereas a lack of potassium promotes the genesis of soluble ferrous sulphate (szomolnokite).

2.7.6 Exchangeable Cations

Miller and Given (1987) showed that as much as 80% of the inorganic material in several US lignites was present as ion-exchangeable cations. Kiss and King (1977) and Durie (1961) have show that the bulk of the inorganic matter in Victorian brown coals is present as salts of carboxylic acids. Since exchangeable cations replace hydrogen ions of carboxyl groups and these groups are lost during the first coalification jump (diagenetic gelification) they are unlikely to be present in the bituminous coals examined in this thesis. However, ion-exchangable cations may be present in weathered bituminous coal (Huggins *et al.*, 1983, see section 2.10.3 ii).

2.8 MEASURES OF COAL GRADE

Determination of the amount and nature of mineral matter in coal is important to evaluate the suitability of coal for industrial use and to correct for the perturbing effect of mineral matter on measures of rank and type. Proper use of such data requires an understanding of the uses and limitations of various methods used to measure inorganic content. Although accurate determination of mineral matter by acid digestion (reviewed by Given and Yarzab, 1978) is possible this tedious technique is rarely applied to coal. This section discusses some of the more common methods used to measure the amount and nature of mineral matter in coal.

2.8.1 Measures of Bulk Mineral Matter Content

(i) ash

Ash is defined as the weight percent noncombustible material that remains after a coal is burned under standard conditions. ASTM D-3174-82 prescribes some standard conditions used for the determination of ash and states (note 1):

> Ash results obtained by this method differ in composition from the inorganic constituents present in the original coal. Incineration causes expulsion of water from the clays and calcium sulfate, of carbon dioxide from carbonates and the conversion of iron pyrites into ferric oxide...

Other changes upon ashing include the fixation of variable amounts of SO_3 by combining with CaO to form calcium sulphate (Rees, 1966). To improve precision for coals with significant amounts of calcite and pyrite an alternate method with a slower heating rate is provided in ASTM standard 3174-73; alternately ash may be mathematically corrected to a sulphate free basis. A slower heating rate allows greater elimination of gaseous sulphur oxides prior to significant carbonate decomposition. The problem of sulphate fixation in the ash is particularly acute for low rank coals where abundant CaO from carboxylate salts readily fixes organic sulphur at comparatively low ashing temperature (Durie, 1961), and suggests that staged combustion to reduce sulphate fixation may be ineffective for low rank coals.

The loss of hydration water of minerals, sulphur from sulphides, and CO_2 from carbonates upon combustion causes the ash yield of bituminous coals to be usually less than the actual inorganic content (with the possible exception of coals with appreciable sulphate fixation). Conversely, the ash yield of low rank coals may be higher than the mineral matter content. Abundant cations in low rank coals, which are present in the coal as salt-form carboxyl groups, are easily oxidized or sulphated during ashing. Additional oxygen and any incorporation of organic sulphur increases the mass of the ash in excess of the amount of inorganic material present in the coal (Kiss and King 1977).

Because ash is an empirical measure of coal grade it will vary in accordance with the analytical method used to determine ash yield. Table 2.9 summarizes the incineration conditions specified by various international standards. In general, lower heating rates can be expected to minimize sulphate fixation.

(ii) low temperature ash

Discrete minerals in coal can be separated from the whole coal with a radio-frequency generated oxygen plasma that oxidizes the organic components, leaving behind relatively unaltered mineral matter (Gluskoter, 1965). Because this oxidation occurs at relatively low temperatures (60 to 200°C) residual mineral

matter isolated by low temperature ashing is little changed and may be examined with conventional X-ray diffraction techniques.

TABLE 2.9
SUMMARY OF SOME METHODS TO MEASURE ASH CONTENT

STANDARD METHOD		HEATING CONDITIONS
AS 1038.3		to 500 °C in 30 minutes then to 815 °C in 60 minutes hold for 60 minutes (or constant mass) (for low rank coals increase furnace air exchanges until 500 °C is reached)
ASTM 3174		to 450-500 °C in 60 minutes then to 700-750 °C in 60 minutes hold for 120 minutes (or constant mass)
ISO 1171	a)*	to 500 °C in 30 minutes then to 815 °C in 30-60 minutes hold for 60 minutes (or constant mass)
	b)	For low rank coals or coals with "high sulphur" or > 2% CO_2 , to 250 °C in 30 minutes then to 500 °C in 30 minutes then to 815 °C in 60 minutes hold for 60 minutes (or constant mass)
CRA method		to 400 °C in 30 minutes, hold 30 minutes then to 815 °C in 50 minutes, hold for 120 min (constant mass, duplicates)

*Note, BS 1016 Part 3 single furnace method is technically equivalent

Miller *et al.*, (1979) showed that the percentage low temperature ash is also a direct measure of the amount of mineral matter in bituminous coal. They specify ashing conditions that minimize both the oxidation of pyrite, and the fixation of organic sulphur as sulphate in the ash. AS-1038.22 (1983) provides instructions for the determination of mineral matter in hard coals by low temperature ashing.

(iii) calculation of mineral matter

Although low temperature ashing and acid digestion techniques can provide a direct measure of the amount of mineral matter in coal, these techniques are tedious. Calculation of the mineral content is a more expedient method and is most often used to allow analytical result to be expressed on a mineral free basis. Table 2.10 lists some formulae that have been used to calculate mineral matter.

TABLE 2.10

MINERAL MATTER FORMULAE

Parr;[1]	MM = 1.08 Ash + 0.55 S
Modified Parr;[2]	MM = 1.13 Ash + 0.47pyr + 0.5Cl
BFC;[3]	MM = 1.10 Ash + 0.53 S + 0.74 CO_2 - 0.36
KMC;[4]	MM = 1.13 Ash + 0.5 S_p + 0.8 CO_2 + 2.8 $S_{SO_4\ coal}$ - 2.8 S_{ash} + 0.5Cl
Kiss and King;[5]	MM = SiO_2 + Al_2O_3 + TiO_2 + K_2O + FeS_2 + Na + Ca + Mg + Fe + NaCl

References: [1]Rees (1966), [2]Given and Yarzab (1975), [3]BS-1016 (part 16)
[4]Millot (1958) and for low rank coals [5]Kiss and King (1977)

The theoretical justification for various mineral matter formulae is reviewed by Rees (1966) and Given and Yarzab (1975). A major difference between these formulae is the necessary assumption of the amount of hydration water lost by clays upon combustion. This is indicated by the ash coefficient which also incorporates an estimation of the proportion of clays in the mineral matter. The Parr formula has been widely criticized because it assumes that essentially all of the sulphur is present in the pyritic form. This assumption is especially in error for the high sulphur bituminous coals of New Zealand. For this reason the modified Parr formula is more suited than the Parr formula for New Zealand coals. Unlike most US coals many New Zealand coals contain significant amounts of carbonate. Here, the BFC formula is appropriate provided sulphur is negligible. The KMC formula is the best general formula for New Zealand bituminous coal since it directly accounts for pyritic sulphur, carbonate as well as the sometimes appreciable sulphate fixation in these coal ashes.

2.8.2 Measures of Specific Inorganic Entities

(i) petrographic techniques

AS 2856 neatly lists some diagnostic features of common minerals that are useful to identify minerals during examination of coal under the reflected light microscope. If oil immersion objectives are used quartz and some feldspars are often invisible (Kemezys and Taylor, 1964). Under oil immersion$_{(RI\ =1.515)}$ in plane polarized light, calcite and dolomite becomes black twice when rotated through 180°, ankerite becomes black just once, and siderite remains visible. In practice, ferroan dolomite is more common than true dolomite ($CaMg(CO_3)_2$) and

ankerite ($CaFe(CO_3)_2$) is difficult to distinguish. Siderite may exhibit a brownish tinge and many carbonates display twinning. Two different sulphide minerals can be distinguished. Pyrite exhibits a variable morphology and frequently displays a gold tint whereas marcasite can be identified by a whiter colour and cockscomb (sometimes radial) morphology when examined in slightly crossed polars. Clay minerals are commonly seen under the microscope except when finely dispersed. Clays can be white or black but are usually brown. They are often finely crystalline, and occur as discrete particles, lenses, or blebs. The liptinite maceral fluorinite as described by Teichmüller (1974) is easily mistaken for small, black, round clay aggregates in reflected light. Bituminite may also be mistaken for clay but like fluorinite can be distinguished by its fluorescence. Clay readily adsorbs cationic dyes and is easily differentiated from huminite (Quick and Kneller, 1987) as well as weathered vitrinite (Lowenhaupt and Gray, 1980) which are stained the complementary colour of the dye.

The precision of petrographic based measurements of mineral matter can be no better than that ascribed to maceral abundance (section 5.4). Furthermore, because of problems associated with the recognition of quartz, clays, and small dispersed minerals, as well as plucking of mineral grains from the polished surface (Davis, 1984), the potential bias in this kind of mineral analysis is high. For these reasons many petrographers prefer to calculate a volume percent mineral matter. A variety of formulae are recommended for this purpose in the ISO (7404/3-1984 E), AS (2856-86), and ASTM (D2799-86) standards.

(ii) determination of carbonates

The amount of carbonate minerals present in coal is commonly determined by digestion with HCl and the amount of CO_2 evolved is determined gravimetrically; CO_2 is proportional to the amount of carbonate present. This technique is only useful for bituminous and higher rank coals since low rank coals yield CO_2 from decomposition of carboxyl or carboxylate groups (Burns *et al.*, 1962). Carbonate species can be differentiated by XRD of low temperature

ash or by microscopic examination of polished specimens (Kemezys and Taylor, 1964).

(iii) X-ray diffraction

X-ray diffraction of low temperature ash is used to identify minerals in coal. With the use of prepared calibration standards, a CaF_2 internal standard, and a rotating sample mount, a semi-quantitative mineralogical analysis (±10%) is claimed (Jenkins and Walker, 1978). Good precision has been reported for pyrite, quartz and calcite but quantification of clay minerals is difficult. Furthermore, phases present in traces less than 5% are often difficult to distinguish within the background signal of low temperature coal ashes (Suhr and Gong, 1983).

(iv) inorganic elemental analysis

ASTM method D-2795 and D-4326 describes some procedures used to determine the major elements in coal ash. A prepared sample of ash is dissolved either directly or after fusion, and the amount of each element in solution is determined by a combination of spectrophotometry, chelatometric titration and flame photometry. Table 2.11 compares the relative precision reported for the two methods. Appropriate methods to determine sulphur in coal ash include the modified British standard method, the Eschka method, and the sodium carbonate fusion method (ASTM D-1757).

TABLE 2.11
COMPARISON OF REPRODUCIBILITY LIMITS OF TWO STANDARD METHODS USED TO MEASURE ELEMENTAL COMPOSITION OF ASH

Element	reproducibility (% absolute) ASTM D-2795 (titration, absorption & emission spectrometry)	reproducibility (% absolute) ASTM D-4326 X-ray fluorescence
SiO_2	2.0	2.04
Al_2O_3	2.0	1.45
Fe_2O_3	0.7	1.02
CaO	0.4	0.53
MgO	0.5	0.55
Na_2O	0.3	0.60
K_2O	0.3	0.16
P_2O_5	0.15	0.16
TiO_2	0.25	0.13

(v) normative analysis

N. Newman (1988) calculated mineral assemblages of west coast, South Island, New Zealand coals from elemental analysis of high temperature ash. The method requires a knowledge of the mineral occurrences in the coal since a single element may occur in more than one mineral species. Suhr and Gong (1983) also used normative analysis calculations. After quantification of kaolinite by infrared analysis and determination of quartz, pyrite, siderite and dolomite by X-ray diffraction the amount of other phases such as montmorillonite and mixed layer clays were estimated using normative analysis techniques.

2.9 COAL WEATHERING

Weathering or "natural oxidation" can significantly reduce coking quality, flotation recovery, and specific energy of coals. Although weathering usually has a negative effect on the technological behaviour of coal, the reduced agglomeration of weathered coal may be beneficial for the production of activated carbons, and efficient operation of fluidized bed combusters or gasifiers. Because of these effects on industrial behaviour weathering has been the focus of many studies. Before reviewing such studies it is important to recognize that coal can be weathered due to a variety of natural and man-made stresses. Retreat mining, stockpiling, and transportation may all contribute to weathering. Coal may also be weathered *insitu*, either at the outcrop or in seams that are close to the surface (particularly in faulted areas). In consideration of the many factors which may influence weathering, it is not surprising that Larsen *et al.*, (1986) identified three different mechanisms responsible for loss of coking properties upon exposure to the atmosphere. Thus like coal rank, coal grade and coal type, no single weathering parameter is likely to provide a measure of the whole range of weathering changes.

Because of the uncertain history of weathering in the natural environment weathering is often simulated by artificial oxidation in the laboratory. Unfortunately the results from laboratory oxidation studies may not be applicable to the studies of coal weathering. Nonetheless, because of the difficulties

associated with studies of weathering this review necessarily draws upon such studies. Lowenhaupt and Gray (1980) suggest that the term weathering be reserved to distinguish natural oxidation processes; this convention is followed in this thesis.

2.10 DETECTION AND MEASUREMENT OF WEATHERING

Few analytical techniques are capable *a-priori* of quantifying natural oxidation; most techniques require "fresh" coal for comparison. Significantly weathered zones in working coal mines can be identified based on lowered crucible swelling values. Weathering can sometimes be detected based on elevated moisture content or diminished calorific value. Subtle weathering of bituminous coal is best detected by lowered Gieseler fluidity. Unfortunately, all of these methods require prior knowledge of the character of the coal in a fresh condition and thus are useful only to detect rather than quantify oxidation.

Reviews of methods used to detect and sometimes measure the extent of coal weathering have been written by Gray *et al.*, (1976), Anderson and Hamza (1982), Gray and Lowenhaupt (1989), Huggins and Huffman (1989), and Davidson (1990). Some of the more common methods are discussed in the following sections.

2.10.1 Petrographic Methods

Table 2.10 lists some petrographic features that can indicate weathered coal upon microscopic examination. The most common microscopic feature of weathered bituminous coal is the occurrence of abundant cracks in vitrinite which, if accompanied by darkened discolouration rims, is certain evidence of weathered coal. In addition to those features listed in Table 2.12, microbrecciation (not related to tectonic deformation) and a large amount of minus 5 micron material in polished particle mounts may also indicate weathered coal. However rank and type also influence the development of fines (Gray, 1982). Fines increase with coal rank to a maximum at the low volatile stage of coalification. Durains produce fewer fines than vitrains and fusains whereas clarains have intermediate characteristics. Increased fines can also result from a

changing sample preparation method. Finally, severely weathered coal particles may also be identified due to a change in polishing hardness and consequent higher relief (J. Newman, 1990 pers. comm.).

TABLE 2.12

MICROSCOPIC FEATURES THAT INDICATE WEATHERED COAL

1.	The vitrinite particles display cracking unrelated to cleat, preparation, or "pseudovitrinite" (slitted telocollinite) causing fines to develop.
2.	A slightly darker discolouration may occur at both grain margins, and along cracks in vitrinite and inertinite.
3.	The edges of the vitrinite may appear rounded
4.	Sulphide minerals may show alteration, clay minerals may swell, cleat and cracks may be coated with secondary minerals.
5.	These conditions may exist simultaneously or in combination but any one is an indicator of weathered coal.

(modified from Lowenhaupt and Gray, 1980 p.67)

It is generally accepted that weathering causes dark oxidation rims in many coals due to the formation of humic acids. These dark rims are present on edges, pores and cracks of particles comprised of vitrinite or inertinite. As noted by Crelling *et al.*, (1979) these features are "best developed in strongly weathered coal" and are not expressed in the initial stages of weathering. However, dark weathering rims are a characteristic of bituminous coals and have not been observed in lower rank coals. Indeed, Marchioni (1983) measured a 6 to 20% relative increase in reflectance in two weathered outcrop samples (subA to hvCb rank). Marchioni suggests that these higher reflectance values were causes by elevated temperatures and low precipitation at the outcrop site. Supporting this is the microscopic observation of bright, high-relief oxidation rims that border thermally oxidized coal particles (Prado, 1977).

In addition to standard microscopic examination of coal, a staining technique may be used to more precisely quantify weathering of high volatile bituminous coals. The technique as introduced by Gray *et al.*, (1976) involves immersion of a polished particle mount in an aqueous solution of KOH and the

cationic dye, Safranin O. Since fresh coals lower than hvBb rank may stain or even dissolve upon immersion in alkali the technique was modified to extend its application to include subB through mvb rank coals (Marchioni, 1983, Gray and Lowenhaupt, 1989). The modified method requires an initial immersion of the polished pellet in an aqueous solution of KOH for ten minutes. Medium and low volatile rank coals may require longer immersion times but etching is not required for hvCb and subB rank coals. This is followed by immersion in a saturated solution of Safranin O in alcohol. The specimen is then rinsed and blown dry. Under the microscope oxidized particles of vitrinite appear green and the volume percent of oxidized components are determined by point counting. The intensity of staining is proportional to the degree of weathering. Petrographic staining is reported to be sensitive to insitu weathering (Marchioni, 1983, Axelson *et al.*, 1987) but does not appear useful to detect deterioration due to sample storage (Quick *et al.*, 1989).

McHugh *et al.*, (1991) showed that fluorometric analysis can be used to detect and quantify weathering of bituminous coals. They showed that open-cast coals display consistently lower fluorescence intensity values than equivalent rank deep mined coals. Their data strongly suggests that coal properties vary according to present depth of burial. It is significant that only Gieseler fluidity and dilation showed similar sensitivity to these changes. Because fluorescence intensity of pristine (deep mined) coals varies with rank and fluorometric analysis is not yet standardized this method requires a rank/fluorescence calibration for fresh coals to be established for each laboratory. Furthermore the method was developed based on a calibration set of Permian coals devoid of alginite or marine influence. Consequently it is unlikely that this approach will be useful for New Zealand bituminous coals which sometimes exhibit considerable isorank variation of fluorescence intensity (Quick and Moore, 1991), are often high in sulphur, and for which fresh, deep mined samples that cover the entire bituminous range would be difficult to procure.

Besides loss of fluorescence intensity weathering also changes the fluorescence alteration response of bituminous coal. Death *et al.*, (1991) have shown that the initial rapid loss of fluorescence intensity upon irradiation (characteristic of fresh bituminous coal) was diminished by weathering. Although Death and his co-workers used a macroscopic system their results agree with microscopic measurements by Quick *et al.*, (1989) who observed that weathering diminished the initial loss of fluorescence intensity upon irradiation.

2.10.2 Alkali Extraction

An alkali-extraction method developed at US Steel Co., has been suggested to be useful to quantify weathering of bituminous metallurgical coals and coal blends (Lowenhaupt and Gray, 1980). One gram of coal is boiled for 2 to 3 minutes with 100 ml of a 1 N solution of NaOH, and the transmittance at 520 nm of the filtrate passing a No. 40 and No. 42 Whatman filter paper is recorded. If the coal is sufficiently weathered to contain humic acids these acids are leached by the caustic solution and discolour the filtrate. Thus the transmittance of the filtrate decreases as the amount of weathering increases. Feedstocks that report less than 80% transmission are rejected for use by US Steel.

Gray and Lowenhaupt (1989) state that the alkali extraction test has a detection limit of about 3 percent weathered coal; coals containing less than 3% weathered coal do not appreciably alter the transmission value from 100 percent. The good sensitivity of the test as well as its speed and simplicity supports their contention (p.272) that "it is an inexpensive and efficient method of avoiding serious problems in coal preparation, cokemaking, and sales". The alkali extraction test is limited to monitoring bituminous coking coals because low rank coals are readily soluble in alkali even when fresh.

Quick *et al.*, (1989) found that the alkali extraction test is relatively insensitive to detect sample deterioration due to sample storage. However unpublished data (D. Glick pers. comm.) shows that alkali solubility of bituminous coal may increase as a consequence of storage. Examination of Glick's data (not shown here) indicate that generation of alkali soluble humic

acids requires both moisture and oxygen availability. Both of these conditions are met in the natural environment.

2.10.3 Indirect Methods

Indirect methods to detect weathering require knowledge of the character of fresh coal. Because weathering diminishes crucible swelling, Gieseler fluidity, and Audibert-Arnu dilation, these methods are sometimes used to detect weathering. Other changes include an increase in oxygen content, inherent moisture, carboxylate cation, CO_X gas upon pyrolysis, and hydrophilic components. Loss of hydrogen and lowered calorific values have also been reported.

(i) moisture

Weathering results in higher moisture contents (Mathews and Bustin, 1984, Fredericks *et al.*, 1983, Ingram and Rimstidt, 1984). Because determination of moisture is fast and inexpensive Fredericks *et al.*, (1983) suggest that determination of moisture may be the most practical way to delineate weathered zones in working coal mines.

(ii) mineral content

Although weathering may increase the inorganic content of coals (Mathews and Bustin, 1984, Fredericks *et al.*, 1983), weathered coals do not always have elevated mineral contents (Ingram and Rimstidt, 1984, Newman, 1989a). The presence of bassinite in the low temperature ash of weakly pyritic weathered coals has been observed by Pearson and Kwong (1979) using XRD and later confirmed by Painter *et al.*, (1980) using FTIR.

Huggins *et al.*, (1983) used SEM with automated image analysis, and other spectrographic techniques to identify and quantify minerals in coal. They found no calcium sulphate in severely weathered oxidized bituminous coal but significant calcium present as carboxylates on the weathered coal particles. Their results suggest that calcium sulphates (such as bassinite) found in the low temperature ash of oxidized bituminous coals are artifacts of the ashing process like those described by Miller *et al.*, (1979) for low rank coals. Thus, as proposed

by Pearson and Kwong (1979), the presence of calcium sulphates in the low temperature ash of weakly pyritic bituminous coal is grounds to suspect significant weathering. Furthermore, Huggins and his co-workers's observations might explain the sometimes elevated high temperature ash contents of weathered coals since fixation of Ca from groundwater as carboxylate salts in the coal would increase ash. Alternately, Newman (1989a) observed lower calcium contents in weathered (outcrop) low rank coal compared to equivalent cored coal. In this instance the weathering was suggested to leach out calcium. This conclusion is supported by the work of Ward (1991) who found leaching with water effective in the removal of significant amount of calcium from low rank coals from Thailand. Ward noted that the leachate was acidic and attributed the removal of calcium to the action of soluble humic acids.

(iii) thermoplastic properties

Severe *insitu* weathering inevitably lowers the crucible swelling index of bituminous coals (Mathews and Bustin, 1984, Gray *et al.*, 1976, Axelson *et al.*, 1987, Marchioni, 1983, Boyapati *et al.*, 1984) and thus is a useful tool to delineate weathered zones in working coal mines. However it is not sensitive to mild weathering such as that which occurs in the stockpile (Boyapati *et al.*, 1984).

Loss of Gieseler fluidity is one of the most sensitive methods to detect weathering (Gray *et al.*, 1976, Boyapati *et al.*, 1984, Marchioni, 1983). The very sensitivity of the method is perhaps its biggest drawback since Gieseler fluidity rapidly declines during laboratory storage unless samples are stored at low temperatures (Boyapati *et al.*, 1984). Indeed, loss of Gieseler fluidity due to laboratory storage can occur long before any detectable change of the ultimate, or proximate analysis is observed (Moxon *et al.*, 1987).

(iv) volatile matter

In a review of methods useful to detect coal weathering Marchioni (1983 p.236) concluded that "changes in coal volatile matter with oxidation cannot be accurately predicted." Nonetheless, higher volatile matter contents are commonly reported for weathered coal (Gray *et al.*, 1976, Crelling *et al.*, 1979, Fredericks *et*

al., 1983, Marchioni, 1983, Mathews and Bustin, 1984, Axelson *et al.*, 1987). Furthermore, the suggestion made by Wellman (1952) that the composition of volatile matter may change upon weathering is supported by Mathews and Bustin (1984) who found the pyrolysis gases of weathered coal contain more CO_2, CO and less CH_4 than equivalent fresh coals. A clear demonstration of the difference between weathering and laboratory oxidation is the observation that laboratory oxidation at elevated temperatures (92°C) decreases volatile matter (Benedict and Berry, 1964) whereas weathering usually leads to higher volatile matter yields.

The difficulty in the use of volatile matter to detect weathering is two-fold. Firstly, change in volatile matter yield can occur solely due to type variation. Also important is the potential dynamic nature of volatile matter change due to weathering. This may be particularly true for New Zealand coals since Suggate (1959) surmised that for some bituminous New Zealand coals volatile matter initially decreased and then increased upon weathering. Although the reason for the apparent anomalous behaviour of these coals is not understood, the possible dynamic variation of volatile matter yield upon progressive weathering further attests to the unreliability of volatile matter yield to detect weathering.

(v) elemental composition

Severely weathered coals can be identified on H/C - O/C (van Krevelen) diagrams since weathering decreases the hydrogen content and increases the oxygen content of coal (Gray *et al.*, 1976, Fredericks *et al.*, 1983, Marchioni, 1983, Mathews and Bustin, 1984). However, the technique is only useful to detect severely oxidized coal and the extent of weathering cannot be directly evaluated due to variation of maceral content and composition.

A number of authors have evaluated the use of carbon vs hydrogen charts to predict the properties of fresh coal from weathered coals (Suggate 1959, Francis 1961, Chandra 1962). Since weathering displaces the position of these coals on the plot in a predictable manner, extrapolation along the oxidation path back to the "mean ulmin" line (i.e., average type line) should reveal the composition of the fresh coal. However Suggate (1959) noted that this method

necessarily assumes coals of "average type". Consequently the results of this procedure cannot be considered conclusive.

(vi) reflectance

Vitrinite reflectance is insensitive to weathering (Marchioni, 1983). In severely weathered coals reflectance is sometimes slightly decreased or increased but these changes are small and reliable values can usually be obtained if measurement of obviously weathered rims, pits and cracks are avoided (Chandra 1962, Pearson and Kwong, 1979, Ingram and Rimstidt, 1984, Mathews and Bustin 1984, Axelson *et al.*, 1987).

(vii) specific energy

Specific energy of coal almost always decreases upon weathering (Fredericks *et al.*, 1983). However, at hvCb and subbituminous rank there is some evidence for a dynamic variation of specific energy upon weathering. Sharp (1986) acknowledges the work of Liotta to explain the initial decline and subsequent rise of specific energy she observed upon laboratory storage of subbituminous coal. A similar variation was observed by Rees *et al.*, (1961) on stockpiled hvCb rank coal. Liotta *et al.*, (1983) found that for artificially weathered coal (a small, crushed sample spread on the ground) oxygen was incorporated in aliphatic ether linkages. Thus the initial decline of specific energy is explained largely as the outcome of loss of aliphatic hydrogen and incorporation of nonalkylateable oxygen. Although no chemical evidence is provided Sharp (1986) states that the subsequent rise in specific energy is due to a loss of carboxyl functionalities found naturally in the coal. The net loss of these oxygen-containing constituents increases specific energy.

2.11 SUMMARY

The characteristics of a coal are determined by geologically constrained processes called coalification, peatification, mineralisation and weathering. Each of these processes involve multiple mechanisms. Consequently, no single parameter can uniquely define either rank, type, grade, or the extent of weathering. Fortunately, all of these processes vary within naturally constrained

limits. Consequently it is suggested that fundamental characterization of coal is possible by selection of a few properties that vary largely in response to these universally shared processes.

CHAPTER THREE
CARBONIZATION

This chapter reviews the influence of coal rank, type, grade and weathering on the carbonization behaviour of coal. It begins with a limited description of the coal to coke transformation in a commercial coking battery and the behaviour of coke in the blast furnace. These sections provide a background for later discussion of the influence of coal properties on carbonization behaviour. The chapter concludes with a discussion of how carbon microtextures relate to the quality of the carbon product.

3.1 THE PRODUCTION OF COKE

Coke is produced in rectangular ovens which are 4 to 8 m high, 12 to 18 m long and .4 to .6 m wide. The ovens are lined with silica bricks (fired to cristobalite) which are maintained at about 1300 °C and separated from adjacent ovens by flues where gas is burned to heat the bricks. Up to one hundred or more adjacent ovens constitute a coking battery. Fifteen to thirty tons of coal are charged through holes in the top of the oven and levelled. Preheated charges, briquettes or stamped charges allow greater amounts of inexpensive high volatile bituminous rank coal to be included in the blend. Volatiles collect at the top of the oven during coking and escape through collector mains; by-product gas and tar are recovered. After 12 to 18 hours coking is complete; the side doors of the oven are removed and the coke is pushed out of the oven into a quench car where it is cooled with water or dry quenched.

Carbonization proceeds from the sides of the coke oven inwards and is marked by the migration of a plastic layer towards the centre of the charge (Gray 1989). The coal to coke transformation occurs in this plastic layer which is about 2 to 5 cm thick. The temperature of the plastic layer is in the region of 325 to 600 °C. The cold side of the plastic layer is relatively impermeable so most of the volatile matter escapes along the hot side through the solidified semi-coke nearer the oven wall.

After solidification the semi-coke mass continues to lose volatile matter and shrinks. This shrinkage causes cracks to develop and weakens the coke. If solidification is extended to a higher temperature more shrinkage is accommodated in the plastic state and fracturing due to contraction in the solid state is minimized. This is why higher rank coals (with higher solidification temperatures) generally produce stronger cokes. Fissuring is also reduced where inert carbons (inertinite macerals, coke breeze) are added to the blend since these constituents contract less than fused constituents and reduce the stress due to shrinkage in the solid state.

3.2 THE BEHAVIOUR OF COKE IN THE BLAST FURNACE

The value of coal selected for metallurgical coke making depends on the contribution it makes to the quality of the coke product which is ultimately a function of the behaviour of the coke in a blast furnace. Thus a limited discussion of the behaviour of coke in the blast furnace is provided since it leads to an understanding of the basis of tests used to assess coke quality. A more comprehensive discussion is provided by Nakamura *et al.*, (1978).

Coke serves three purposes in the blast furnace: (1) it serves as fuel, (2) it is used as a reducing agent, and (3) it supports the burden to allow uniform flow of the reducing gases through the charge. Figure 3.1 shows a schematic cross section of a blast furnace and where coke degradation affects efficient blast furnace operation. In the upper part of the blast furnace the burden remains at around 950 °C and the coke is little changed. As the burden enters the fusion zone the coke reacts with CO_2 and moisture and about 25 to 30% of the coke is consumed as it descends towards the tuyeres. Within the fusion zone (about 1300 °C) the coke layers serve as gas distribution channels. Below the fusion zone coke remains the only solid phase through which liquid iron and slag percolate down towards the hearth; the temperature in this region increases up to about 1600 °C in the lower part of the furnace. At the level of the tuyeres most of the remaining coke is burned at temperatures above 2000 °C and CO is produced. Of particular importance is the permeability of slits (coke layers) in the fusion

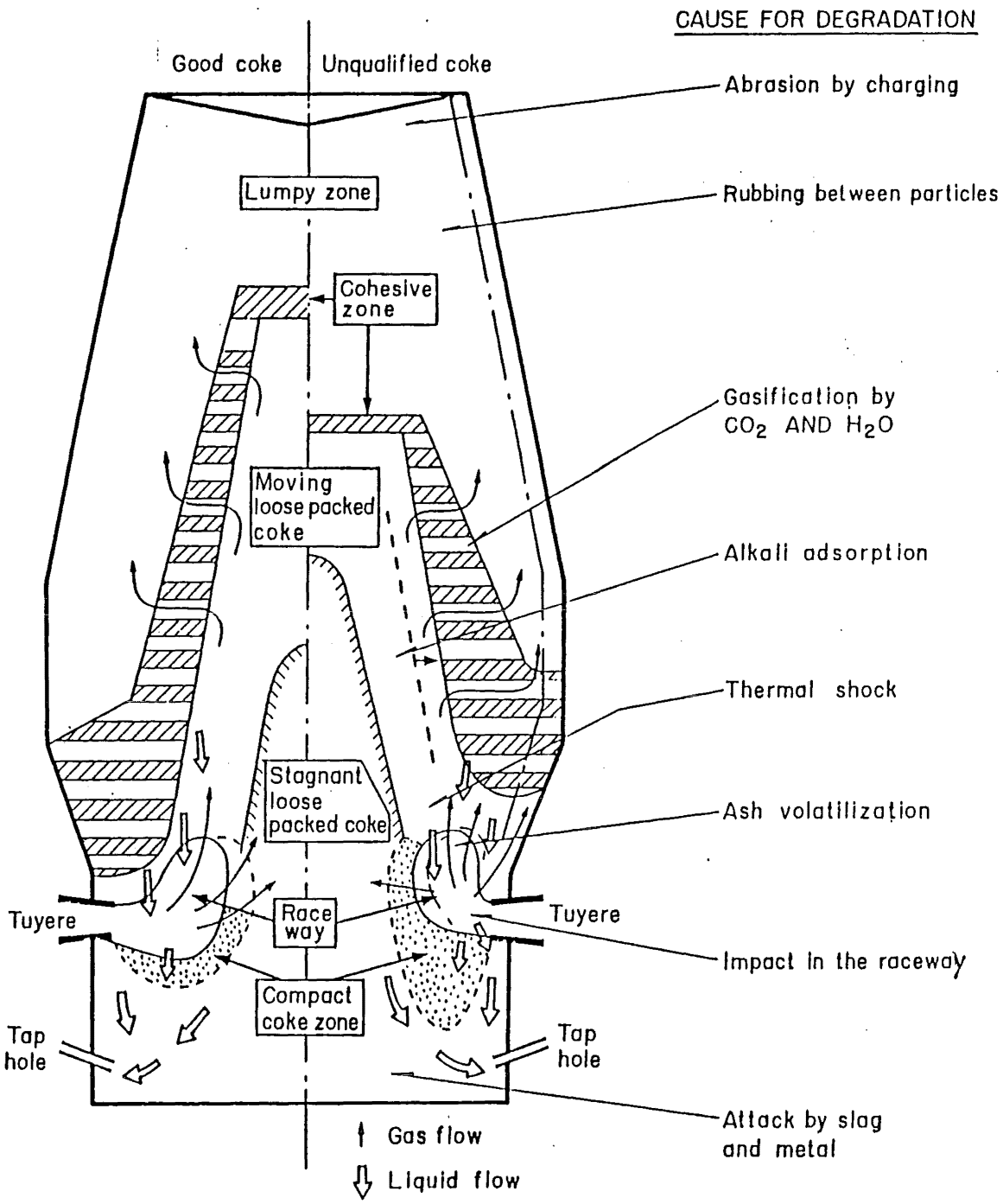

Figure 3.1 Schematic cross section of a blast furnace showing the change of the cohesive zone and raceway due to coke quality. From Goscinski *et al.*, (1985), after Ishikawa *et al.*, (1983).

zone, and permeability in the raceway (combustion zone adjacent to the tuyeres). If permeability is reduced due to the generation of fines, even gas flow is disrupted and blast furnace efficiency declines (Ishikawa *et al.*, 1983). Thus the maintenance of good coke strength after carbon solution loss to avoid the production of fine coke is an important coke quality parameter. Cold strength

and abrasion resistance remain important since these parameters relate to coke performance in the upper part of the furnace.

Injection of gas, oil, tar, or coal through the tuyeres provides additional reducing gases and lowers the requirement for coke as a reducing agent and fuel but increases the importance of good coke strength after reaction to maintain permeability (Peacey and Davenport, 1979). Planned increases in the pulverized coal injection rate in Japan will reduce the amount of coke in the blast furnace and necessitate an increase in the coke strength after reaction to maintain uniform flow of the reducing gases through the burden. To account for this new demand on coke strength after reaction, Tateoka (1990) suggests that a new measure of coke strength after more extensive solution loss and extended residence time will need to be developed.

3.3 COAL PROPERTIES AND CARBONIZATION

3.3.1 Rank and Carbonization

Industrial carbons may be broadly divided into two classes based on their structural style. Graphitizable carbons are made from carbonaceous materials that pass through a plastic phase upon pyrolysis whereas non-graphitizable carbons are made from feedstocks that do not fuse upon pyrolysis (Edwards, 1989). With rare exceptions, the ability of coal to fuse into a coherent mass upon pyrolysis is a defining characteristic of bituminous rank (AS-2096, ASTM-D388).

The thermoplastic behaviour of coal increases to a maximum value and then decreases as coal rank advances through the bituminous rank stages. The progressive increase in thermoplastic behaviour results from two coalification processes: catagenetic loss of oxygen and the generation of bitumen. Upon pyrolysis, oxygen in coal may abstract hydrogen or form crosslinks. Thus catagenetic loss of oxygen through the early stages of bituminous rank enhances fluidity since more hydrogen is available to stabilize free radicals and any cross-linking due to oxygen is diminished. Along with this loss of oxygen, low molecular weight extractable constituents form in response to coalification (bituminisation). During pyrolysis these constituents serve as both hydrogen donors and, more

importantly, transfer vehicles that shuttle hydrogen from the aromatic network to stabilize free radicals; this delays eventual polymerization reactions and allows the development of an isotropic plastic phase (Neavel 1982). In addition, these constituents may also temporarily stabilize free radicals and enhance molecular mobility thereby improving the chances for eventual contact with hydrogen (Grint *et al.*,1985).

The latter half of the bituminous stage of coalification is marked by a progressive decline of thermoplastic character. Concurrently, both the temperature of maximum fluidity and the solidification temperature increase. The loss of thermoplasticity is due to late catagenetic liberation of hydrogen, and eventual incorporation of the mobile phase into the aromatic network. The loss of hydrogen increases the tendency of free radicals to form crosslinks upon pyrolysis which promote polymerization and diminish plasticity. The concurrent increase of solidification temperature suggests that the solvating mobile phase becomes more thermally stable and the aromatic network becomes more strongly crosslinked with advancing rank. This explains, in part, why medium and low volatile bituminous rank coals produce larger anisotropic carbon forms (flow and ribbon microtextures) than high volatile bituminous coals (Rhoades *et al.*, 1981, Patrick *et al.*, 1973, 1979); the higher thermal stability allows further breakdown of the aromatic network and more time for alignment of the aromatic fragments into ordered carbon structures. The importance of high solidification temperatures to maintenance of stability is also suggested by the work of Benedict *et al.*, (1968b) at Bethlehem Steel. This research group observed that, where blends contain more than ~23% lvb rank coal, coke strength is essentially that of the lvb rank coal alone.

3.3.2 Type and Carbonization

Accurate differentiation of inert and reactive constituents in coals selected for coke making is important since there is an optimum proportion of inert constituents for a given coal blend. Inerts function to reduce fissuring (Loison *et al.*, 1989), thicken pore walls, and depress the development of large vacuoles

(Cudmore, 1984). The optimum amount of inerts varies, according to the capacity of the thermoplastic phase to cement the inert components into a coherent mass. If this capacity is exceeded cold strength (stability) declines and the coke will abrade easily. Cold strength also declines where the optimum inert content is not met. In these instances the coke will crush more easily. Schapiro *et al.*, (1961) observed that the optimum amount of inerts varied with vitrinite reflectance. Their relationship is shown in Figure 3.2. The shape of the curve shown in Figure 3.2 can be compared to the thermoplastic behaviour of coal (excluding weathered or inertinite rich coals) through these ranks which is schematically illustrated in Figure 3.3. Comparison of the two figures suggests that the optimum inert content increases with the thermoplasticity of coal.

The proportion of potentially reactive or inert constituents in raw coals is usually estimated from the maceral composition. Following earlier Russian studies, workers at US Steel developed a coke strength prediction method based on petrographic criteria (Schapiro *et al.*, 1961, Schapiro and Gray, 1964). The failure of the US Steel coke strength prediction method to accurately predict the cold-strength of cokes made from coals with elevated inertinite contents has been attributed to inadequate methods to differentiate reactive and inert constituents belonging to the inertinite group. Diessel and Bailey (1989) and Pearson (1984, *in* Price *et al.*, 1988) have published improved petrographic methods to distinguish reactive inertinite. Although the provincial behaviour of inertinite macerals is widely acknowledged, industrial characterization methods that account for provincial variation of vitrinite group macerals are less common. An exception is the recognition of a relatively infusible constituent, pseudovitrinite, in the coke strength prediction method used at Bethlehem Steel (Benedict *et al.*, 1968b). There is no corresponding petrographic method that directly accounts for relatively more fusible vitrinite in carbonization feedstocks. The reason for this may relate to the scarcity of perhydrous vitric coals rather than lack of recognition of type variation within the vitrinite group. Gray (1989) notes that larger mosaic carbons are produced in coals with high Gieseler fluidity compared to coals of

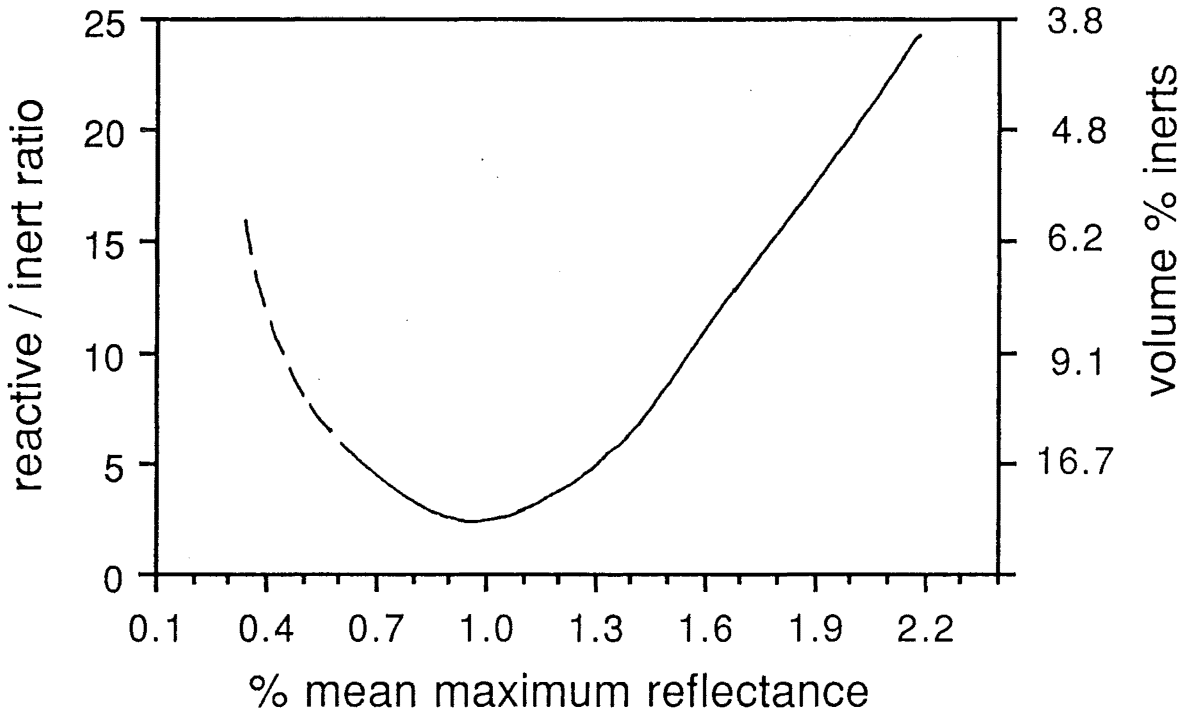

Figure 3.2 Diagram illustrating how the optimum inert content of coal varies with reflectance of component vitrinites (modified from Schapiro *et al.*, 1961).

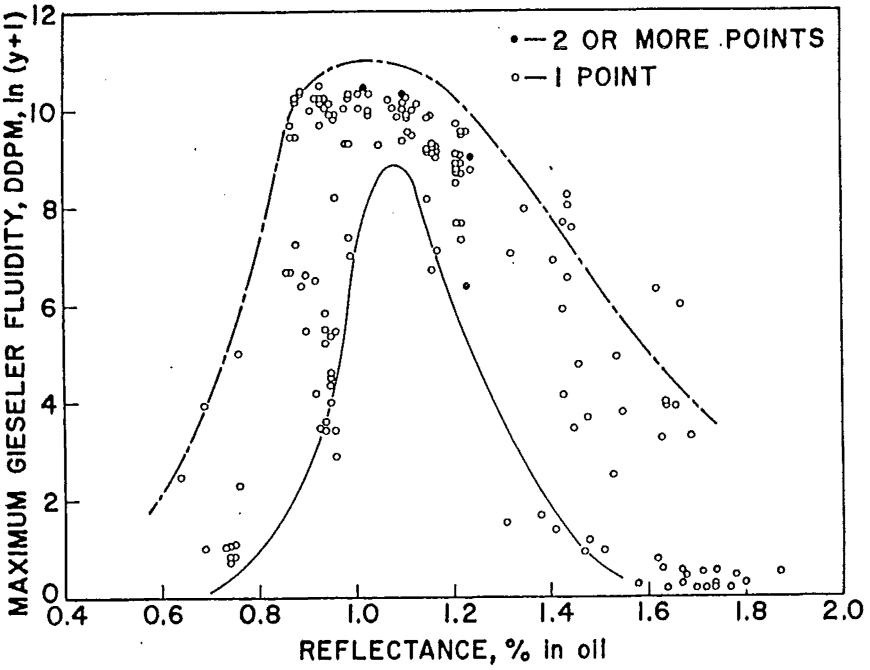

Figure 3.3 Schematic illustration showing how Gieseler fluidity varies with vitrinite reflectance (from Schapiro and Gray, 1964).

lower fluidity and equivalent reflectance. Compositional variation within the vitrinite group has long been recognized; structured vitrinite (telocollinite, vitrinite A) is relatively hydrogen poor whereas unstructured vitrinite (desmocollinite, vitrinite B) is relatively hydrogen rich (Brown *et al.*, 1964). The sometimes high Gieseler fluidity and volatile matter of New Zealand bituminous coals, which are often enriched in desmocollinite (Brown *et al.*, 1964, Newman 1985, 1989b, Lavill, 1987) suggests that type variation within the vitrinite group should be considered for accurate evaluation of New Zealand coal for industrial carbonization.

The work of Harrison *et al.*, (1964) also suggests that variation in vitrinite type may be important for petrographic methods to predict coke strength. Harrison and his co-workers found that the US Steel method underestimated the coke strength of coke made in pilot coke ovens (700 lb charges) using Illinois coals. Since Illinois coals lack abundant inertinite the failure of the original US Steel method may have been due to variation in the nature of the vitrinite.

Cook and Edwards (1971) examined cokes made in the laboratory from blends of vitric New Zealand coal (Stockton and Paparoa) and inertic Australian coal (Bulli). They observed that the optimum vitrinite content for blends containing these New Zealand coals were below those predicted by the US Steel method. Although the thermoplastic nature of much of the "inertinite" in the Bulli coal may have been a contributing factor to the lack of correspondence with the US Steel prediction method, their conclusion is consistent with the notion that variation within the vitrinite group may influence coking behaviour.

Type variation within the vitrinite group can be measured by counting the proportion of recognizable submacerals that comprise the vitrinite group. Although industrially significant variation within the vitrinite group is widely acknowledged these differences are difficult to measure with precision. For example, Newman (1985) has shown that substantial variation of volatile matter may occur where vitrinite submaceral proportions are similar and both inertinite and exinite content is low. The subjective nature of maceral analysis may also

limit the use of petrographic data. For example, the ICCP does not recognize pseudovitrinite presumably because of poor repeatability in round robin exercises directed towards its identification in coal. Finally, the limited precision of point count analysis should be considered. Brown *et al.*, (1982) showed that the predicted ASTM stability of some coals will vary by more than ±5 points due to the inherent imprecision of point count analysis (see section 5.4).

Teichmüller and Teichmüller (1982) observe that many bituminous coals with high organic sulphur contents are perhydrous and display high thermoplasticity and low softening temperatures. Since the addition of sulphur to coal reduces fluidity (reviewed by Loison, *et al.*, 1963) their high fluidity must be a consequence of hydrogen enrichment rather than a direct effect of sulphur. Nonetheless, the presence of organic sulphur compounds may explain the lower thermal softening temperatures of sulphur rich coal. Sinninghe Damste *et al.*, (1989c) suggest that the sulphur bridges which protected the hydrogen rich, biogenic precursors from bacterial degradation may be preferentially broken upon catagenesis. They caution that the importance of this early breakdown requires knowledge of the different types of sulphur containing moieties. George *et al.*, (1991) developed a method for quantification of organic sulphur forms in coal. Their results show that as rank advances, organic sulphur in coal progressively changes from thermally labile aliphatic forms to more refractory aromatic sulphur forms. Programmed temperature pyrolysis studies (Boudou, 1990) support this idea and show that the peak temperature of H_2S generation increases with rank. The loss of hydrogen due to thermally induced change of aliphatic sulphides to aromatic forms (Fromm and Achert 1903, in Kelemen *et al.*, 1991) suggests a similar loss of hydrogen occurs upon catagenetic change of aliphatic sulphides to aromatic forms. If so, any positive correlation between organic sulphur and thermoplastic behaviour will progressively weaken as coal rank advances. However, where organic sulphides are abundant they are prone to break at low temperature thereby enhancing molecular mobility and depressing the softening temperature.

3.3.3 Grade and Carbonization

Nearly all of the inorganic constituents of coal are retained in the coke. These constituents reduce the amount of useful carbon since they dilute the coke and also consume carbon and flux required for their own reduction. Perch (1981) reviewed the effect of coke ash on blast furnace performance. Although the effect was variable a one percent increase in coke ash typically increased coke consumption by more than 2%.

The composition of the inorganic material in coal is also important. Essentially all the phosphorus in coke is detrimentally incorporated into the iron. Sodium and potassium vaporize in the lower part of the blast furnace and condense in the upper part leading to restrictions in gas flow and uneven burden descent. Inorganic composition is particularly important where high coke strength after reaction (CSR) is desired. The catalytic effect of alkalis on CO_2 gasification is demonstrated by the inclusion of a catalytic index term in various methods used to predict CSR (reviewed by Goscinski *et al.*, 1985, Valia, 1989). The negative effect of alkalis on coke strength after reaction may also be due to the intercalation of these cations within the aromatic structure. These molecular defects are preferential sites for solution loss of carbon.

Gill *et al.*, (1985) examined the effect of inorganic species on reactivity of a low ash New Zealand coking coal (Buller, Ro_{max} = 1.1%) by adding increments of specific inorganic oxides and minerals to the coal. The coal was carbonized and reacted with CO_2 at 1100 °C and 1600 °C. At 1100 °C SiO_2 and Al_2O_3 were essentially inert and the influence of the inorganic additions on coke reactivity increased in the order Si=Al<Mg<Fe<Ca<<Na<K. From 1100 to 1600 °C they observed that Si, Ca and Mg additions degraded the binder phase although extensive solution loss was also apparent from Na and K. An important conclusion of their study is that the standard coke strength after reaction test (1100 °C) may not provide an equitable measure of coke strength. Cokes with high CSR may degrade at higher temperatures below the fusion zone due to ash carbon reactions not measured at 1100 °C. They also observed isotropic carbon

growth in the laboratory cokes around FeS_2, K_2CO_3 and Na_2CO_3 mineral additions. Thus enhanced reactivity of coke due to alkalis might be partly due to the effect of these inorganics during coking rather than an entirely catalytic effect in the blast furnace.

3.3.4 Weathering and Carbonization

The adverse effects of natural weathering of coal on resulting coke quality are well known (Gray *et al.*, 1976, Crelling *et al.*, 1979, Boyapati *et al.*, 1984, Mikula and Mikhail, 1987, Gray and Lowenhaupt, 1989, Valia, 1990). They include, decreased cold coke strength, lower coke strength after reaction, green (smoky) coke oven pushes, lower bulk density of coke oven charges, diminished by-product tar recovery and quality, and poor handling characteristics.

Although the effects of weathering on coke making are well known, the mechanisms responsible for both weathering and the consequent deterioration of thermoplastic properties are not fully understood. Proposed weathering mechanisms include increased oxygen content, loss of donatable hydrogen, and increased cross link density. The rapid initial loss of Gieseler fluidity upon weathering is probably due to the loss of donatable hydrogen; swelling properties lost after mild oxidation can be renewed where hydrogen is restored to the coal but the mechanism for loss of swelling upon extended oxidation remains uncharacterised (Larsen *et al.*, 1986). Ignasiak *et al.*, (1974) concluded that hydroxyl oxygen introduced upon oxidation was responsible for the formation of crosslinks upon pyrolysis whereas Clemens *et al.*, (1989) found no evidence of increased crosslinking in semicokes made from oxidized coals and explain the loss of plasticity as a result of the loss of donatable hydrogen. Liotta *et al.*, (1983) found diminished crucible swelling upon weathering and attributed this loss to the formation of ether crosslinks in the parent coal. Although these (and many other) studies have contributed to our understanding of oxidation, what happens during weathering ("oxidation" in the natural environment) is less clear. Of particular significance are results presented by McHugh *et al.*, (1991) which suggest systematic rheological differences between surface and equivalent deep

mined coal. Thus what constitutes a fresh (non-weathered) coal is difficult to define since freshly mined coal from open cast operations may not be the same as freshly mined coal from underground workings.

Since severely weathered vitrinite remains inert upon coking (Benedict *et al.*, 1968, Thompson and Benedict, 1974, Rhoades *et al.*, 1981) petrographic based methods to predict coke strength will be in error unless severely weathered vitrinite can be quantified and designated as an inert component. Safranin O staining can be used to detect severely weathered coal but the technique is not sensitive to mild weathering and is not well suited to detect weathering above high volatile bituminous rank (Gray and Lowenhaupt, 1989). Fluorometric analysis shows diminished fluorescence intensity for even slightly weathered coal (McHugh *et al.*, 1991, Quick and Moore, 1991). Mitchell *et al.*, (1991) further investigated the use of fluorometric analysis to monitor coal degradation during storage and found that the technique is rank dependent; at 600 nm emission wavelength, loss of fluidity is matched by loss of fluorescence intensity only between 0.65 and 1.1% mean maximum reflectance. The use of longer wavelengths may extend the sensitive rank range of the test. Using 650-750 nm emission McHugh *et al.*, (1991) report good sensitivity at 1.15% random reflectance although loss of fluorescence intensity was less marked at 1.2% random reflectance and insignificant at 1.8% random reflectance.

Deliberate additions of finely ground, weathered coal to a blend might be beneficial where additional inerts are required to reduce fissuring (Valia, 1990). However, the presence of weathered coal in a feedstock will diminish coke strength after reaction. The loss of thermoplasticity due to weathering reduces the Gieseler fluid temperature range and thus the time interval that the coal is in a plastic state thereby hindering alignment of the aromatic fragments into ordered carbon structures. Since less ordered carbon forms are more reactive (Gray, 1989) coke strength after reaction will decline. Loss of coke strength after reaction has been observed to correlate with the loss of thermoplasticity that occurs during stockpile storage (Price *et al.*, 1988, Valia, 1990). Crelling *et al.*,

(1979) noted that even small amounts (7%) of weathered coal in a blend can double coke reactivity. Thus some weathered coal can probably be accommodated into a blend without greatly affecting coke stability but coke strength after reaction is likely to decline where even small amounts of weathered coal are present.

3.4 CARBON MICROTEXTURES

Microscopic examination of industrial and laboratory carbons has led to the recognition of different kinds of carbon texture that, under uniform carbonization conditions, vary according to the rank and type of the parent coal. Marsh and Smith (1978) briefly review some of the early studies of microscopic examination of industrial carbons and naturally carbonized coal. Patrick *et al.*, (1979) showed that the kind of microscopic texture that develops from vitrinite is related to the vitrinite reflectance of the parent coal. Where maximum vitrinite reflectance is less than about 0.8% the product semicokes display an isotropic texture. With increasing reflectance of the parent vitrinites, anisotropic mosaic textures are formed. The size of the individual circular anisotropic macrocrystallites that comprise the mosaics progressively increase as reflectance approaches about 1.1%. Through the medium volatile stage of coalification the individual mosaic units become elongated, usually in the direction of the bedding plane of the original vitrinite. Longer still are the ribbon or flow type carbon textures that appear above about 1.5% reflectance, which corresponds to the beginning of the low volatile stage of coalification. Vitrinite above about 1.9% reflectance is non-coking and, although the resulting carbons are anisotropic, they display inherited botanic structures.

The above discussion applies to typical vitrinite; some varieties of vitrinite tend to be non-coking and include pseudovitrinite (Benedict *et al.*, 1968), weathered vitrinite, and brecciated vitrinite (Gray 1982). Furthermore, Gray (1989) notes that larger size anisotropic carbons are produced from coal with high fluidity for a given level of vitrinite reflectance.

Presently, a variety of words are used to describe the optical microstructure of carbons. Coin (1987) provides a comparison of the diverse nomenclatures reported in the literature. The terms used in this thesis to describe the optical microtexture of carbons are described in section 4.4.2.

3.4.1 Origin of Carbon Microtexture

The development of anisotropic carbon microstructures in metallurgical coke is explained by Marsh (1982) as the result of mesophase solidification via polymeric cross-linking. The molecular structure of solid mesophase is inherited from its liquid crystal precursor. These liquid crystals form through homogeneous nucleation of large aromatic sheets that grow in an isotropic fluid phase by dehydrogenative polymerization reactions.

Although the development of an isotropic plastic phase is a necessary precondition for the formation of liquid crystals and mesophase, it does not guarantee that such structures will develop. For example, high volatile bituminous rank coals produce small sized anisotropic units despite relatively high fluidity. Marsh (1982) explains that the relatively abundant heteroatoms at these ranks initiate cross linking reactions within the isotropic melt at temperatures below those required for growth of liquid crystals and mesophase. Thus, only if fluidity can be maintained to higher temperatures will mesophase develop within the high volatile bituminous ranks. This explains the observation by Patrick *et al.*, (1973) who found that the development of optical anisotropy occurs at higher temperatures in low rank bituminous coals compared to higher rank bituminous coals.

Although the growth of liquid crystals and mesophase works well to explain the origin of optical microtexture from high and medium volatile bituminous rank vitrinite, this process does not fully explain the development of anisotropy in low volatile bituminous and higher rank coals. Patrick *et al.*, (1979) as well as Moreland *et al.*, (1988) reason that the growth of some flow type anisotropy and all "patterned-anthracitic" (called basic anisotropy in this thesis) must occur in

the solid state, without an isotropic fluid precursor. Although the nature of this transformation remains uncharacterised it probably involves increasing diameters and structural order of aromatic layer groups along the original bedding plane. Such solid state transformations also occur within solidified mesophase as carbonization temperatures continue to increase (Goodarzi and Murchison, 1972, Murchison, 1978). The fundamental difference between solid state transformations that occur within mesophase derived mosaics and those that occur within solid chars from high rank (or oxidized) non-graphitizing vitrinites is that the lateral growth of aromatic units within the mosaic units is restricted.

3.4.2 Carbon Microtexture and Reactivity

Carbon reactivity describes the tendency of a carbonaceous solid to lose mass upon exposure to gaseous CO_2, H_2O, O_2, or H_2 at elevated temperatures. The retention of coke strength after reaction with CO_2 is a desirable quality in metallurgical coke and is discussed in this section. Other gasification reactions also occur in the blast furnace, for example reaction with H_2O, but these processes are rarely examined. It is worth noting that reactivity is a desirable trait where the aim of carbonization is to produce activated carbons or gaseous pyrolysis products.

The intrinsic reactivity of a carbon solid depends on the accessible surface area, the molecular structure of the exposed carbons, and the presence of catalysts. Since the optical texture of carbons depends on the size and ordering of molecular structural units, optical texture provides an indication of reactivity. Catalytic effects due to inorganic constituents are discussed in section 3.3.3. The effect of porosity/surface area is not considered in this thesis.

Shapiro and Gray (1963) related the microtexture of metallurgical coke to the weight loss after reaction with CO_2. They found that cokes rich in isotropic carbons were very reactive whereas those with mosaic and lenticular carbons displayed lower reactivity; cokes rich in ribbon type carbons showed intermediate levels of reactivity. Fujita *et al.*, (1983) examined cokes before and after reaction

with CO_2 and found that inert derived components and isotropic carbons were most reactive and reactivity progressively declined with increasing size of the anisotropic units. Perhaps most significantly, they observed that the reactivity of each kind of carbon form was generally independent of the coke in which it occurred. Marsh and Kuo (1989) discuss the variation of reactivity with optical texture in terms of the carbon surface topochemistry. Reactivity is promoted by disordered carbons which present unpaired electrons or valence vacancies. Basal plane carbons are resistant to attack by CO_2 whereas carbon atoms on the edges of the aromatic layers and at defects or dislocations within the layers are more easily consumed. In the first instance solution loss proceeds along the c axis of the anisotropic units which leads to micro-cracks parallel to the basal plane of the aromatic layers. The random orientation of mosaic carbons prevents any preferred orientation of these cracks and good strength after reaction is observed in cokes with well developed mosaic texture. In the second instance defects due to heteroatoms, such as sulphur, within the sheets are likely sites of attack by CO_2. This may explain the negative effect of sulphur in empirically derived equations used to predict coke strength after reaction (Valia 1989).

The above discussion is largely based on studies of CO_2 reactivity near 1100 °C; what happens at higher temperatures in the blast furnace is probably different. Gill *et al.*, (1985) argue that at higher temperatures in the deadman (centre of the furnace below the fusion zone) coke-ash reactions predominate rather than solution loss due to reaction with CO_2. Reactivity with other gases is also not accounted for by the standard CSR test. Coin *et al.*, (1982) noted that in the oxidizing conditions of the raceway, coke made from "higher rank coal" [Port Kembla] resisted combustion. Despite high stability and CSR, this coke presented permeability problems near the raceway apparently due to the accumulation of fines. In this instance the accumulation of fines may have been a consequence of incomplete combustion of inertinite macerals like that reported for pulverized coal combustion (Sanyal, 1983). Alternately fines may have been generated due to physical weakening of the coke due to high temperature coke-ash reactions near

the raceway. Whatever the cause, these examples illustrate the difficulty of obtaining a single measure of coke quality that can be used to evaluate the merit of carbonization feedstocks.

CHAPTER FOUR
SAMPLES AND METHODS

This chapter begins with a description of the coal samples examined in this thesis and analytical methods used for their examination. Methods used to carbonize these coals and examine the resulting carbons are also described.

4.1 SAMPLES

Table 4.1 lists the number, type, origin, and storage conditions of the 165 samples used in this study. Figure 4.1 shows the location of the Greymouth, Pike River, Reefton, Garvey Creek, and Buller coalfields from which these coal samples originated. The coals examined here are Late Cretaceous or Eocene in age and occur in the Paparoa or Brunner coal measures respectively (Figure 4.2). General stratigraphic sections for the Greymouth and Pike River coalfields are shown in Figure 4.3. The late Cretaceous to early Tertiary setting of the west coast, South Island region (Figure 4.1) is discussed by Nathan *et al.*, (1986). Paparoa and Brunner coal measure depositional environments are discussed by Newman (1985). Coal seams that occur in the Paparoa coal measures are laterally discontinuous and devoid of marine influence compared to the generally continuous seams in the Brunner coal measures which accumulated in association with a widespread marine transgression.

Ply samples are splits taken from vertically adjacent intervals through single seams whereas seam samples represent the entire seam thickness. Ply samples were provided by Coal Corporation of New Zealand (CC), Greymouth Coal Limited (GCL) and through an exploration drilling program funded by the Foundation for Research Science and Technology (UC samples). Run-of-mine samples from the Coal Research Association of New Zealand (CRANZ) 1989-1990 mine sampling program were split from bulk reserve samples which originated from stockpiles either at the mine or stockyard bins. Samples belonging to a weathering series were taken at monthly intervals over one year from the surface of two, ~15 tonne experimental stockpiles at Ngakawau. Grab samples are those simply taken from the face of a working coal mine.

TABLE 4.1

LIST OF COAL SAMPLES

Sample Suite	Number of samples	Type	Coalfield and Area	Origin	Mass (grams)	Storage Conditions
DH 1480	17	ply	Buller No. 2 Block	CC	~ 400	plastic bags, ambient
DH 1481	17	ply	Buller No. 2 Block	CC	~ 400	plastic bags, ambient
DH 1489	23	ply	Buller No. 2 Block	CC	~ 400	plastic bags, ambient
DH 1490	27	ply	Buller Webb Block	CC	~ 400	plastic bags, ambient
DH-1492	3	ply	Buller Webb Block	CC	~ 400	plastic bags, ambient
Weathering series	20	Stock-pile	Buller, No.2 Block & Sullivan N.	CRANZ	~ 400	plastic bags and foil laminate bags, in freezer
Island Block series	7	grab	Island Block Mine, Reefton/Garvey Creek	Mine-face	~ 2 kg	plastic bags, ambient
Run-of-mine A series	6	mine/ bin	Various	CRANZ	~ 500	plastic bags, ambient
Run-of-mine B series	8	mine/ bin	Various	CRANZ	~ 500	Plastic pails, then foil laminate bags, in freezer,
DH-1494	12	ply	Buller,Upper Waimangaroa	UC	100 to 4000	foil laminate bags, in freezer
PRDH-7	19	ply & seam	Pike River	UC	100 to 4000	foil laminate bags, in freezer
DH-712	6	ply	Greymouth Rapahoe sector	GCL	~ 400	plastic bags, ambient

To minimize the loss of thermoplastic properties some samples were stored in hermetically sealed foil laminate bags. Special care was taken with cored samples from Buller drillhole 1494 (Upper Waimangaroa sector) and Pike River drillhole 7. These cores were shipped to the University of Canterbury several days after drilling and quickly processed. They were sent to CRANZ for analysis and then returned to the University of Canterbury. After processing they were continuously stored in an operating domestic freezer except when in transit.

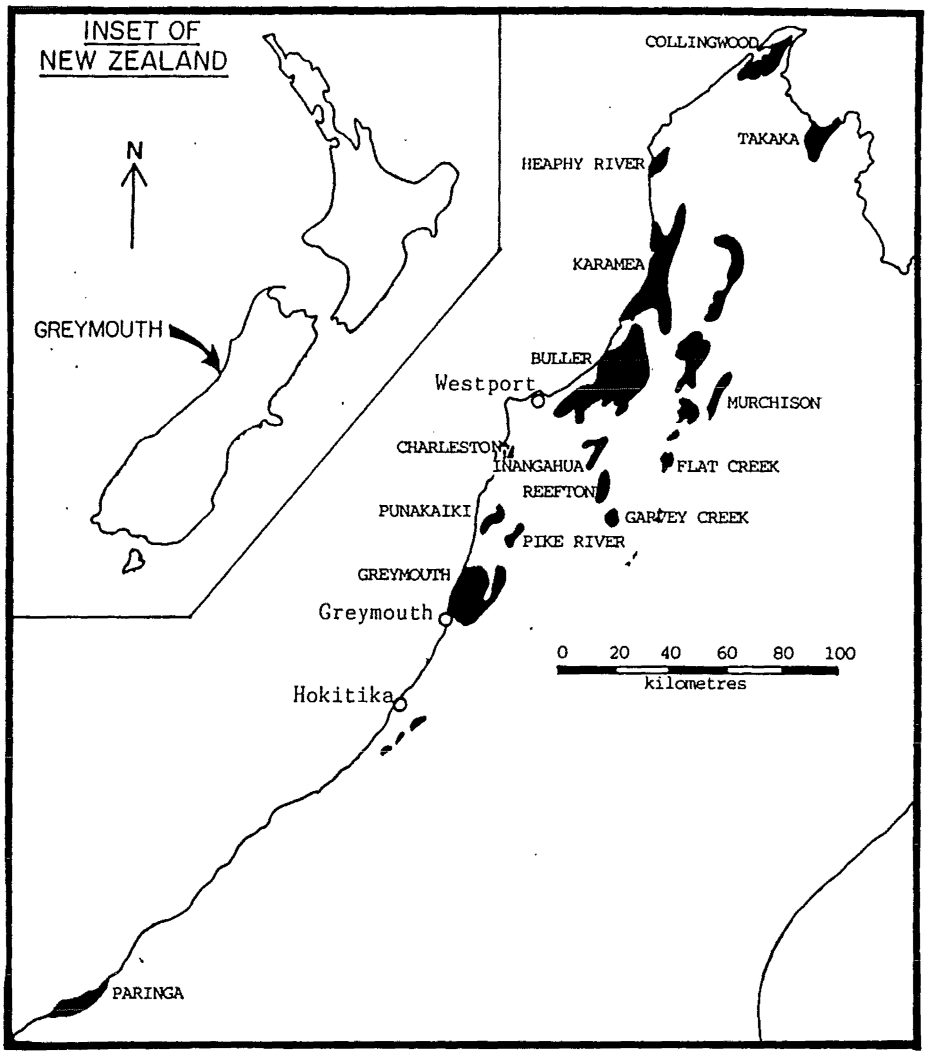

Figure 4.1 Location map showing the coalfields in the west coast, South Island, New Zealand (From N. Newman, 1988).

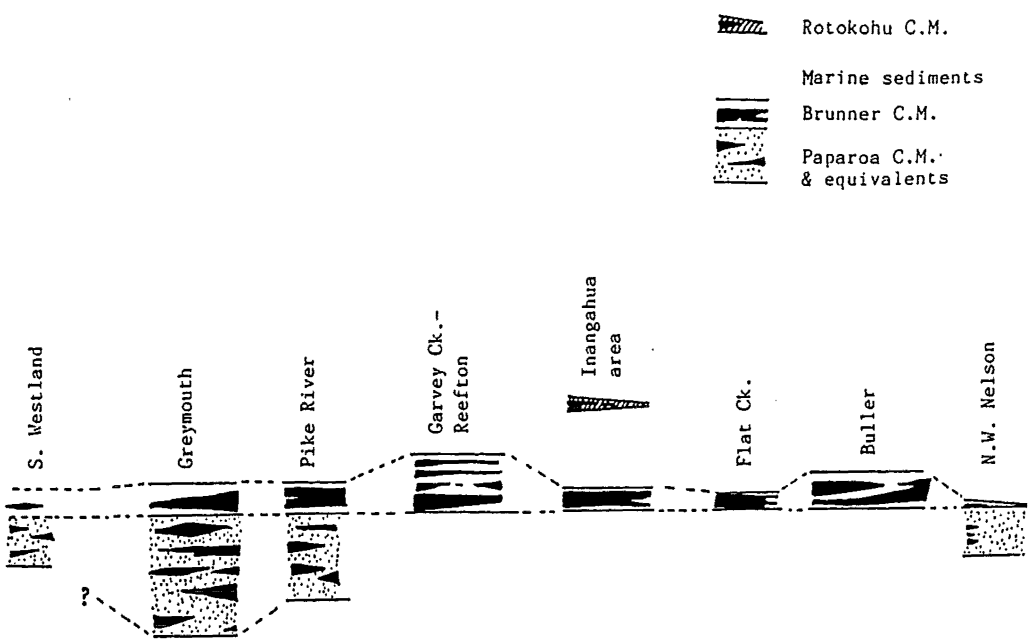

Figure 4.2 Lithostratigraphic relationships of some west coast, South Island, coalfields; not to scale (from N. Newman 1988).

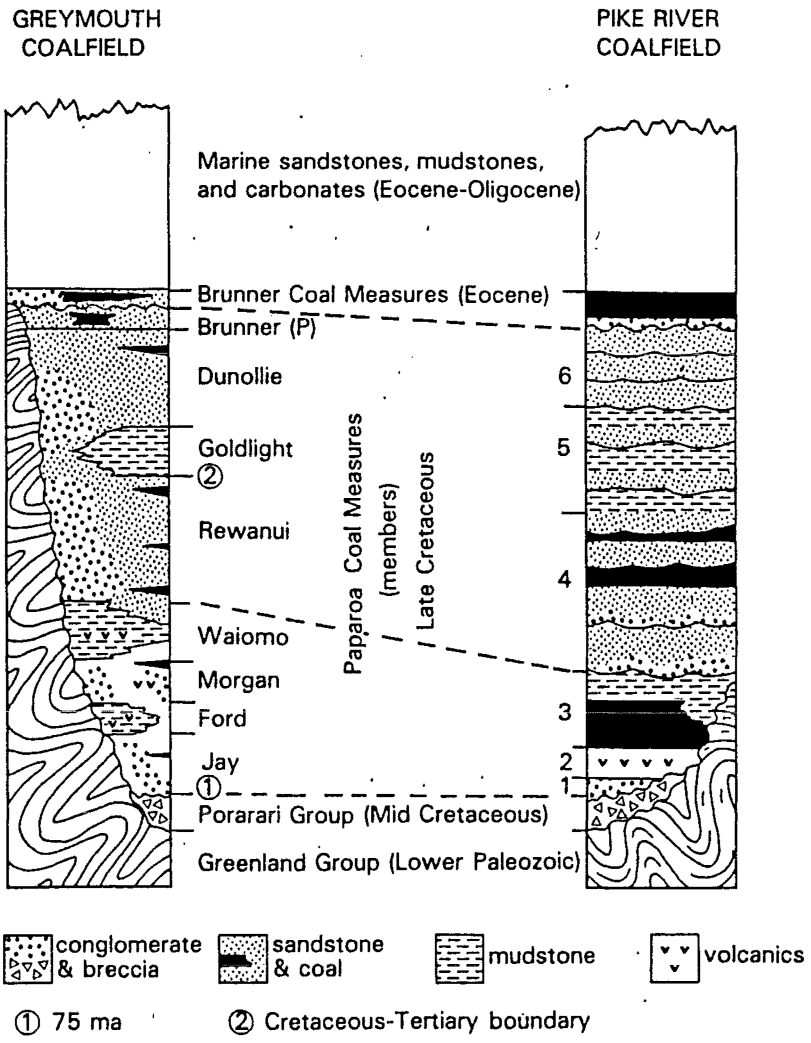

Figure 4.3 General stratigraphic columns showing Paparoa and Brunner coal measures in the Greymouth and Pike River coalfields (from Newman and Newman, in press).

4.2 DATA

Much of the data presented in this thesis was either purchased from the Coal Research Association of New Zealand or provided by the Coal Corporation of New Zealand. Analytical data for the Run-of-mine series A, and Island Block series samples are provided in Table 6.4. Raw, uncorrected data for all other coal samples as well as the results of point count analysis of carbon microtextures are listed in Appendix E. Reflectance data for the carbonized coals are presented in Table 4.4.

4.3 METHODS, COAL ANALYSES

Table 4.2 lists some analytical methods used in this study. Where appropriate, some of the tests are discussed. The discussion is limited to significant deviations from standard methods and explanation of non-standard methods. Details of the method used for preparation of polished coal specimens for microscopic analyses are provided in Appendix A.

TABLE 4.2
ANALYTICAL METHODS

* Total Moisture	ISO 1988-1975(E)
* Air-dried Moisture	in-house
* Ash	ISO 5068
* Volatile Matter	ISO 562 - 1981(E)
* Specific Energy	ISO 1928 - 1976(E)
* Total Sulphur	ASTM D4239-83
* Forms of Sulphur	AS1038 - Part 11
* Carbon, Hydrogen Nitrogen	Leco infrared, in-house
* Crucible Swelling	ISO 501 - 1981
* Gieseler Fluidity	ASTM D2639 - 74
* CO2	ISO 925-1980
** Ash Composition	XRF in-house
*** Rock Eval Pyrolysis	in-house
**a Maceral Analysis	AS-2856
**a Reflectance Analysis	ISO-7404/5
**a Fluorometric Analysis	in-house
**a Chemical Etching	Quick and Moore 1991
**a Safranin O Staining	modified after Gray *et al.*, (1976)

* as determined at CRANZ
** as determined at the University of Canterbury
**a as determined at the University of Canterbury (by the author)
*** undertaken at the University of British Columbia

4.3.1 Air-dried Moisture

Air-dried moisture reports the moisture content of a minus 72 BS mesh coal specimen equilibrated at 70% relative humidity and 20 °C to a constant weight. Typical equilibration time for bituminous coal is less than one day; drying time is 2 hours in a nitrogen flushed oven.

4.3.2 Ash

The ashing temperature cycle used by CRANZ is similar to that specified for brown coal and lignite.

4.3.3 Crucible Swelling

Crucible swelling numbers greater than 9 are reported by CRANZ as 9+, 9++, and 9+++ and, to facilitate computer manipulation, are reported here as 9.5, 10, and 10.5. 9+++ indicates that the crucible was completely filled and the two other designations (+, ++) are between it and 9. Note that a crucible swelling index 9+++ probably corresponds to the maximum possible "free swelling index" (ASTM D-720) of 11.5.

4.3.4 Ash Composition

Major elements in ash were determined using an XRF technique where specimens are prepared by fusion of coal ash and flux (lithium tetraborate - lithium carbonate mix) and pressed into glass disks. Ammonium nitrate was used as an oxidant and Lanthanum oxide used as a heavy absorber. The fusion disk preparation method is described in detail by Weaver (1987) and is similar to that outlined in ASTM D-4326 (1987). A deviation from these methods is that the ash samples were not desiccated prior to preparation of the fusion disks. Where elements were calculated to a coal basis or for calculation of mineral content the reported data were corrected to a "loss on ignition free basis" which is close to an ignited ash basis. The weight percent dry ash reported by CRANZ was used for both of these calculations. Loss on ignition is the measured weight loss of the ash upon heating the ash/flux mixture to 1000 °C. Ashes prepared at the University of Canterbury were obtained from milled coal samples, ignited at 600 °C until the organic matter was visibly absent, followed by roasting at 800 °C for 1 hour. The mean, minimum and maximum compositional values determined for 38 ash specimens examined in this study are listed in Table 4.3 together with the same values reported for the 27 standards used for calibration. For comparative purposes the values listed in Table 4.3 are on a loss on ignition free basis. Examination of Table 4.3 shows that the composition of the coal ashes typically varies within the range of the calibration standard composition (except for Al_2O_3 and P_2O_5). Although the sulphate values for the calibration standards are highly skewed, with only one standard reporting a value greater than 0.5%,

determination of 5 specimens doped with 4 to 13% SO_3 showed general agreement with the known sulphate additions (data not shown).

TABLE 4.3
COMPOSITION OF COAL ASHES AND CALIBRATION STANDARDS

ELEMENT	COAL ASH SPECIMENS			CALIBRATION STANDARDS		
	minimum wt.%	mean wt.%	maximum wt.%	minimum wt.%	mean wt.%	maximum wt.%
SiO_2	0.5	32.3	83.9	0.3	50.7	99.6
TiO_2	0.1	0.9	3.9	0.0	0.6	3.9
Al_2O_3	0.4	12.1	38.6	0.1	9.8	18.2
Fe_2O_3	0.7	22.8	95.8	0.1	10.0	95.7
MnO	0.0	0.1	0.2	0.0	0.2	0.8
MgO	0.0	5.6	25.8	0.0	10.3	50.8
CaO	0.1	11.7	60.0	0.0	10.8	79.9
Na_2O	0.0	1.0	3.6	0.0	2.3	8.7
K_2O	0.0	0.8	3.6	0.0	2.6	15.5
P_2O_5	0.0	0.4	5.6	0.0	0.2	1.1
SO_3	0.0	10.6	42.4	0.0	2.2	58.7

4.3.5 Rock Eval

Rock Eval pyrolysis was accomplished at the Department of Geological Sciences, University of British Columbia (Vancouver Canada). The test is not recognized in national coal standards, and is more commonly used by the petroleum industry for rapid evaluation of downhole kerogen type and maturation trends.

4.3.6 Vitrinite Reflectance

The mean maximum reflectance of vitrinite was measured in general accordance with ISO-7404/5 except that means were usually recorded from 50 rather than the 100 or more measurements specified in the standard. Both desmocollinite (common) and telocollinite (often rare) were measured but not differentiated. Details of the instrumentation and calibration method used for reflectance analysis are provided in Appendix B.

4.3.7 Fluorometric Analysis.

The fluorometric analyses in this study report the mean fluorescence intensity of vitrinite and inertinite at 550-650 nm, induced by irradiating the coal surface with intense blue light (395-485 nm). The mean intensity was calculated from 100 or more measurements on vitrinite and inertinite macerals randomly encountered during traverses of the pellet surface; particles of liptinite and mineral matter were ignored. Calibration was accomplished with a Wild Leitz masked uranyl glass standard arbitrarily assigned an intensity value of 100. Where appropriate, individually calibrated, coated neutral density filters were used to reduce the fluorescence intensity of the standard to levels comparable with the coal. A dry, 40X/0.85NA objective was used and a nitrogen flow maintained over the irradiated coal surface to prevent loss of fluorescence intensity upon irradiation. Details of the instrumentation and calibration method for fluorometric analysis are provided in Appendix C.

4.3.8 Maceral Analysis

Maceral analyses were undertaken in normal (white) light and in the fluorescence mode (blue light) in general accordance with AS-2856. Results from the white and blue light analyses were combined according to the "two scan" method described by Davis (1987); the volume percent mineral matter parameter required by this method was calculated according to ASTM-2799. In all cases a minimum of 500 white light and 500 blue light maceral counts were obtained. Figure 4.4 shows that the volume percent liptinite determined in blue light was generally lower than that determined using white light illumination. This difference is generally due to less liptodetrinite being counted in the fluorescence mode. No correlation exists between the measured ash content and the difference between liptinite counted in white reflected light and liptinite counted in the fluorescence mode. The higher liptodetrinite counts in white light is suggested to have resulted from mis-identification of small voids in the coal as liptodetrinite.

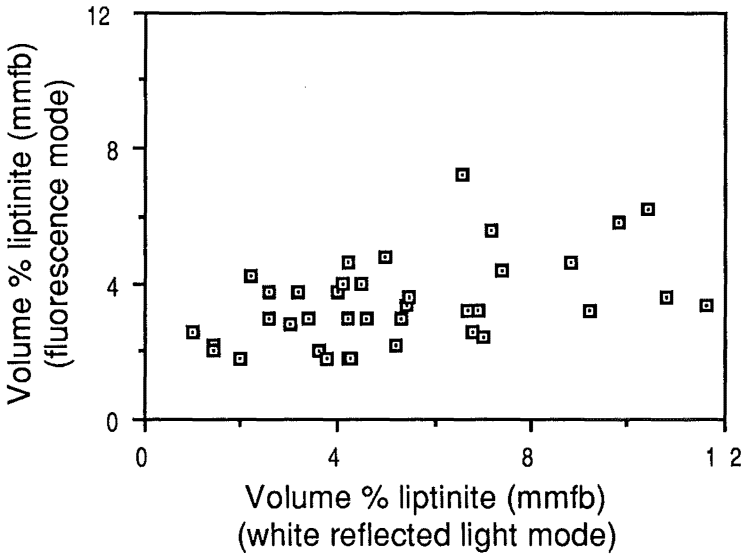

Figure 4.4 Comparison of the liptinite content determined in white reflected light with that determined using the fluorescence mode.

Maceral analyses were undertaken according to AS-2856; this standard method provides concise, petrographic criteria for the identification of macerals and is particularly well suited for industrial purposes. As explained by Potonie (1954) petrographic nomenclatures are suited for industrial purposes but are different than petrological nomenclatures which are better used for geological studies of maceral origin and genesis. Thus, the maceral fluorinite counted in this thesis conforms to AS-2856 petrographic criteria but genetically is probably a terpene resin rather than an essential oil or lipid (Teichmüller, 1974). Likewise, all of the eugelinite counted in coals from the Brunner coal measures is, in a petrological sense, better described as meta-exudatinite (Teichmüller, 1982 p.260) or inverted exudatinite (Newman, 1985).

4.3.9 Etching Analysis

Polished specimens from the Brunner coal measures, Pike River coalfield, were etched prior to petrographic analysis. The polished pellet surface was immersed for 10 seconds in a hot, decanted, freshly boiled etching solution (100 ml H_2O, 5 ml H_2SO_4, 25 g $KMnO_4$) followed by immersion in a cold cleaning solution (100 ml H_2O, 5 ml H_2SO_4, 25 g Na_2SO_3) and finally ultrasonically cleaned in water and dried with a blast of filtered air. For good results the etching solution is used once per specimen and discarded; decanting the solution allows

about 6 etched specimens to be prepared from one batch made according to the recipe given above. The optimum etching time was established by trial and error.

Chemical etching of the polished coal surface differentiates macerals based on their relative susceptibility to oxidative attack (relief) and resulting optical texture. Petrographic analyses on etched coal specimens were undertaken using a 40X/0.85NA oil immersion objective. Mineral matter was ignored and the following constituents were point counted.

(i) Amorphous matrix included any organic constituent that showed low relief compared to adjacent material, or could not be included in another category. Rare, featureless particles that displayed no differential relief were included in this category. In these rare instances it was impossible to determine if the material under the cross-hair showed either "high" or "low" relief.

(ii) Tissue included all material with recognizable cellular structure, and typically exhibited high relief. Recognizable cellular structure is defined here as any component that exhibits at least one intact cell lumen.

(iii) Particulate matrix included all high relief material greater than about 2 microns in maximum dimension that did not display cellular structure. This size limitation was adopted as a matter of convenience. Small particulate matrix commonly presented edge hits where the cross hair of the microscope intersects the edge of the particle and the surrounding material. The relief of the surface was such that the edges of these particles were often indistinct and the edge of the particle sometimes appeared larger than the particle itself. In these instances a count was registered for the surrounding material.

(iv) Liptinite was counted separately in the fluorescence mode and included all bright fluorescent material except for occasional carbonates which displayed fluorescence presumably due to associated organic matter. The two scans were combined in the same way as conventional maceral analyses.

4.3.10 Staining Analysis.

Some polished specimens were stained with the cationic dye Safranin O to reveal weathered grains of bituminous coal. Polished pellets were immersed overnight in a staining solution (1 g Safranin O, 100 ml H_2O and 100 ml alcohol) rinsed with water and dried with a blast of filtered air. The KOH etching step often used in this method (Gray *et al.*, 1976, Marchioni, 1983) was omitted because of the tendency of weathered grains to dissolve in alkaline solution.

Petrographic analyses of specimens stained with Safranin O were undertaken using a 40X/0.85NA oil immersion objective. Staining was not observed where an air objective was used. The procedure differs from other petrographic analyses in that grains of coal are counted rather than macerals which comprise the grains. For example, where staining occurred along cracks or particle edges and the cross-hair intersected the central un-stained area of the particle, a count was registered for a stained component. In retrospect, a lower power objective or smaller grain size would have been more appropriate since the visible area of the coaly particles often exceeded the field of view. The intensity of staining varied from a pale green to a darker olive green. In this study the intensity of staining was not differentiated. Rare, pure mineral grains were ignored.

4.4 PREPARATION AND ANALYSIS OF CARBONS

Table 4.4 lists the coal samples selected for carbonization. Each coal was stage ground to minus 1 mm, split to about 50 g and singly packed into a metal retort (Figure 4.5). A perforated aluminium foil disk, glass wool and quartz gravel was used to fill any remaining head space and a vented cap screwed on to secure each charge. The retorts were placed in a vented Carbolite muffle furnace; the furnace accommodated 5 retorts in the uniform heating zone at the rear of the furnace chamber. A programmable controller was set to provide a heating rate of 3 °C per minute and a hold time of one hour at a final temperature of 900 °C. During carbonization some of the coals expelled a plastic phase from the retort

vent. At the end of each run the retorts were allowed to cool naturally, disassembled and the carbon product recovered for analysis. Photographs of the recovered carbons are shown in Appendix F.

The recovered carbons were stage ground to minus 1 mm and polished specimens produced for microscopic examination. The specimens were prepared in the same manner as described for the coal samples (Appendix A) except for some preliminary grinding on fixed 80 grit zirconium oxide disks.

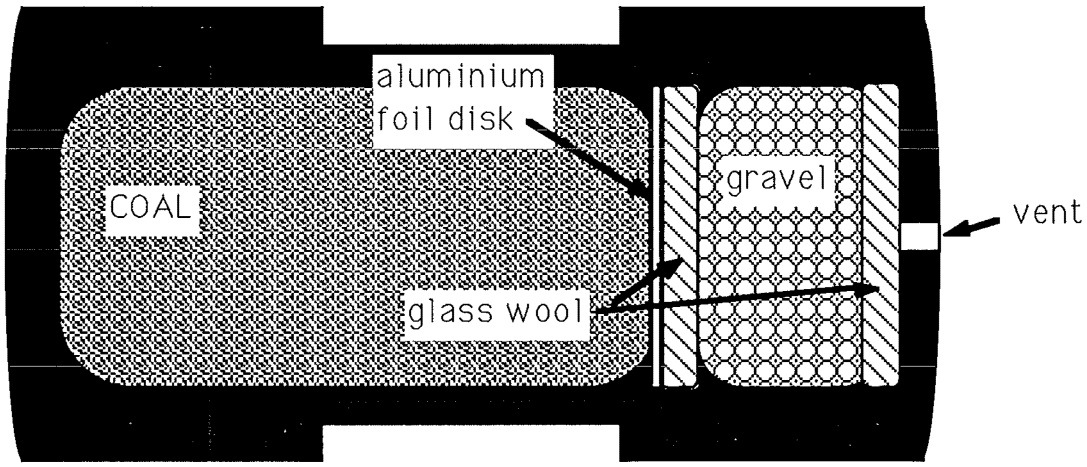

Figure 4.5 Illustrated cross section of metal retort used to hold coal charges during carbonization (actual size).

4.4.1 Reflectance Analysis of Carbons

The mean apparent average, maximum, and minimum reflectance (in oil) as well as mean apparent anisotropy of the carbons are shown in Table 4.4. These data are based on the measurement of thirty particles for each analysis. During 360° stage rotation two maxima and two minima were recorded from each particle and each pair of values averaged to obtain the minimum and maximum reflectance. The anisotropy of each particle was determined by subtraction of the minimum from the maximum value. The average reflectance of each particle was determined by dividing the sum of the recorded readings by four.

TABLE 4.4

ANALYTICAL DATA FOR CARBONIZED COALS

Parent Coal ID	Vitrinite Ro max	Mean Apparent %Carbon Reflectance (in oil)				OTI[1]	Notes [2]
		average	maximum	minimum	anisotropy[3]		
50/639	.56	6.64	6.74	6.54	.20	0.0	d,p,GM
50/641	.51	6.51	6.57	6.45	.13	0.0	d,p,GM
46/741	.56	7.10	7.59	6.61	.99	2.0	d,p,UW
46/743	.67	7.43	7.94	6.92	1.01	0.9	d,p,UW
46/747	.69	7.33	7.60	7.05	.55	0.6	d,p,UW
46/836	.66	6.84	8.05	5.62	2.43	3.0	d,p,PRb
46/841	.74	7.17	8.40	5.95	2.45	4.1	d,p,PRb
46/845	.67	6.94	8.35	5.53	2.83	3.0	d,p,PRb
46/919	.93	7.12	8.00	6.24	1.76	1.6	d,f,PRp
46/922	.89	7.02	7.93	6.12	1.80	3.5	d,f,PRp
46/923	.83	7.04	8.28	5.80	2.49	4.1	d,f,PRp
46/924	.88	6.80	7.73	5.86	1.88	3.1	d,f,PRp
a90-93	1.10	7.58	9.42	5.74	3.68	4.0	d,p,ST
a90-102	1.09	7.55	9.37	5.73	3.64	3.5	d,p,ST
a90-136	.98	7.26	8.71	5.81	2.90	3.6	d,p,ST
a90-140	1.17	7.33	8.80	5.87	2.94	3.7	d,p,ST
a90-151	1.13	7.31	9.28	5.33	3.95	3.9	d,p,ST
a90-599	1.24	7.19	10.08	4.31	5.77	6.3	d,p,WB
a90-621	1.31	7.41	9.65	5.16	4.49	4.6	d,p,WB
a90-636	1.22	7.26	8.40	6.12	2.28	1.0	d,p,w,WB
a90-646	1.27	7.31	9.28	5.33	3.95	0.0	d,p,w,WB
46/068	.59	6.67	6.73	6.61	.12	0.0	s,GM
46/064	.62	6.70	6.77	6.64	.14	0.0	s,GM
45/936	.73	6.83	6.92	6.73	.19	0.0	s,RG
45/978	.74	7.07	7.28	6.85	.43	0.1	s,BU
45/965	.75	6.94	7.06	6.83	.23	0.0	s,GM
45/971	1.20	7.80	10.76	4.85	5.91	6.3	s,BU
46/426	1.60	8.54	13.01	4.06	8.95	17.9	s,GM

1 Optical Texture Index, defined in text below.

2 Notes:

d	drillhole core	UW	Upper Waimangaroa Sector, Buller coalfield
f	full seam sample	ST	Stockton Sector, Buller coalfield
p	ply sample	WB	Webb Sector, Buller coalfield
s	stockpile sample	GM	Greymouth coalfield
w	weathered coal	RG	Reefton, Garvey Creek coalfield
		BU	Buller coalfield (Cascade Mine)
		PRb	Pike River coalfield, Brunner coal measures
		PRp	Pike River coalfield, Paparoa coal measures

3. Maximum minus Minimum reflectance (recorded to three decimal places and rounded)

The mean reflectance values listed in Table 4.4 are reported as "apparent" values for two reasons. Vitrinite in bituminous coal is usually considered to display a uniaxial negative optical character (Davis, 1978). Consequently, true maximum reflectance should be obtained on any random surface whereas minimum reflectance will range from the true minimum (reflecting surface parallel to bedding) to the maximum reflectance value (reflecting surface normal to bedding). Biaxial vitrinite has been noted in anthracite (Cook *et al.*, 1972) and bituminous coal (Stone and Cook, 1979, Levine and Davis, 1984). Stone and Cook (1979) suggested that biaxial vitrinite is common in bituminous coals. Their conclusion is supported by Kilby (1988) who also identified coals with uniaxial positive reflectance indicatrix. Figure 4.6 shows a reflectance cross plot (after Kilby, 1988) for the carbon obtained from coal sample 46/426 which is interpreted to show a biaxial negative reflectance indicatrix. Thus the reflectance parameters shown in Table 4.4 are probably "apparent" rather than true values.

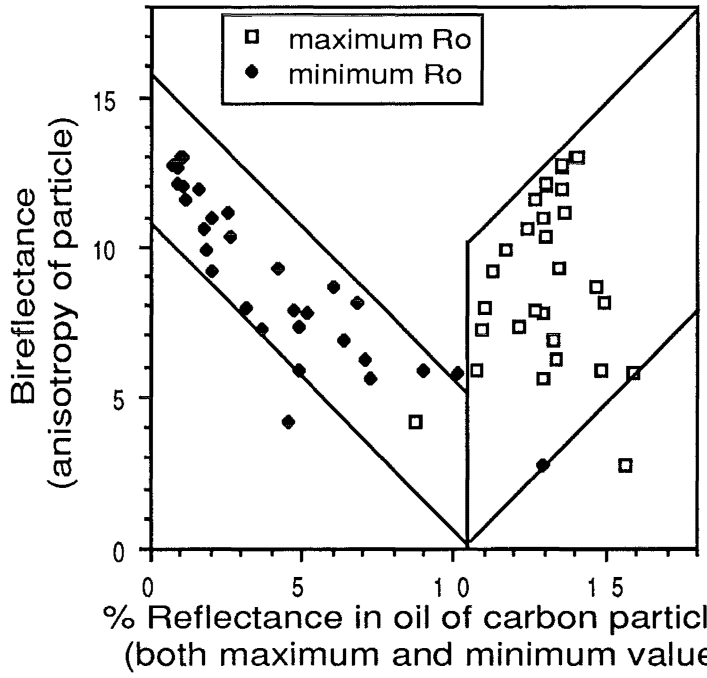

Figure 4.6 Reflectance cross-plot of carbon from coal sample 46/426 interpreted to show a biaxial negative reflectance indicatrix.

A second reason that apparent values are reported in Table 4.4 relates to the heterogeneous character of the reflecting carbon surfaces. The data in Figure 4.6 were obtained by measuring comparatively large anisotropic domains which

are characteristic of cokes made from low volatile bituminous rank coal. However, the size of the individual mosaic units in the other carbon samples was rarely large enough for individual measurement. As noted by Murchison (1978 p.429) "... any reflectance measurement upon a carbonized maceral with a mosaic texture will be comprised of a number of units". Since the alignment of the stacked aromatic sheets in adjacent units may vary, the reflectance in polarized light of individual adjacent units within the measurement area will behave independently at any given angle of stage rotation. Rather than reduce the measurement area to a size less than the 2.8 um diameter used for measurement of vitrinite reflectance, a 5.5 um measuring spot (with 14.1 um illuminated field stop) was used. The larger spot size was selected to reduce variation resulting from drift over small mosaic units upon stage rotation. Further details of the calibration method used for reflectance analysis of the carbon specimens are provided in Appendix B.

4.4.2 Carbon Texture Analysis

Representative optical photomicrographs of the carbon textures observed in this study are shown in Plates 4.1 and 4.2. The identification of these carbon textures was largely based on the size of the isochromatic domains. The interference colours were induced using an H-PL-Pol plane glass illuminator, crossed nicols with the polariser set to 45°, and an Epiplan 40X/0.85NA Pol air objective. Brighter, more intense interference colours would have been observed had an antiflex lens system been used. Nonetheless, the arrangement used in this study was useful and the isochromatic domains sufficiently well developed for the recognition of carbon textures. Nomenclature used to classify these textures was modified from Edwards (1989) and is summarized in Table 4.5. Results of the point count analyses for these carbon textures are based on 250 counts per specimen.

Plate 4.1
Carbon Microtextures

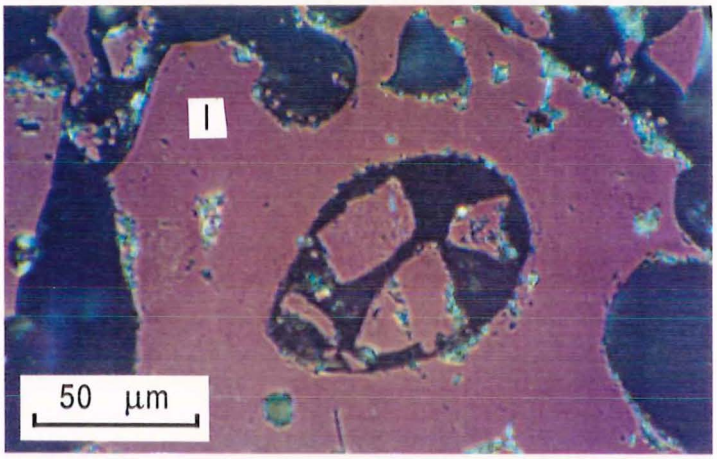

Isotropic texture

from coal 45/965

mean Ro_{max} vitrinite = 0.75

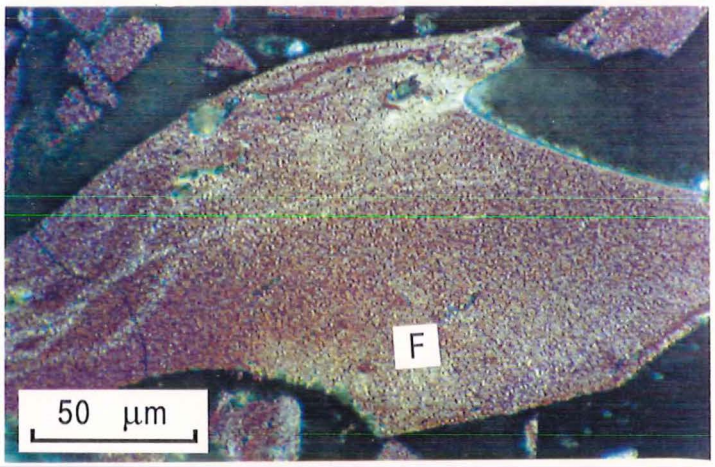

Fine Mosaic texture

from coal 46/919

mean Ro_{max} vitrinite = 0.93

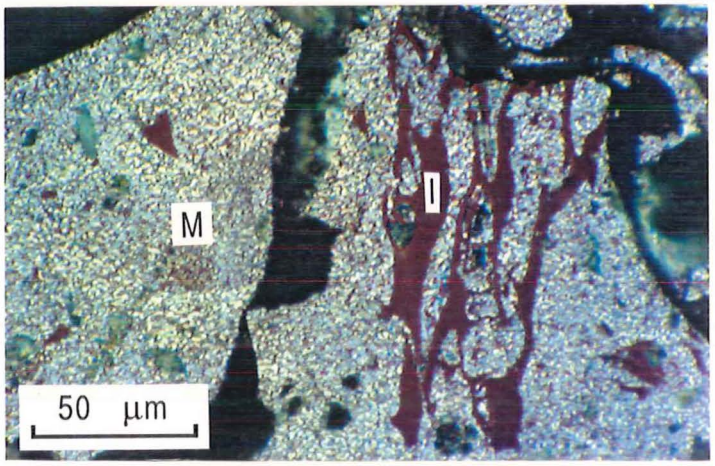

Medium Mosaic texture

from coal 46/923

mean Ro_{max} vitrinite = 0.83

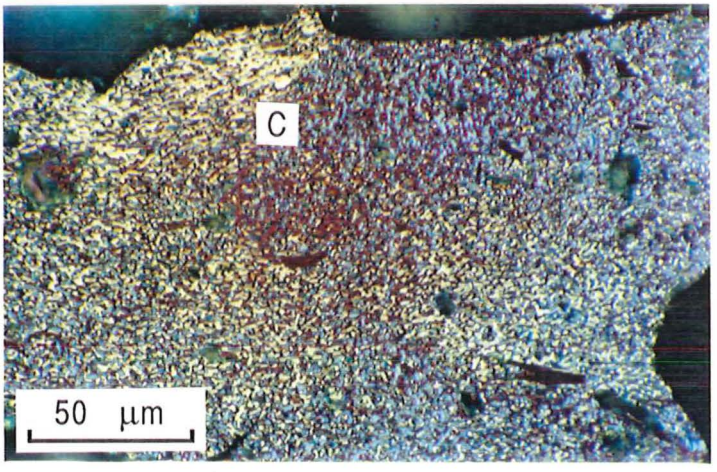

Coarse Mosaic texture

from coal 46/923

mean Ro_{max} vitrinite = 0.83

Plate 4.2
Carbon Microtextures

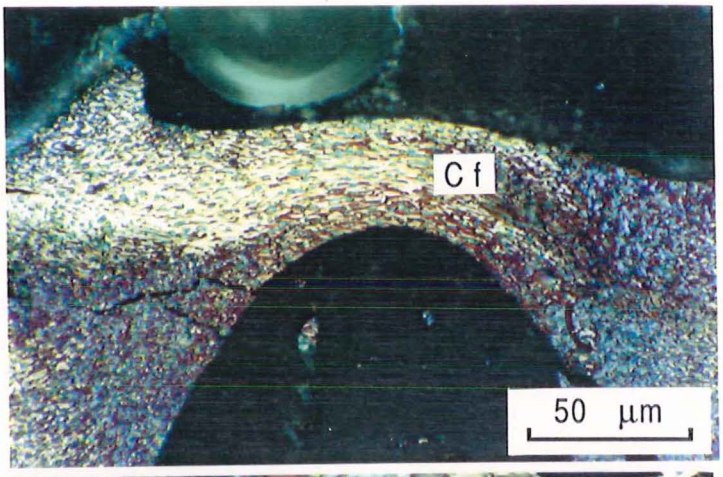

Coarse Flow texture

from coal 46/923

mean Ro_{max} vitrinite = 0.83

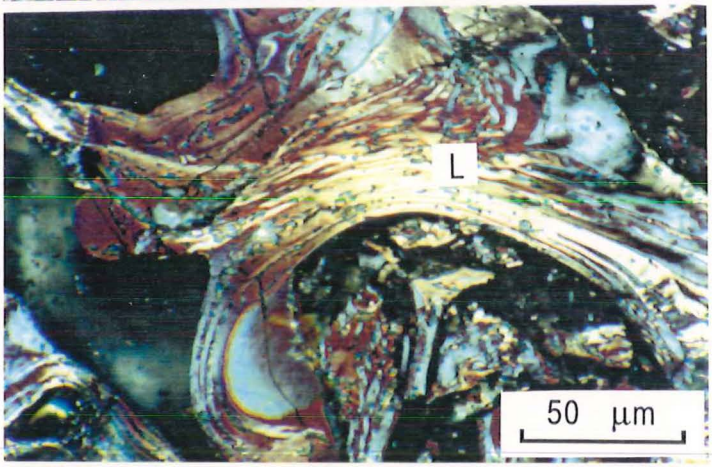

Lamellar Flow texture

from coal 45/971

mean Ro_{max} vitrinite = 1.20

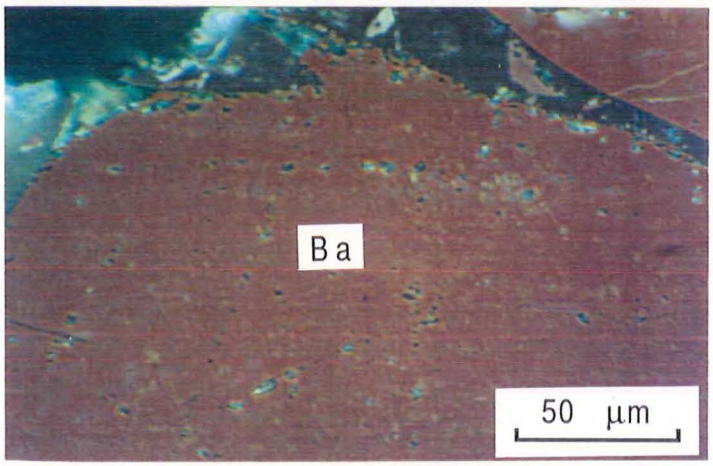

Basic Anisotropy texture

from coal a90-646

mean Ro_{max} vitrinite = 1.27

weathered coal

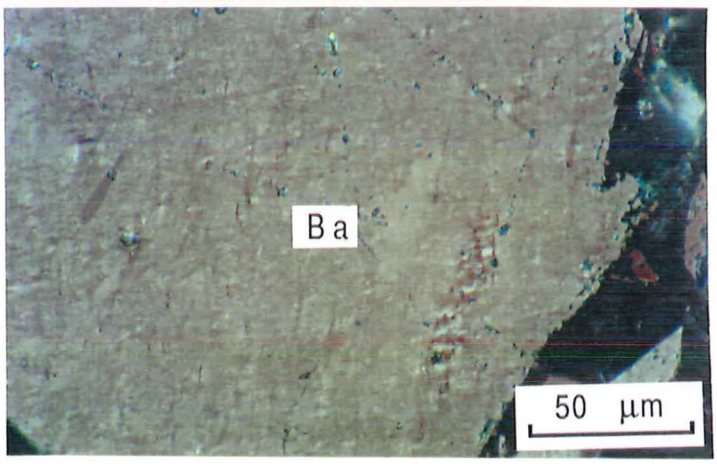

Basic Anisotropy texture

Same image as above with

90° clockwise stage rotation

weathered coal

TABLE 4.5

NOMENCLATURE USED TO DESCRIBE OPTICAL TEXTURE

Texture Name	Optical Character	OTI factor
Isotropic carbon forms	no optical activity	0
Fine grain mosaics	<0.8 um diameter	1
Medium grain mosaics	0.8 - 2.4 um	3
Coarse grain mosaics	2.4 - 10 um	7
Coarse flow domains	elongate, 10 - 20 um	20
Lamellar flow domains	plastic, > 20 um	30
Basic anisotropy	anisotropic with inherited structure	0

modified from Edwards (1989)

Isotropic carbon forms remain purple upon stage rotation. This behaviour is also characteristic of anisotropic carbons where the basal plane of the carbon is parallel with the specimen surface. However, as noted by Marsh and Smith (1978) isotropic carbons are distinguished by a lighter purple hue than that displayed by the basal plane of anisotropic carbons. The differentiation of isotropic and fine mosaic morphologies was based on the appearance of a fine granular texture.

Fine grain mosaics were identified based on the appearance of a granular texture where individual mosaic units were less than 0.8 um in maximum dimension. Medium grain mosaics were recognized where the size of the individual mosaic units varied between 0.8 and 2.4 um. Coarse grain mosaics were recognized where the size of the individual mosaic units varied between 2.4 and 10 um in maximum dimension. Coarse flow domains were recognized as any isochromatic domain composed of elongated grains greater than 10 um in maximum dimension. Lamellar flow domains showed plastic deformation with long range order greater than 20 um. Basic anisotropy was recognized where both anisotropy and inherited structure (bedding plane alignment) were observed upon stage rotation.

Within individual particles, the mosaic units were typically uniform in size. However, the distribution of mosaic sizes was continuous, without abrupt changes from one size to another. Moreland *et al.*, (1988) observed the same behaviour and stated (p.731): "Any classification scheme therefore involves

arbitrarily chosen classes. Structures typical of each class are easy to recognize, but differentiating between structures at the interface between classes is highly subjective." Thus, the classification of mosaic textures according to visually recognized, arbitrary size classes is inherently imprecise and reproducibility is likely to be poor.

Edwards (1989) stresses that petrographic analysis of optical texture is a comparative technique and that the results of this kind of analysis depends on the resolution of the microscope. Piller (1977) states that the resolving power of a microscope is primarily a function of the numerical aperture of the objective and a theoretical limit of resolution can be calculated according to the following relationship.

$$d = \frac{\lambda}{NA_{Obj} + NA_{Con}} \qquad \text{(eq. 4.1)}$$

where:

d	is the smallest resolvable distance (um)
λ	is the wavelength (um)
NA	is the numerical aperture (numeral)
Obj	is the objective, and,
Con	is the condenser.

Using Equation 4.1 the theoretical limit of resolution attained in this study can be shown to be 0.3 um where NA = 0.85 and λ = 0.55 um; the objective serves as the condenser in reflected light.

4.4.3 Optical Texture Index

The optical texture index (OTI) is a single value calculated from the results of the point count analysis of the carbon textures. The use of a single value, rather than the volume percent of seven different components, simplifies comparisons of the optical texture of carbon materials. The OTI was calculated by multiplying the volume percent (expressed as a fraction) of each carbon texture times the corresponding OTI factor listed in Table 4.5 and summing the results. The OTI of the carbons examined in this thesis are listed in Table 4.4.

4.5 SUMMARY

Analytical methods used in this thesis have been listed and briefly described. The significance of the resulting data are discussed in chapter 5 where some limitation of various analytical methods are also examined. Finally, measures of carbonization and pyrolysis behaviour are predicted in chapter six where fundamental characterization of coal according to combined reflectance and fluorescence microscopy is advocated.

CHAPTER FIVE
EVALUATION AND LIMITATIONS OF ANALYTICAL DATA

This chapter begins with the application of some tests that were undertaken to identify errors in the data set. These tests also allow interpretation and thus provide insight into the nature of the subject coals. Because microscopic analyses are emphasised in this thesis, some inherent limitations of point counting techniques are described. The chapter concludes with a discussion of some limitations of the Gieseler fluidity test and the determination of moisture.

5.1 THE MOTT-SPOONER TEST

The Mott-Spooner "test" compares the determined specific energy with the specific energy value calculated (by any appropriate equation) from the elemental composition of coal. The name of the test was coined by Given and Yarzab (1975) who used an equation published by Mott and Spooner (1940) to calculate the specific energy of coals from their elemental composition and subtracted the calculated specific energy from the determined specific energy; the resulting difference is called the Mott-Spooner Difference (MSD). Where this value is large Mott and Spooner (1940) suggest that the analyses should be repeated. Numerous equations have been proposed in the literature for calculation of specific energy from elemental composition; Table 2.2 summarizes a few of the equations used for coal. In this section an equation presented by Given *et al.*, (1986) is used to calculate specific energy. Although Given and his co-workers reported that this formula provides no better estimate of specific energy than that proposed by Mott and Spooner, it is preferred here since it is based on modern theoretical values for the heats of combustion of the elements and CO. Given and his co-workers discuss in some detail the derivation of the oxygen coefficient used in their equation. The coefficient appropriate for oxygen varies according to the way oxygen is combined in the coal (i.e., hydroxyl, ether or carbonyl). The effect of different oxygen coefficients applicable to bituminous coals was found by Given *et al.*, (1986) to be insignificant, and a global term was adopted. A necessarily

empirical term included in the equation is a factor related to the enthalpy of decomposition. Despite finding statistically significant, provincial differences in the enthalpy of decomposition, Given and his co-workers observed that a global term for the enthalpy of decomposition was as effective in predicting specific energy as individual terms for subsets of samples. The acceptance of a global term for the enthalpy of decomposition probably relates to the limits of analytical precision which obscure the significance of variation in the enthalpy of decomposition where single coals are evaluated.

Calculation of specific energy from ultimate analyses requires that data be expressed on a dry mineral matter free (dmmf) basis. Unfortunately it is not possible to directly measure organic CHNOS or to entirely attribute the heat of combustion to the organic fraction of coal. For this reason approximation formulae are used to correct these raw values to a dmmf basis. The formulae used in this thesis are shown below.

$$MM = 1.13A + 0.5Sp + 2.8Ss - 2.8\left(\frac{0.4SO_3 \cdot A}{100}\right) + 0.08CO_2 \qquad \text{(eq. 5.1)}$$

$$MJ/kg_{dmmf} = \left(MJ/kg - 0.126Sp\right)\cdot\left(\frac{100}{100 - MM}\right) \qquad \text{(eq. 5.2)}$$

$$C_o = \left(C - 0.273CO_2\right)\cdot\left(\frac{100}{100 - MM}\right) \qquad \text{(eq. 5.3)}$$

$$H_o = \left[H - .014A + .018Sp + .019CO_2 + .014\left(\frac{SO_3 \cdot A}{100}\right)\right]\cdot\left(\frac{100}{100 - MM}\right) \qquad \text{(eq. 5.4)}$$

$$N_o = N \cdot \left(\frac{100}{100 - MM}\right) \qquad \text{(eq. 5.5)}$$

$$S_o = \left(S - Sp - Ss\right)\cdot\left(\frac{100}{100 - MM}\right) \qquad \text{(eq. 5.6)}$$

$$O_o = 100 - C_o - H_o - N_o - S_o \qquad \text{(eq. 5.7)}$$

where,

MM	is dry weight percent mineral matter
MJ/kg	is dry specific energy
C	is dry weight percent carbon
H	is dry weight percent hydrogen

N	is dry weight percent nitrogen
S	is dry weight percent sulphur
O	is dry weight percent oxygen
A	is dry weight percent ash
Sp	is dry weight percent pyritic sulphur
Ss	is dry weight percent sulphate sulphur in coal
SO_3	is weight percent sulphate in ash
CO_2	is dry weight percent gas evolved upon reaction with HCl

and the subscripts,

dmmf	specifies a dry mineral matter free basis
o	specifies organic, dry mineral matter free basis
calc	specifies that the value is calculated rather than determined

The mineral matter formula (eq. 5.1) is the KMC formula (King *et al.*, 1936) as modified by Millott (1958). The chlorine parameter is omitted and the equation expressed using values corrected to a dry basis. With one exception, Equations 5.2 to 5.7 are those described in BS 1016 part 16 (1981) expressed using values corrected to a dry basis. Equation 5.4 includes an additional term (SO_3) that accounts for the appreciable sulphate fixation in some New Zealand bituminous coal ashes. The reason for inclusion of this term is discussed by Given and Yarzab (1975). Finally it is important to note that H reports dry hydrogen where the contribution due to moisture has been removed by calculation. This is standard practice for reporting ultimate analyses on a dry basis by the Coal Research Association of New Zealand laboratories.

Specific energy was calculated according to Equation 5.8. The coefficients were derived from those presented by Given *et al.*, (1986) using a multiplication factor of 0.002326 to convert BTU/lb to MJ/kg rather than adopting the alternate formula presented in kJ/kg. Regression between coefficients in the alternate formulae presented by Given *et al.*, (1986) resulted in a non-zero intercept, presumably due to rounding errors.

$$MJ/kg_{dmmf,calc.} = 0.3278C_o + 1.419H_o + 0.09257S_o - 0.1379O_o + 0.6373 \qquad \text{(eq. 5.8)}$$

Using the resulting calculated specific energy, the Mott-Spooner difference (MSD) can be calculated as shown below.

$$MSD = MJ/kg_{dmmf} - MJ/kg_{dmmf\ calc.} \qquad \text{(eq. 5.9)}$$

Table 5.1 lists the values obtained using the above equations for some New Zealand coals for which appropriate analytical data were available. The coals listed in Table 5.1 are from drillhole 1494 and drillhole 7; raw analytical data for these coals are provided in Tables E.6, E.7 and E.8 (appendix E).

TABLE 5.1
CALCULATED VALUES FOR SOME NEW ZEALAND COALS

Lab No	C_o	H_o	N_o	S_o	O_o	MM dry	MJ/kg determined dmmf	MJ/kg calculated dmmf	MSD
46/750	84.6	6.2	1.4	1.3	6.5	36.6	35.37	36.34	-.97
46/739	81.7	6.0	1.1	3.2	8.0	3.5	34.47	35.17	-.70
46/740	81.6	5.9	1.3	3.4	7.9	2.8	34.19	34.94	-.75
46/741	81.6	6.0	1.1	3.4	7.8	6.5	34.53	35.19	-.66
46/742	81.4	5.8	1.1	3.3	8.5	1.8	34.25	34.61	-.36
46/743	82.1	5.6	1.1	2.7	8.5	1.8	34.31	34.64	-.32
46/744	83.4	5.7	1.2	1.7	8.0	6.5	34.40	35.10	-.70
46/745	82.7	5.7	1.2	1.3	9.2	0.6	34.28	34.65	-.37
46/746	82.7	5.6	1.1	1.2	9.4	0.2	34.28	34.54	-.26
46/747	82.7	5.6	1.2	1.2	9.3	0.8	34.26	34.54	-.28
46/748	82.9	5.6	1.1	1.1	9.3	0.4	34.25	34.58	-.33
46/749	83.9	5.7	1.1	1.0	8.2	3.2	34.44	35.25	-.82
46/847	83.9	6.0	1.1	3.1	5.9	9.3	35.99	36.15	-.16
46/835	82.9	6.3	1.0	2.9	6.8	9.8	35.71	36.12	-.41
46/836	83.4	6.1	1.0	3.3	6.1	2.3	35.53	36.15	-.63
46/837	83.3	6.1	1.1	3.0	6.5	2.8	35.35	35.94	-.59
46/838	84.1	6.2	1.0	2.4	6.3	1.1	35.92	36.33	-.41
46/839	85.3	6.3	0.9	1.6	5.8	1.3	36.14	36.88	-.73
46/840	85.2	6.1	1.0	1.1	6.5	3.8	35.74	36.48	-.74
46/841	84.1	6.1	1.0	1.4	7.4	2.3	35.86	36.03	-.17
46/842	83.4	6.1	1.1	2.2	7.3	5.6	35.59	35.77	-.18
46/843	84.1	6.1	0.9	3.0	5.9	2.0	36.10	36.35	-.25
46/945	81.7	6.3	1.0	3.3	7.8	48.0	33.28	35.59	-2.31
46/844	84.0	6.2	0.9	3.8	5.1	1.8	36.26	36.64	-.39
46/845	85.0	6.3	0.9	3.9	3.8	3.4	36.49	37.28	-.79
46/846	85.6	6.4	0.8	3.6	3.5	13.4	37.07	37.66	-.59
46/919	87.6	5.7	1.1	0.7	5.0	15.0	36.05	36.76	-.70
46/920	88.7	5.8	1.2	0.6	3.7	23.6	36.83	37.46	-.63
46/921	88.4	5.8	1.3	0.7	3.9	23.3	36.59	37.31	-.72
46/922	87.1	5.9	1.1	0.9	4.9	19.7	36.23	37.01	-.78
46/923	88.5	6.0	1.4	0.4	3.7	22.0	37.01	37.64	-.63
46/924	87.6	6.0	1.4	0.3	4.7	13.4	36.52	37.21	-.68

5.1.1 Discussion of the Mott-Spooner Test Results

The Mott-Spooner test can be used to suggest the presence of analytical error, evaluate mineral matter approximation formulae, and demonstrate provincial differences in coal structure. These applications are discussed below.

(i) detection of analytical errors

Where the difference between the experimental and calculated specific energy is large, this difference can sometimes be attributed to analytical error. Given *et al.*, (1986) suggest that where the absolute MSD exceeds 250 BTU/lb (0.58 MJ/kg) the analytical data are probably wrong, but caution that no precise limits of acceptability can be stated. Most of the samples listed in Table 5.1 exceed this limit and all show a negative MSD. Although the consistently negative MSD values may suggest the presence of systematic analytical bias it does not prove it. Because values from eleven different analyses are used in the Mott-Spooner test detection of significant bias in one or more of the analyses is difficult. Nonetheless, it is possible to examine the relative importance of some of the analytical values and suggest likely sources of error. For example, the reproducibility of carbon, hydrogen, and nitrogen determinations are reported to be 0.3% C, 0.15% H, and 0.1% N (BS1016, part 16) and correspond to changes in the calculated specific energy of 0.14, 0.23, and 0.01 MJ/kg respectively. Furthermore, reproducibility of the determined specific energy is reported as 0.30 MJ/kg. If these reproducibility values are considered as indicators of the relative likelihood of analytical bias then systematic bias in the determination of specific energy or hydrogen rather than carbon and nitrogen more easily accounts for the consistently negative MSD values. However, BS1016 part 16 (p.6) states, "[systematic errors] can be detected and measured only by comparing results with a known true value or with the result obtained by a method known to be accurate." This task is outside the scope of this thesis. Nevertheless, examination of unpublished, international round robin laboratory exchanges show no indication of consistently high hydrogen values or low specific energy values for the laboratory employed in this study (CRANZ). Furthermore, using a completely different data set, Suggate (1959) also observed consistently high calculated values of specific energy for some New Zealand coals using the equation presented by Mott and Spooner (1940). Thus, despite the consistently negative MSD values, the presence of systematic bias in the data set is doubtful.

(ii) inappropriate mineral correction formulae

Provided the raw data are accurate, the difference between the measured and calculated specific energy will be minimized where the effect of mineral matter is properly accounted for. Given and Yarzab (1975, p.21) note, "In a large set of analyses it [MSD] can be used to test the validity of various bases for reporting the data." They go on to show systematic variation of MSD values due to inaccurate mineral matter approximation formulae. This approach to validate mineral approximation formulae is not considered here since complete data are available for only 32 samples. However, many of the samples listed in Table 5.1 have negligible mineral matter and no significant correlation between MSD and ash content or any other variable was noted. Thus, it is unlikely that the consistently negative MSD values can be attributed to an inappropriate mineral matter correction formulae. Nonetheless the Mott-Spooner test is not appropriate where mineral matter content is high; Examination of Table 5.1 shows that 46/750 and 46/945 report mineral matter contents of 37 and 48% and the largest MSD values (-0.97 and -2.31 respectively).

(iii) enthalpy of decomposition

Since both the analytical data and the mineral correction formula appear valid then the consistently low MSD values must be due to provincial variation in the enthalpy of decomposition. The enthalpy of decomposition is related to the enthalpy of formation of a compound. The total heat released by a compound upon combustion will equal the summation of the energy due to the individual elements minus the heat of formation (ΔH_f) of the compound ($-\Delta H_f$ = enthalpy of decomposition). Because Equation 5.8 is based on theoretical constants rather than empirically derived values, the average enthalpy of decomposition for a set of coals can be estimated. The enthalpy of decomposition is represented by the last term in Equation 5.8.

The enthalpy of decomposition for a single coal can be calculated by omitting the last term in equation 5.8 and subtracting the result from the determined specific energy. In consideration of the analytical precision associated

with the various analytical determinations, the result for a single coal is meaningless. However, an average value for a set of coals provides a reasonable estimate of the enthalpy of decomposition for the set as a whole. The average enthalpy of decomposition calculated for coals listed in Table 5.1 with less than 10% ash (23 samples) is 0.16 MJ/kg (which is 0.48 MJ/kg less than the "global" term shown in equation 5.8). All of these coals are from Brunner coal measures at Pike River coalfield and the Upper Waimangaroa sector in the Buller coalfield. Figure 5.1 shows the average enthalpy of decomposition for these coals compared to some US coals.

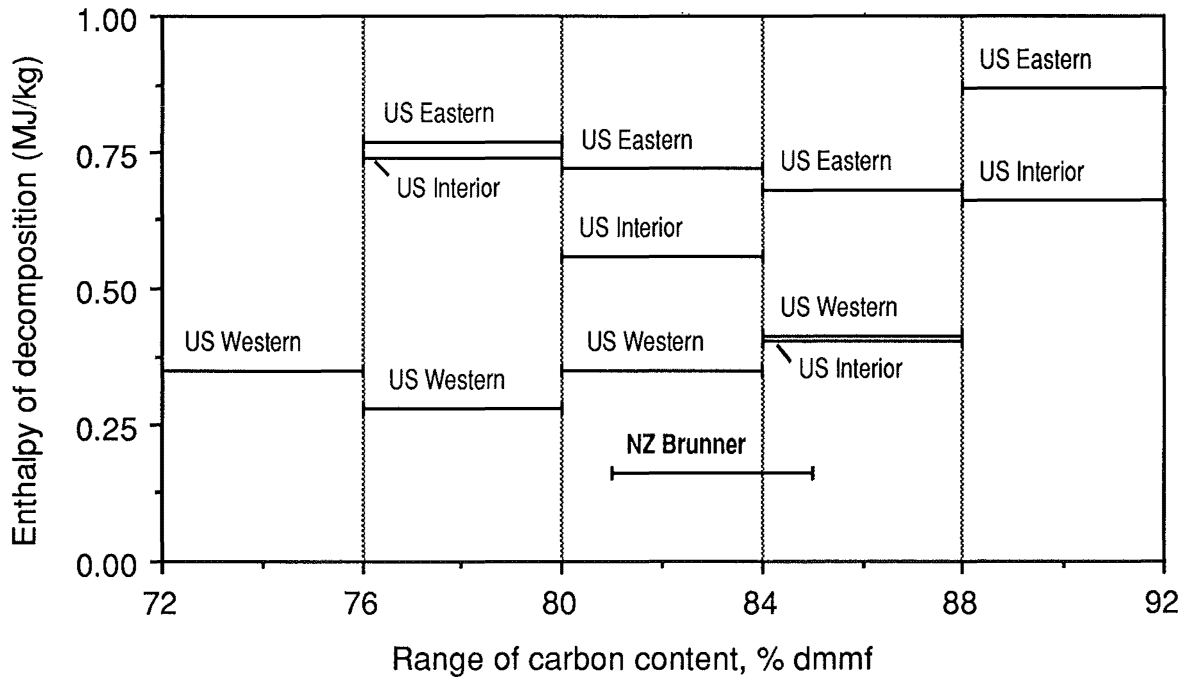

Figure 5.1 Comparison of the enthalpy of decomposition of some New Zealand and US bituminous coals classified by rank and province (adapted from Given *et al.*, 1986).

5.2 SIGNIFICANCE OF THE ENTHALPY OF DECOMPOSITION

The comparatively low enthalpy of decomposition of the New Zealand coals as shown in Figure 5.1 illustrates both similarities and differences with US coals. The Eocene age New Zealand coals plot near coals from the western (largely late Cretaceous age) and interior (Carboniferous) United States. The New Zealand coals plot farthest from coals from the eastern US (Carboniferous age). The relative parity with western US coals compared to eastern US coals might be a

consequence of the respective paleo-floral assemblages of these coals. Carboniferous age coal-forming plants tended to be lignin rich compared to the cellulose rich plants that contibuted to late Cretaceous and Tertiary coals. This idea is supported by the abundant fungal sclerotinite in these New Zealand coals which averaged 0.3% compared to 0.0%, 0.03%, and 0.1% sclerotinite for Carboniferous, late Cretaceous, and Tertiary age US coals respectively (Robinson, 1990). The New Zealand coals are also similar to typically high sulphur Carboniferous age coals from the interior US. Damberger (1974) concludes that Illinois basin coals (interior US) were coalified at a shallow depth compared to similar rank coals from Pennsylvania (eastern US). The New Zealand coals may also have experienced a comparatively high geothermal gradient; how variation in the geothermal gradient might effect the enthalpy of decomposition is not clear. The New Zealand coals considered here report an average organic sulphur (dmmf) content of 2.4%; interior US coals are typically rich in organic sulphur. Thus, a comparatively low enthalpy of decomposition might be explained as a consequence of organic sulphur enrichment where significant amounts of sulphur are present as thermally labile sulphides. Finally, the low inertinite contents of these New Zealand coals (avg. < 2%) may also have contributed to the observed low enthalpy of decomposition. Since the heat of formation increases with aromaticity (Given *et al.*, 1986), and inertinite group macerals are more aromatic than vitrinite and liptinite macerals (Choi *et al.*, 1989), the enthalpy of decomposition should increase where inertinite is high and decrease where inertinite is low.

5.2.1 Coal Structure and the Enthalpy of Decomposition

The low enthalpy of decomposition of the New Zealand coals shown in Figure 5.1 can be used to suggest variation in coal structure. The lower bond energy of New Zealand coal suggests that they should decompose at lower temperatures compared to US coals. Figure 5.2 compares the initial Gieseler softening temperatures of the New Zealand coals with the initial Gieseler softening temperatures of some US coals. Although there is some overlap, Figure 5.2 shows

that the New Zealand coals collectively exhibit a comparatively low initial softening temperature at equivalent carbon content.

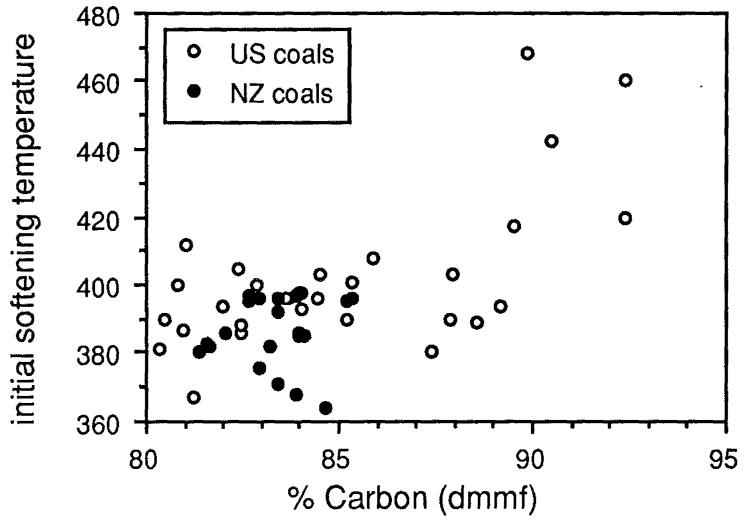

Figure.5.2 Scatterplot showing how the initial Gieseler softening temperature of selected New Zealand coals compares to some US coals. New Zealand coals are those listed in Table 5.1 where ash is <10% ; US coal data courtesy of Penn State Coal Data Base.

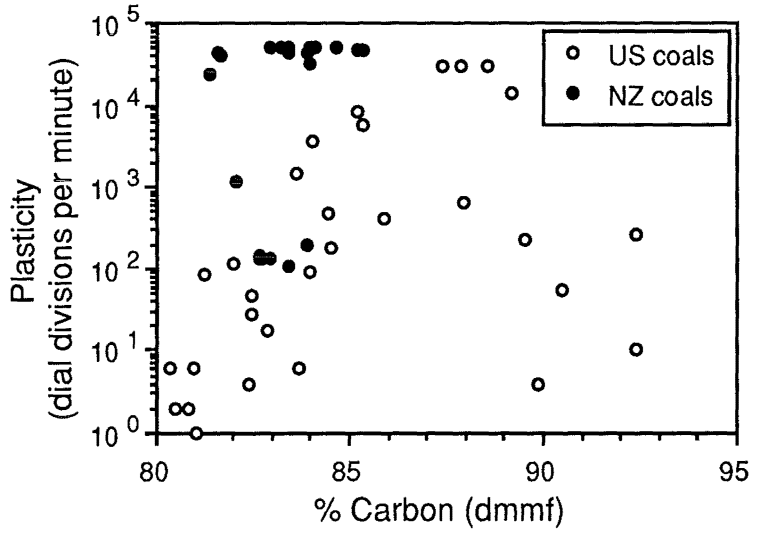

Figure 5.3 Scatterplot showing how the Gieseler fluidity of selected New Zealand coals compares to some US coals. New Zealand coals are those listed in Table 5.1 where ash is <10% ; US coal data courtesy of Penn State Coal Data Base.

Given *et al.*, (1986) showed that the heat of formation of hydrocarbons increases with aromaticity which suggests that the New Zealand coals listed in Table 5.1 are less aromatic than US coals. Thus these New Zealand coals should possess a comparatively large amount of mobile phase material rather than the more aromatic network phase. Lin *et al.*, (1986) have related the concept of

mobile phase to the development of thermoplasticity; as mobile phase material increases, thermoplasticity is enhanced. The higher plasticity of these New Zealand coals compared to US coals of equivalent carbon content is shown in Figure 5.3 and supports this interpretation.

5.3 CORRELATIONS WITH ASH COMPOSITION

Another way that analytical data can be examined is by comparing two different measurements that vary largely in response to a single property. For example, the amount of CO_2 evolved upon mixing the coal with acid should correlate with the amount of Ca and Mg in fresh bituminous rank coal where Ca and Mg occur in carbonate minerals. Figure 5.4 compares the calculated CO_3 in dry coal with Ca plus Mg in dry coal. The data show a reasonable correlation about a line of stoichiometric equivalence. The sample plotting highest above the line corresponds to the rider seam encountered in drillhole 1494 (sample 46/750) and reports 32% ash. How does the extra calcium and magnesium occur in sample 46/750? This sample contains a relatively high amount of phosphorus (0.79% in dry coal). Since phosphorus is reported to occur in crandallite ($CaAl_3(PO_4)_2(OH)\cdot H_2O$) in New Zealand bituminous coals (Newman 1988) the amount of calcium associated with the calculated crandallite abundance for sample 46/750 (assuming all phosphorus is present in crandallite) was subtracted from the total calcium in coal and the sample replotted. As can be seen in Figure 5.4 the deviation of sample 46/750 from the line is not due solely to the presence of crandallite. In this instance the excess Ca and Mg is probably associated with clay minerals. Other samples from DH-1494 deviate from the equivalence line where carbonate is low, and the detection limit for CO_2 determination is approached. The precision of the CO_2 determination is reported to be ±0.035 % (absolute) and the average CO_2 yields from samples in Buller DH-1494, Pike River DH-7 Paparoa coal measures, and Pike River DH-7 Brunner coal measures are 0.03%, 0.46%, and 2.72% respectively. Thus the deviation of the DH-1494 samples (shown as open circles in Figure 5.4) is explained as a consequence of analytical precision rather than intrinsic variation of the coals.

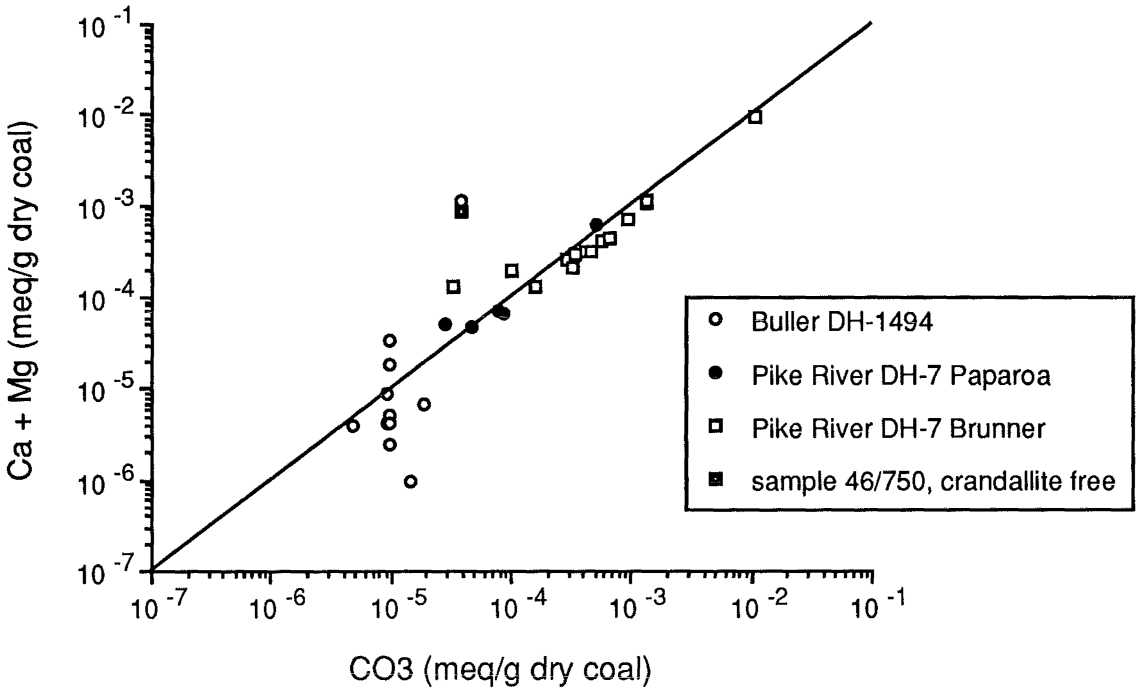

Figure 5.4 Scatterplot showing how calcium plus magnesium vary with carbonate in dry coal for coal samples. DH-1494 are ply samples Upper Waimangaroa sector Buller Coalfield; DH-7 are whole seam samples from the Paparoa coal measures and ply samples from the Brunner coal measures, Pike River coalfield; Sample 46/750 is an outlier and is also plotted (adjacent point) on a crandallite free basis.

Where iron carbonates (ankerite, ferrous dolomite, siderite) are low, the amount of iron in coal should correlate with the pyritic sulphur content of fresh coal. Using data from Sheat (1984), N. Newman (1988) reported that the correlation between iron and the sum of sulphate and pyritic sulphur more closely approximates the stoichiometric composition of pyrite than the correlation obtained where iron is plotted against pyritic sulphur alone. Newman considered that sulphide minerals are the only significant source of iron in low-ash un-oxidized coals from the Webb-Baynes area of the Buller coalfield. For the coals considered in this thesis sulphate sulphur is low (average 0.01%, max 0.03%) compared to Sheat's data (average 0.08%, max 0.23%). Figure 5.5 shows iron in coal plotted against pyritic sulphur. A similar plot (not shown) where iron is plotted against the sum of sulphate and pyritic sulphur shows no significant differences. The "ideal" line drawn on the plot corresponds to the stoichiometric composition of FeS_2 expressed in weight percent. Two additional lines drawn on the plot correspond to the allowable error (repeatability) for the determination of

pyritic sulphur which is reported as ±0.035% where $S_{pyritic}$ <0.5% and ±0.047% where $S_{pyritic}$ >0.5% (BS1016, part 16). Examination of Figure 5.5 shows a close correspondence between the two variables for Brunner coals from the Pike River and Buller coalfields. The single coal that plots clearly above the upper error line does not report enough iron to account for the measured amount of pyrite. Analytical error is more difficult to assess where coals plot below the lower error line. For example, samples from the Paparoa coal measures in the Pike River coalfield fall below the line and may contain siderite which is abundant in Paparoa coals in the nearby Greymouth coalfield (N. Newman 1988). Other possible sources of iron include chlorite and illite which have been identified in both Brunner and Paparoa coal measures (Pankhurst *et al.*, 1986).

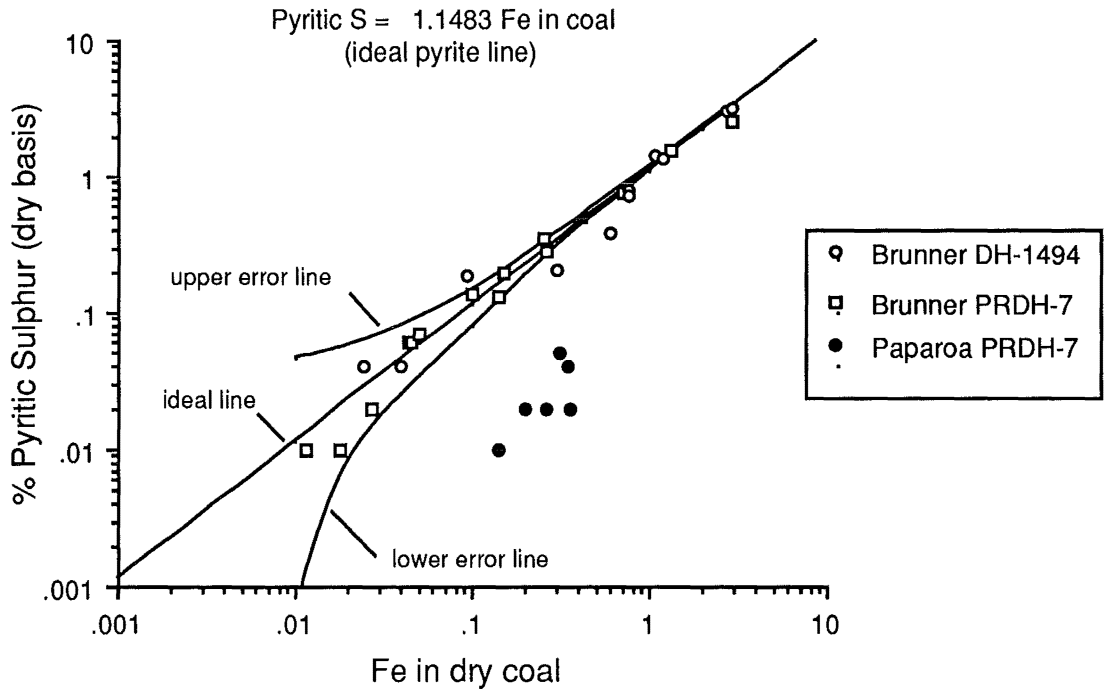

Figure 5.5 Scatterplot showing how the weight percent pyritic sulphur in dry coal varies with the weight percent iron in dry coal. The coal samples plotted are; DH-1494 ply samples Upper Waimangaroa sector Buller Coalfield; PRDH-7 whole seam samples from the Paparoa coal measures and ply samples from the Brunner coal measures, Pike River coalfield.

The calculations used for expression of an inorganic element on a whole coal basis (e.g., Ca and Mg in Figure 5.4 and Fe in Figure 5.5) were undertaken based on the weight percent of the respective oxide determined in an ash

specimen prepared at the University of Canterbury and the weight percent dry ash reported by CRANZ laboratories. Consequently, errors due to variable amounts of sulphate in ash due to differences in ashing conditions in the two laboratories are likely. Regardless of the vagaries of sulphate fixation, analytical error in the determination of the elemental composition of coal ash is indicated where the sum of the oxides is greater than 100% and suggested where the sum is significantly less than 100%. Analytical bias is also suggested where one or more elements correlate with the sum. This approach was found useful to verify the oxide composition determined by XRF spectroscopy in this thesis. Significantly improved results were obtained where additional standards were used so that the compositional range of the standards approximated the compositional range of the specimens.

5.4 LIMITATIONS OF POINT COUNT ANALYSES

Maceral analysis, staining analysis, etching analysis, and carbon texture analysis are all based on counting the occurrence of constituents observed under the microscope during incremental traverses of polished particle mounts (point counting). The historical development and theoretical basis of point counting is reviewed by Galehouse (1971). Bustin (1991) investigated the influence of point-counting methodology on the precision and accuracy of maceral analysis. Other factors that influence the precision and accuracy of point count analyses include representative sampling, sample division and sample preparation. This section is limited to discussion of the theoretical precision associated with point counting technique.

5.4.1 Precision of Point Count Analysis

The theoretical precision associated with the measured volume percent of a maceral depends on the total number of points encountered during the incremental traverse of the polished particle mount, and the determined volume % of the component. According to methods AS-2856 and ISO-7404/3, the

theoretical standard deviation (σ_t) for a single maceral component can be calculated as:

$$\sigma_t = \sqrt{\frac{p(100 - p)}{n}} \qquad \text{(eq. 5.10)}$$

where p is the percentage of counts registered for a component and n is the total number of points counted. Equation 5.10 is based on a normal distribution and assumes negligible errors in maceral identification and random sampling. For components in proportions between 10 and 90% the probable error at 95% confidence (E_{95}) can be calculated as:

$$E_{95} = 2(\sigma_t) \qquad \text{(eq. 5.11)}$$

The maximum difference between repeated analyses by the same operator on the same polished surface, using the same microscope, at the 95% confidence interval (19 out of 20 analyses) is called the repeatability and is calculated as:

$$\text{repeatability at 95\% confidence} = \left(2\sqrt{2}\right)\sigma_t \qquad \text{(eq. 5.12)}$$

For components present in proportions below 10% and above 90% estimation of confidence limits based on normal distribution statistics (eq. 5.10) are increasingly inaccurate; in this range Poisson distributions can be used. However, Poisson distribution statistics fail as component proportions approach 50%. Furthermore both normal and Poisson distribution statistical methods to estimate confidence limits are increasingly inaccurate as the total number of counts grows small. As explained by Burstein (1971) only the binomial distribution model provides exact confidence limits at stated confidence levels. He adds (p.4) that estimation of precision according to the "binomial distribution entails laborious calculations". For this reason he provides tables and simple formulae that permit determination of binomial confidence levels with a relative accuracy of at least 0.999 for any sample size at six different confidence levels.

Table 5.2 shows the theoretical standard deviation, probable error, and repeatability for different maceral proportions calculated by Equations 5.10, 5.11, and 5.12, at 95% confidence for an analysis of 500 total counts. Also shown in Table 5.2 are the corresponding upper and lower binomial confidence limits

calculated using the method and tables of Burstein (1971). Burstein's method also allows for the singular determination of upper or lower confidence levels (the levels shown in Table 5.2 are the two-sided confidence levels). The use of one-sided confidence levels is applicable to situations where petrography is used to check that a feedstock component does not exceed or fall below a specified threshold.

TABLE 5.2
CALCULATED ESTIMATES OF PRECISION FOR DIFFERENT MACERAL ABUNDANCES (95% CONFIDENCE, N=500 COUNTS)

Measured % of a component	Theoretical Standard Deviation eq. 5.10	Probable Error at 95% Confidence eq. 5.11	Repeatability eq. 5.12	Lower 95 % Confidence Limit (Burstein, 1971)	Upper 95% Confidence Limit (Burstein, 1971)
2	0.6*	1.3*	1.8*	1.0	3.6
5	1.0*	1.9*	2.8*	3.3	7.3
10	1.3	2.7	3.8	7.5	13.0
25	1.9	3.9	5.5	21.3	29.0
50	2.2	4.5	6.3	45.5	54.5
75	1.9	3.9	5.5	71.0	78.7
90	1.3	2.7	3.8	87.0	92.5
95	1.0*	1.9*	2.8*	92.7	96.7
98	0.6*	1.3*	1.8*	96.4	99.0

*Values Doubtful

It should be noted that the precision shown in Table 5.2 is the theoretical limit that can be attained; the precision can only be improved by increasing the total number of counts. For example, using the method of Burstein (1971) if 1000 counts are made (n=1000), the lower and upper 95% confidence limits for a component present at 25 volume percent are 22.3 and 27.8 compared to 21.3 and 29.0 shown in Table 5.2 where n=500. Recommendations regarding the total number of points that should be counted vary. Both AS-2856 and ISO-7404/3 recommend a total of 500 counts be obtained and use equations 5.10 and 5.12 to obtain repeatability values. The ASTM method D-2799 requires a minimum of two separate analyses of 1,000 counts (2,000 total counts). If the mean variation of the components is greater than 2% a third set of 1,000 is required and the two sets with less than 2% mean variation are averaged and reported (or all 3 sets are averaged). The mean variation ($\Delta \overline{V}$) is calculated by;

$$\Delta \overline{V} = (\Delta V_{vitrinite} + \Delta V_{exinite} + \Delta V_{resinite} + \Delta V_{micrinite} + \Delta V_{semifusinite} + \Delta V_{fusinite})/6 \qquad \text{(eq. 5.13)}$$

where ΔV of the listed macerals is simply the difference between the volume percent of the individual macerals determined on each set of 1000 counts. The ASTM

method may appear to offer greater precision due to the larger number of total counts required. However the standard allows a Whipple graticule to be used and 4 points (separated by 100 μm on the image plane) to be counted for each field of view, provided a total magnification of 400X is obtained. Since all 4 counts can be recorded even if the 4 points fall on the same particle of coal, the total number of particles examined is not much greater than the 500 counted if a single crosshair were used. Further, if a Whipple disk is used more than 1 count will inevitably be recorded on a single particle of coal where the size of the particles significantly exceed 0.1 mm. Thus random sampling is not assured and no statement of precision is possible. Indeed, Equation 5.13 offers no assurance as to the precision attained and is provided only as a guide to the analyst. The likelihood of counting a single particle more than once is less where only one count is registered per field of view but not eliminated since all of the published standards reviewed here recommend a point to point and line to line distance less than the maximum particle size.

Since the identification of macerals is subjective it is not surprising that the observed reproducibility of maceral analysis between different operators or laboratories is reported to be 1.5 to 2 times greater than the calculated repeatability for a single component (AS-2856). Furthermore, although the theoretical precision increases with the number of points counted, individual bias in the identification of macerals limits the accuracy of the technique. Using artificial coal blends, Bustin (1991) has shown that the errors associated with the identification of components are so great that no improvement in accuracy was observed after as few as 200 counts.

5.5 LIMITATIONS OF GIESELER FLUIDITY

Callcott (1987) notes that the imprecision of the Gieseler plasticity test is "notorious". This imprecision is recognized to be largely due to the sensitivity of the test to weathering and sample deterioration in the laboratory (section 2.10.4 iii). This sensitivity is implicit in the test method (ASTM-2639-74); it requires mild drying and prompt analysis of the sample to minimize alteration of thermoplastic

properties. A further limitation, which appears to be significant for some New Zealand coals, is suggested here. In order to explain the problem, part of the apparatus used for determination of Gieseler fluidity (Figure 5.6) as well as the values reported by the method are briefly described. A comprehensive description of the method is provided in ASTM D-2639-74.

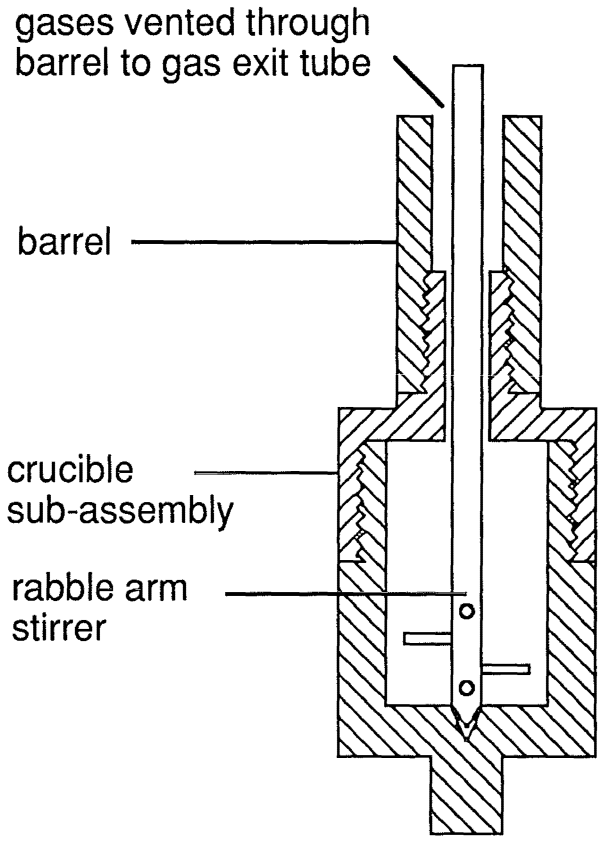

Figure 5.6 Illustration showing a cross section of the crucible sub-assembly, rabble arm stirrer, and barrel components of the Gieseler plastometer.

5.5.1 Description of the Gieseler Fluidity Test

The Gieseler fluidity test reports diagnostic values obtained by measuring the response of a 5 g, minus 425 um coal charge that is heated at 3 °C/min from 350 to more than 500 °C. The coal is packed in a crucible around a rabble arm stirrer to which 40 g of torque is applied (Figure 5.6). The five grams of packed coal cover the stirrer rabble arms and about half of the crucible remains empty. As the coal charge is heated it softens and the rabble arm stirrer turns; one revolution equals 100 dial divisions. The temperature and dial divisions of

movement are recorded at one minute intervals. The diagnostic values reported by the test are defined as follows.

Initial Softening Temperature is the temperature where continuous movement of the dial begins.

Maximum Fluid Temperature is the temperature that corresponds to the highest rate of dial movement.

Solidification Temperature is the temperature where dial movement stops.

Maximum Fluidity reports the highest rate of dial movement recorded for a one minute interval and is expressed in dial divisions per minute (ddpm).

Fluid Temperature Range is sometimes reported and corresponds to the temperature interval of continuous dial movement.

The test is done in duplicate and provided that the diagnostic test parameters agree within prescribed limits the average values of the duplicates are reported. Where duplicate analyses disagree repeated determinations are required. Although the diagnostic values calculated from duplicate or multiple analyses are useful, it is instructive to examine the raw data from a single test run. These data can be presented in a plot that shows variation in dial movement with increasing temperature. For example, Figure 5.7 shows the steady increase and subsequent decline of ddpm with increasing temperature.

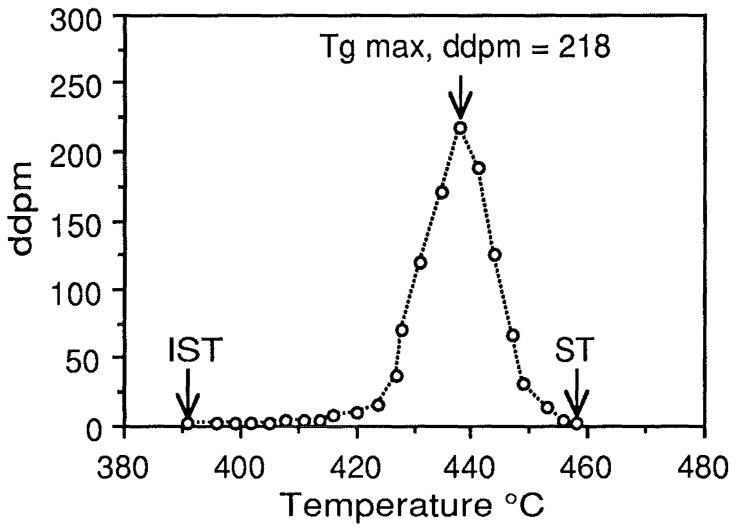

Figure 5.7 Plot showing the rise in dial division per minute (ddpm) movement with increasing temperature for coal sample 46/745. The notations correspond to the initial softening temperature (IST), maximum fluid temperature (Tg max), solidification temperature (ST) and the maximum fluidity expressed as dial divisions per minute (ddpm).

5.5.2 A Problem with Gieseler Fluidity

During the course of this study relationships between the various characteristic values reported by the Gieseler test and other measured properties were sought. For example, Habermehl *et al.*, (1981) reports that Tg max varies with rank. Likewise, vitrinite reflectance is a useful rank parameter. The relationship between these two parameters for some US and New Zealand coals is shown in Figure 5.8. The departure of certain New Zealand coals, (samples from the Buller and Pike River coalfields, Ro max near 0.65 in Figure 5.8), from the regression line established for US coals supports the idea of anomalous (low) vitrinite reflectance for some New Zealand coals (Newman and Newman, 1982, Newman, 1987). This demonstration of provincial behaviour suggested that the reflectance vs Tg max scatterplot might allow identification of coals with anomalous reflectance. Furthermore, the potential use of Tg max as a rank parameter was considered. For this reason the relationship shown in Figure 5.8 was examined in more detail.

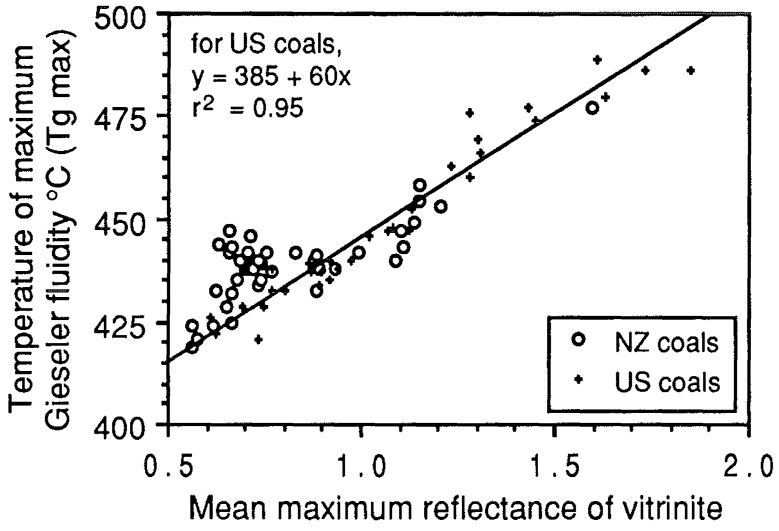

Figure 5.8 Mean maximum vitrinite reflectance vs temperature of maximum Gieseler fluidity (Tg max) for US and New Zealand (NZ) coals. The correlation line is from linear regression on reflectance and Tg max for 32 US whole-seam coals (US data courtesy of Penn State Coal Data Base).

Figure 5.9 shows a significant correlation between Tg max and vitrinite reflectance for serial ply samples from a seam encountered in Buller drillhole 1494 and a lack of correlation between vitrinite reflectance and Tg max for serial

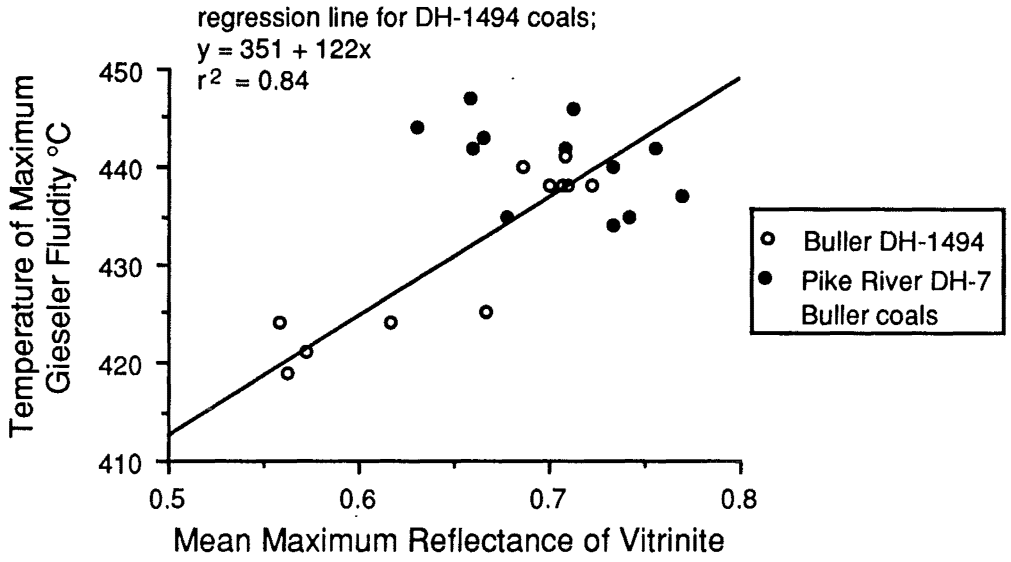

Figure 5.9 Relationship between mean maximum reflectance of vitrinite and the temperature of maximum gieseler fluidity for serial ply samples in seams encountered in drillhole 1494 (Buller coalfield, Upper Waimangaroa sector) and drillhole 7 (Brunner coal measures, Pike River coalfield). The linear regression line is for samples from DH-1494 only.

ply samples from a seam encountered in Pike River drillhole 7. Examination of the raw data for the Gieseler analyses suggested an explanation for the different behaviours of coals from drillhole 1494 and drillhole 7 shown in Figure 5.9. Figure 5.10 shows how the Gieseler dial rotation varied with increasing temperature for a single test of sample 46/741. The bi-modal profile shown in Figure 5.10 contrasts with a more "typical" profile shown in Figure 5.7. Kirov and Stephens (1967) note that the Gieseler test is misleading for some high swelling coals; Figure 5.10 verifies their concern although crucible swelling is a poor predictor of potential problems since sample 46/741 reports a crucible swelling index of only 4.5. It is suggested that the reason for the irregular profile relates to the insufficient head space in the crucible sub-assembly to accommodate the swollen coal mass during the test. Upon heating, the coal softens and swells and the stirrer begins to rotate. If the swollen coal mass exceeds the capacity of the crucible sub-assembly it forces coal into the retort barrel (Figure 5.6) that creates additional friction and slows the rate of dial rotation. Here, excessive swelling may have occurred prior to extensive formation of a plastic phase and solids were carried along with the plastic coal into the barrel. Alternately, a swollen but entirely plastic mass may have been extruded into the barrel. By whatever

mechanism the dip in the rate of dial rotation shown in Figure 5.10 is suggested to be a consequence the coal and/or plastic mass swelling into the barrel. The net result is a "low" value of Tg max compared to what might have been recorded with no swelling into the barrel.

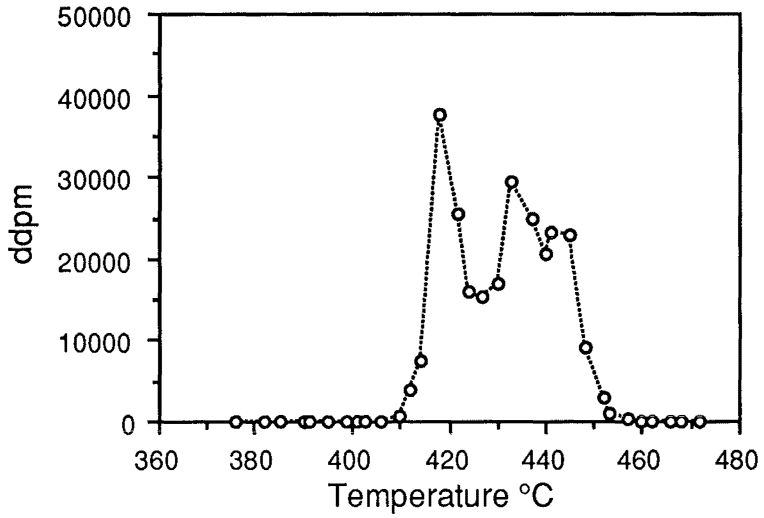

Figure 5.10 Plot showing the irregular rise in dial division per minute (ddpm) movement with increasing temperature for coal sample 46/741.

Upon examination of the raw data, bimodal patterns were observed in 21 out of 31 cases. In most instances Tg max was not affected since the ddpm peaked after the initial dip. However, all of the DH-1494 samples in Figure 5.9 with Tg max values less than 430 °C showed irregular ddpm/temperature profiles like that shown in Figure 5.10. Therefore, the correlation shown in Figure 5.9 is suggested to be an artifact of the test method. The reason for an erratic ddpm - temperature profile exhibited by some coals and not by others is not known but may relate to a combined effect of high vitrinite content, high organic sulphur content, and hvbB-hvAb rank coals. In these instances the sulphur may have formed crosslinks, increasing the viscosity of an early formed thermoplastic phase which impeded the migration of gaseous volatile matter and induced swelling. Such crosslinking reactions are favoured by the relatively low heating rate (Derbyshire *et al.*, 1989) used in the Gieseler test compared to the crucible swelling test and may explain why the crucible swelling of the affected coals is not appreciably different than the unaffected coals from drillhole 1494.

Regardless of the underlying cause, "swelling into the barrel" is suggested to sometimes bring about an anomalously low temperature of maximum fluidity. Because the effect cannot be predicted the results of the Gieseler test should be annotated to indicate where an erratic ddpm-temperature profile has occurred and the significance of Tmax judged accordingly. It is more difficult to determine if swelling into the barrel has perturbed other values reported by the Gieseler test. In some cases ddpm appears to have been slightly lowered, but the other values appear largely unaffected. Finally it should be noted that the anomalously low Tmax suggested to be caused by "swelling into the barrel" does not explain the sometimes high temperature of maximum fluidity for some New Zealand coals compared to US coals of equivalent reflectance (Figure 5.8).

5.6 LIMITATIONS OF AIR-DRIED MOISTURE ANALYSIS

The moisture content of coal is used to evaluate rank and has direct significance for evaluation of industrial behaviour. The simplicity of the measurement of moisture belies the sensitivity of this parameter to variation due to sample handling and preparation. Suggate (1956a) showed that day to day variation of temperature and relative humidity in the laboratory precludes a reproducible moisture determination. To provide reproducible results the use of standardized conditions (20 °C, 70% relative humidity) were adopted by the New Zealand Dominion Laboratories for the routine determination of "air-dried" moisture; this practice is continued by the Coal Research Association of New Zealand today. The following discussion is not intended to disparage the use of air-dried moisture for routine analyses but to point out the limitations of air-dried moisture values for evaluation of coal rank or industrial behaviour.

The use of air-dried moisture to estimate moisture holding capacity (equation 2.3) is misleading where moisture holding capacity is used as a surrogate for bed moisture. Figure 5.11 shows that equation 2.3 significantly underestimated the total moisture content of both stockpile samples and rapidly processed fresh core samples even if increased by 1.4% (suggested by Gray 1983). The failure of equation 2.3 to predict the total moisture content of the coals

examined in this thesis suggests that a dependable relationship between air-dried moisture and bed moisture is probably unattainable. Because bed moisture is an important but inconvenient rank parameter, equilibrium moisture may be used as a proxy for bed moisture of bituminous and subbituminous rank coal. For this purpose determination of equilibrium moisture in accordance with Australian or ASTM standard methods, rather than determination of moisture holding capacity by the less rigourous British or ISO method, is suggested.

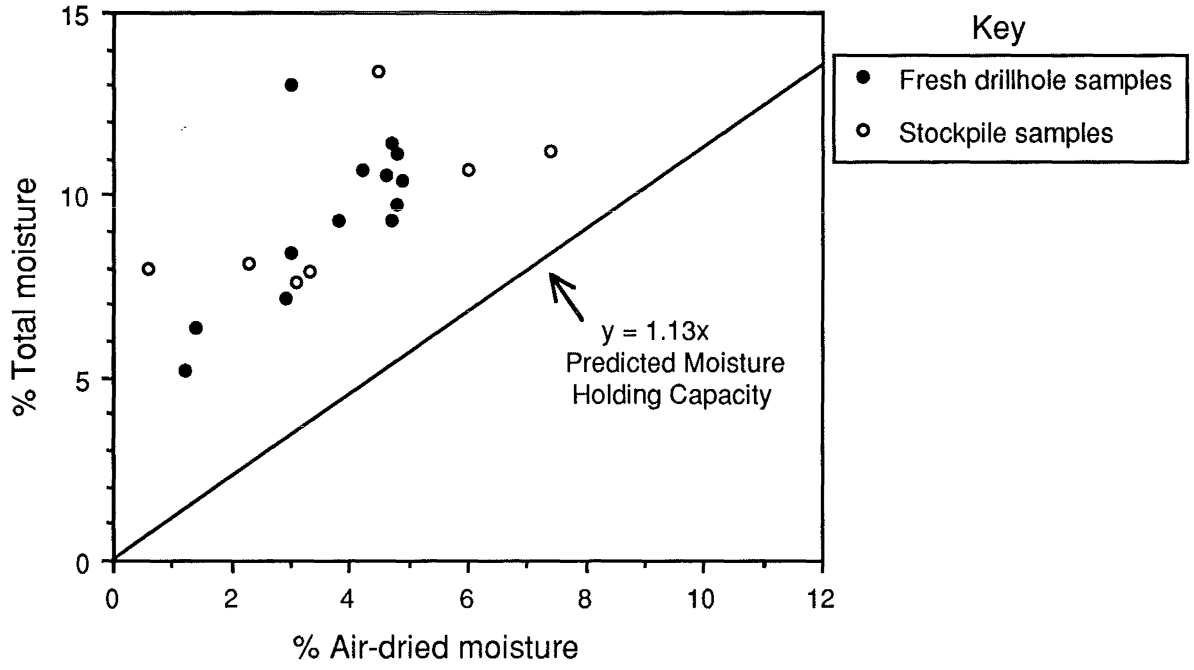

Figure 5.11 Relationship between Air-dried moisture and Total Moisture observed for some bituminous New Zealand coals compared to the predicted relationship (equation 2.3 from Gray, 1983) between Air-dried moisture and Moisture holding capacity.

5.7 SUMMARY

Analytical data collected in this study were evaluated by the Mott-Spooner test and scatterplots where inorganic compositional data were compared. These tests successfully identified errors in the data set. For example, relationships shown in Figures 5.4 and 5.5 were significantly improved where the compositional range of the standards approximated the compositional range of the specimens (original data not shown). More importantly the tests allow interpretation and

provide insight into the nature of the subject coals (e.g., the comparatively low enthalpy of decomposition of New Zealand coals listed in Table 5.1).

The precision of analyses based on point counting techniques has also been discussed. This discussion has significance where data obtained by point counting are used in chapter six to predict industrial carbonization behaviour.

Low Gieseler Tmax values, presumably caused by swelling of the coal into the retort barrel, obscures the significance of this potential rank parameter. Likewise, it appears doubtful that a reliable relationship between air-dried moisture and equilibrium moisture is possible.

CHAPTER SIX
EVALUATION OF NEW ZEALAND COALS FOR CARBONIZATION

This chapter examines the predicted and observed carbonization behaviour of some New Zealand bituminous coals. Carbonization behaviour is predicted based on established methods. The applicability of these methods to New Zealand coals is suggested to be limited where perhydrous or weathered vitrinite is encountered and the use of fluorometric analysis is advocated to account for these occurrences. Finally, relationships between coal properties and observed carbonization behaviour are examined. The combined use of reflectance and fluorometric analysis to predict diverse measures of carbonization and pyrolysis behaviour is demonstrated.

6.1 PREDICTION OF THE COKING QUALITY OF NEW ZEALAND COALS.

Because commercial performance testing is expensive, predictive calculations are sometimes used to evaluate the coking behaviour of individual coals and hypothetical coal blends. These methods are generally successful where applied to coals that are similar to those used to establish the predictive formula but, as the following discussion will illustrate, are likely to fail if applied to dissimilar coals. However, as noted by Brown *et al.*, (1982) even where the inadequacy of a predictive method can be shown this does not necessarily mean that there are no systematic relationships between the variables used in the method and coke quality.

Many of the coal samples examined in this thesis are thin ply samples and are atypical of the coal product that would be produced if an entire seam or bench were mined. These narrow ply samples would be difficult to acquire in a quantity sufficient for an actual commercial performance test. Consequently, the results of the predictive calculations discussed here would be difficult to verify. Nonetheless, thin ply samples offer advantages where relationships between coal properties and carbonization behaviour are sought. Figure 6.1 shows a reflectance histogram for the whole seam encountered in drillhole 1481 (Brunner coalfield). Note the highlighted contributions of two ply samples from the top and

the middle of the coal seam. The vitrinite populations in these two ply samples are clearly different and both are more homogeneous than the parent, whole-seam population. Homogeneous vitrinite populations allow more precise relationships between coal properties and carbonization behaviour to be established than where more heterogeneous, whole seam or run of mine samples are examined.

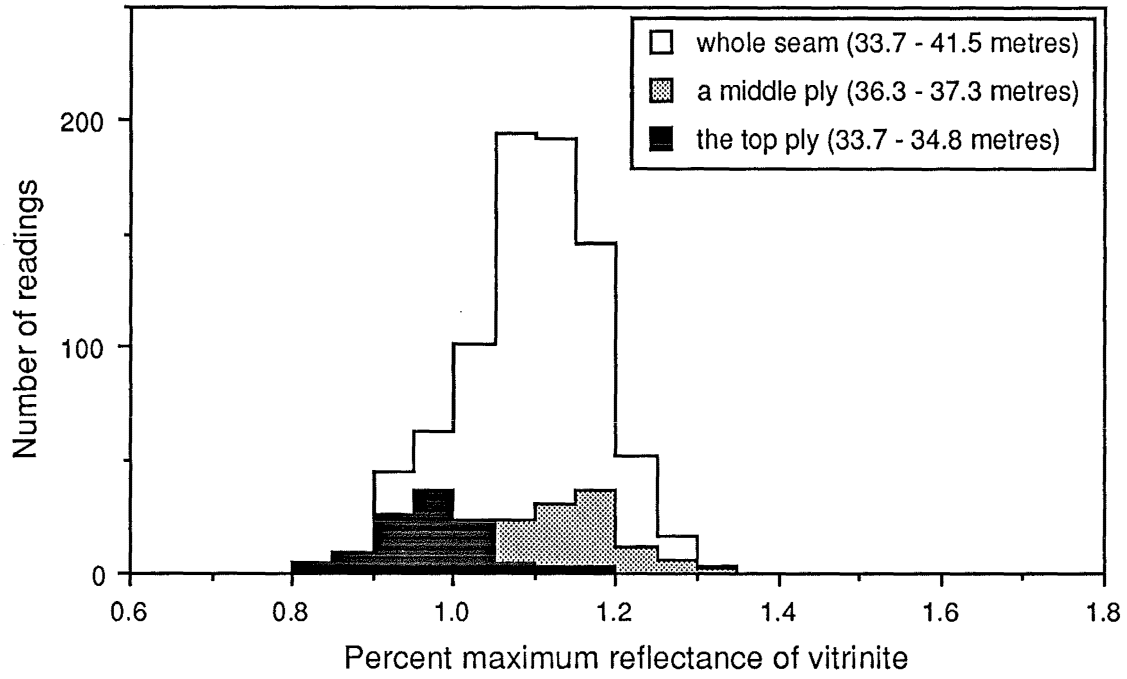

Figure 6.1 Composite reflectance histogram showing the vitrinite reflectance populations in a coal seam encountered in drillhole 1481 (Buller coalfield, Eocene age). The top ply is an ~1 metre thickness at the top of the seam (samples a90-134 , a90-135, a90-136) and the middle ply is a 1 metre thickness from the middle of the seam (samples a90-140, a90-141). Figure modified from Quick and Moore (1991).

6.2 PREDICTION OF COKE STABILITY

6.2.1 US Steel Method

Brown *et al.*, (1982) simplified the US Steel coke strength prediction method (Schapiro *et al.*, 1961) and produced a convenient graph (Figure 6.2) that shows the relationship between vitrinite reflectance, inert content and predicted coke strength (ASTM tumbler stability). Although this graph is useful Brown and his co-workers show that it offers poor precision for some coals due to the limited precision of point count analysis. For example, if a coal with a vitrinite reflectance of 1.0% and a total inert content of 10% is plotted on Figure 6.2 a coke strength near 35 is predicted. As shown in Table 5.2 if the point count analysis is

based on 500 total counts the actual amount of inert components can only be stated as between 13% and 7.5% (at 95% confidence). These limits correspond to predicted coke strength values near 40 and 30 respectively. Thus, the inherent precision of point count analysis limits reliable prediction of coke strength for some coals that plot where the "iso-strength" lines in Figure 6.2 are close together.

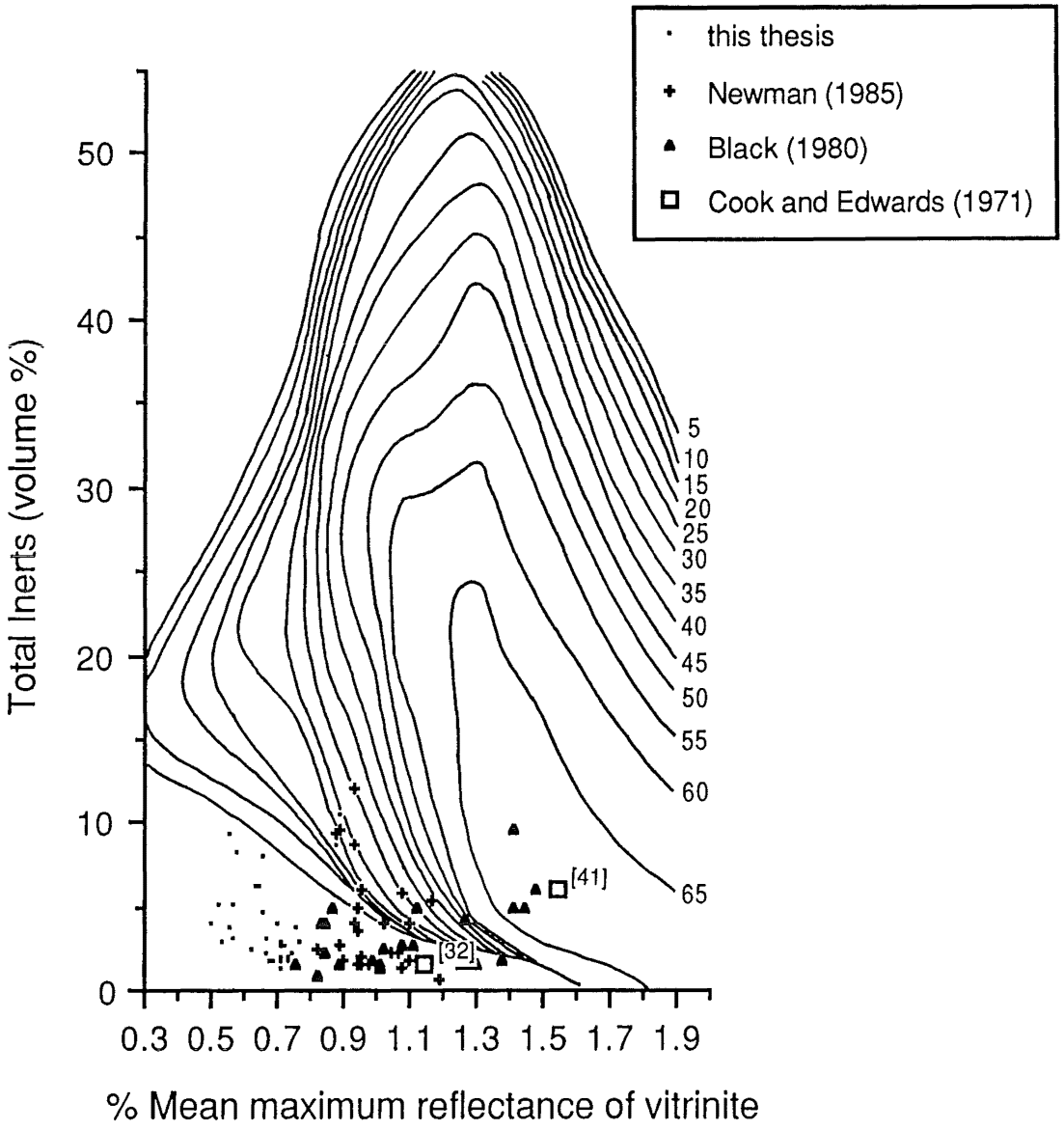

Figure 6.2 Relationship between percent inerts, mean maximum reflectance of vitrinite and coke strength according to a simplified US Steel model. Iso-stability lines show ASTM tumbler stability. Figure adapted from Brown *et al.*, (1982), analytical data from this thesis, and selected data from Newman (1985), Black (1980), and Cook and Edwards (1971). Bracketed numbers are measured ASTM stability values for the two coal samples examined by Cook and Edwards (1971).

Cook and Edwards (1971) measured the ASTM tumbler stability of two cokes made from New Zealand coals ("Stockton coal" Ro_{max} = 1.15%, and "Paparoa coal" Ro_{max} = 1.54%). Their data allow the correspondence between the determined coke strength and that predicted by the US steel method to be evaluated. The two New Zealand coals examined by Cook and Edwards are plotted on Figure 6.2 and the determined ASTM coke strength values are indicated in brackets adjacent to the points; one of the coals shows a higher and the other a lower determined coke strength value than predicted. Neavel (1981) also used the US Steel method to produce a similar (but not identical) graph to that shown in Figure 6.2. However, in Neavel's graph both of these coals report a lower measured coke strength than predicted. The reason for the difference between the graph presented by Neavel (1981) and that shown in Figure 6.2 is not known but may be due to the use of different coking coefficients by the respective authors. Since the original publication of the US Steel method (Schapiro *et al.*, 1961) these values have been widely modified and the actual coefficients used by individual laboratories are rarely stated.

Regardless of the precision attributed to the US Steel coke strength prediction method, Figure 6.2 shows that most New Zealand coals lack sufficient inert components to produce a strong coke but are well suited for blending with coals that contain excessive amounts of inert components. Indeed, Cook and Edwards (1971) have shown that blends of inert rich Bulli coal and inert deficient Stockton coal produce a coke strength that is higher than that produced where either of these coals is coked alone. In addition to improving coke strength, Cook and Edwards's data show that where either New Zealand coal was present in a blend the abrasion resistance of the resulting coke (hardness) increased (presumably due to better incorporation of the inert components in the coke matrix).

6.2.2 MOF Diagram

Okuyama *et al.*, (1970) published a convenient graph where mean maximum reflectance and log maximum Gieseler fluidity (ddpm) are used to graphically evaluate the coking quality of individual coals and coal blends. This

graph is reproduced in Figure 6.3 and shows the position of some New Zealand coals examined in this thesis. The shaded area in the middle of the graph shows the field of blended coal for coke making; the solid line indicates the expected relation between reflectance and fluidity for coals with low inertinite content. Coals that plot above this line can be expected to lack inert components and possess a more thermoplastic variety of vitrinite whereas coals that fall below the line typically contain a larger amount of inert components. The position of many New Zealand coals on the plot indicates their vitrinite rich character and lack of significant inert components. However due to high mineral contents some New Zealand coals examined here plot below the line (Paparoa coals from the Pike River coalfield). Alternately, two New Zealand coals (Buller) that lack both inertinite and mineral matter but are weathered also plot below this line.

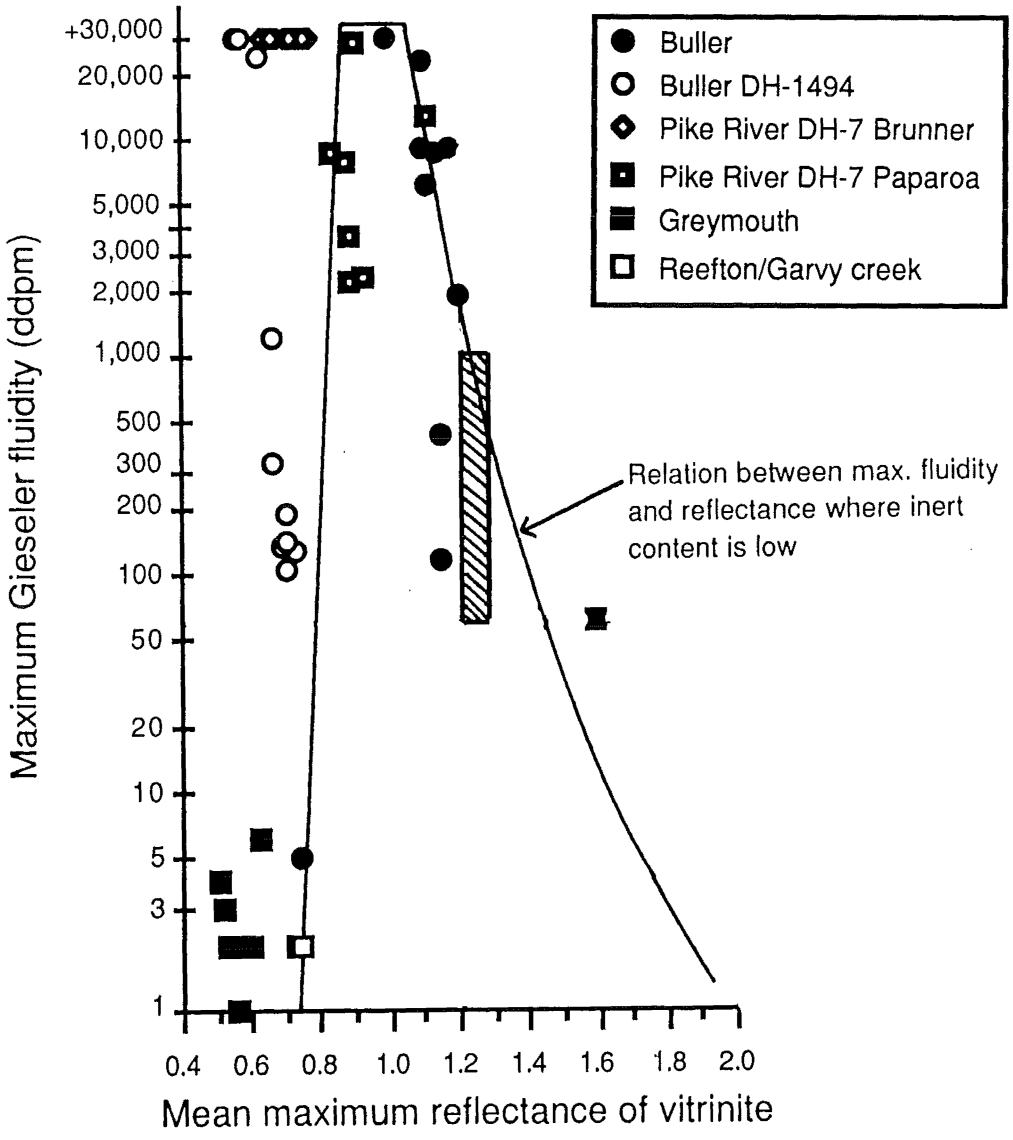

Figure 6.3 MOF diagram (modified from Okuyama *et al.*, 1970).

The MOF diagram works because coals that plot in the shaded area posses the optimum amount of inert components and the proper rank distribution of reactive components. However, where weathered coals are included in the blend, the method is likely to fail. Furthermore, Price *et al.*, (1988) report high coke strength (>55 ASTM stability) for cokes made from inertinite rich Canadian coals where maximum fluidity is less than 15 ddpm; these coals plot below the shaded area in Figure 6.3. Despite these limitations, the plotted position of the New Zealand coals shown in Figure 6.3 is consistent with the notion that most New Zealand coals are best used where blended with higher rank coals that contain abundant inert components.

6.3 PREDICTION OF COKE STRENGTH AFTER REACTION

In addition to good coke strength, the maintenance of coke strength after reaction (CSR) is also important for efficient operation of large diameter blast furnaces. Accordingly, numerous methods have been proposed in the literature to predict CSR.

6.3.1 Nippon Steel Diagram

Figure 6.4 shows a plot attributed to Nippon Steel that graphically illustrates the relationship between CSR, vitrinite reflectance and inertinite content. Goscinski *et al.*, (1985, p.27) state that this graph "is handy for the novice in quickly assessing the potential after reaction strength of an intended coal product." As indicated in Figure 6.4 CSR can be expected to increase with vitrinite reflectance and then decline. Figure 6.5 was graphically derived from the relationship shown in Figure 6.4; reflectance and inert content of points of equivalent CSR (estimated from figure 6.4) were plotted and lines connecting these points were manually drawn using a flexible ruler. Data from some coals examined in this thesis are also shown. The CSR characteristics of coals at 1.5% vitrinite reflectance are not shown in Figure 6.4 consequently there is a break in the iso-CSR lines at this value in Figure 6.5. Based on coke reactivity studies by Schapiro and Gray (1963), Goscinski *et al.*, (1985) note that CSR declines above 1.55% vitrinite reflectance. The dashed vertical line in Figure 6.5 corresponds to this CSR maximum and is in agreement with the low CSR values predicted for higher rank coals to the right of the line.

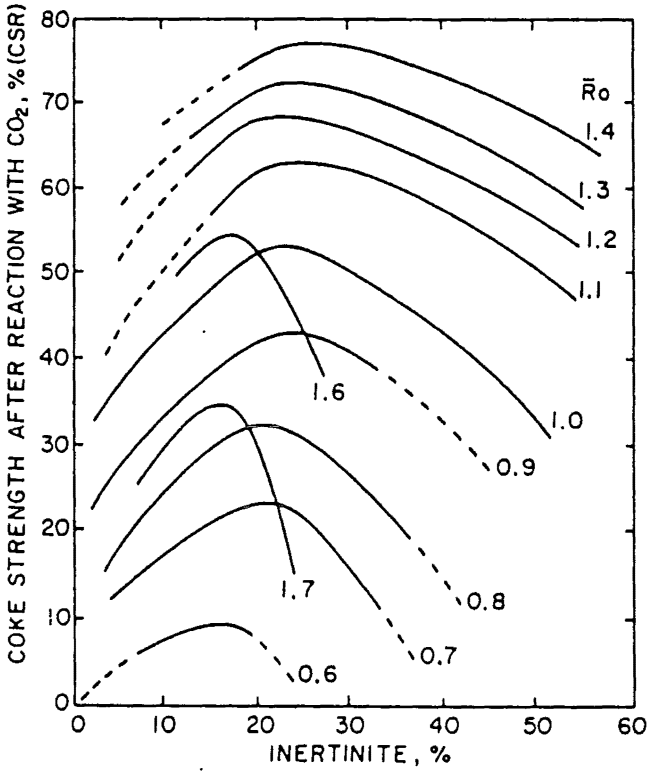

Figure 6.4 Relationship between mean maximum reflectance of vitrinite, inert content and CSR; figure attributed to Nippon Steel, by Goscinski *et al.*, (1985).

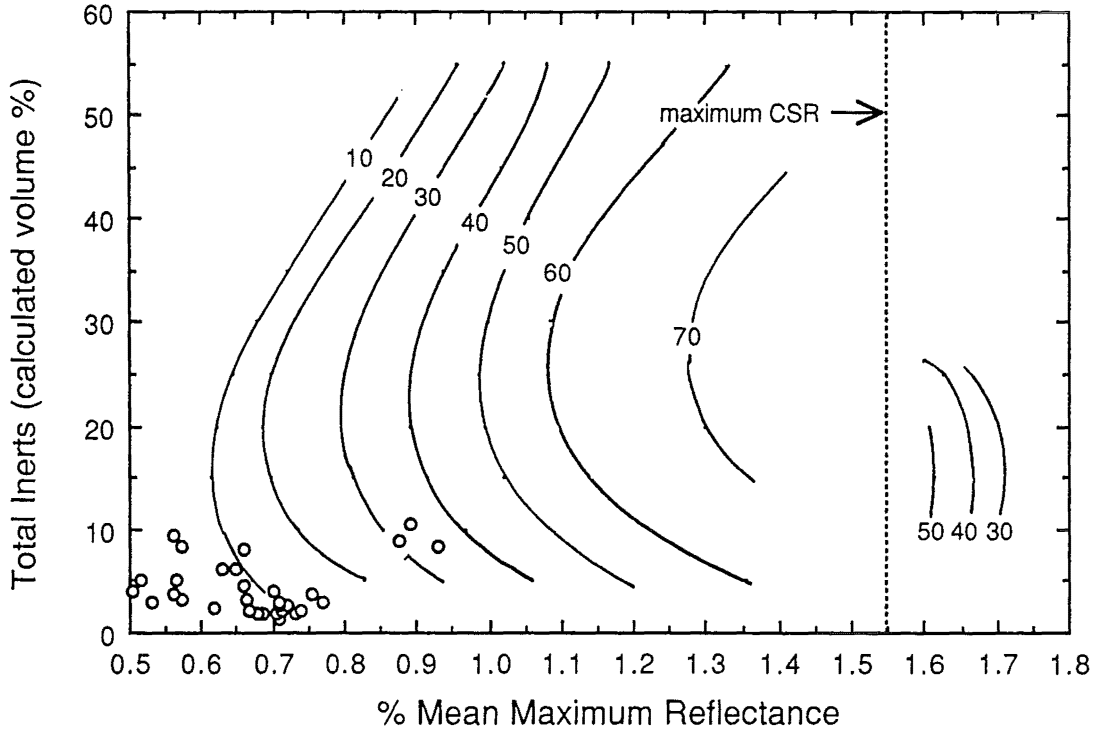

Figure 6.5 Relationship between mean maximum reflectance of vitrinite, inert content and CSR. Figure constructed from relationship shown in Figure 6.4. CSR is indicated by annotated lines on the graph. The dashed vertical line shows the position of maximum CSR. The plotted points indicate the position of some coals examined in this study.

Figure 6.5 shows that CSR increases with increasing vitrinite reflectance until 1.55% reflectance and then declines. It also shows that at any given level of vitrinite reflectance there is an optimum inert content for maximum CSR. In consideration of the high reactivity of organic inert derived components in coke the influence of inertinite on CSR deserves further comment. Inert constituents, particularly where small, serve to thicken pore walls in the carbonized product thereby reducing the porosity and surface area of the carbon product. Since less surface area is subject to attack by CO_2, CSR is enhanced. Because many New Zealand coals lack appreciable inerts they inevitably report lower CSR values, according to Figure 6.5, than might otherwise be expected on the basis of vitrinite reflectance alone. Since New Zealand coals are inevitably blended with coals that contain more abundant inertinite, Figures 6.4 and 6.5 underestimate the value of New Zealand coal as a blend component.

More complex predictive estimates of CSR have been proposed where the inorganic content of the feedstock is also considered. Goscinski *et al.*, (1985) review CSR prediction methods used by British Steel, Nippon Steel, ISCOR, and Kobe Steel. They note that these methods use maximum reflectance, organic inert content, Gieseler fluidity, and measures of ash composition. These methods incorrectly assume that CSR increases linearly with reflectance. Although ash composition is emphasised in these models the total amount of ash is not considered. A more recent method published by Valia (1989) is examined below since it does account for total inorganic content and relies on the Gieseler thermoplastic range rather than linear relationships with vitrinite reflectance to predict CSR.

6.3.2 Inland Steel CSR prediction

The Inland Steel CSR prediction method is fully explained by Valia (1989) where CSR is predicted according to the following equations.

$$CSR = 28.91 + 0.63 * \text{Gieseler plastic range} - \text{Catalytic Index} \quad \text{(eq. 6.1)}$$

and.

$$\text{Catalytic Index} = 9.64 * \text{Alkali Index} + 14.04 * \text{Sulphur} \quad \text{(eq.6.2)}$$

and,

$$\text{Alkali Index} = \text{Ash} * \frac{CaO + MgO + Fe_2O_3 + Na_2O + K_2O}{SiO_2 + Al_2O_3} \qquad \text{(eq. 6.3)}$$

where ash and sulphur are on a dry basis and the sum of the oxides equals the weight percent ash. These calculations were applied to some data for New Zealand coals and the results are shown in Table 6.1. Examination of Table 6.1 shows impossible (negative) CSR values predicted for many of the coals examined in this thesis. The results illustrate the limitation of predictive methods derived from regression methods for evaluation of coals that are not similar to those that were used to establish the predictive method. In this regard it is important to note that Valia (1989, p.86) states "The CSR prediction method is applicable to individual coals and coal blends within the limits of the materials used in this study".

Why do the New Zealand coals listed in Table 6.1 provide such improbably low (negative) predicted CSR values? Examination of Table 6.1 shows that the lowest CSR values are associated with high alkali index values. The profound effect of the alkali index on predicted CSR is shown in Figure 6.6. The reason for the high alkali index values relates to the use of a ratio of the oxides in the calculation of the alkali index (Equation 6.3) and the exceptionally high base to acid ratios of many of the coals listed in Table 6.1. The average base to acid ratio of the coals listed in Table 6.1 is 5.5. This value can be compared to an average base to acid ratio of 0.5 (σ = 0.2) reported for 626 eastern US coals and 0.9 (σ = 0.5) for 586 western US coals (Winegartner and Rhodes, 1975). Valia (1989) notes that the catalytic index of the coals used to establish the predictive method ranged from 15 to 40. Thus the predicted CSR for coals that exhibit catalytic index values outside this range are probably wrong. However where coals are within this range the predicted CSR values cannot be summarily rejected. Figure 6.7 graphically illustrates the relationship expressed in equation 6.1 and shows the plotted position of coals that fall within the calibrated range of the method.

TABLE 6.1

INLAND STEEL CSR PREDICTION APPLIED TO SOME NEW ZEALAND COALS

Lab No *	Suite **	Ash (dry)	Sulphur (dry)	Plastic Range	Alkali Index	Catalytic Index	CSR (predicted)
46/750 s (rider)	DH-1494	32.4	1.2	61	7	82	-15
46/739 p	DH-1494	2.5	4.5	91	5	111	-25
46/740 p	DH-1494	1.9	4.7	87	43	479	-396
46/741 p	DH-1494	4.3	6.4	89	165	1683	-1598
46/742 p	DH-1494	1.2	4.0	82	14	194	-113
46/743 p	DH-1494	1.3	3.4	76	11	149	-73
46/744 p	DH-1494	4.3	4.7	66	46	507	-437
46/745 p	DH-1494	0.4	1.5	71	0	23	50
46/746 p	DH-1494	0.2	1.2	67	0	19	53
46/747 p	DH-1494	0.6	1.4	66	2	38	32
46/748 p	DH-1494	0.3	1.1	64	0	16	53
46/749 p	DH-1494	2.7	1.1	67	0	17	54
50/639 p	DH-712	7.3	0.4	31	1	11	37
50/640 p	DH-712	1.2	0.3	48	0	6	53
50/641 p	DH-712	1.0	0.3	59	0	5	61
50/643 p	DH-712	3.4	0.3	50	0	7	54
50/644 p	DH-712	6.3	0.5	37	0	10	42
50/645 s	DH-712	5.1	0.4	45	0	9	49
46/847 p	PRDH-7 Br	7.3	5.4	107	14	211	-114
46/835 p	PRDH-7 Br	8.0	4.2	104	30	348	-254
46/836 p	PRDH-7 Br	2.2	3.6	111	19	237	-138
46/837 p	PRDH-7 Br	2.4	3.1	96	25	283	-194
46/838 p	PRDH-7 Br	0.8	2.5	92	4	70	17
46/839 p	PRDH-7 Br	1.1	1.6	86	10	116	-33
46/840 p	PRDH-7 Br	2.7	1.1	85	56	555	-473
46/841 p	PRDH-7 Br	1.9	1.4	84	38	389	-307
46/842 p	PRDH-7 Br	4.0	2.1	88	107	1057	-973
46/843 p	PRDH-7 Br	1.6	3.0	97	28	312	-222
46/844 p	PRDH-7 Br	1.6	4.0	99	18	231	-139
46/845 p	PRDH-7 Br	2.6	4.1	124	5	108	0
46/846 p	PRDH-7 Br	11.8	4.0	114	2	78	22
46/919 s	PRDH-7 Pap	13.2	0.6	68	1	19	52
46/920 s	PRDH-7 Pap	20.9	0.5	76	1	15	62
46/921 s	PRDH-7 Pap	20.6	0.5	70	1	17	56
46/922 s	PRDH-7 Pap	17.4	0.7	86	1	17	66
46/923 s	PRDH-7 Pap	19.6	0.3	88	3	37	48
46/924 s	PRDH-7 Pap	11.7	0.3	82	3	38	43
a90-3482 p	DH-1492	0.8	3.5	0	0	51	-22
a90-3484 p	DH-1492	0.1	1.2	74	0	17	58
a90-3486 p	DH-1492	3.3	4.3	102	1	66	28
Lavill (1987)	Stockton	0.3	0.9	96	0	14	75
Lavill (1987)	Stockton	3.2	3.1	114	1	51	50

notes to table: * s seam sample; p ply sample; ** Br Brunner coal measures; Pap Paparoa coal measures

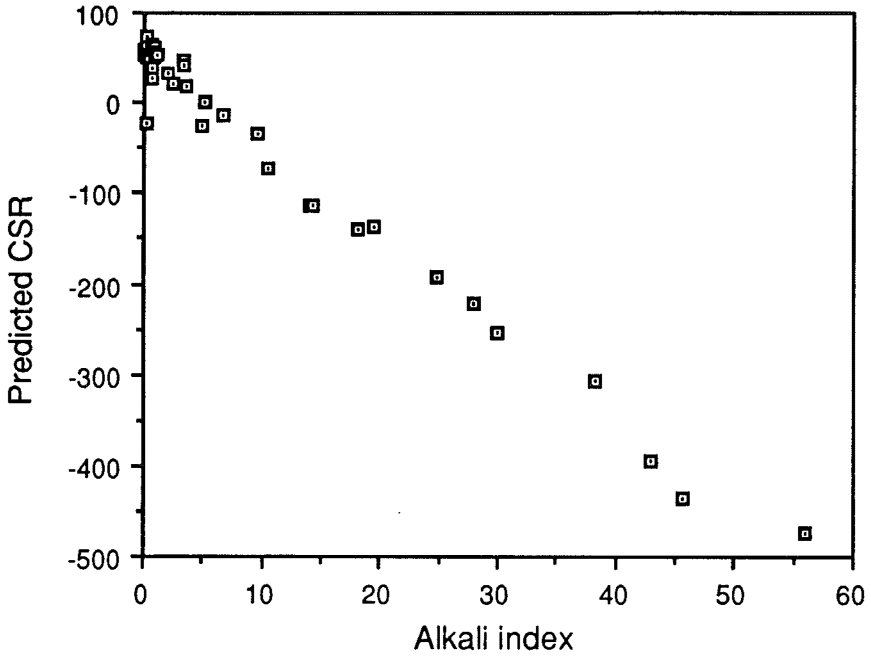

Figure 6.6 Scatterplot showing how the predicted CSR of some New Zealand coals varies with the Alkali index. Data from Table 6.1. Note that coal samples 46/741 and 46/842 are off the figure scale.

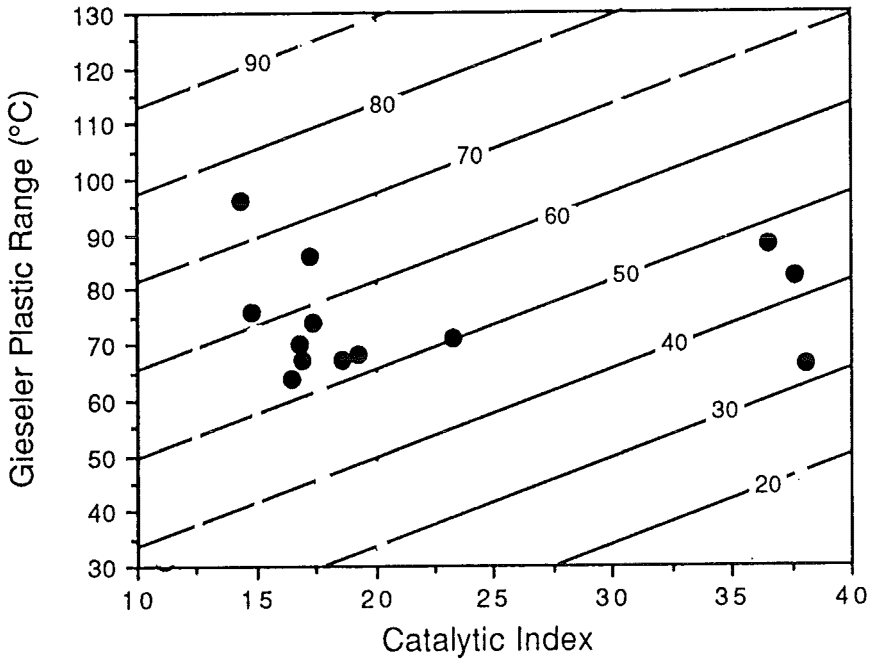

Figure 6.7 Graphic illustration of the relationship between the catalytic index, Gieseler plastic range and CSR expressed in equation 6.1. Plotted New Zealand coals are within the calibrated range of the method.

6.4 DISCUSSION OF PREDICTIVE METHODS

Achievement of high coke strength requires an optimum amount of inerts which varies according to the capacity of the thermoplastic binder phase to fuse these components together. The amount of potentially inert components is calculated based largely on the results of point count analysis. As discussed in section 6.2.1 the precision associated with point count analysis may lead to unacceptable errors associated with this kind of predictive method.

CSR can be attributed to three characteristics of coke: 1) the available surface area subject to attack by CO_2, 2) the catalytic effect of alkalis and the presence of molecular defects due to the presence of heteroatoms, and 3) the physical arrangement of the carbon crystallites present in the coke. The porosity and surface area of coke are not considered in this thesis. However, since good cold strength of coke also depends on the presence of adequately thick cell walls it is suggested that for cokes with good cold strength the effect of porosity is likely to be small. The effect of alkalis and heteroatoms on CSR is widely acknowledged. However, as suggested in section 6.3.2, current methods to predict CSR will need to be improved if universal applicability is to be achieved. Although the correspondence between reactivity and ash composition and content of New Zealand coals has not been measured the alkali rich character of many New Zealand coal ashes is not a good attribute for cokemaking. Nonetheless, the negative CSR values predicted for many of the New Zealand coals examined in this thesis (Table 6.1) are impossible. A more useful approach to evaluate the effect of alkalis on CSR would be to avoid the use of ratios and use a summation of the mole percent of specific inorganic cations in the coal as regression variables. The possible mitigating effect of alumina and silica on alkali catalysed reactivity (Price *et al.*, 1988) could be accounted for by subtraction of these cation abundances rather than calculation of base/acid ratios.

Regardless of the accuracy of these predictive methods it is worth noting that the value of a coal for carbonization can only be validly judged by examination of the contribution it makes to a particular blended product. Indeed

few coals are capable of producing an acceptable coke product if used alone. Where blend composition is known, accurate predictive methods are required for valid appraisal of the contribution that component coals make to a blend. Most predictive methods use vitrinite reflectance to predict the behaviour of the binder phase. These methods work because the thermoplastic character of coal waxes and wanes through the bituminous ranks and the binder phase is largely derived from vitrinite macerals. However, the assumption that vitrinite reflectance alone is an accurate predictor of the thermoplastic behaviour of the binder phase is suggested to be wrong where New Zealand coals are considered. As will be shown in the following sections the influence of perhydrous or weathered vitrinite in New Zealand coals is not accounted for by vitrinite reflectance alone and the combined use of reflectance and fluorometric analysis is advocated.

6.5 Vitrinite Reflectance and Carbonization Behaviour

The general increase and decrease of thermoplasticity as coal advances through the bituminous ranks is well known (see Figures 3.3 and 6.3). However the relationship is poorly defined due to the effects of infusible constituents, undetected weathering, or vitrinite submaceral variation on thermoplastic behaviour. Habermehl *et al.*, (1981) note that the effect of inert components varies according to the capacity of the infusible components to absorb the "plasticising material" upon pyrolysis; where the inert material does not absorb this material the reduction of (log) fluidity is essentially linear with the volume percent inert components, but where small amounts of activated carbon or coke are added more significant reductions in fluidity have been reported. The variable effects of undetected weathering may also contribute to the lack of a precise relationship between vitrinite reflectance and thermoplastic behaviour. The lack of a precise correlation between reflectance and thermoplasticity has also been attributed to variation in the composition of vitrinite (Newman, 1985b). For example, Figure 6.8 shows some New Zealand coals that are not weathered and do not contain appreciable inert material but still exhibit a significant variation of fluidity at equivalent levels of vitrinite reflectance. Since thermoplasticity relates

to the ability of a coal to bond inert components into a coherent mass, methods to predict coke quality are likely to fail where vitrinite reflectance alone is used to estimate the binding capacity of the vitrinite in coal. Vitric New Zealand coals with anomalously high fluidity should be able to bind more inerts whereas vitric New Zealand coals with anomalously low fluidity (due to weathering) may yield a more friable coke unless fewer inerts are added to the blend.

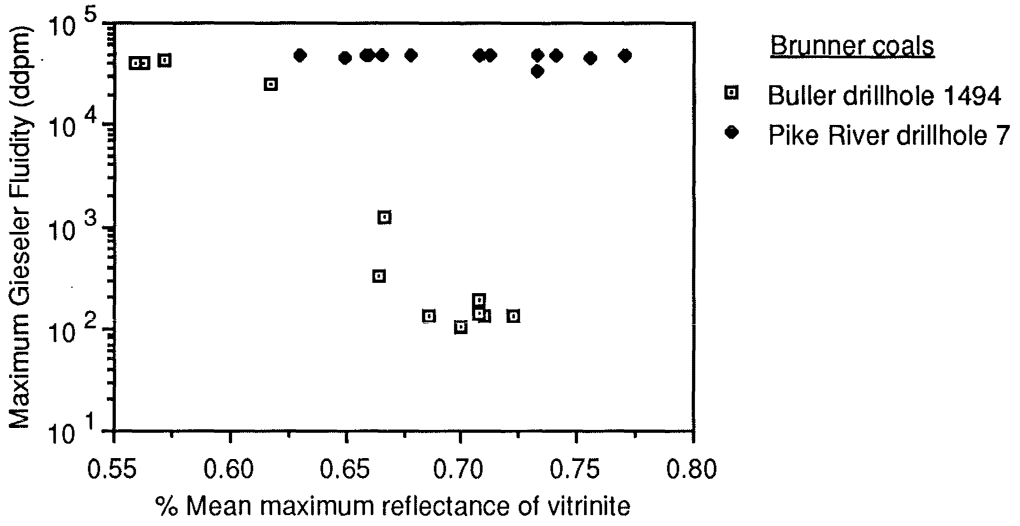

Figure 6.8 Relationship between vitrinite reflectance and Gieseler fluidity for some ply samples from two New Zealand coal seams.

The capacity of a coal blend to assimilate inerts upon coking can only be beneficial since inerts function to reduce post-solidification shrinkage fractures that weaken the coke. In addition to inert content, coke strength is further controlled by the amount that the binder phase shrinks after solidification. Since higher solidification temperatures allow more shrinkage to be accommodated in a plastic state, high solidification temperatures promote coke strength. Figure 6.9 shows the general increase in Gieseler solidification temperature with increasing vitrinite reflectance for some New Zealand and US coals. Some New Zealand coals (largely Brunner coals from the Pike River coalfield) show higher solidification temperatures than might be expected based on vitrinite reflectance.

The general increase and decrease of CSR with increasing vitrinite reflectance through the bituminous ranks has been attributed to the development of a mosaic texture (Marsh, 1982). Diessel and Wolf Fischer (1986) report that isotropic and fine grain mosaic carbons undergo solution loss more quickly than

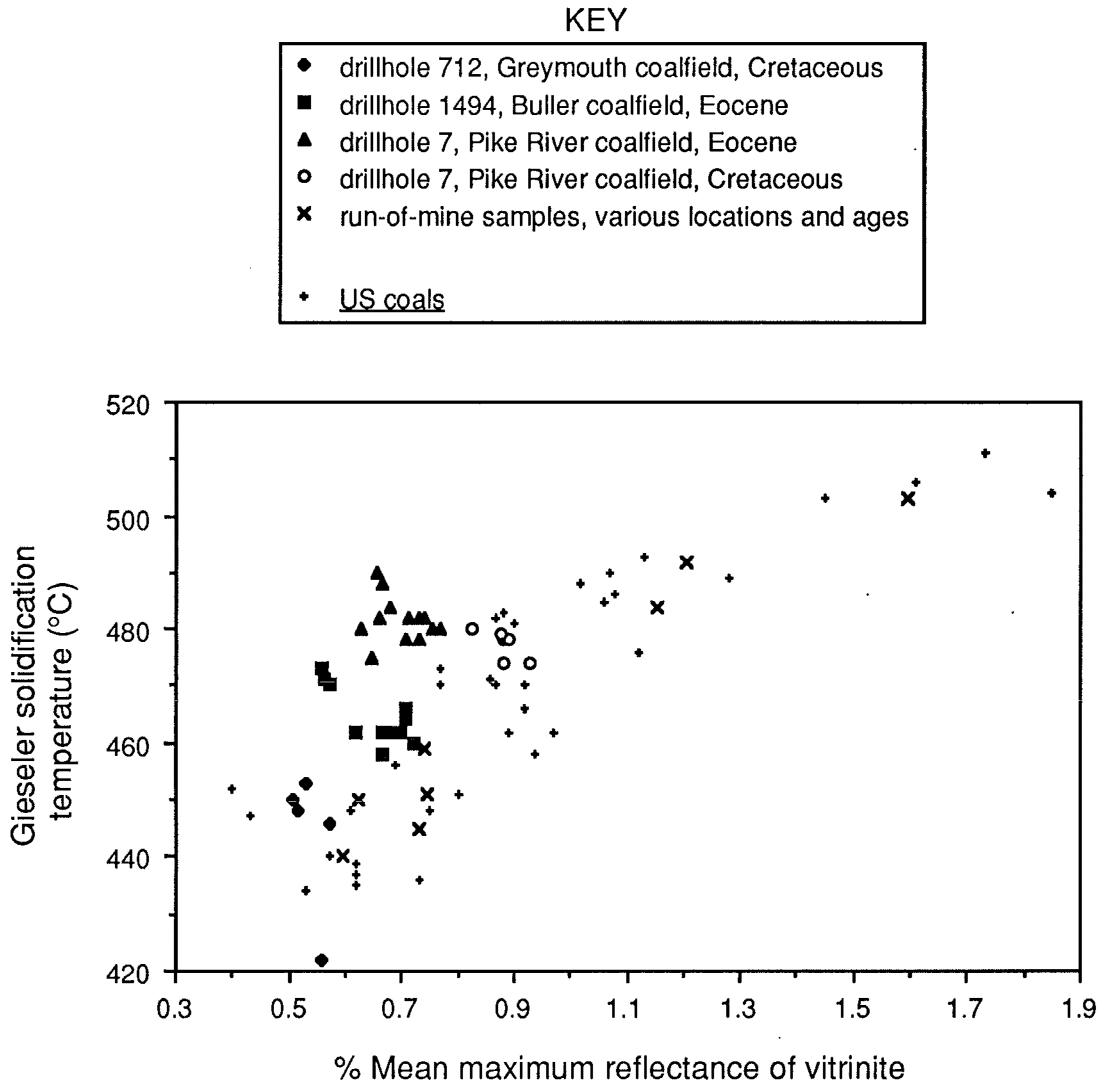

Figure 6.9 Relationship between vitrinite reflectance and Gieseler solidification temperature for some New Zealand and US coals (US coal data courtesy of the Penn State Coal Data Base).

larger anisotropic units. Figure 6.10 shows how the optical texture index of carbons made from 28 New Zealand coals compares to the vitrinite reflectance of the parent coals. Although Figure 6.10 shows a general correspondence between vitrinite reflectance and optical texture of the carbonized products this relationship is not as good as that observed by Patrick *et al.*, (1973, 1979) and Diessel and Wolf Fischer (1987) for Paleozoic coals. Patrick and his co-workers examined 23 hand-picked vitrains from British, Carboniferous coals that ranged between 0.8 and 1.8 % maximum reflectance. Diessel and Wolf Fischer (1987) examined a set of coals comprising 10 Australian (Permian) and 20 German (Ruhr, Carboniferous) coals that ranged between 0.8 and 1.5% mean random

telocollinite reflectance. The lack of correlation shown in Figure 6.10 might be explained for two reasons. Firstly, some of these coals are weathered and yield isotropic carbons or smaller sized mosaic carbons than equivalent fresh coals. Secondly, some of these coals (circled) are perhydrous (high fluorescence intensity, section 6.6) and yield larger sized mosaic carbons than might be expected based on their vitrinite reflectance.

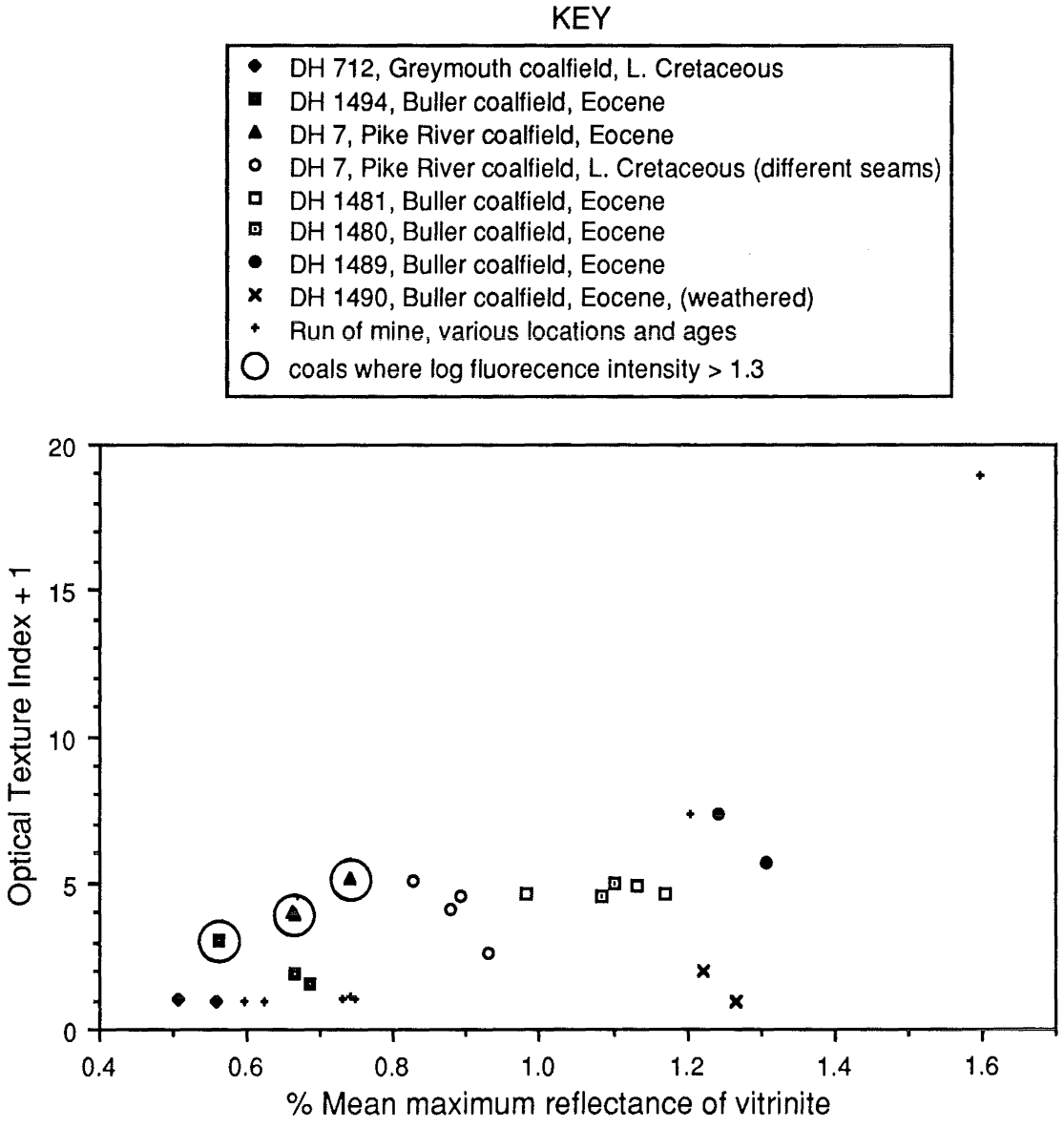

Figure 6.10 Relationship between vitrinite reflectance and the optical texture index of carbons made from some New Zealand coals.

The examples given in this section illustrate some potential problems where vitrinite reflectance is used alone to predict the carbonization behaviour of New Zealand coals. These problems are attributed to the presence of either perhydrous or weathered vitrinite. Despite the suggested limitations of vitrinite

reflectance to predict carbonization behaviour, vitrinite reflectance offers some significant advantages. Unlike other coal quality parameters, vitrinite reflectance is independent of group maceral variation and does not require adjustment for inorganic content. Nonetheless, if New Zealand coals are to be used effectively some means to identify perhydrous and weathered vitrinite is needed. In the following sections the idea that fluorometric analysis can be used to detect and quantify perhydrous and weathered vitrinite is advanced. Finally, various measures of carbonization and pyrolysis behaviour are predicted where both reflectance and fluorometric analysis are used as characterization parameters.

6.6 PERHYDROUS VITRINITE.

Semantically, perhydrous vitrinite is simply vitrinite that contains more hydrogen than "normal" vitrinite. Although the hydrogen content of whole coals can be measured directly, the hydrogen content of the vitrinite macerals in coal is not easily measured. Consequently, perhydrous vitrinite is not strictly defined and the phrase is used here in a conceptual sense. Where perhydrous vitrinite is present, measures of carbonization and pyrolysis behaviour such as Gieseler fluidity and volatile matter yield are often higher than expected for "normal" coals of equivalent group maceral content and rank.

6.6.1 Recognition of Perhydrous Vitrinite

Perhydrous vitrinite can sometimes be visually recognized under reflected light as, vitrinite B, desmocollinite, degradinite, detrovitrinite, saprovitrinite or dark vitrinite but these identifications are inherently subjective and do not lend themselves to precise measurement of the degree of hydrogen enrichment. For example, Newman (1989) has shown examples of vitric New Zealand coals where significant variation of volatile matter does not correspond to vitrinite submaceral variation. Thus, compositional variation within the vitrinite group is not always revealed by conventional petrographic examination. Newman (1987) observed better differentiation of vitrinite group macerals where the polished surface of the coal specimen was etched prior to microscopic examination. Figure 6.11 shows how the volume % amorphous matrix revealed by etching corresponds to variation

of volatile matter for serial ply samples from a vitric coal seam encountered in Pike River coalfield drillhole 7 (Brunner coal measures, Eocene age). The significant correlation (r^2=0.79) between amorphous matrix and volatile matter shown in Figure 6.11 is evidence that oxidative etching can be used to chemically differentiate components within the vitrinite group. Quick and Moore (1991) reported an even better correlation (r^2=0.89) where mean vitrinite--inertinite fluorescence intensity of the ply samples in this seam was used to predict volatile matter.

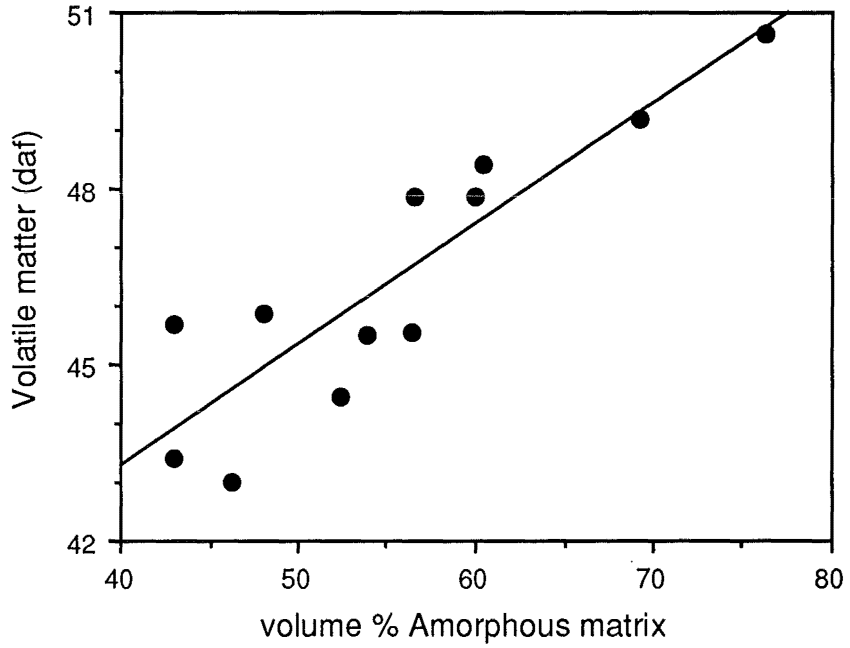

Figure 6.11 Relationship between volume % amorphous matrix and dry ash free volatile matter for some ply samples from a seam encountered in Pike River drillhole 7, (Brunner coal measures). Volatile matter corrected to a dry, ash free basis according to BS1016 part 16 (from Quick and Moore, 1991).

Given the lack of convenient methods to directly measure the elemental composition of individual macerals fluorometric analysis is used here to recognize and quantify perhydrous vitrinite in New Zealand coals. The method used for fluorometric analysis is discussed in section 4.3.7 and Appendix C. It should be noted that the mean fluorescence intensity values reported in this thesis were obtained on both vitrinite and inertinite macerals. Inertinite is rare in these coals and the mean fluorescence intensity values are not significantly different where low fluorescence values, presumably due to inertinite, were removed from the data set. Figure 6.12 shows the correlation between fluorescence intensity and organic

hydrogen content for some ply samples from two coal seams where ash is less than 10%. Despite the lack of a convincing correlation fluorometric analysis is considered here to be a satisfactory tool for the recognition and measurement of perhydrous vitrinite. The weak correlation (r^2=0.71) is suggested to result, in part, from the variable abundance of hydrogen rich liptinite. Coals that reported more than 5% liptinite are circled in Figure 6.12; all of these coals fall above the regression line. Multivariate regression where both fluorescence intensity and total liptinite content are used to predict total hydrogen of these coals reports a coefficient of determination (R^2) of 0.83. The resulting equation ($H_{organic}$= 4.72 + 0.75*logFLI + 0.06*liptinite) predicts that 1% liptinite will contribute 0.06% hydrogen to the whole-coal hydrogen content. The upper and lower confidence limits for a coal with 5% liptinite are 7.3 and 3.3% (Table 5.2) and correspond to a ±0.12% unexplained variation of hydrogen content which can be compared to the reported precision of the hydrogen determination (±0.07, BS1016 part 16).

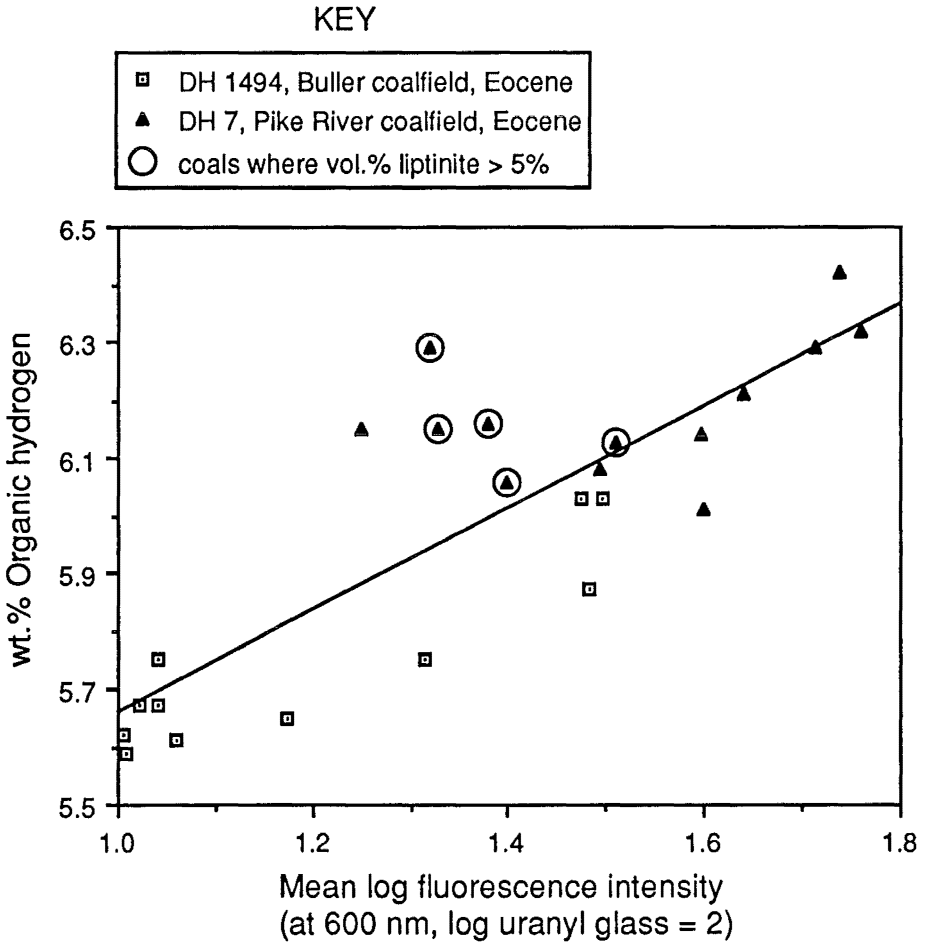

Figure 6.12 Scatterplot showing the relationship between the mean fluorescence intensity of vitrinite and inertinite in some New Zealand coals and organic hydrogen content. Organic hydrogen contents of these coals are listed in Table 5.1.

Better, albeit indirect, evidence for the use of fluorescence intensity to detect and measure perhydrous vitrinite is shown in Figure 6.13. The general relationship between "high" fluorescence intensity and "low" vitrinite reflectance in perhydrous coals is known (Teichmüller and Teichmüller, 1982 p.72, Wolf *et al.*, 1983, Diessel and Wolff-Fischer, 1989) but rarely quantified. Figure 6.13 shows the relationship between vitrinite reflectance and fluorescence intensity of serial ply samples from six New Zealand coal seams. Because serial ply samples are used, the effect of coalification on both vitrinite reflectance and fluorescence intensity can be ignored (Suggate, 1959). This approach provides a way to both detect and quantify perhydrous vitrinite.

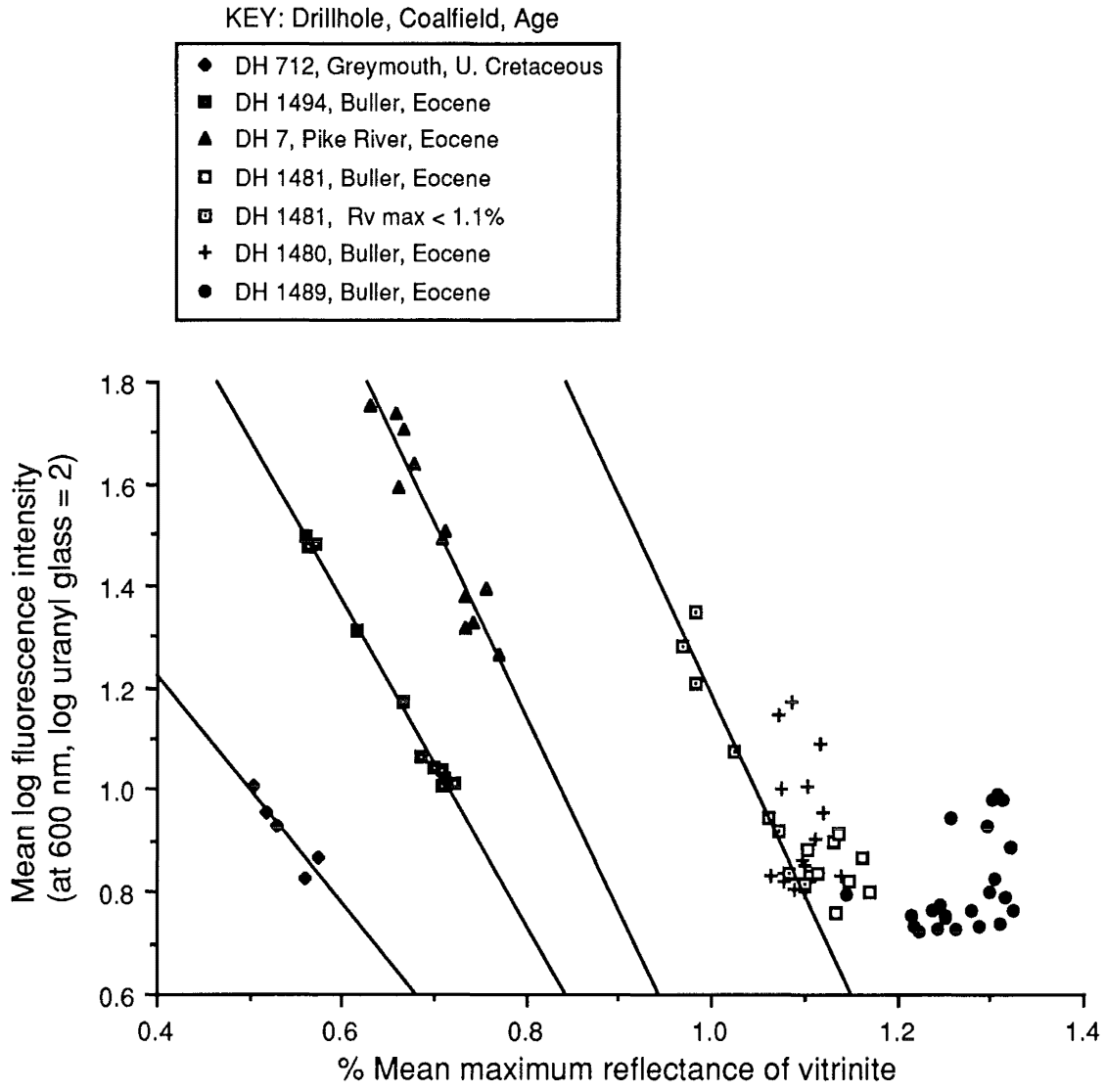

Figure 6.13 Relationship between vitrinite reflectance and fluorescence intensity for serial ply samples from six New Zealand coal seams. Linear regression lines for serial ply samples in DH-712, DH-1494, DH-7, and, where < 1.1% reflectance, DH-1481. These lines report a coefficient of determination (r^2) of 0.84, 0.99, 0.91, and 0.96 respectively.

Linear regression lines for sets of serial ply samples from four seams are shown in Figure 6.13. Above about 1.1% reflectance no significant correlations were observed. The lack of correlation above this threshold may be due to several factors. The coal seams encountered in drillholes 1480, 1481 and 1489 occur at a shallow depth (~7 to 33 metres) compared to those encountered in drillholes 712, 1494, and 7 (~119 to 386 metres depth). McHugh *et al.*, (1991) suggest that incipient weathering due to shallow present depth of burial reduces fluorescence intensity. Conversely, vitrinite reflectance is not changed by mild weathering (section 6.7). Thus the fluorescence intensity of samples from these drillholes may be lower than would otherwise be expected if they were deeply buried.

Alternately, the lack of a relationship between fluorescence intensity and vitrinite reflectance for serial ply samples above 1.1% may relate to the wavelength of maximum vitrinite fluorescence intensity; the relationship between reflectance and fluorescence intensity of serial ply samples measured at different emission (or excitation) wavelengths remains to be investigated. The 550-650 nm measurement wavelength was selected in this thesis for practical and theoretical reasons discussed below.

Teichmüller and Durand (1983) reported that the wavelength of maximum vitrinite fluorescence intensity shifts from near 650 to above 700 nm as coalification advances through the high volatile bituminous ranks (0.5 to 1% random reflectance). They noted (p.209) that "it was not possible for methodical reasons to measure wavelengths higher than 710 nm". It is important to note that these workers only measured desmocollinite and densinite, presumably because fluorescence intensity of other vitrinite macerals was not high enough to obtain reproducible spectra. In this regard Crelling *et al.*, (1989) state "at this time full spectral analysis of vitrinite and inertinite is not possible on a routine basis using existing fluorescence systems"; they later note that spectral analysis of all coal macerals is possible where a photo-diode array with image intensifier is used. Using this system and "UV" (365 nm) excitation Crelling and his co-workers show spectra for vitrinite, pseudovitrinite, semifusinite, and fusinite that occur in

a hvBb rank coal from Illinois (US). All three spectra show similar intensity maximums (near 780 nm) but differences between these macerals are best expressed near 600 nm.

Although the wavelength of maximum vitrinite fluorescence intensity increases with coal rank, the fluorescence intensity at a fixed wavelength increases and then decreases through the bituminous ranks. Diessel, (1991) compared the fluorescence intensity of vitrinite and inertinite populations in both a Carboniferous (German, Ruhr, Ro_{random} = 0.95) and Australian (Permian, Bulli, Ro_{random} = 1.00) coal at 546, 650, and 700 nm. Variation within the vitrinite and inertinite group macerals was best expressed at 650 nm compared to 546 and 700 nm. Lin (1988) suggested that the build up of mobile phase material (bituminisation) in the vitrinite delays the spectral red-shift (Teichmüller and Durand, 1983) that accompanies the progressive advance of coal rank. The enrichment of mobile phase material has been suggested to be the causative factor responsible for the thermoplastic behaviour of coal.

The practical reasons for using 550-650nm emission wavelengths include high sensitivity of the photomultiplier tube in this region and, perhaps more importantly, leakage of longer wavelengths by the excitation filter. Dichroic excitation filters in the range of 450 nm require additional blocking strategies for good blocking above 700 nm which inevitably decrease excitation light transmission. A dichroic filter blocks a limited range of light, approximately 1.2 times the centre wavelength on either side of the passband (Omega Optical). Blocking beyond this range requires additional low and high side filters. For effective dielectric blocking to 1 micron an appropriate excitation filter approaches 5 mm thickness (Pers. comm., Paul Millman, Omega Optical Co.). (Thinner filters where metallic coatings are used for blocking are available but these blocking elements significantly reduce the transmission of the excitation filters.) This thickness does not allow placement in the Ploem filter cube holder used in this study. Crelling *et al.*, (1989, p.20) note the advantage of this placement is that it provides a "significantly higher proportion of excitation energy to the sample by

the notable reduction in the distance through which the excitation light must travel." Although the logic of this explanation is not clear, the practical effect of this placement is easy to demonstrate. Accordingly, a 3.2mm, 440nm CWL, 90nm HBW excitation filter with good blocking in the range of 550-650nm was selected for use in this study; good blocking at higher wavelengths requires a thicker filter or metallic blocking elements. Thus the selection of measurement wavelengths used in this study is the outcome of a compromise to achieve high excitation efficiency, good blocking in the measurement wavelengths and sensitivity to perhydrous vitrinite (enrichment of mobile phase material) emission.

6.6.2 Measurement of Perhydrous Vitrinite

The relationships shown in Figure 6.13 suggest that for deeply buried coals between 0.5 and 1.1% reflectance, fluorometric analysis can be used to adjust measured vitrinite reflectance values to account for low reflectance due to the presence of perhydrous vitrinite. The proposed correction is mathematically expressed as:

$$Ro_{adjusted} = Ro_{measured} + \frac{(FLI - 1)}{3.4} \qquad \text{(eq. 6.4)}$$

where,

Ro = % mean maximum reflectance of vitrinite,
FLI = log (base10) mean fluorescence intensity of vitrinite at 600 nm emission, relative to a uranyl glass standard = 100 on a linear scale,

and the value 3.4 is obtained from the average slope of the four regression lines shown in Figure 6.13. A hypothetical example of the proposed correction method is graphically illustrated in Figure 6.14. Examination of Figure 6.14 shows the plotted position of a coal with a measured reflectance of 0.64% and a mean log fluorescence intensity of 1.34. This point is graphically shifted along a line, with a slope ($\Delta FLI/\Delta Ro$) equal to -3.4, to a position where the log fluorescence intensity equals one. The adjusted reflectance is indicated on the X axis below this position.

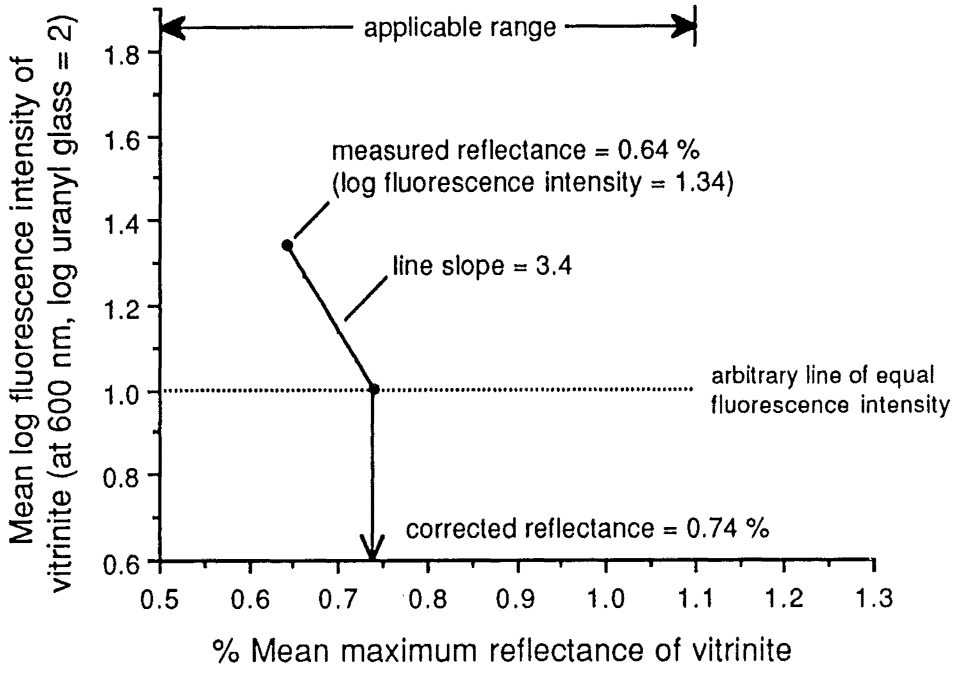

Figure 6.14 Graphic illustration of the proposed reflectance correction for perhydrous vitrinite. The method is applicable to bituminous rank vitrinites between 0.5 and 1.1% maximum reflectance. It is inappropriate for weathered coals or coals that have deteriorated due to laboratory storage or shallow present day burial.

It should be noted that the proposed line of equivalent fluorescence intensity shown in Figure 6.14 (and implicit in equation 6.4) has no special significance. For example the line could have been plotted at a position where log FLI equals 0.8 (in this instance the mathematical expression of the relationship would be adjusted reflectance equals measured reflectance plus (FLI - 0.8)/3.4). Regardless of what value is used for the line of equal fluorescence intensity the effect of the reflectance adjustment is the same in that reflectance variation for coals with the same coalification history is reduced. Figure 6.15A shows how the measured reflectance of serial ply samples from a single seam (drillhole 7, Pike River coalfield, Brunner coal measures, Eocene age) varies through the coal seam. After adjusting the measured reflectance values according to equation 6.4, variation of reflectance through this seam is shown to be diminished (Figure 6.15B).

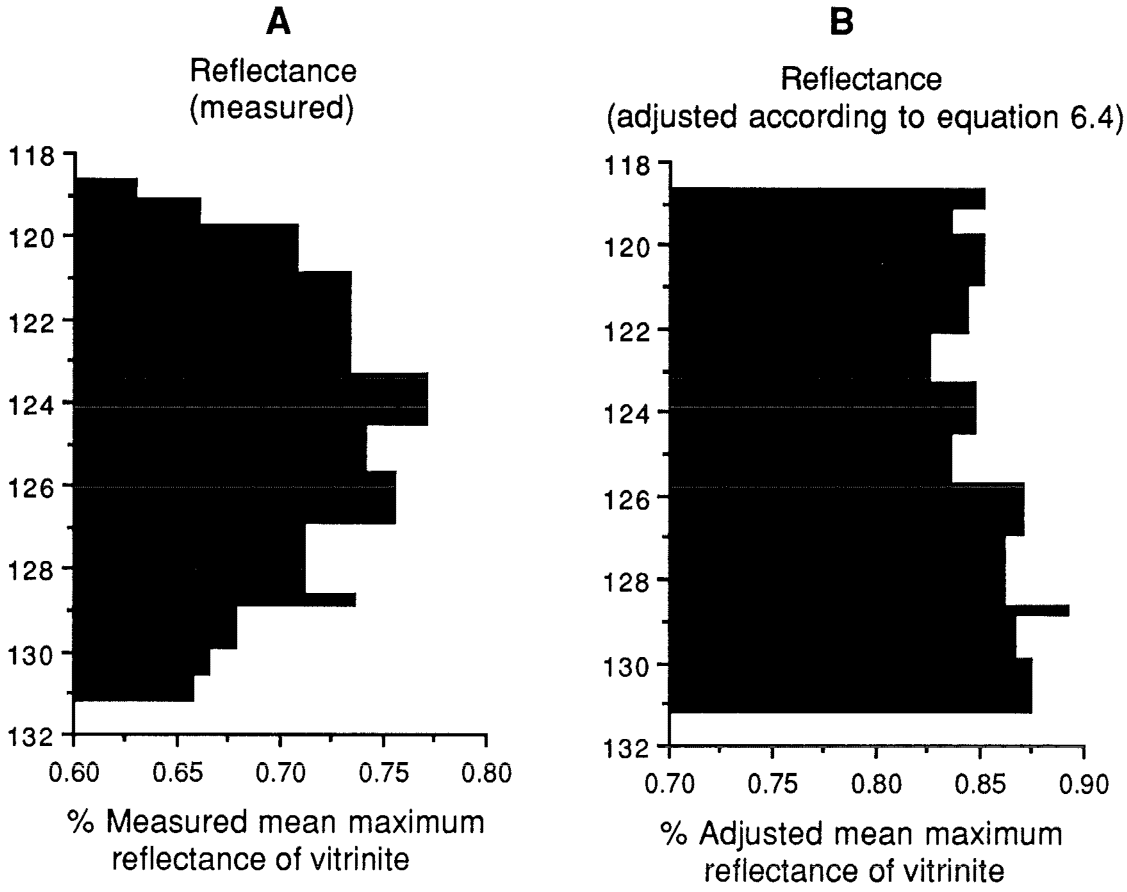

Figure 6.15 Comparison of measured (A) and adjusted (B) reflectance variation through a single coal seam encountered in drillhole 7, Pike River coalfield, Brunner coal measures (Eocene).

Equation 6.4 may be used where the measured vitrinite reflectance is between 0.5 and 1.1 % provided that weathered coal, shallow buried coal, or coal that has deteriorated due to laboratory storage is excluded. Where these conditions are met Equation 6.4 provides a way to proportionally adjust the measured reflectance of vitrinite to an arbitrary basis in accordance with the measured level of fluorescence intensity.

Measurement of fluorescence intensity and vitrinite reflectance on serial ply samples from additional bituminous coal seams should allow refinement of the proposed reflectance adjustment for perhydrous coals (eq. 6.4). It is hoped that collection of additional serial ply samples from fresh, deeply buried mvb and lvb rank coals will extend the useful range of the technique. However, since suppressed vitrinite reflectance probably has multiple causes (section 2.3.2 iv), it is doubtful that the method can be indiscriminately applied to all coals with "anomalous" reflectance. Nonetheless, the proposed correction has value given

the importance of vitrinite reflectance as a maturation parameter for petroleum exploration.

It is significant that although weathering reduces fluorescence intensity, vitrinite reflectance remains unchanged (Figure 6.16). The dissimilar response of fluorescence intensity and vitrinite reflectance to weathering indicates that "high" fluorescence intensity and "suppressed" vitrinite reflectance, although both apparently indicative of perhydrous vitrinite, are different expressions of hydrogen enrichment.

6.7 WEATHERING AND CARBONIZATION

Figure 6.16 shows the variation of vitrinite reflectance, maximum Gieseler fluidity, and mean vitrinite/inertinite fluorescence intensity of monthly samples taken over a one year interval from the surface of two, ~15 ton piles of coal at Ngakawau, New Zealand. Figure 6.16A shows that reflectance does not vary upon stockpile storage except for random scatter due to analytical precision (~ ±0.015%) and additional variation attributed to sampling from the surface of the stockpiles. Figure 6.16B shows the progressive loss of Gieseler fluidity during stockpile storage. The scatter in Figure 6.16B is attributed, in part, to the inherent difficulty of stockpile sampling and the "notorious" imprecision of the Gieseler test (Callcott 1987). Additional scatter may be a consequence of occasional swelling of the coal into the retort barrel during the Gieseler test which is suggested to slightly lower maximum Gieseler fluidity (section 4.7.2). This second explanation appears likely given the steady loss of fluorescence intensity upon stockpile storage shown in Figure 6.16C compared to the more irregular trends shown in Figure 6.16B.

Comparison of Figures 6.16B and Figure 6.16C shows that the Stockton No 2 coal exhibited generally lower fluidity values but consistently higher fluorescence intensity values than the Sullivan north coal. This observation is consistent with earlier observation by Quick *et al.*, (1988) who observed that fluorescence intensity at 600 nm reaches a maximum near 0.97% Ro_{max} whereas

Gieseler fluidity reaches a maximum near 1.15% Ro_{max}. Had longer wavelength emission filters been used, such that fluorescence intensity showed a maximum at 1.15% vitrinite reflectance, then fluorescence intensity and Gieseler fluidity could be expected to show the same relative response. Although this (superficially) suggests that longer measurement wavelengths are more useful for evaluation of carbonization behaviour than the 600 nm centre wavelength used in this study, this idea is not supported where other measures of carbonization behaviour are considered. For example, although Gieseler fluidity peaks near 1.15% Ro_{max}, the Gieseler temperature range reaches a maximum near 1.3% Ro_{max} (Quick *et al.*, 1988) and coke strength after reaction is highest where parent coals are near 1.55% Ro_{max} (Figure 6.5). Thus, fluorescence intensity at any single wavelength cannot be simply correlated with diverse measures of carbonization behaviour.

Figure 6.16 shows that weathering changes thermoplastic behaviour but does not influence vitrinite reflectance. Consequently, established relationships between carbonization behaviour and vitrinite reflectance do not apply where weathered coal is present. This observation shows the need for reliable methods to detect and quantify weathering. If weathering can be quantified then relationships between the degree of weathering and carbonization behaviour can be sought.

Where inert content is low, severely weathered bituminous coals can easily be recognized based on low crucible swelling but low level weathering is more difficult to identify. The loss of fluorescence intensity due to weathering, as illustrated in Figure 6.16C, supports the laboratory studies by McHugh (1986), Quick *et al.*, (1989) and McHugh *et al.*, (1991). Importantly, McHugh *et al.*, (1991) suggest that weathering is not restricted to outcrop and is inevitable in coals with relatively shallow present day burial depth. Their idea is supported by the data shown in Table 6.2 for three, low ash, vitrinite rich serial ply samples from Drillhole 1492 (Buller coalfield). The top ply sample is severely weathered and

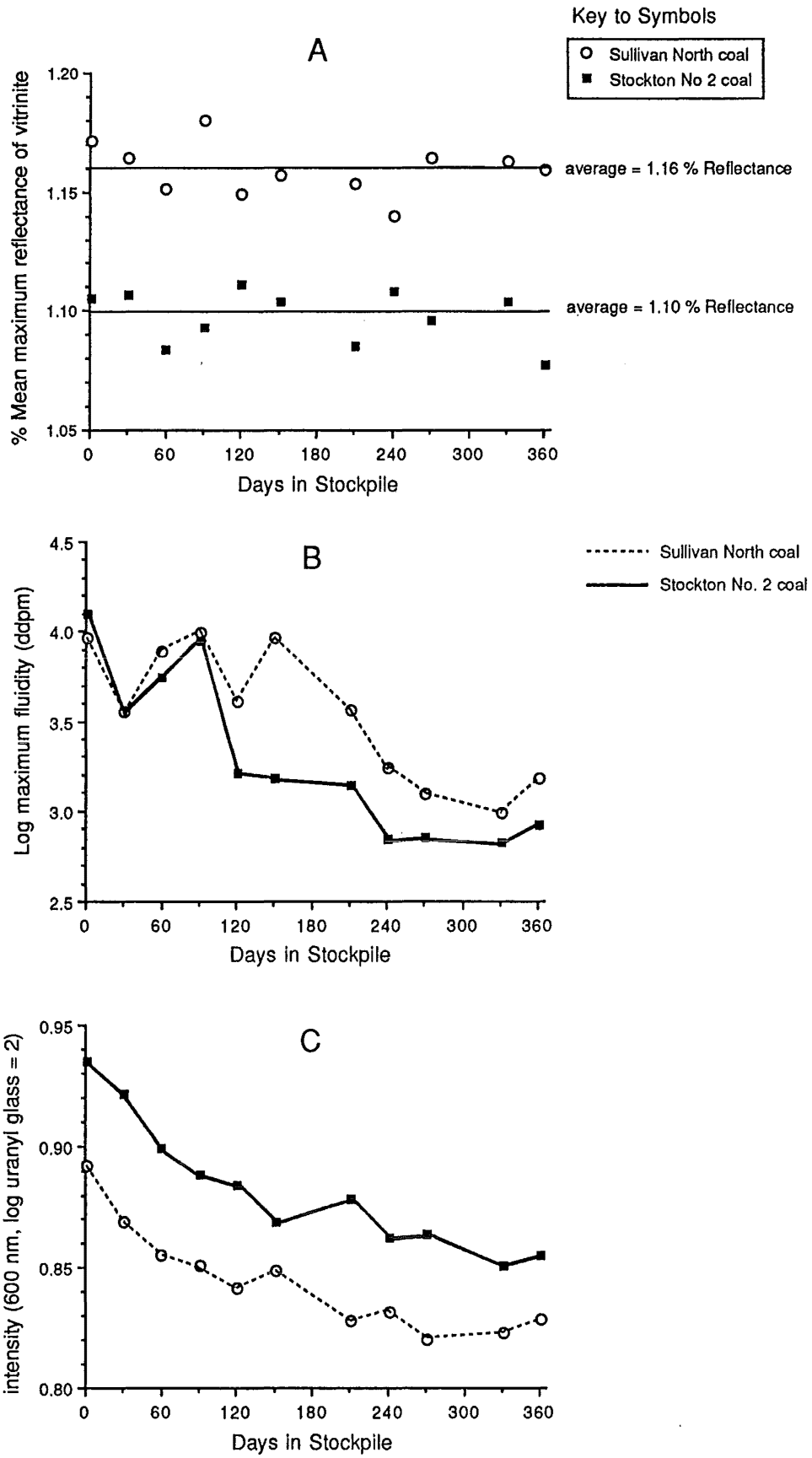

Figure 6.16 The effect of one year outdoor storage on (A) vitrinite reflectance, (B) maximum Gieseler fluidity, and (C) vitrinite & inertinite fluorescence intensity. Reflectance and fluorescence data shown for coal samples taken from the surface of two, 15 ton stockpiles is listed in Appendix E. Gieseler fluidity data for these coals courtesy of Coal Corp. of New Zealand.

reports a crucible swelling index of zero. Despite a high swelling index, the middle ply is moderately weathered; vitrinite rich coals with reflectance values near 1.1% reflectance should exhibit Gieseler fluidities near 10,000 ddpm (see Figures 3.3 and 6.3). Although similar rank Buller coals commonly show relatively low fluidity near the middle of the seam, the low Gieseler fluidity of this coal and its occurrence immediately below a severely weathered intersection suggests that it has lost fluidity due to weathering. Table 6.2 shows that severe weathering may occur as deep as 26 meters of present day burial depth. McHugh and her co-workers have observed lower fluorescence intensity at 73 meters burial depth compared to equivalent coal present at 177 meters depth. These observations support the notion that where coking coal is produced from open-cast operations incipient weathering is inevitable and severe weathering is possible.

TABLE 6.2
COAL PROPERTIES IN A WEATHERED COAL SEAM
(drillhole 1492, Buller coalfield, Eocene)

Sample ID	Depth (meters)	Reflectance (Ro_{max})	% Stained	Crucible Swelling Index	Max. Gieseler Fluidity (ddpm)
a90-3482	26.1 to 28.3	0.98	78.8	0	0
a90-3484	28.3 to 37.6	1.15	0.6	9	445
a90-3486	37.6 to 39.6	1.14	0.5	9	8,780

6.8 PREDICTION OF CARBONIZATION BEHAVIOUR

In this section, prediction of carbonization behaviour by the combined use of vitrinite reflectance and fluorescence intensity is advocated. Vitrinite reflectance is used as a rank parameter and fluorescence intensity is used as a type and weathering parameter. Multivariate regression is used to predict observed carbonization behaviours where reflectance and fluorescence intensity are used as predictor variables.

As discussed in section 6.5, the thermoplastic behaviour of coal has been correlated with vitrinite reflectance. For New Zealand coals the relationship is poor due to the presence of both perhydrous and weathered vitrinite. Thus

prediction of carbonization behaviour will fail where only vitrinite reflectance is considered. Quick *et al.*, (1988) has shown that fluorescence intensity alone is a poor predictor of maximum Gieseler fluidity. Similarly, Figure 6.17 shows that fluorescence intensity alone is a poor predictor of Gieseler plastic temperature range. This is because coals with relatively high reflectance (circled in Figure 6.17) report relatively high Gieseler plastic temperature range values at equivalent levels of fluorescence intensity. Thus, both reflectance and fluorescence intensity must be considered in order to predict carbonization behaviour.

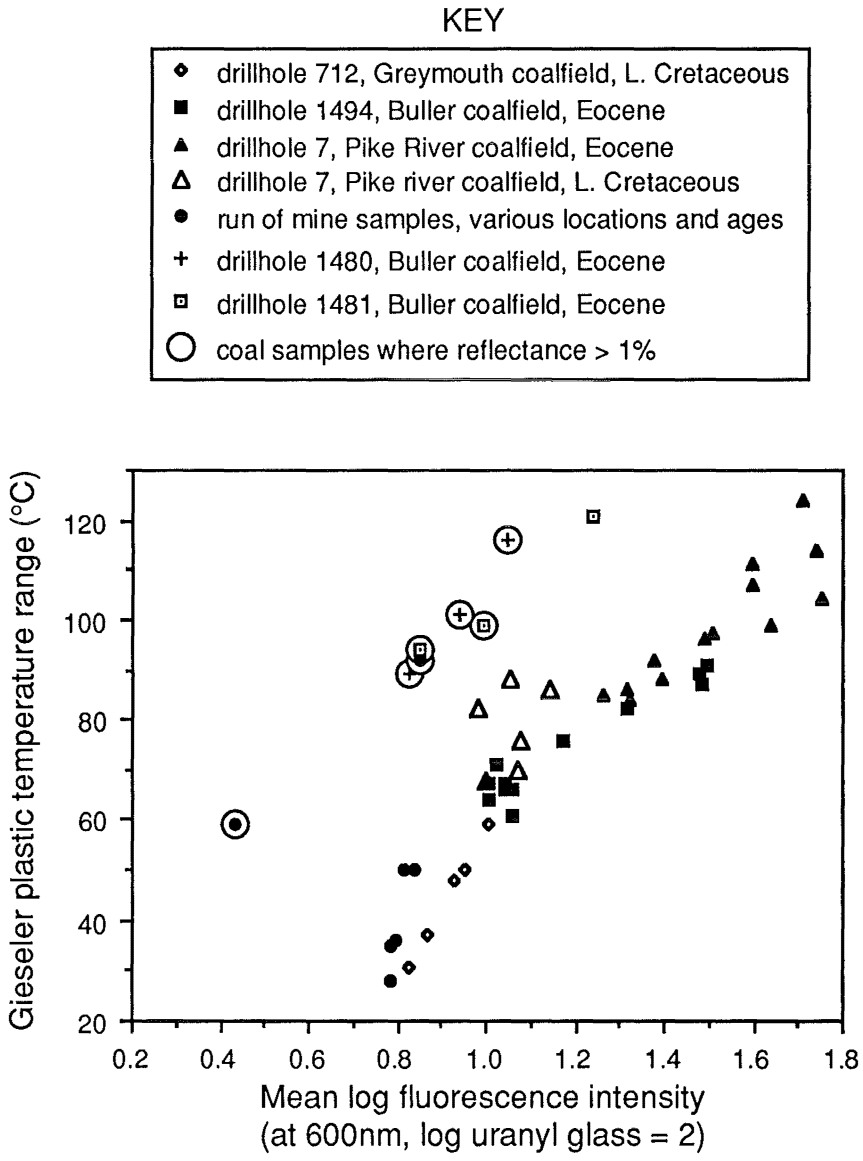

Figure 6.17 Relationship between fluorescence intensity and Gieseler fluid temperature range for some New Zealand coals.

It is important to note the limitations of the data presented in this thesis. For example, Gieseler fluidity data are available for 50 coals. However, five of these coals show ash yields greater than 15%, and only one coal reports a reflectance value greater than 1.2% (46/426). The small number of high ash coals precludes reliable evaluation of the effect of inorganic content on thermoplastic behaviour and they are not considered. Because data for only one high reflectance coal is available, reliable prediction above 1.2% reflectance is not possible and this sample is sometimes removed from the data set. Thus the resulting regression analyses are only valid within a restricted range of ash and reflectance values. Different relationships can also be expected where fluorescence intensity is measured using different excitation/emission wavelengths or different calibration standards.

6.8.1 Prediction of Gieseler Fluidity

Multivariate linear regression on 44 New Zealand coals where ash is less than 15% and mean maximum reflectance is between 0.4 and 1.2%, showed that the Gieseler thermoplastic range can be predicted according to the following equation.

$$\text{Predicted Gieseler Temp. Range (°C)} = 96.1*Ro + 76.8*FLI - 81.7 \qquad \text{(eq. 6.5)}$$

where,

Ro = % mean maximum reflectance of vitrinite, and,

FLI = log (base10) mean fluorescence intensity of vitrinite at 600 nm emission, relative to a uranyl glass standard = 100 on a linear scale.

This equation provides a coefficient of determination (R^2) of 0.91 and a standard deviation of the residuals of ±5 °C. To test the wider applicability of equation 6.5 an independent data set is required. Because fluorometric analysis is not a standardized method this is not easily accomplished. Nonetheless, data published by Quick *et al.*, (1988) for 23 US coals, where Ro_{max} is <1.2% and ash is <15%, (19 Carboniferous, 3 Late Cretaceous, 1 Paleocene age coal originating from 10 different US States) were used for this purpose. Quick *et al.*, (1988) measured vitrinite-inertinite fluorescence intensity using similar excitation and

emission wavelengths (390-490nm excitation, 570-630nm emission) and the same style calibration standard (Leitz masked uranyl glass standard). Because these workers calibrated to an arbitrary value of uranyl glass = 10.72 on a 100 scale, their data were multiplied by a factor of 9.33 to achieve parity with the raw data presented in this thesis. When equation 6.5 was applied to the adjusted data from Quick et al., (1988) good agreement between the predicted and the measured Gieseler plastic temperature range was observed; the standard deviation of the residuals was ±6 °C. Because of the close agreement between the two data sets all of the data were used to obtain a new predictive equation shown below.

Predicted Gieseler Temp. Range (°C) = 92.1*Ro + 79.9*FLI - 86.3 (eq. 6.6)

Equation 6.6 reports a coefficient of determination of 0.88 and a standard deviation of the residuals of ±5 °C. The relationship between the predicted and observed Gieseler thermoplastic range for 44 New Zealand and 23 US coals is shown in Figure 6.18.

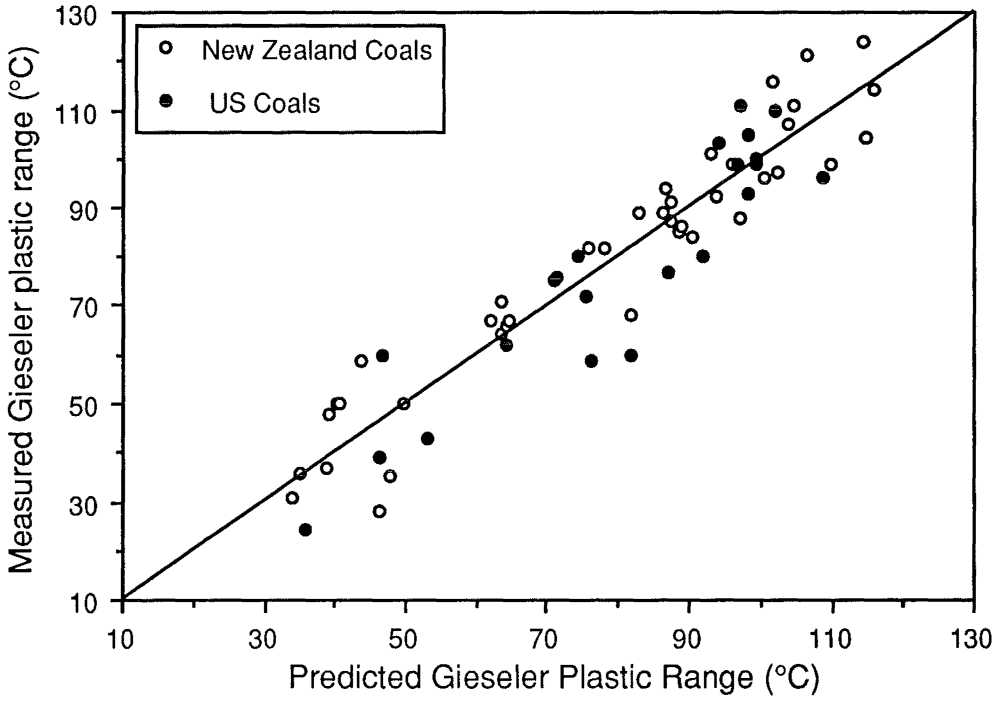

Figure 6.18 Relationship between the measured and predicted (equation 6.6) Gieseler plastic range (°C) for some New Zealand and US coals where reflectance is between 0.4 and 1.2% and dry ash content is less than 15%. US coal data from Quick *et al.*, (1988).

More analytical data are required to extend the relationship shown in Figure 6.18 to include higher rank coal. However if additional data become available an additional predictive term (Ro_{max}^2) will probably be required to account for the known loss of thermoplastic range above 1.3% reflectance. It is worth noting that the US coals shown in Figure 6.18 lack abundant inertinite; whether this relationship can be extended to include inertic coals remains to be demonstrated. Nonetheless, it is significant that analytical data obtained in a different laboratory on different set of coals could be used with the data presented in this thesis to predict the Gieseler plastic range.

The relationship between vitrinite reflectance, mean log fluorescence intensity of vitrinite and inertinite (FLI), and Gieseler fluidity shown in equation 6.6 is graphically illustrated in Figure 6.19 along with the plotted position of the samples used to establish the equation. Examination of Figure 6.19 shows that the slope ($\Delta FLI/\Delta Ro_{max}$) of the lines of equal Gieseler plastic range equals -1.16. This value can be compared to the average slope for serial ply samples where $\Delta FLI/\Delta Ro_{max}$ is shown to equal -3.4 (Figure 6.13). Thus both FLI and Ro need to be considered for prediction of thermoplastic behaviour.

6.8.2 Prediction of Optical Texture Index

The lack of correlation between the optical texture index (OTI) and vitrinite reflectance (Fig. 6.10) was attributed to the presence of either weathered or perhydrous vitrinite. A good relationship between the Gieseler solidification temperature and the log of the optical texture index is shown in Figure 6.20.

(i) hydrogen and OTI

Why does the Gieseler solidification temperature correlate with the optical texture index? Before the development of liquid crystals, crosslinking reactions due to the presence of heteroatoms predominate. Only after the demand for hydrogen by these reactive heteroatoms has been satisfied can the hydrogen effectively function to stabilize thermally cleaved aromatic fragments and allow

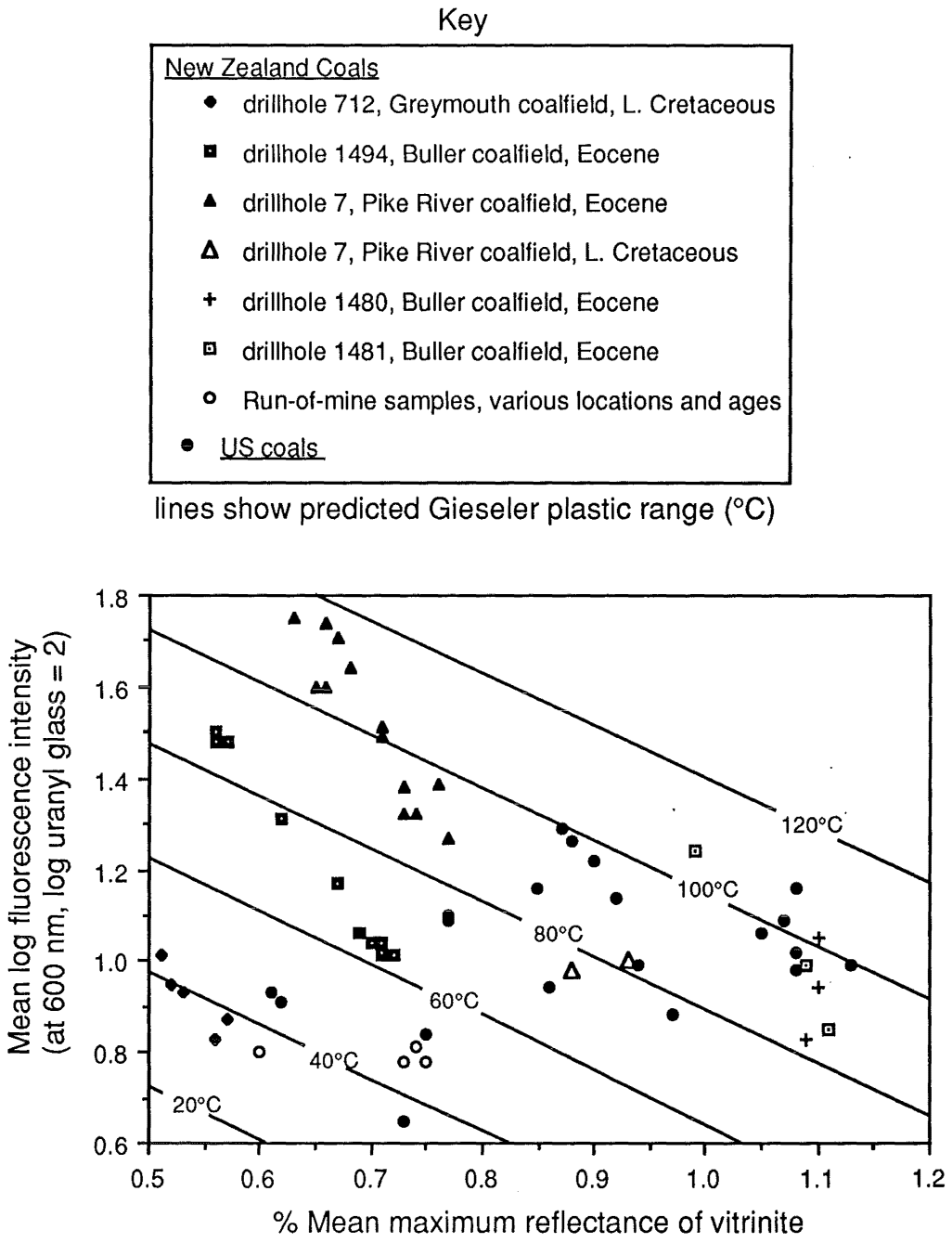

Figure 6.19 Graphic illustration of the relationship between reflectance fluorescence intensity and Gieseler plastic range (°C) expressed in equation 6.6. The plotted position of the samples used to establish the equation are also shown. US coal data from Quick *et al.*, (1988).

sufficient mobility for alignment of the aromatic layers into ordered units. Thus the stabilization or gaseous evolution of oxygen or sulphur-containing reactive moieties consumes hydrogen that would otherwise be used to stabilize free radicals and allow the alignment of aromatic lamallae into liquid crystal precursors of mosaic microtextural units. If this is true then the development of anisotropic microtextures should depend on the amount of hydrogen remaining after consumption by oxygen and sulphur atoms. This "available" hydrogen may

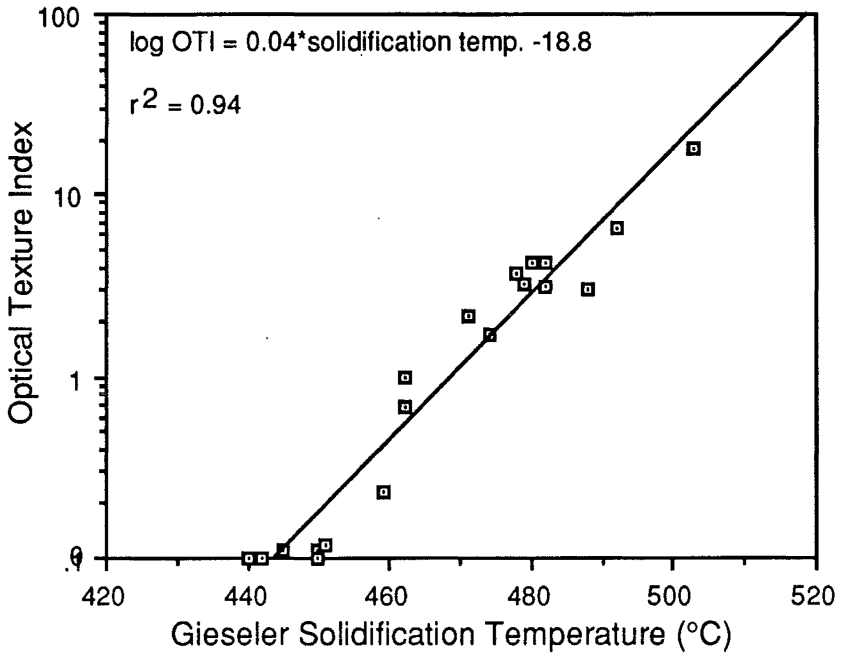

Figure 6.20 Correlation between the Gieseler solidification temperature of parent coals and the optical texture index of carbon products for 19 carbon specimens listed in Table 4.4, excluding samples a90-93 to a90-646 where Gieseler fluidity was not measured.

be estimated by stoichiometric calculation of the amount of hydrogen consumed by sulphur and oxygen to produce H_2S and H_2O; this quantity is subtracted from the total hydrogen. The relationship between available hydrogen and Gieseler solidification temperature for coal samples listed in Table 5.1 where ash is <30% is shown in Figure 6.21 (reliable calculation of elemental composition is difficult where ash is high). The regression line shown in Figure 6.21 reports a coefficient of determination (r^2) of 0.90 compared with a value of 0.78 where total organic hydrogen is plotted against Gieseler solidification temperature. For coals that pass through an isotropic liquid phase upon pyrolysis, available hydrogen rather than total hydrogen appears to be a better predictor of solidification temperature, and thus optical texture index. Above mvb rank, optical microtexture is largely a consequence of solid state transitions (basic anisotropy, and some lamellar flow textures) where the availability of hydrogen is probably less important. The nature of these solid state transitions remains uncharacterised but does not involve an isotropic liquid phase (Moreland *et al.*, 1988).

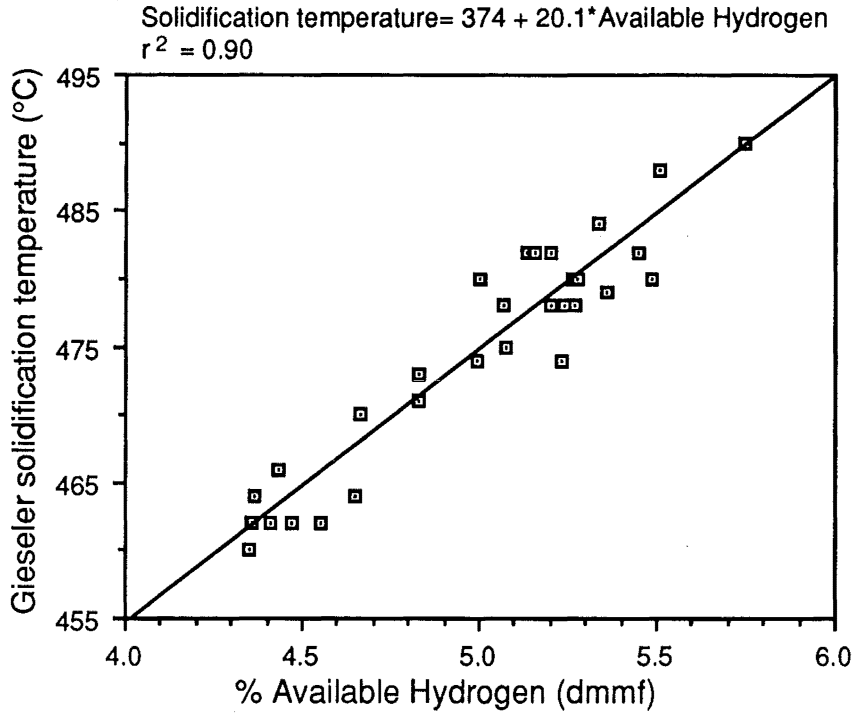

Figure 6.21 Relationship between available hydrogen content and solidification temperature for some New Zealand coals (coal samples are those listed in Table 5.1 excluding sample 46/750 and 46/945 which contain >30% ash (available hydrogen = H_o - 0.126*O_o - 0.0629*S_o).

Despite the good correlation between the available hydrogen content and solidification temperature shown in Figure 6.21 the substantial analytical requirements for calculation of organic hydrogen (equation 5.4) hinder its use for routine predictive purposes. For example, calculation of the available hydrogen values used in Figure 6.21 required 10 different analytical determinations. Complete analytical data are available for only 10 of the 28 coals selected for carbonization (coals from the Pike River coalfield and the Upper Waimangaroa sector of the Buller coalfield, Table 4.4). For these few data, where "available" hydrogen is used to predict log OTI a positive correlation is observed (r^2=0.84). Note that these ten coals vary in reflectance between 0.56 and 0.88 and the positive relationship between OTI and hydrogen can be expected to change at higher rank since OTI tends to increase with increasing rank whereas hydrogen content declines above mvb rank. Nonetheless, the positive relationship between available hydrogen and OTI supports the notion that where optical microtexture develops through an isotropic melt abundant available hydrogen promotes the development of progressively larger anisotropic domains.

Since thermoplastic behaviour is essentially a molecular reaction the importance of hydrogen is better understood in terms of the molar rather than the weight percent abundances reported by ultimate analysis. Where molar abundance is considered the low molecular weight of hydrogen compared to that of carbon or oxygen imposes exacting demands on analytical precision. For example, the precision (± 2σ) of air dried, weight% carbon and hydrogen determinations are ± 0.135 and ± 0.07 respectively (BS1016, part 16). If analytical error due to moisture and mineral matter corrections are ignored these values can be shown to correspond to an acceptable error of 0.07 mole% carbon and 0.30 mole% hydrogen for a hypothetical coal with 83% C, 6% H, 1% N, and 2% S on a weight percent dmmf basis. Besides showing the effective precision of elemental analysis, consideration of the mole% composition of coal neatly illustrates the importance of hydrogen; in the hypothetical coal described above (6 wt.% H) 44 out of every 100 atoms are hydrogen. The relative abundance of hydrogen in coal is easily overlooked (and rarely emphasised in texts) where only the weight percent elemental composition is considered.

(ii) OTI predicted by fluorescence and reflectance

Where both vitrinite reflectance and the mean log fluorescence intensity are used to predict OTI for (26) coal samples listed in Table 4.4 (excludes samples a90-636 and a90-646 that lack fluorescence data) a coefficient of determination (R^2) of 0.66 is obtained. The R^2 value increases to 0.79 where the highest rank (46/426, Ro_{max} = 1.6) coal is not included in the regression. This improved correlation can be explained as a result of different origins of carbon microtexture; optical microtexture of lower rank bituminous coals is suggested to develop through a liquid isotropic phase, to liquid crystal, to mesophase, and finally mosaic microcrystallite structure. Above about 1.3% reflectance solid state transformations become increasingly important. Thus OTI may exhibit a nonlinear relationship with rank necessitating an additional term in the regression equation. Indeed, where log mean fluorescence intensity, Ro_{max}, and Ro_{max}^2 are used as regression variables to predict OTI a coefficient of determination (R^2) of 0.87 is obtained. Unfortunately the data set is highly skewed toward low rank bituminous coals (only one coal above 1.3% Ro_{max}).

Consequently a convincing relationship using these three predictor variables is not possible. Despite the acknowledged limitations of the data, a systematic relationship between OTI and both reflectance and fluorescence intensity is suggested.

6.8.3 Prediction of the Reflectance of Carbonized Coals.

Figure 6.22 shows how the maximum, average, and minimum reflectance of the carbonized coal specimens compare with the mean maximum reflectance of the parent coals. Maximum and average carbon reflectance as well as the optical anisotropy of the carbons increase with increasing vitrinite reflectance whereas minimum carbon reflectance decreases with increasing vitrinite reflectance. The general increase of average carbon reflectance with increasing reflectance of the parent vitrinites suggests that the aromaticity of the carbon product is predetermined by the aromaticity of the parent coal. The decrease of minimum carbon reflectance is thought to be due to the increasing diameter of the aromatic lamallae in the carbons. Increasing bireflectance reflects the progressive alignment of aromatic lamallae into more perfect crystallites. Figure 6.23 shows

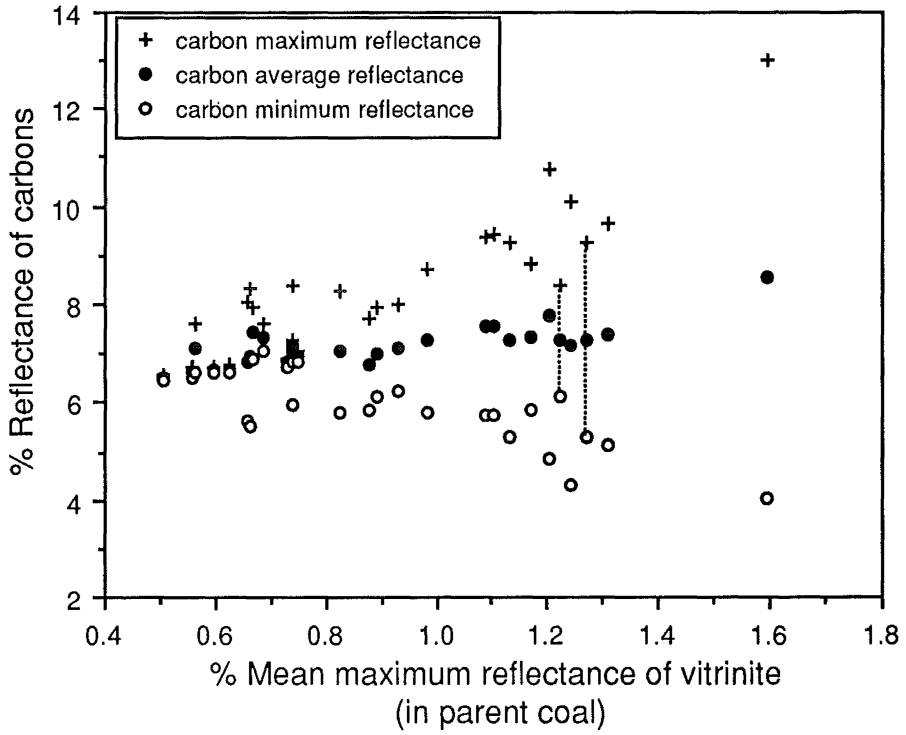

Figure 6.22 Relationship between the reflectance of the parent coal and the maximum, average and minimum reflectance of the derived carbon specimens. Analytical data from Table 4.4, the dashed lines show the anisotropy of two coals (a90-636, a90-646) that are thought to be severely weathered.

the relationship between optical anisotropy and OTI. Carbons made from coal samples a90-636 and a90-646 (weathered coals) are shown to deviate from this relationship. Analytical data for these outliers are provided in Table 6.3; low crucible swelling of vitric coals at this rank is indicative of severe weathering. The comparatively low OTI values of the derived carbons is a consequence of the predominance of basic anisotropy microtextures. Examination of Table 6.3 suggests that safranin O staining is not a sensitive indicator of weathering at these ranks since only 18% of the organic matter in sample a90-636 was stained but 81% of the derived carbon did not pass through a plastic stage upon carbonization. It is also worth noting that these two coals exhibit a slightly lower apparent anisotropy than might be expected based on their level of vitrinite reflectance (Figure 6.22).

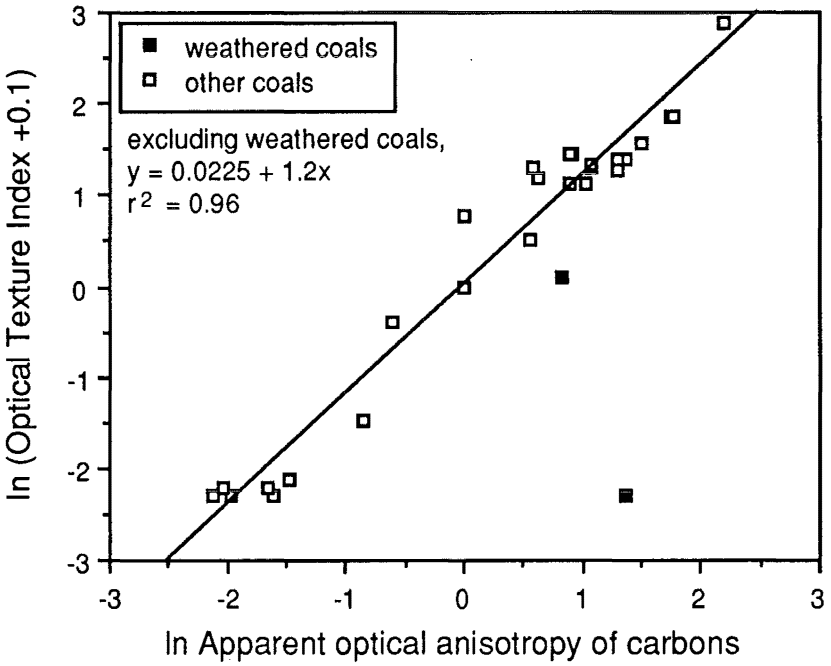

Figure 6.23 Relationship between the optical anisotropy of carbonized coals and OTI. Note the position of two coals (a90-636, a90-646) that are thought to be severely weathered (analytical data from Table 4.4).

Figure 6.24 shows how reflectance and fluorescence intensity of the parent coals can be used to predict the optical anisotropy of the carbonized coals. The good relationship between measured and predicted anisotropy supports the combined use of reflectance and fluorescence to predict carbonization behaviour.

TABLE 6.3
SOME ANALYTICAL DATA FOR TWO WEATHERED COAL SAMPLES AND DERIVED CARBONS (from drillhole 1490, Buller coalfield, Eocene)

Coal Properties				Properties of Derived Carbons		
ID number	Ro_{max} (vitrinite)	Crucible Swelling Index	vol. % Stained	vol.% Basic Anisotropy microtexture	OTI	Optical Anisotropy (carbon)
a90-636	1.22	0.5	18.2	81.2	1.0	2.28
a90-646	1.27	0.0	45.7	92.4	0.0	3.95

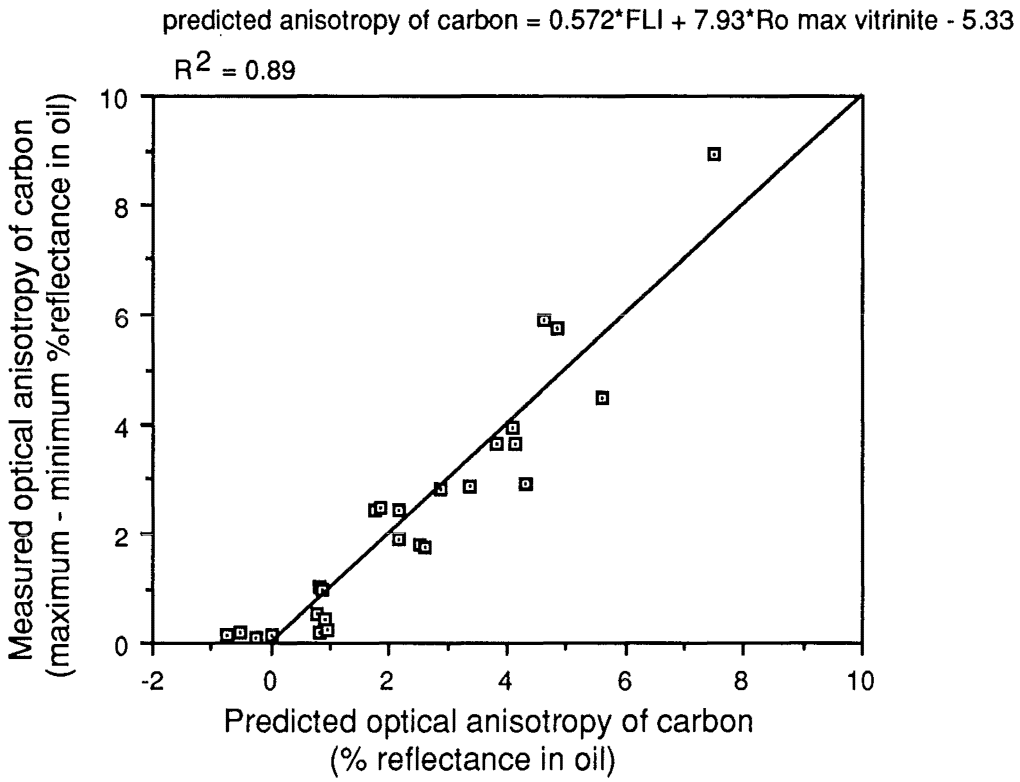

Figure 6.24 Relationship between predicted and measured optical anisotropy. Coals plotted are listed in Table 4.4. Samples a90-636 and a90-646, for which fluorescence intensity was not measured, are omitted.

6.9 REFLECTANCE, FLUORESCENCE AND PYROLYSIS BEHAVIOUR.

The preceding discussion has suggested that the carbonization behaviour of coal can be estimated by consideration of both reflectance and fluorescence intensity. In this section the relationship between these parameters and both Rock Eval pyrolysis, and volatile matter are examined. Because the coals examined in this study typically contain more than 90% vitrinite it is uncertain if these relationships would apply to inertinite rich coals. Because neither reflectance or fluorometric analysis account for the presence of liptinite, it is

unlikely that relationships established in the following sections could be validly applied to liptinite rich coals.

6.9.1 Prediction of Rock-Eval Pyrolysis Values

(i) Tmax

Figure 6.25 relates vitrinite reflectance and Rock-Eval Tmax. If the three outliers (a90-97, a90-100, a90-102, boldface in Table 6.4) are ignored a linear relationship is observed. The anomalously low Rock-Eval Tmax values are not understood and three different explanations are suggested.

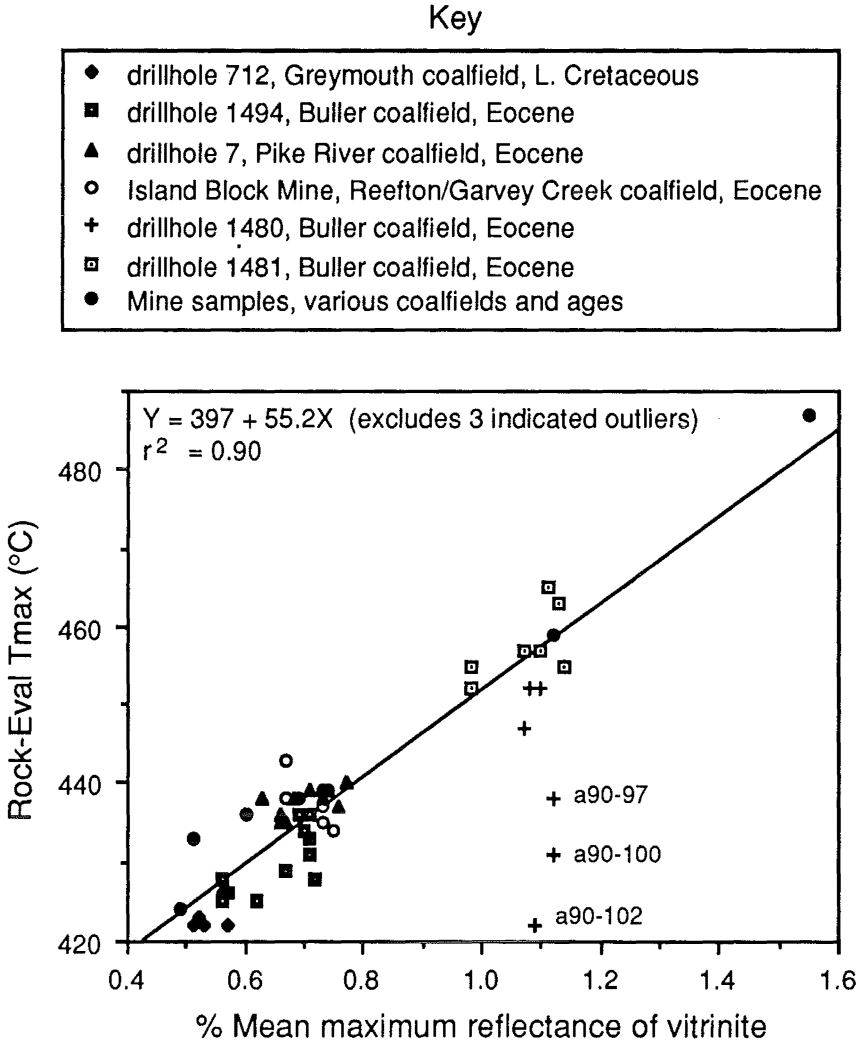

Figure 6.25 Relationship between mean maximum reflectance of vitrinite and Rock-Eval Tmax (data from Table 6.1).

Peters (1986) notes that resinite, migrated oil or solidified bitumen is sometimes associated with low Tmax values in source rocks. In such instances S1 is high, PI is high, and the S2 peak is bimodal. Because raw pyrograms were not examined this possibility was not fully explored. Nonetheless, compared to

TABLE 6.4

ROCK EVAL DATA FOR SOME NEW ZEALAND COALS

Coal ID number	drillhole No Mine name	% Ro_{max}	Rock-Eval Data TOC wt%	Tmax (°C)	S1 mgHC/g	S2 mgHC/g	S3 mgHC/g	Sulphur % total (dry)	% pyritic (dry)
46/739	DH-1494	0.56	51.0	428	8.90	311	1.50	4.5	1.4
46/740	DH-1494	0.57	56.8	426	9.54	286	1.18	4.7	1.4
46/741	DH-1494	0.56	50.8	425	8.22	322	1.29	6.4	3.3
46/742	DH-1494	0.62	47.3	425	7.73	269	1.28	4.0	0.8
46/743	DH-1494	0.67	47.3	429	7.86	273	1.09	3.4	0.7
46/744	DH-1494	0.70	47.8	434	6.02	237	1.68	4.7	3.1
46/745	DH-1494	0.71	32.2	433	5.75	228	0.90	1.5	0.2
46/746	DH-1494	0.71	54.1	431	5.58	258	2.00	1.2	0.0
46/747	DH-1494	0.69	58.4	436	5.33	226	1.22	1.4	0.2
46/748	DH-1494	0.72	68.3	428	6.82	267	1.41	1.1	0.0
46/749	DH-1494	0.71	61.8	436	7.17	258	1.19	1.1	0.0
a90-88	DH-1480	1.08	40.0	452	7.20	212	1.46	0.5	
a90-89	DH-1480	1.10	28.6	452	7.84	195	1.16	0.5	
a90-95	DH-1480	1.14	36.5	455	8.73	201	1.16	1.2	
a90-97	**DH-1480**	**1.12**	**17.1**	**438**	**9.64**	**73**	**1.21**	**2.5**	
a90-100	**DH-1480**	**1.12**	**25.8**	**431**	**9.69**	**73**	**1.54**	**4.0**	
a90-102	**DH-1480**	**1.09**	**21.7**	**422**	**14.77**	**57**	**1.10**	**4.3**	**0.2**
a90-103	DH-1480	1.07	38.9	447	14.39	190	1.08	4.4	
a90-134	DH-1481	0.98	45.4	452	13.46	197	1.23	6.4	
a90-136	DH-1481	0.98	42.7	455	11.68	208	1.88	3.6	1.4
a90-138	DH-1481	1.07	38.8	457	10.66	206	2.16	1.1	
a90-143	DH-1481	1.10	25.4	457	11.66	182	2.27	0.8	
a90-148	DH-1481	1.10	31.7	465	8.53	181	1.65	1.1	
a90-151	DH-1481	1.13	43.0	463	11.41	157	3.14	4.5	2.7
a90-152	DH-1481	1.14	38.4	455	11.32	157	2.05	2.7	
C90-8	Island Block	0.73	36.0	439	4.55	229	5.89	1.3	
C90-7	Island Block	0.74	41.5	439	6.82	227	5.60	0.9	
C90-6	Island Block	0.73	41.4	437	2.28	188	5.22	1.1	
C90-5	Island Block	0.75	45.8	434	3.91	193	5.36	0.9	
C90-4	Island Block	0.73	45.5	435	2.37	190	5.93	1.7	
C90-3	Island Block	0.67	36.9	438	4.84	194	5.06	0.8	
C90-2	Island Block	0.67	50.9	443	3.31	178	7.11	1.8	
45/075	Sullivan	1.12	31.5	459	7.69	170	1.45		
45/076	New Creek	0.49	31.0	424	2.17	104	14.69		
44/197	Ferndale	0.51	30.7	433	1.42	101	12.97		
44/963	Strongman	0.60	39.4	436	4.91	212	4.64		
44/934	Moody Creek	0.69	49.6	438	3.88	187	4.76		
44/816	Roa	1.55	29.0	487	3.13	92	1.75		
50/639	DH-712	0.56	60.9	426	1.32	185	4.19	0.3	
50/640	DH-712	0.53	68.6	422	3.02	220	4.30	0.3	
50/641	DH-712	0.51	61.7	422	2.63	267	4.66	0.3	
50/643	DH-712	0.52	56.9	423	2.33	239	4.17	0.3	
50/644	DH-712	0.57	70.7	422	2.02	230	3.91	0.5	
46/835	DH-7	0.63	59.6	438	19.29	346	0.97	4.2	1.6
46/836	DH-7	0.66	61.5	435	19.84	351	2.06	3.6	0.4
46/837	DH-7	0.71	65.8	433	13.75	301	1.11	3.1	0.1
46/838	DH-7	0.73	58.0	438	13.91	324	1.00	2.5	0.1
46/839	DH-7	0.73	57.6	439	11.92	327	1.00	1.6	0.0
46/840	DH-7	0.77	55.6	440	11.15	298	1.34	1.1	0.0
46/841	DH-7	0.74	53.4	439	5.58	318	1.02	1.4	0.0
46/842	DH-7	0.76	55.2	437	8.62	324	1.30	2.1	0.1
46/843	DH-7	0.71	60.5	439	11.92	344	3.07	3.0	0.1
46/844	DH-7	0.68	57.6	438	16.32	329	0.75	4.0	0.2
46/845	DH-7	0.67	75.8	435	18.44	380	1.89	4.1	0.3
46/846	DH-7	0.66	76.7	436	21.25	373	1.62	4.0	0.8

unaffected coal samples from Drillhole 1481, the S1 values of the affected samples are not high. The high PI values for these coals is a result of comparatively low S2 rather than high S1 values.

Peters (1986) also comments that some organic rich samples generate sufficient pyrolyzate to saturate the FID detector, resulting in low S2 and low Tmax. As noted above the affected samples exhibit comparatively low S2 and Tmax values. However, without knowledge of the sample weights charged into the pyrolyzer, this explanation must remain speculative.

Another explanation is suggested by the low TOC values for the affected coal samples. Although TOC determined by Rock Eval pyrolysis is usually low for coals (R. M. Bustin pers. comm.) the affected samples report significantly less carbon than the unaffected coals. If TOC was determined by summing the carbon in the pyrolyzate with that determined upon combustion of the pyrolysis residue, then perhaps the low TOC value is an artifact of organic matter being incorporated into a refractory pyrolysis residue rather than evolving at higher temperatures during S2 peak generation. The incorporation of relatively large amounts of organic matter into a refractory pyrolysis residue might be promoted by sulphur induced cross-linking. The low Tmax may result from thermally labile organic sulphides which might promote decomposition at a lower temperature before eventually participating in any crosslinking reactions. Although high sulphur contents are also found in Drillhole 1481, some limited analyses suggest that in these instances a significant amount of the sulphur is present in mineral sulphide which probably remains inert at Rock-Eval pyrolysis temperatures.

Regardless of the cause of the anomalous Tmax values shown in Figure 6.25 the data listed in Table 6.4 suggest that anomalous Tmax values can be recognized where S2 is low. For the instrumental conditions and coal samples considered here the results of Rock Eval pyrolysis are unreliable where S2 is less than 80 mg HC/gram sample. The anomalous samples (boldface type in Table 6.4) are not considered any further.

The correlation between reflectance and Rock-Eval Tmax (r^2=0.90) shows no significant improvement where both reflectance and fluorescence intensity are used as predictor variables. Thus Tmax does not appear to be significantly affected by the amount of mobile phase material present in coal, and may simply vary with aromaticity or network phase structural rigidity. This explanation is favoured if reflectance is considered as a measure of aromaticity or structural rigidity of the network phase. The general increase in the enthalpy of decomposition with increasing rank (Figure 5.1) supports this idea. Indeed where equation 6.4 is applied to these coals to remove the perturbing effect of hydrogen enrichment on vitrinite reflectance the coefficient of determination decreases to 0.85. Thus Tmax and reflectance are apparently responding largely to a single causative factor unrelated to either fluorescence intensity or bitumen enrichment. This explanation is consistent with the notion expressed in section 6.7 that suppressed vitrinite reflectance and high fluorescence intensity are expressions of different phenomena, although presumably related in origin.

Examination of Figure 6.25 shows that the data are negatively skewed; only one coal sample reports a reflectance value greater than 1.2% Ro_{max}. It is worth noting that the regression equation and coefficient of determination are not materially changed where this coal sample is excluded from the regression analysis. Nonetheless the lack of coal samples above 1.2% Ro_{max} constrains prediction of S1 and S2 discussed below.

(ii) S1 and S2

The relationship between vitrinite reflectance and both S1 and S2 is shown in Figure 6.26 and is consistent with the trends observed by Teichmüller and Durand (1983) who examined a larger, more diverse set of coals. Both S1 and S2 show significant variation at equivalent reflectance. S1 shows a general increase up to about 1% reflectance and then declines. S2 shows a general decrease and less variation with increasing reflectance.

Examination of Figure 6.26 shows that reflectance alone is a poor predictor of S1 or S2. Plots of mean fluorescence intensity with both S1 and S2 (not shown)

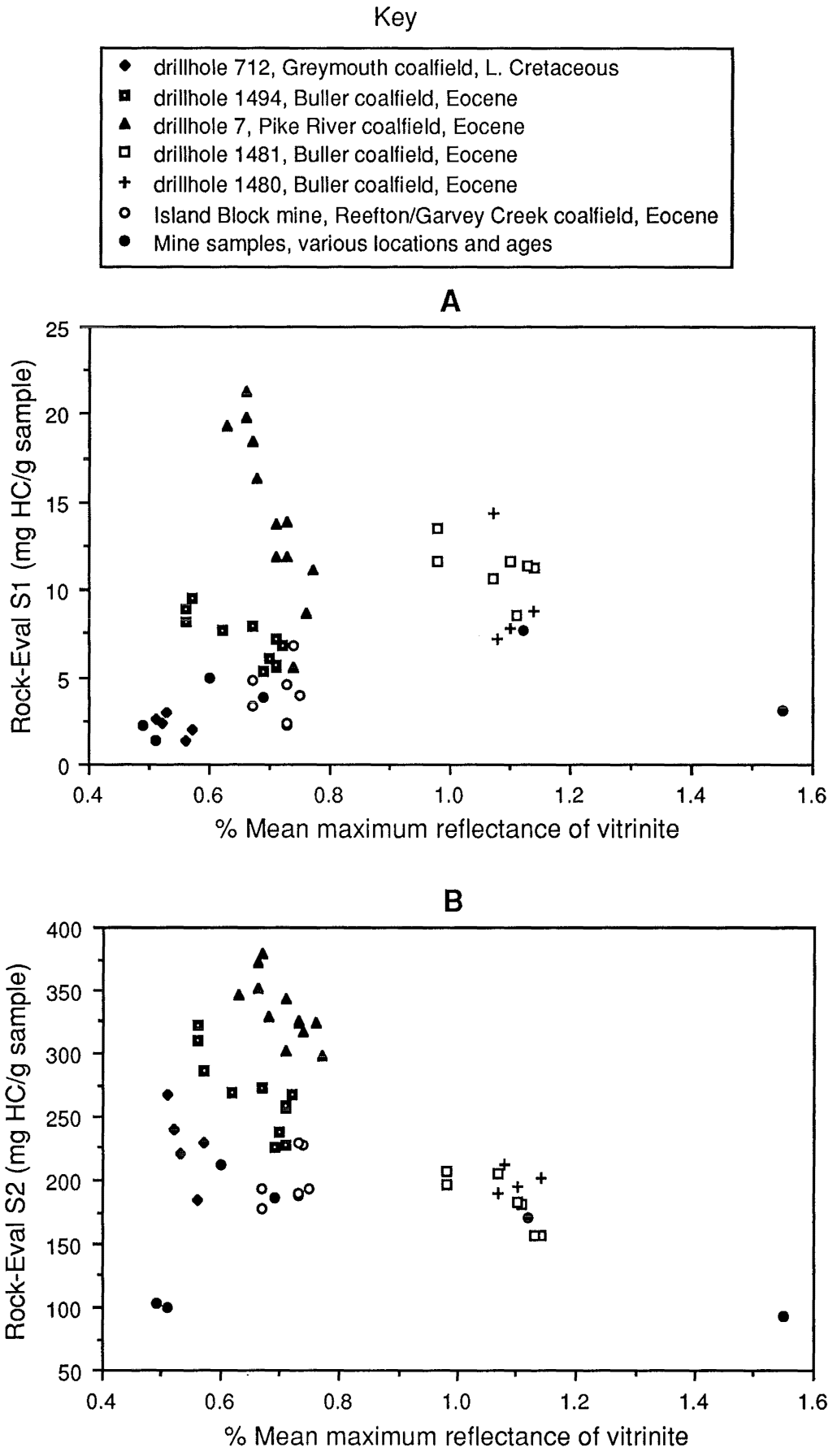

Figure 6.26 (A) Scatter plot showing how S1 varies with vitrinite reflectance. (B) Scatter plot showing how S2 varies with vitrinite reflectance. Analytical data from Table 6.4 excluding anomalous samples (boldface type in Table 6.4).

show positive, but weak, correlations (r^2 = 0.60 and 0.78 respectively). Because the data set is highly skewed toward low reflectance values the single high rank coal (44/816) was omitted from these and subsequent calculations. Consideration of both reflectance and fluorescence intensity provides a better estimation of S1 and S2 where,

$$S1 = 15.41*Romax + 0.38*FLI - 9.14 \quad \text{(eq. 6.7)}$$

$$S2 = -92.08*Romax + 175.8*\log FLI + 130.7 \quad \text{(eq. 6.8)}$$

and; Romax = % mean maximum reflectance of vitrinite, and

FLI = Mean fluorescence intensity of vitrinite and inertinite at 600 nm where a uranyl glass standard = 100.

The coefficients of determination reported by equations 6.7 and 6.8 are 0.89 and 0.86 respectively. Figures 6.27A and 6.27B graphically illustrate the relationships expressed in equations 6.7 and 6.8 and the position of analytical data used to derive them. Examination of Figure 6.27 or equations 6.7 and 6.8 show that between 0.5 and 1.2% vitrinite reflectance, S1 increases with increasing reflectance and S2 decreases with increasing reflectance. Both S1 and S2 are shown to increase with increasing fluorescence intensity.

6.9.2 Prediction of Volatile Matter Yield

Figure 6.28 shows the relationship between vitrinite reflectance and volatile matter for 130 bituminous rank New Zealand coal samples where ash is < 20%. Examination of Figure 6.28 shows that reflectance is a relatively poor predictor of volatile matter below 1% reflectance. McCartney and Teichmüller (1972) observed a similar relationship between reflectance and volatile matter for a much larger set of coal specimens (n= 2,660) from Europe and the United States.

Below 1.0% reflectance a better estimate of volatile matter yield of the bituminous New Zealand coals is obtained where both reflectance and fluorescence intensity is considered according to equation 6.9.

$$VM = 50.1 - 22.1*Romax + 8.3*FLI \quad \text{(eq. 6.9)}$$

where, VM = volatile matter (dry ash free basis),

Romax = % Mean maximum reflectance of vitrinite and,

FLI = Mean log fluorescence intensity of vitrinite and inertinite at 600 nm where log uranyl glass standard = 2.

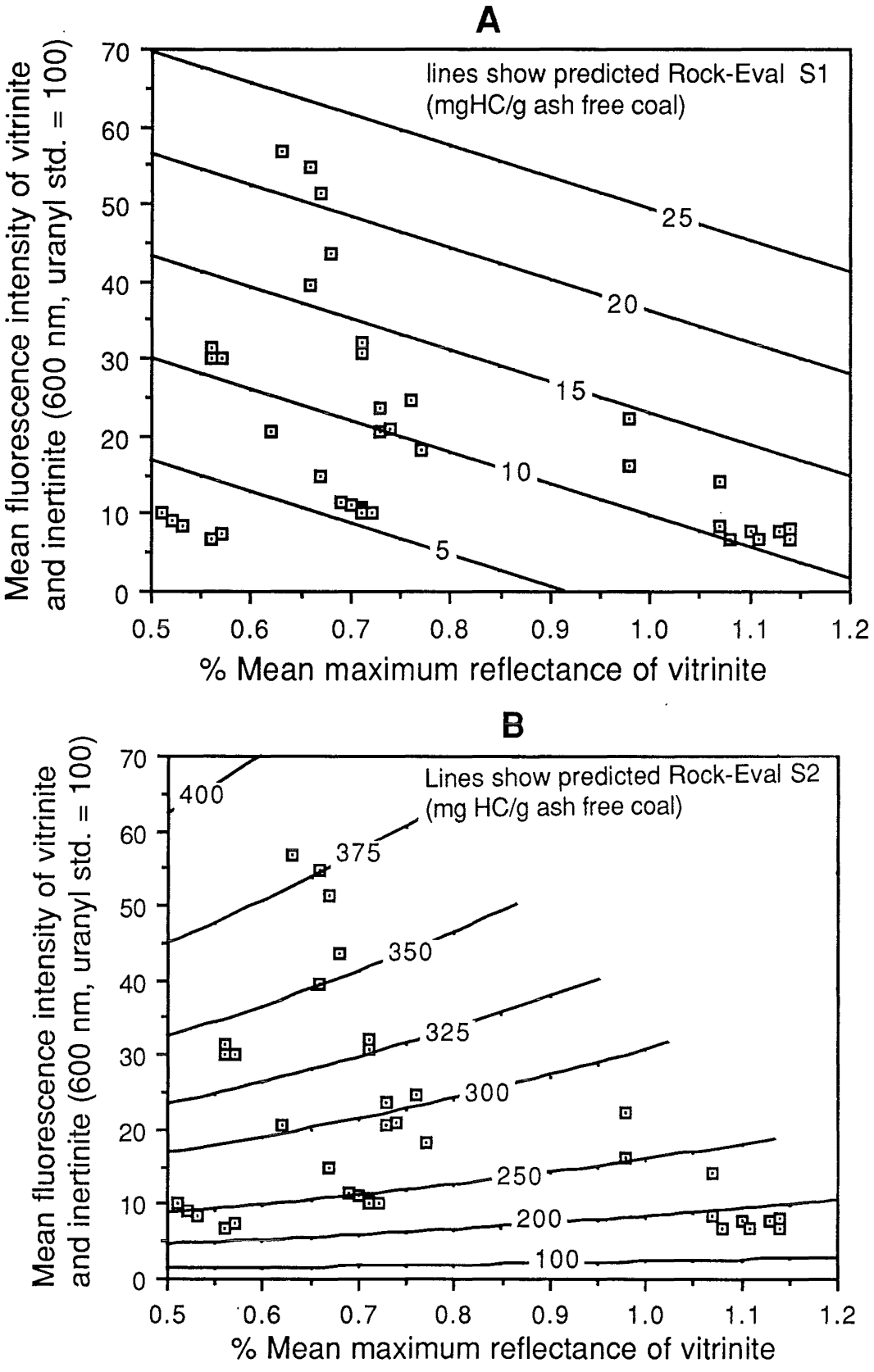

Figure 6.27 (A) Relationship between reflectance, fluorescence intensity and S1 predicted according to equation 6.7. (B) Relationship between reflectance, fluorescence intensity and S2 predicted according to equation 6.8. Analytical data used to derive the relationship are shown and include all samples listed in Table 6.4 except, Island Block samples, Mine samples, and samples a90-89, a90-97, a90-100 and a90-102. S1 and S2 are corrected to an ash free basis.

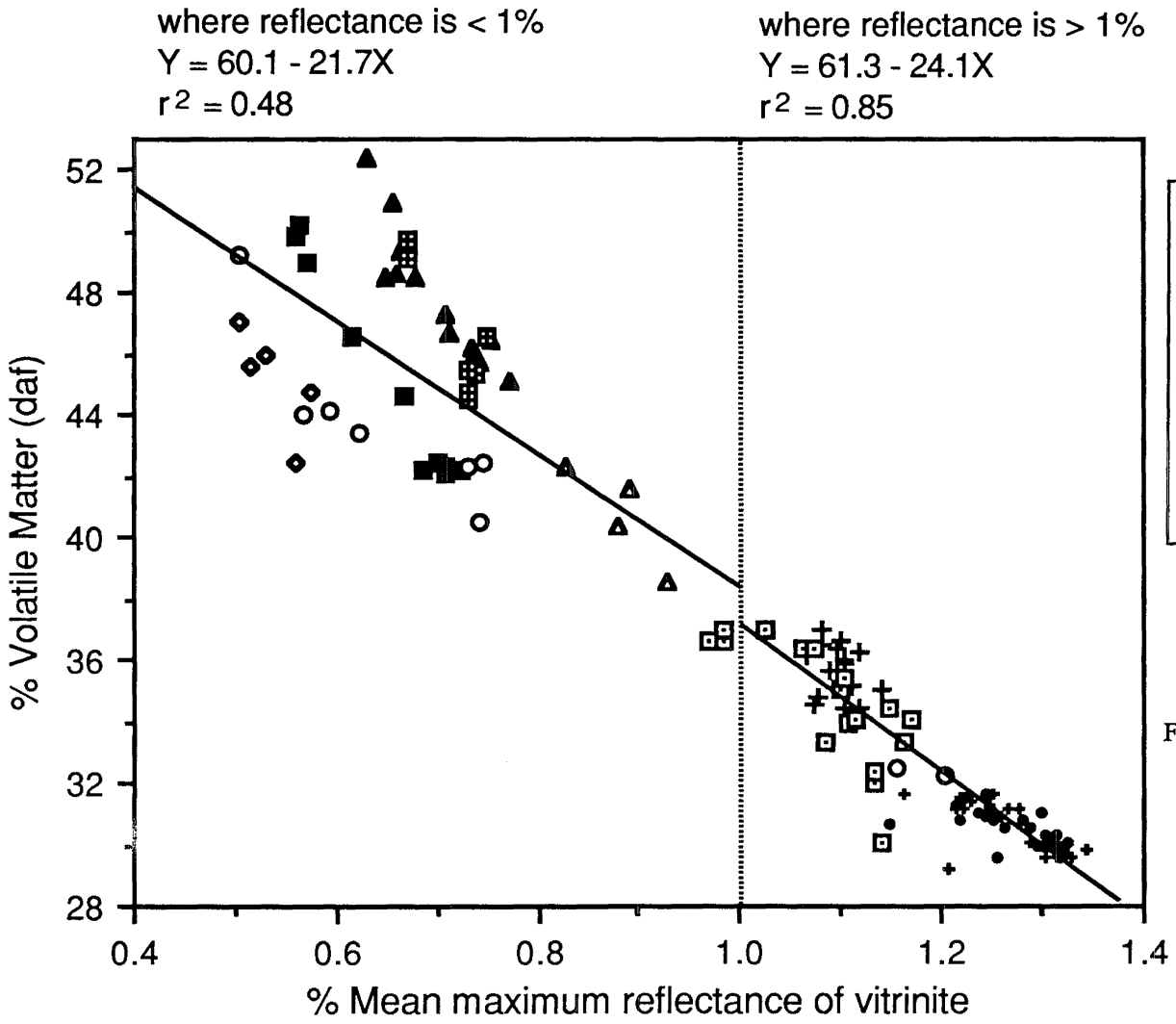

Key

- drillhole 712, Greymouth coalfield, L. Cretaceous
- drillhole 1494, Buller coalfield, Eocene
- drillhole 7, Pile River coalfield, Eocene
- drillhole 7, Pike River coalfield, L. Cretaceous, (whole seams)
- Island Block mine, Reefton/Garvey Creek coalfield, Eocene
- run of mine, various locations and ages
- drillhole 1480, Buller coalfield, Eocene
- drillhole 1481, Buller coalfield, Eocene
- drillhole 1489, Buller coalfield, Eocene
- drillhole 1490, Buller coalfield, Eocene

Figure 6.28 Scatterplot showing the relationship between reflectance and volatile matter above and below 1% Ro_{max} for some bituminous rank New Zealand coals. Note; sample a90-102 omitted (analytical error) and sample 46/426 (Ro_{max} = 1.6%) off figure scale.

Equation 6.9 was derived from 41 New Zealand coals and provided a coefficient of determination (R^2) equal to 0.90 compared to 0.51 where reflectance alone is used to estimate volatile matter of these coals. The relationship between reflectance, fluorescence intensity and volatile matter expressed in equation 6.9 is graphically illustrated in Figure 6.29. The coal samples used to establish the relationship are plotted on the figure.

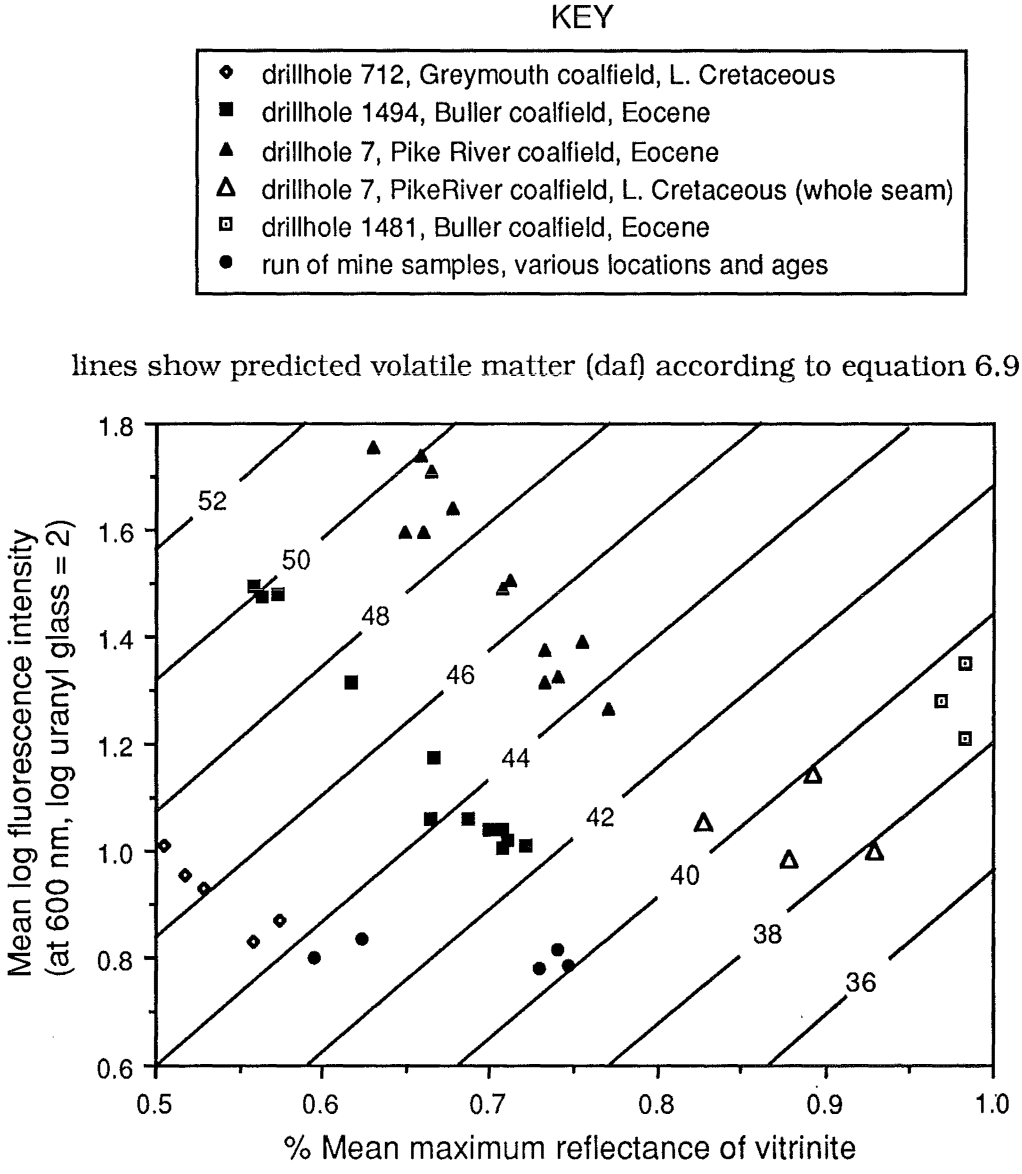

Figure 6.29 Relationship between reflectance, fluorescence intensity, and predicted volatile matter yield (dry, ash free basis) for some New Zealand coals. The lines indicate the volatile matter yield predicted by equation 6.9; the position of the coal samples used to derive equation 6.9 are plotted on the figure.

The correlation between vitrinite reflectance and volatile matter above 1% Ro_{max} is not improved where both fluorescence intensity and vitrinite reflectance are used to predict volatile matter. Above this threshold, the volatile matter of

vitrinite rich coals can be estimated according to vitrinite reflectance alone (r^2 = 0.85, Figure 6.28).

6.10 SUMMARY

Most carbonization and pyrolysis behaviours of coal (Gieseler fluidity, microscopic measurements on carbonized coal products, Rock-Eval S1 and S2, and volatile matter below 1% reflectance) cannot be adequately predicted by any single parameter. However, where both vitrinite reflectance and mean vitrinite/inertinite fluorescence intensity are considered significant relationships with both carbonization and pyrolysis behaviour can be demonstrated. The combined use of these two parameters reflects the geological origin of coal. Reflectance is used as a rank parameter and fluorescence is used as a type/weathering parameter. Because fluorescence intensity varies with both weathering and coal type it is not well suited for geological investigations unless appropriate sample origin and laboratory preparation/storage conditions are assured. Nonetheless, fluorescence intensity appears to be well suited as a parameter for prediction of carbonization behaviour. This is because weathered vitrinite or subhydrous vitrinite inevitably shows both lower fluorescence intensity and lower thermoplasticity than equivalent fresh or perhydrous vitrinite. However, the relative effects of weathering and type variation on both fluorescence and carbonization behaviour remain to be investigated.

The relative lack of samples that report reflectance greater than about 1.3% is a significant limitation of this study. More analytical data are required for extension of this work to include higher rank coals. Nonetheless, within the limits of the materials examined, it is suggested that the combined use of fluorescence intensity and reflectance to predict carbonization behaviour will work for all vitrinite rich coals regardless of origin. The successful prediction of Gieseler plastic temperature range using both data collected in this study and data published for some US coals supports this idea (Figure 6.18). However, it remains uncertain if relationships established in this study can be applied to inertinite or liptinite rich coals.

CHAPTER SEVEN
CONCLUSIONS

This chapter lists some conclusions relevant to the evaluation of New Zealand bituminous coal for industrial carbonization. A discussion of selected analytical techniques pertinent to evaluation and classification of New Zealand coal follows. The chapter ends with a discussion of some ideas related to coal genesis, and suggestions for future research.

7.1 CARBONIZATION BEHAVIOUR AND RANK, TYPE, GRADE, AND WEATHERING

Conventional petrographic analysis of New Zealand coking coals shows that they are best used where blended with inert rich coking coals. Analytical data presented in chapter six show that numerous measures of laboratory carbonization behaviour can be estimated where both reflectance and fluorescence intensity are considered. Reflectance is used as a rank parameter and fluorescence is used as a combined type-weathering parameter. These results support the notion that fundamental characterization of coal according to geologically constrained causative factors is useful for industrial characterization of carbonization feedstocks.

The effect of coal grade on carbonization product behaviour is not directly evaluated in this thesis. Nonetheless, negative predicted CSR values (Table 6.1) demonstrate the need for further research to improve current predictive methods. The low CSR values are thought to be a consequence of the alkali rich character of most of the New Zealand coals examined in this thesis. Initial laboratory studies of CO_2 reactivity of carbons made from a range of alkali rich coals might help nominate specific coals for more rigourous commercial evaluation in blended feedstocks. Given the importance of CSR for efficient operation of the blast furnace, such studies might be useful to ensure that New Zealand coals are not unfairly disadvantaged in export markets where CSR is of concern.

Fluorescence intensity has been shown to be especially sensitive to incipient weathering that occurs in the stockpile. Severe weathering that occurs in the seam is easily recognized by safranin O staining. Weathered coal can also

be recognized where characteristic carbon microtextures are produced upon carbonization. Each of these analytical techniques to detect and measure weathering has advantages and limitations.

Besides being sensitive to weathering, fluorescence intensity also varies according to inherited attributes of the macerals and the degree of coalification. Where type variation is small, and selected vitrinite macerals (telocollinite) are considered, the extent of weathering may be estimated by examining deviations from reflectance vs fluorescence trends established for fresh coals (McHugh *et al.*, 1991). The large variation of fluorescence intensity values for fresh New Zealand coals (e.g., drillhole 1494, Buller coalfield, Figure 6.13) hinders this approach.

Safranin O staining allows the detection of weathered bituminous rank coal without knowledge of the characteristics of equivalent fresh coal. Because safranin O staining is based on point-counting stained maceral occurrences the precision of the method is limited (section 5.4). Furthermore, the technique is not sensitive to weathering near 1.2% Ro_{max} (Table 6.3) and probably is best used below 1% Ro_{max}.

At 1.2% Ro_{max} the presence of basic anisotropy texture in carbonized coals indicates weathering. However basic anisotropy is also characteristic of carbons made from fresh lvb and higher rank coals (Mooreland *et al.*, 1988). Although it is probable that weathering influences optical texture below 1% reflectance this possibility was not examined. Finally, carbon microtextures are also controlled by variation of coal type. For example, coals with relatively high fluorescence intensity produce larger carbon forms than coals of the same reflectance but lower fluorescence intensity (Figure 6.10).

With increased pulverized coal injection rates and consequent higher CSR requirements for coke charged into the blast furnace it is likely that demands on coking coal quality will become more stringent. The adverse effect of even small amounts of weathered coal on CO_2 reactivity (Crelling *et al.*, 1979) indicates a need for a program to develop and implement convenient, sensitive methods to detect weathered coking coal.

7.2 CARBONIZATION MECHANISMS AND COAL STRUCTURE

The optical texture of carbonized coal specimens was found to correlate with the Gieseler solidification temperature. Where carbon microtextures form through an isotropic melt, the Gieseler solidification temperature is, in turn, suggested to be controlled by the amount of hydrogen available to stabilize reactive aromatic fragments cleaved from the network phase. At higher rank, where optical texture develops through uncharacterized solid state transformations, the importance of available hydrogen is suggested to diminish.

The comparatively low enthalpy of decomposition of certain Eocene age coals from the Pike River and Buller coalfields is consistent with the low inertinite contents of these coals. If low inertinite content is the reason for the low enthalpy of decomposition then coals with high inertinite content should exhibit a comparatively high enthalpy of decomposition. This possibility remains to be investigated. A low enthalpy of decomposition is also consistent with the notion that a significant amount of the organic sulphur in these coals is present as thermally labile sulphide linkages.

Regardless of the actual cause of the low enthalpy of decomposition values, a lower mean activation energy for thermal degradation is advantageous in conversion processes should these coals ever be used to produce liquid fuels. Of more immediate significance, the consequent low thermal softening temperatures should be advantageous if these coals are used as binding agents in the preparation of briquettes for carbonization. In this regard any sulphur penalty might be offset by the lower temperatures required for briquette manufacture.

7.3 ANALYTICAL METHODS TO EVALUATE COAL.

7.3.1 Gieseler Fluidity

The results of the Gieseler fluidity test may be misleading for some New Zealand coals presumably due to swelling of the semi-molten mass into the retort barrel. For reporting purposes raw data tapes should be examined and any irregular temperature *vs* ddpm profiles noted.

7.3.2 Fluorometric Analysis

Predictive equations obtained in this study were successfully applied to published fluorometric data obtained with a different microscope and different coals. The mutual agreement suggests that it should be possible to standardise fluorometric analysis using existing standards and equipment. Despite this agreement, the general applicability of the predictive equations and relationships established in this thesis is not known.

Fluorometric analysis of coal is convenient where a dry objective and inert gas flow over the the specimen is used. This arrangement eliminates the need for frequent switching between the white light and fluorescence mode of illumination. The inert gas flow eliminates negative alteration (Davis *et al.*, 1990) and minimizes otherwise unavoidable analytical errors arising from variable amounts of irradiation prior to and during the measurement process. Since the uranyl glass standard is significantly brighter than most vitrinite and inertinite the use of neutral density filters during calibration is recommended; this technique improves instrumental sensitivity and precision.

Fluorescence intensity values reported in this thesis were obtained using 550-650nm measurement wavelengths (half bandwidth). Theoretical and practical reasons for selecting this measurement bandpass are discussed in section 6.6.1. The fluorescence intensity of New Zealand coals at longer or shorter emission wavelengths remains to be investigated.

Although the thermoplastic behaviour of coal waxes and wanes through the bituminous ranks different measures of thermoplastic behaviour reach a maximum at different reflectance values. Similarly, fluorescence intensity waxes and wanes through the bituminous ranks and with increasing measurement wavelengths fluorescence intensity reports a maximum value at progressively higher levels of vitrinite reflectance. Thus, regardless of what emission wavelength is selected, prediction of diverse measures of carbonization behaviour requires consideration of both reflectance and fluorescence data.

7.3.3 Moisture

The use of air-dried moisture to estimate moisture holding capacity (equation 2.3) is misleading where moisture holding capacity is used to estimate original bed moisture. In the absence of bed moisture values determination of equilibrium moisture in accordance with Australian or ASTM standard methods (rather than moisture holding capacity determined by the less rigourous British or ISO method) is suggested.

Air-dried moisture (equilibrated at 20°C, 70% relative humidity) is inevitably higher than "air dried" moisture determined after the sample has been previously dried at up to 40°C (e.g., as part of the determination of total moisture according to ASTM D-3302). Where New Zealand coal is sold to export markets the relatively high "air-dried" moisture content is misleading and commercially disadvantageous.

7.4 SOME IDEAS RELATED TO COAL GENESIS

The fluorescence intensity of vitrinite waxes and wanes through the bituminous ranks. Within the high volatile bituminous stage of coalification fluorescence intensity generally increases with increasing vitrinite reflectance. This phenomenon has been explained as a consequence of the catagenetic build-up of mobile phase material (Lin *et al.*, 1986). The general increase of fluorescence intensity with increasing reflectance through the high volatile bituminous stage of coalification stands in sharp contrast to the inverse relationship between fluorescence intensity and vitrinite reflectance observed for serial ply samples in this thesis. Thus, within these ranks, fluorescence intensity varies according to both the level of coalification and inherited attributes of the vitrinite.

Other workers have shown that fluorescence intensity declines with increasing reflectance above mvb rank; the data presented in this thesis support this general trend. However for serial ply samples within single seams where Ro_{max} >1.1% no significant correlations between reflectance and fluorescence

intensity were noted (Figure 6.13). Likewise, above 1% reflectance no relationship between fluorescence intensity and volatile matter was observed (Figure 7.1). Figures 7.2, 7.3, and 7.4 graphically illustrate the vertical variation of volatile matter, fluorescence intensity, and vitrinite reflectance through single seams encountered in drillholes 1480, 1481 and 1489. The figures are annotated with Gieseler fluidity data (where available) for composite samples made by combining adjacent ply samples. Examination of the seam profiles shows that in all cases reflectance varies inversely with volatile matter. Indeed, above 1% reflectance volatile matter can be estimated from reflectance alone (Figure 6.28).

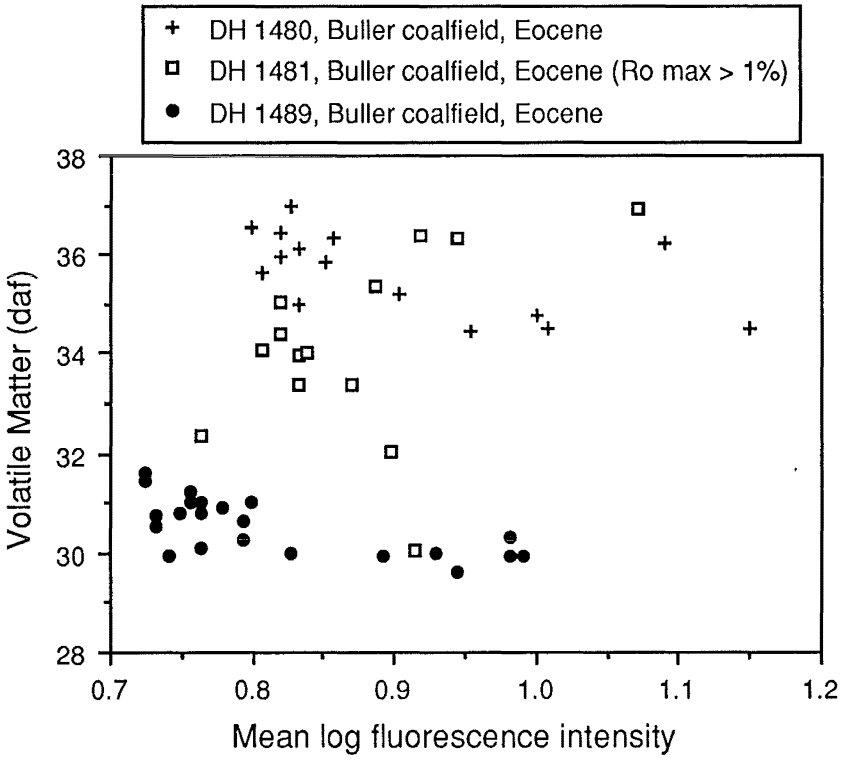

Figure 7.1 Scatterplot showing the lack of correlation between fluorescence intensity and volatile matter for serial ply samples where reflectance is greater than 1%.

The lack of correlation between fluorescence intensity and volatile matter where reflectance is greater than 1% (Figure 7.1) may be due to the shallow present burial depth of these three coal seams. Without additional data for deeply buried coals where reflectance is greater than 1% this possibility cannot be discounted. It is also not known if the lack of correlation between fluorescence intensity and volatile matter is simply an artifact of the emission wavelength used in this study. This possibility remains to be investigated.

7.4.1 Causes of Fluorescence Variation

It is improbable that vertical variation of fluorescence intensity through a single seam can be entirely attributed to any single mechanism. Abundant terpene resins observed as megascopic lumps in New Zealand coals suggests that resin impregnated wood may have contributed to some perhydrous vitric coals and enhanced fluorescence intensity. Furthermore, relatively abundant sclerotinite (section 5.2.1) suggests that (aerobic) fungal degradation may have had a significant effect on the coal-forming peat resulting in diminished fluorescence intensity. Accumulated bacterial remains may also have contributed to high fluorescence intensity. The results of this study are used to suggest two different anaerobic degradation mechanisms that may have contributed to the observed vertical variation of fluorescence intensity. Although only two mechanisms are discussed it suggested that the observed variation of fluorescence intensity through any single seam is the result of multiple mechanisms including, those listed above, the effect of weathering, and probable diverse coalification paths for different maceral precursors.

Within drillholes 1480, 1481, 1489, 1494 and Pike River drillhole 7, the fluorescence intensity values generally correspond to variation in total sulphur (Figures 7.2, 7.3, and 7.4, 7.5, 7.6). Limited analyses of forms of sulphur data suggest that exceptions to the positive relationship between sulphur and fluorescence intensity are due, in part, to the presence of pyritic sulphur and a better relationship might be obtained where only organic sulphur is considered. More analytical work is needed to determine if this trend is consistent for all high sulphur coals. However, examination of Figure 7.7 shows that, where sulphur content is low (drillhole 712), in-seam variation of fluorescence intensity for serial ply samples is not related to variation of sulphur content. An explanation for

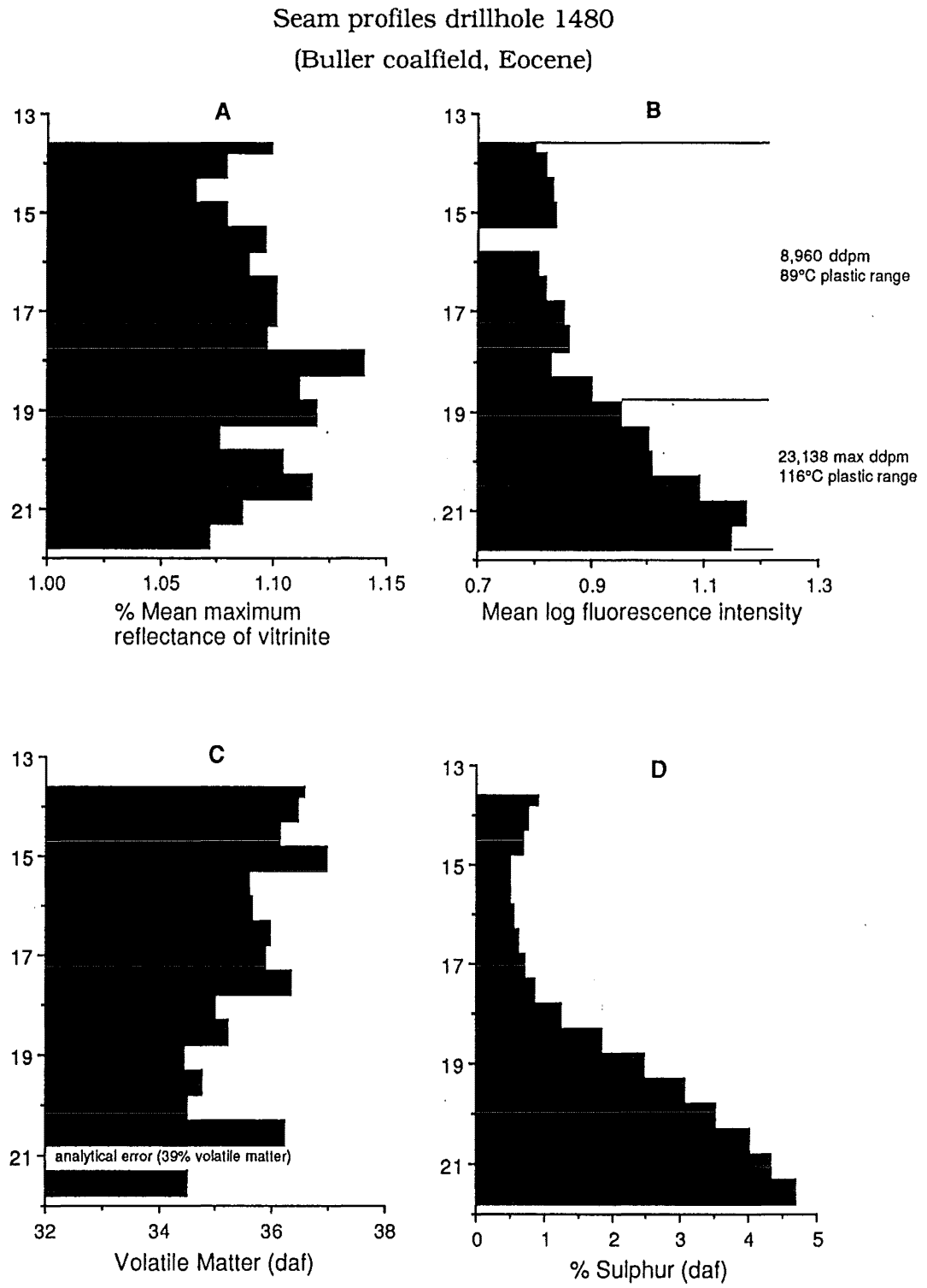

Figure 7.2 Vertical variation of selected coal properties through a coal seam encountered in drillhole 1480 (Buller coalfield, Eocene age), vertical axes show depth from surface (metres). **A**) vertical variation of reflectance. **B**) vertical variation of vitrinite-inertinite fluorescence intensity at 600nm relative to a masked uranyl glass standard = 100 on a linear scale (no data for ply sample between 15 and 16 metres). **C**) vertical variation of volatile matter on a dry ash free basis (ply sample with anomalous volatile matter at 21 metres (a90-102) omitted. **D**) vertical variation of sulphur expressed on a dry ash free basis. Note annotated Gieseler fluidity data for specimens made by combining adjacent ply samples for indicated seam sections.

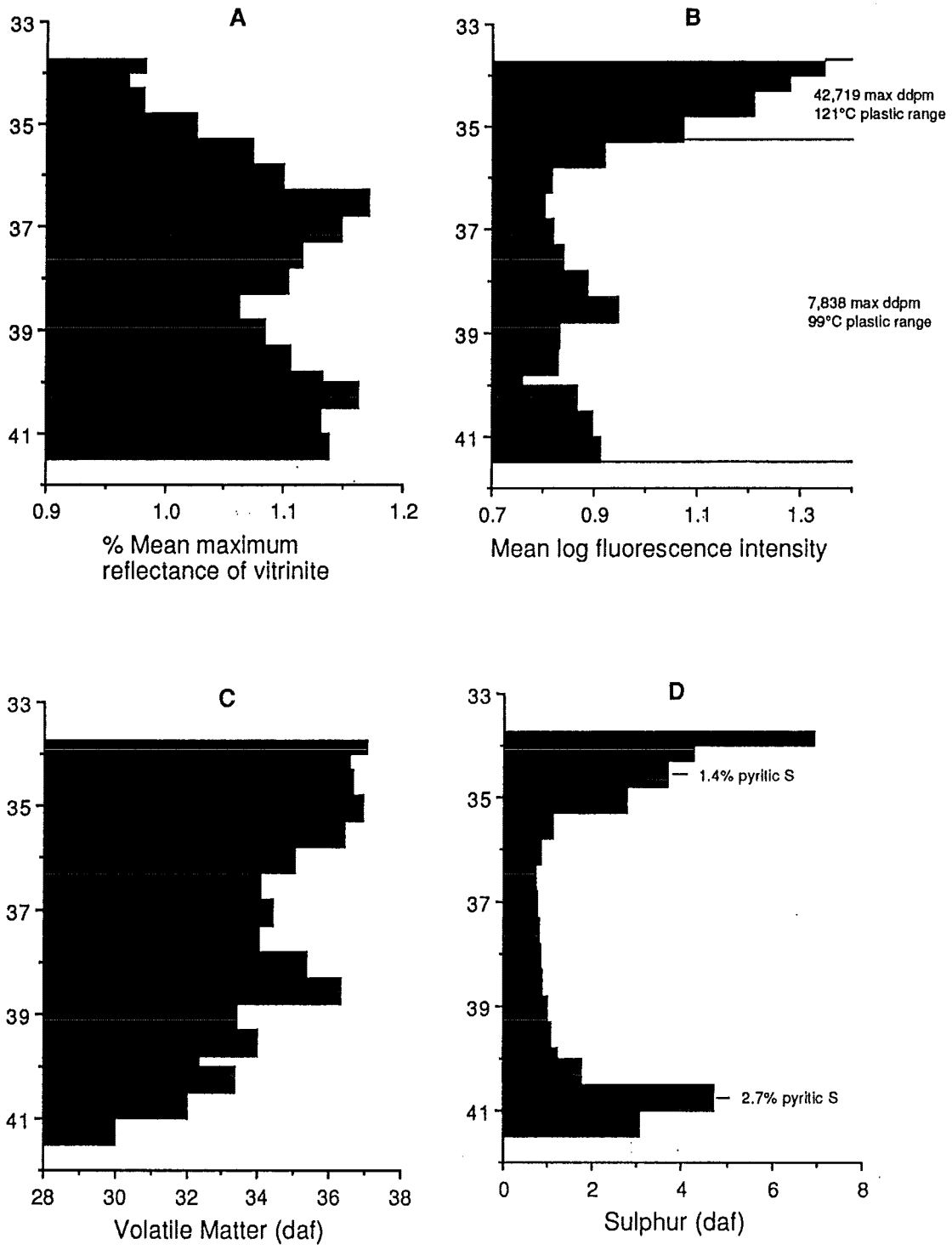

Figure 7.3 Vertical variation of selected coal properties through a coal seam encountered in drillhole 1481 (Buller coalfield, Eocene age), vertical axes show depth from surface (metres). **A**) vertical variation of reflectance. **B**) vertical variation of vitrinite-inertinite fluorescence intensity at 600nm relative to a masked uranyl glass standard = 100 on a linear scale; note annotated Gieseler fluidity data for specimens made by combining adjacent ply samples for indicated seam sections. **C**) vertical variation of volatile matter on a dry ash free basis. **D**) vertical variation of total sulphur expressed on a dry ash free basis; note annotated pyritic sulphur (dry) values for two ply samples.

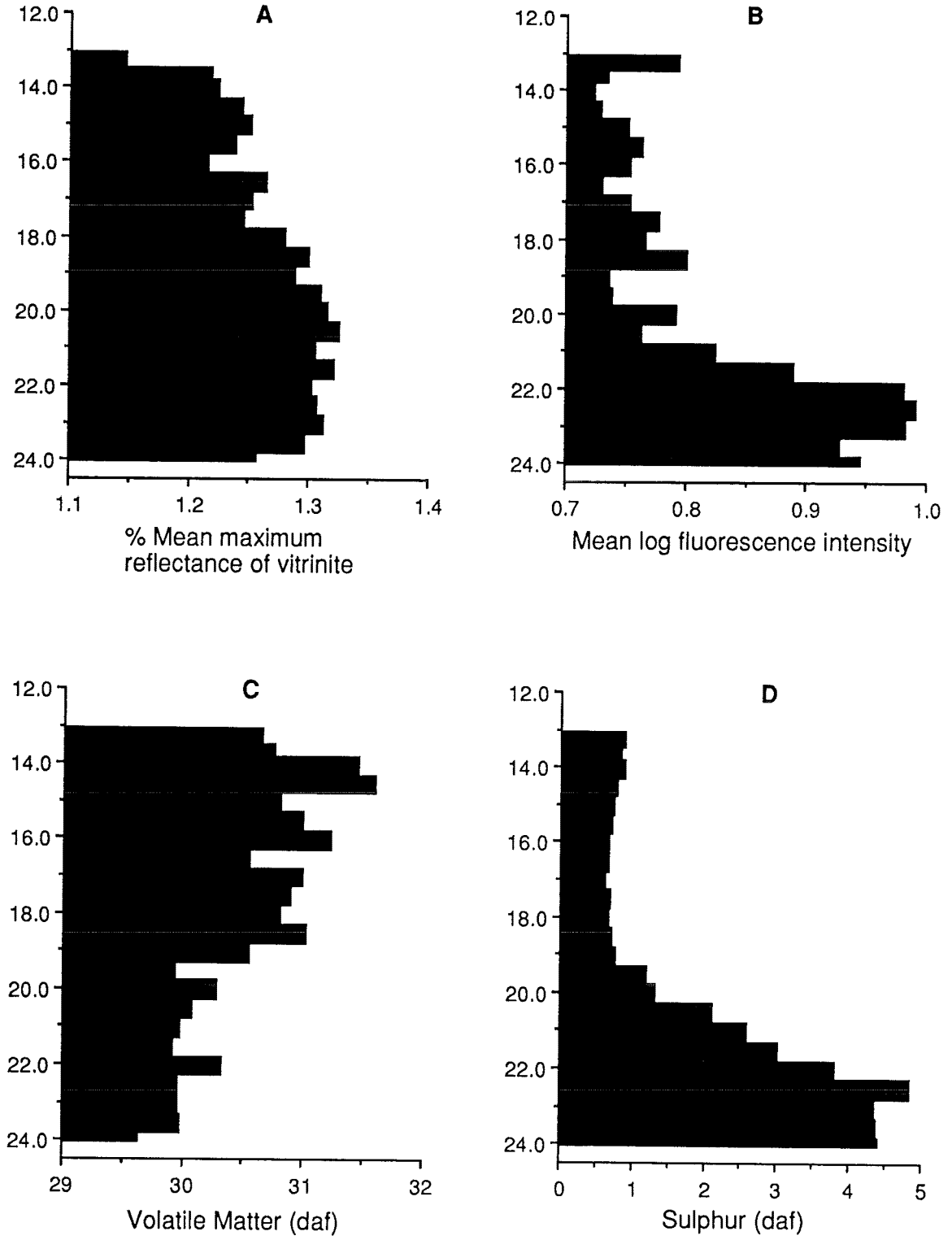

Figure 7.4 Vertical variation of selected coal properties through a coal seam encountered in drillhole 1489 (Buller coalfield, Eocene age), vertical axes show depth from surface (metres). **A**) vertical variation of reflectance. **B**) vertical variation of vitrinite-inertinite fluorescence intensity at 600nm relative to a masked uranyl glass standard = 100 on a linear scale. **C**) vertical variation of volatile matter on a dry ash free basis. **D**) vertical variation of sulphur expressed on a dry ash free basis.

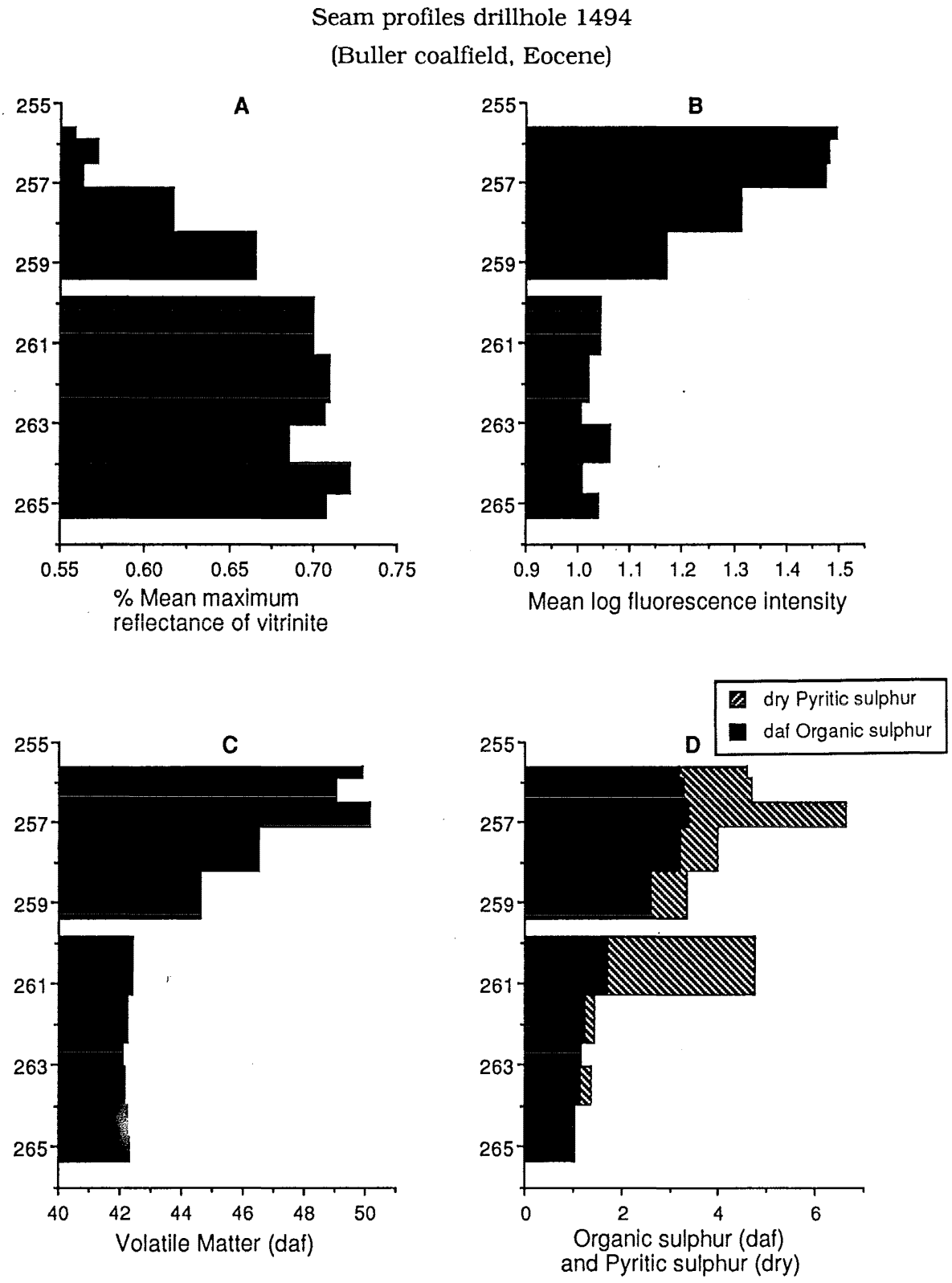

Figure 7.5 Vertical variation of selected coal properties through a coal seam encountered in drillhole 1494 (Buller coalfield, Eocene age), vertical axes show depth from surface (metres). **A**) vertical variation of reflectance. **B**) vertical variation of vitrinite-inertinite fluorescence intensity at 600nm relative to a masked uranyl glass standard = 100 on a linear scale. **C**) vertical variation of volatile matter on a dry ash free basis. **D**) vertical variation of organic sulphur (dry ash free basis) and pyritic sulphur (dry basis). Note, no core recovery near 259.5 metres.

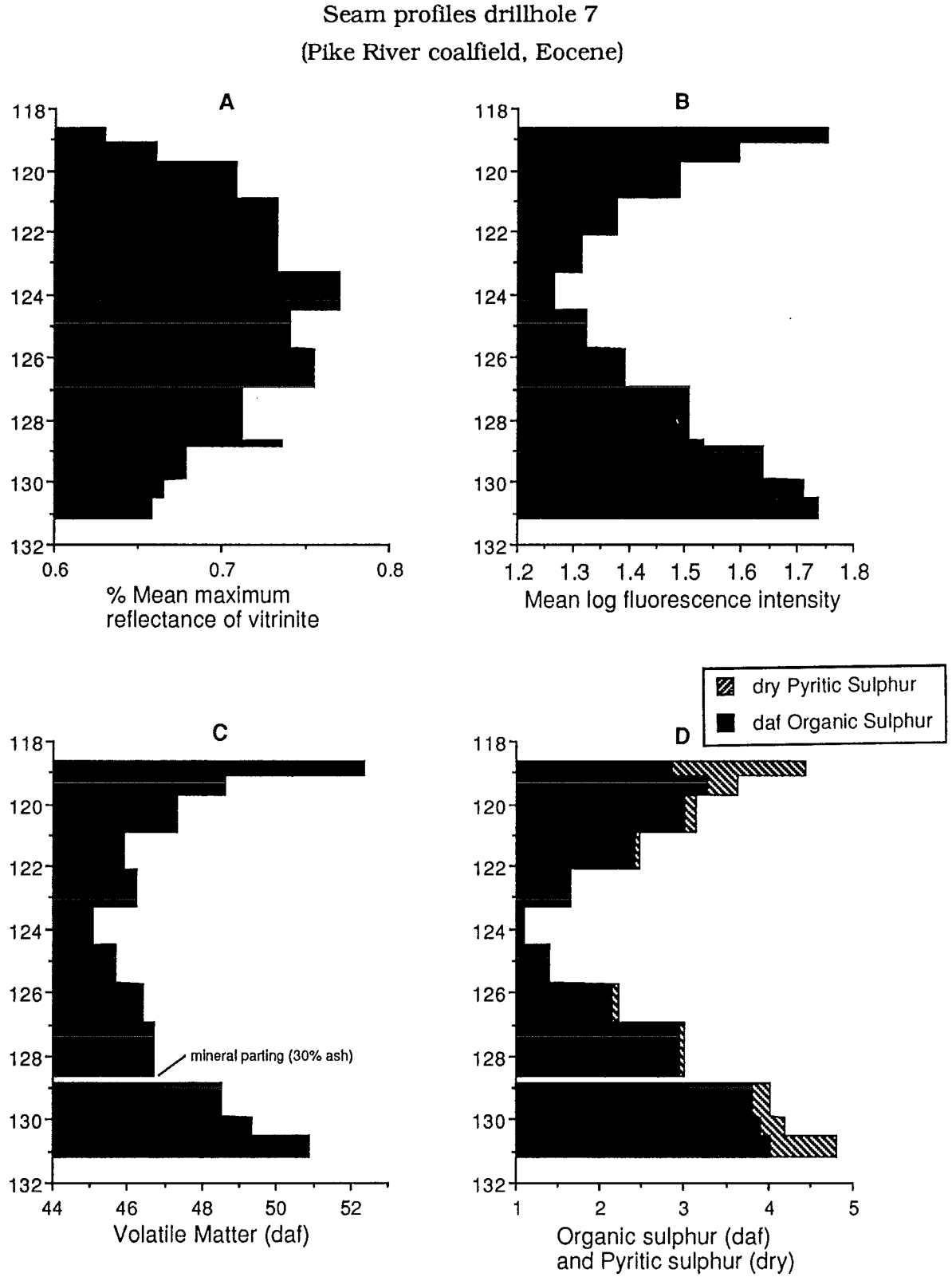

Figure 7.6 Vertical variation of selected coal properties through a coal seam encountered in drillhole 7 (Pike River coalfield, Eocene age), vertical axes show depth from surface (metres). **A)** vertical variation of reflectance. **B)** vertical variation of vitrinite-inertinite fluorescence intensity at 600nm relative to a masked uranyl glass standard = 100 on a linear scale. **C)** vertical variation of volatile matter on a dry ash free basis, note data for high ash carbonate rich ply sample near 128.8 metres (46/945) not shown. **D)** vertical variation of organic sulphur (dry ash free basis) and pyritic sulphur (dry basis), no data for ply sample near 128.8 metres (46/945).

Seam profiles drillhole 712
(Greymouth coalfield, L. Cretaceous)

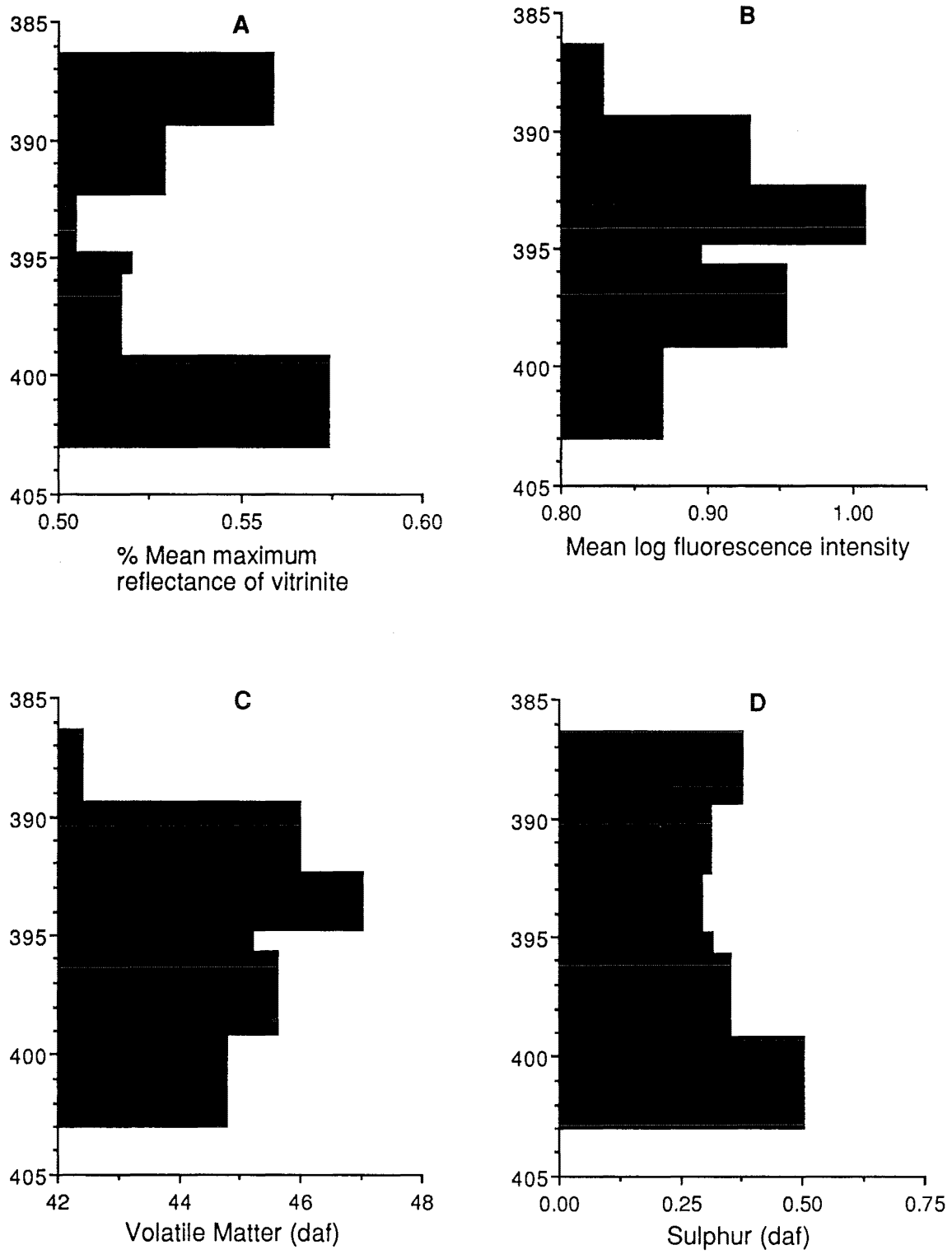

Figure 7.7 Vertical variation of selected coal properties through a coal seam encountered in drillhole 712 (Greymouth coalfield, L. Cretaceous age), vertical axes show depth from surface (metres). **A**) vertical variation of reflectance. **B**) vertical variation of vitrinite-inertinite fluorescence intensity at 600nm relative to a masked uranyl glass standard = 100 on a linear scale. **C**) vertical variation of volatile matter on a dry ash free basis. **D**) vertical variation of sulphur expressed on a dry ash free basis.

these trends is offered below. Figure 7.7 shows the vertical variation of fluorescence intensity and vitrinite reflectance through a coal seam encountered in drillhole 712. Fluorescence intensity is highest and reflectance is lowest in the middle of the seam. The seam profiles shown in Figure 7.7 are distinctive in this respect; the other seams examined in this study generally show high reflectance and low fluorescence intensity in the middle of the seam. Different microbial degradation mechanisms are suggested to be contributing genetic factors responsible for these contrasting fluorescence and reflectance profiles.

The acidic conditions that characterize a coal-forming mire inhibit biological degradation of peat. However anaerobic degradation can be expected to be greater at the top and bottom margins of the seam where base exchange with adjacent inorganic sediments locally increase the pH (Taylor and McKenzie, 1926) and enables primary fermentive anaerobes to decompose polymers to CO_2, H_2, and H_2O (Brock and Madigan, 1988). Where sulphate ion is absent, methanogenic bacteria convert the hydrogen to methane gas. Consequently hydrogen is diminished at the seam margins and fluorescence intensity should be highest in the centre of the seam; this mechanism is consistent with the observed fluorescence variation through the seam encountered in drillhole 712 (Figure 7.7). Relative hydrogen enrichment as a consequence of inhibited microbial decomposition due to low eh and pH might explain the occurrence of some, low sulphur, perhydrous coals where the paleofloral assemblage produced a cellulose rich biomass. Cellulose is relatively rich in hydrogen (Figure 2.4) and is thought to have made proportionally greater contributions to younger coals compared to Carboniferous coals (Robinson, 1990). Given the susceptibility of cellulose to hydrolysis by fungi this mechanism necessarily requires restricted aerobic decay.

Where sulphate ions are present methanogenesis is inhibited and the hydrogen produced by primary fermentive anaerobes is used by secondary, sulphate reducing bacteria that produce H_2S rather than methane (Belyaev *et al.*, 1980). Unlike methane, hydrogen sulphide is reactive and, in the absence of reducible iron, readily combines with otherwise labile functionalised lipids and

enriches the organic matter in hydrogen (Sinninghe Damste *et al.*, 1989a,b). This mechanism is consistent with the observed association between high sulphur and fluorescence intensity shown in Figures 7.2 to 7.6.

Although fluorescence intensity is often low at the centre of the many of the seams examined in this study close examination of the seam profiles shown in Figure 7.3 reveals slightly higher fluorescence intensity near the seam centre (~38.5 metres depth) that is not related to the presence of sulphur. In this area (Webb Block, Buller coalfield) Newman (1991) has shown that sulphur enrichment occurred after burial of the coal-forming peat beneath more than 40 metres of fluvial sediments. This suggests early methanogenic microbial decomposition followed by later modification of the peat due to the activity of sulphate reducing bacteria. Thus, as observed earlier by Newman (1985), compositional variation of the vitrinite cannot be reliably predicted on the basis of sulphur content.

Close examination of the fluorescence and sulphur profiles shown in Figure 7.5 (drillhole 1494) also suggest multiple mechanisms responsible for the observed variation of fluorescence intensity. Although both fluorescence intensity and sulphur are higher at the top of the seam, and support the idea of hydrogen enrichment via natural vulcanization of otherwise labile hydrogen rich precursors, organic sulphur is fairly uniform in the top half of the seam whereas fluorescence intensity progressively increases upwards. In this instance, a larger proportion of accumulated bacterial remains towards the top of the seam may have increased fluorescence intensity. In addition, a rising water table during peat accumulation (Newman, 1985b) may also have contributed to the upward increase of fluorescence intensity. Here, inhibited aerobic decay and consequent hydrogen enrichment (e.g., inhibited loss of cellulose upon hydrolysis by fungi), due to progressive drowning of the paleo-mire is also consistent with the observed upward increase of fluorescence intensity.

Whatever the actual causes of vertical variation of fluorescence intensity the above discussion suggests that within any single seam multiple causes are likely. Despite the acknowledged limitations of the data presented here

fluorometric analysis appears to be a useful tool to investigate the enigmatic genesis of coal.

7.4 FUTURE WORK

Within the high volatile bituminous stage of coalification perhydrous vitrinite generally exhibits "suppressed" reflectance. Indeed, between 0.5 and 1.1% Ro_{max} the use of fluorometric analysis to account for suppressed vitrinite reflectance has been suggested (section 6.1.1). What happens to perhydrous vitrinite upon further coalification cannot be deduced based on the results of this study. However if perhydrous vitrinite is likened to liptinite macerals then by the time the low volatile stage of coalification is reached the reflectance of perhydrous vitrinite may exceed that of the associated vitrinite. For example, AS-2856 shows that sporinite reflectance exceeds vitrinite reflectance above about 1.5% Ro_{max}. Likewise, Jacob and Hiltman (1985) have shown that the reflectance of native bitumen is lower than associated vitrinite below 1.0% random reflectance and higher than associated vitrinite above 1.0% random reflectance. The importance of vitrinite reflectance as a maturation parameter suggests that investigation of the fate of perhydrous vitrinite upon continued coalification is a worthy topic.

Although our understanding of the chemical basis of fluorescence emission of coal macerals has improved (Lin, 1988), interpretation of the chemical significance of fluorescence from solids (such as macerals) remains a challenging topic. Nonetheless, advances in analytical technique, such as the introduction of longer wavelength dichroic excitation filters (Diessel, 1985) and the use of inert gas to eliminate alteration (Davis *et al.*, 1990), suggest that fluorometric analysis is sufficiently well developed for routine use to predict industrial behaviour. The modification of existing conventional microscopes capable of reflectance analysis to induce measurable fluorescence intensity is easily accomplished with existing commercially available light sources and filters. However, for fluorometric analysis to become a standard method will require specification of analytical conditions that can be achieved with existing microscopes systems. The most important obstacle to overcome to obtain reproducible data is agreement on a

suitable standard. Excitation wavelengths in the region of 400-500nm are suitable as are emission wavelengths between 550 to and 700nm provided that wide bands are used (to maximize the fluorescence signal) and leakage from excitation filters within the measurement bandpass is minimized. After these conditions are met, reproducible data on a diverse set of coals should be obtained.

REFERENCES

Allardice, D. J., and Evans, D. G., (1978) Moisture in coal. In: C. Karr (ed), Analytical Methods of Coal and Coal Products, Vol. 1, Academic Press, New York, p.247-262

Alpern, B., (1971) Influence de la temperature sur les mesures de reflectance en immersion dans l'huile. Bull. Soc. fr. Mineral. Cristallog., 94:179-180

Alpern, B., Lemos de Sousa M. J., and Flores D., (1989) A progress report on the Alpern coal classification. In: P.C. Lyons and B. Alpern (eds) Coal: Classification, Coalificaton, Mineralogy, Trace-element Chemistry and Oil and Gas Potential. Int. J. Coal Geol., 13:1-19

Anderson N. E., and Hamza, H. A., (1982) The characterization of oxidized coal - a review. In: A. M. Al Taweel (ed) Coal Phoenix of the 80's, Proceedings of the 64th CIC Coal symposium, Ottowa, p.117-124

Axelson, D. E., Mikula R. J., and Munoz, V. A., (1987) Characterization of coal oxidation in-situ and on a stockpile. In: J. A. Moulijn *et al.*, (eds) 1987 International Conference on Coal Science. Elsevier Science Publishers, Amsterdam, p.423-422

AS Australian Standard. Standards Association of Australia, Standards House, 80 Arthur St, North Sydney NSW

------ 1038.3-1989 Methods for the analysis and testing of coal and coke, Part 3: Proximate analysis of higher rank coal. 15p.

------ 1038.22-1983 Methods for the analysis and testing of coal and coke, Part 22: Direct determination of mineral matter and water of hydration of minerals in hard coal.

------ 2096-1987 Classification and Coding Systems for Australian Coals. 8p.

------ 2434.2-1983 Methods for the analysis and testing of brown coal and brown coal char. Part 2 - Determination of the volatile matter in low rank coal. 9p.

------- 2486-1981 Microscopical determination of the reflectance of coal macerals. 12 p.

------- 2856-1986 Coal - Maceral Analysis. 22p.

ASTM (1987) Annual book of ASTM Standards, volume 05.05, Gaseous Fuels; Coal and Coke. American Society for Testing and Materials, 1916 Race Street, Philadelphia PA 19103

------ Method D 388-84 Standard classification of coals by rank; p.225-230

------ Method D 720-83 Free swelling index of coal; p.257-263

------ Method D 1757-84 Test methods for sulfur in ash from coal and coke. p.271-275

------ Method D 2639-74 Plastic properties of coal by the constant torque Gieseler plastometer; p.341-347

------ Method D 2795-86 Analysis of coal and coke ash. p.349-356

------ Method D 2797-85 Preparing coal samples for microscopical analysis by reflected light. p.361-366

------ Method D 2798-85 Microscopical determination of the reflectance of the organic components in a polished specimen of coal. p.367-374

------ Method D 2799-86 Microscopical determination of volume percent of physical components of coal. p.371-374

------ Method D 3174-73 Ash in the analysis sample of coal and coke from coal.

------ Method D 3174-82 Ash in the analysis sample of coal and coke from coal. p.385-388

------ Method D 3175-82 Volatile matter in the analysis sample of coal and coke. p.389-392

------ Method D 4326-84 Major and minor elements in coal and coke ash by X-ray fluorescence. p.481-484

Axelson, D. E., Mikula, R. J., and Munoz, V. A., (1987) Characterization of coal oxidation in-situ and on a stockpile. In: J. A. Moulijn *et al.*, (eds) 1987 International Conference on Coal Science, Elsevier, Amsterdam, p.419-422

Barker, Ch., E., (1989) Temperature and time in the thermal maturation of sedimentary organic matter. In: N. Naeser and T. McCulloh (eds) Thermal History of Sedimentary Basins, Springer-Verlag, New York, p.73-98

Barker, Ch., E., and Pawlewicz, M. J., (1986) The correlation of vitrinite reflectance with maximum temperature in humic organic matter. In: G. Buntebarth and L. Stegena (eds), Paleogeothermics, Evaluation of Geothermal Conditions in the Geological Past, Springer-Verlag, Berlin, p.79-93

Bass Becking, L. G. M., Kaplan, I. R., and Moore, D., (1960) Limits of the natural environment in terms of pH and oxidation-reduction potentials. Jour. of Geol., 68:243-284

Beafore F. J., Cawiezel K.E., and Montgomery C. T., (1984) Oxidized coal - what it is and how it affects your preparation plant performance. Jour. Coal Qual., no. 2, 3:17-23

Belyaev, S. S., Yy-Lein, A., and Ivanov, M. V., (1981) Role of methane-producing and sulphate reducing bacteria in the destruction of organic matter. In: P. A. Trudinger and M. R. Walter (eds) Biochemistry of Ancient and Modern Environments. Springer -Verlag, Berlin, p.235-242

Benedict, L. G., and Berry, W. F., (1964) Recognition and Measurement of coal Oxidation. paper presented to the Geol. Soc. of America, Coal Group, Nov. 19, Miami, Bituminous Coal Research publ., Monroeville Pa, 41p.

Benedict, L. G., Thompson, R. R., Shigo III, J. J., and Aikman, R. P., (1968) Pseudovitrinite in Appalachian coking coal. Fuel, 47:125-143

Benedict, L. G., Thompson, R. R., and Wenger, R. O., (1968b) Relationship between coal petrographic composition and coke stability. Blast Furnace and Steel Plant, 56:217-224

Berner, R. A., (1984) Sedimentary pyrite formation: An update. Geochim. et Cosmochim. Acta, 48:605-615

Berry, L. G., and Mason, B., (1959) Mineralogy. W. H. Freeman Co., San Francisco, 630 p.

Black, P. M., (1980) A Reconnaissance Survey of the Petrology of New Zealand Coals. New Zealand Energy Research and Development Committee, Rept. no. 51, 49 p.

Bostic, N., (1986) Smoothness and relief of polished sections. The Society for Organic Petrology newsletter, 3:4-6

Boudou, J. P., (1990) Coal desulfurization by programmed temperature pyrolysis and oxidation. In: W. L. Orr and C. M. White (eds) Geochemistry of Sulfur in Fossil Fuels. ACS Symposium Series 429, p.345-364

Boyapati, E., Oates, W. A., Moxon, N. T., Day, J. C., and Baker, C. K., (1984) The weathering characteristics of coking coals. Fuel, 63:551-556

Brock, T. D., and Madigan, M. T., (1988) Biology of Microorganisms. Prentice-Hall, Englewood Cliffs NJ, 835p.

Brown, H. R., Cook, A. C., and Taylor, G. H., (1964) Variations in the property of vitrinite in isometamorphic coal; Fuel, 43:111-124

Brown, K., Diessel, C., McHugh, E., Wolf, M., and Wolff-Fischer, E., (1985) The fluorescence properties of Carboniferous and Permian coking coals. Proc. International Conf. on Coal Science, Sydney p.649-652

Brown, N. A., Coin, C. D. A., and Gill, W. W., (1982) Prediction of coke quality. BHP Tech. Bull., 26:1:27-30

BS 1016 (1981) Methods for the Analysis and Testing of coal and coke. British Standards Institution, 2 Park Street, London, W1A 2BS

------ part 3, (1973) Proximate Analysis of Coal and Coke. 14p.

------ part 16, Methods for reporting of results. 14p.

Budge, C. F., (1972) Moisture equilibrium isotherms for New Zealand coals. New Zealand Journal of Science, 15:39-51

Budge, C. F., and MacKnight, F. J., (1976) Forms of sulphur in New Zealand coals. N. Z. Jour. Sci., 19:237:241

Buiskool Toxopeus, J., (1983) Selection criteria for the use of vitrinite reflectance as a maturity tool. In: J. Brooks (ed) Petroleum Geochemistry and Exploration of Europe, Blackwell Scientific, p.259-307

Burnham, A. K., and Sweeney, J. J., (1989) A chemical kinetic model of vitrinite maturation and reflectance. Geochim. et Cosmochim. Acta., 53:2649-2657

Burns, M. S., Durie, R. A., and Swaine, J., (1962) Significance and chemical evidence for the presence of carbonate minerals in brown coals. Fuel, 41:373-383

Burstein, H., (1971) Attribute Sampling. McGraw-Hill Inc., New York, 464p.

Bustin, R, M., (1991) Quantifying macerals: some statistical and practical considerations. Int. J. Coal Geol., 17:213-238

Callcott T, (1987) Fluidity of coking coals; Volume 1 Coal Research Conference Proceedings, paper R7-1, Wellington, 2-4 Nov. 9p.

Cardott, B. J., (1987) Petrography of some typical Oklahoma coals. Abstracts with program Fourth Ann. mtg., The Society for Organic Petrology 30 Sept.-3 Oct. San Francisco. p.9

Carpenter, A. M., (1988) Coal Classification. IEA Coal Rept. 12, International Energy Agency, London, 104 p.

Casagrande, D. J., (1987) Sulphur in peat and coal. In: A. C. Scott (ed) Coal and Coal-bearing Strata: Recent Advances. Geological Society Special Publication No. 32, p.87-105.

Casagrande, D. J., Siefert, K., Berschinski, C., and Sutton, N., (1977) Sulfur in peat-forming systems of the Okefenokee Swamp and Florida Everglades, Origins of sulfur in coal. Geochim. et Cosmochim. Acta, 41:161-167.

Cecil C. B., Stanton, R. W., Dulong, F. T., and Cohen, A. D., (1979a) Experimental coalification of Taxodium peat from the Okefenokee swamp, Georgia. In: A. Donaldson, M. Presley and J. Renton (eds) Carboniferous Coal Guidebook supplement. West Virginia Geological and Economic Survey Bulletin B-37-3, p.129-141

Cecil, C. B., Renton, J. J., Stanton, R. W., and Dulong, F., (1979b) Some geologic factors controlling mineral matter in coal. In: A. Donaldson, M. Presley, and J. Renton (eds) Carboniferous Coal Guidebook, volume 1. West Virginia Geological and Economic Survey, Bulletin B-37-1, p. 224-239.

Cecil, C. B., Renton, J. J., Stanton, R. W., and Finkelman, R. B., (1979c) Mineral matter in coals of the central Appalachian Basin. 9th Internat. Cong. Carbonif. Strat. Geol., Abstracts. Urbana, p.33.

Chandra, D., (1962) Reflectance and microstucture of weathered coals. Fuel, 41:185-193

Choi, C-y., Muntean, J. V., Thompson, A. R., and Botto, R. E., (1989) Characterization of coal macerals using combined chemical and NMR spectroscopic methods. Energy and Fuels, 3:528-533

Clemens, A. H., Matheson, T. W., Lynch, L. J., and Sakurovs, R., (1989) Oxidation studies of high fluidity coals. Fuel, 68:1162-1167

Coin, C. D. A., (1987) Coke microtextural description comparison of nomenclature, classification, and methods. Fuel, 66:702-705

Coin, C. D. A., Gill, W. W., and Hart, A. T., (1982) Blast furnace coke reactions. BHP Tech. Bull., 26:1:31-33

Connolly, C. A., (1989) Thermal diagenesis of the Wilrich Member shale, Spirit River Formation, northwest Alberta. Bull. Can. Petrol. Geol., no.2, 37:182-187

Cook, A. C., (1975) The spatial and temporal variation of the type and rank of Australian coals. In: A. C. Cook (ed) Australian Black Coal - Its Occurrence, Mining, Preparation and Use. Austalian Institute of Mining and Metallurgy, pp. 63-84

Cook, A. C., and Edwards, G. E., (1971) Vitrinite content and coke strength. Fuel, 50:41-72

Cook, A. C., Murchison, D. G., and Scott, E., (1972) Optically biaxial anthracitic vitrinites. Fuel, 51:180-184

Correa da Silva, Z. C., (1989) The rank evaluation of South Brazilian Gondwana coals on the basis of different chemical and physical parameters. In: P. C. Lyons and B. Alpern (eds) Coal: Classification, Coalification, Mineralogy, Trace-element Chemistry, and Oil and Gas Potential. Int. J. Coal Geol., 13: 21-39

Creaney S., Pearson D.E., and Marconi L.G., (1980) Anomalous coking properties of the Wolgan Seam NSW Australia. Fuel, 59:438-440

Crelling, J. C., Schrader R. H., and Benedict, L. G., (1979) Effects of weathering on coking properties and coke quality. Fuel, 58:542-546\

Crelling, J. C.,Bensley, D. F., Landis, C. B., and Rimmer, S. M., (1989) Lecture notes for workshop on fluorescence microscopy. Workshop held at the Coal Characterization Laboratory, Dept, of Geology, Southern Illinois University at Carbondale, 1-2 Nov. 1989, 122p.

Cudmore, J. F., (1984) Coal utilization. In: C. R. Ward (ed) Coal Geology and Coal Technology, Blackwell Scientific, Victoria, pp.113-150

Damberger H. H., (1974) Coalification patterns of Pennsylvanian coal basins of the eastern United States. In: Geological Society of America Special Paper 153, p.53-74

Davidson, R. M., (1990) Natural Oxidation of Coal. IEA Coal Research, IEA/CR29, 76p.

Davis, A., (1971) The optical properties of some Bowen Basin vitrinites. Proceedings of the 2nd Bowen Basin Symposium, Brisbane, Geological Survey of Queensland, rept. no. 62, p.61-76

Davis, A., (1978) The reflectance of coal. In: C. Karr (ed) Analytical Methods of Coal and Coal Products, Vol. 1, Academic Press, New York, p.27-81

Davis, A., (1984) Coal petrology and petrographic analysis. In: C. R. Ward (ed) Coal Geology and Coal Technology, Blackwell Scientific, Victoria, pp.74-112

Davis A., (1987) Combined white-/blue-light maceral analysis. The Society for Organic Petrology Newsletter, no. 2, 4:6-7

Davis, A., Russell, S. J., Rimmer, S. M., and Yeakel, D. J., (1984) Some genetic implications of silica and aluminosilicates in peat and coal. Int. J. Coal Geol., 3:293-314

Davis, A., Rathbone, R. F., Lin, R., and Quick, J. C., (1990) Observations concerning the nature of maceral fluorescence alteration with time. Org. Geochem., 16:897-906

Davis, A., Mitchell, G. D., Derbyshire, F. J., Rathbone, R. F., and Lin, R., (1991) Optical properties of coals and liquifaction residues as indicators of reactivity. Fuel, 70:352-360

Death, D. L., Eberhardt, J. E., and Read, R., (1991) Laser induced macrofluorescence of coal: oxidation and macroalteration. Fuel, 70:1073-1077

Derbyshire, F. D., Davis, A. D., and Lin, R., (1989) Considerations of physicochemical phenomena in coal processing. Energy and Fuels, 3:431-437

Diessel, C. F. K., (1983) Carbonization reactions of inertinite macerals in Australian coals. Fuel, 62:883-892

Diessel, C. F. K., (1984) Coal Geology, Part 1. Australian Mineral Foundation, workshop course 282/84, 17-23 May, New Zealand, 382p.

Diessel, C. F. K., (1985) Fluorometric analysis of inertinite. Fuel, 64:1542-1546

Diessel, C. F. K., (1990) Current trends in coal microscopy, Proc 4th Australian Coal Conference, Dec, 3-5, Brisbane 16p.

Diessel, C. F. K., (1991) The ICCP ring analysis - an interesting comparison of two coals and their cokes. Twenty Fifth Newcastle Symposium, on Advances in the Study of the Sydney Basin. 12-14 April, Newcastle NSW, p.251-260

Diessel, C. F. K., and McHugh, E., (1986) On the correlation of fluorescence intensity and reflectance in vitrinites and inertinites in relation to the degree of coalification and coking behaviour. Glueckauf-Forschungshefte, 47:60-70 (in german, anon. english translation)

Diessel, C. F. K., and Wolff-Fischer (1986) Comparative investigations on coals and cokes in relation to the question of the inertinite reactivity. Glueckauf-Forschungshefte, 47:203-211 (in german, translation by J. and A. Zeder)

Diessel, C. F. K., and Wolff-Fischer (1987) Coal and coke petrographic investigations into the fusibility of Carboniferous and Permian coking coals. Int. J. of Coal Geol., 9:87-108

Diessel, C. F. K., and Bailey, J. G., (1989) The application of petrographic techniques to carbonisation and combustion research at the University of Newcastle AusIMM Mineralogy-Petrology Symposium, February, 89 Sydney NSW, p.117-121

Diessel, C. F. K., and Wolff-Fischer (1989) The application of fluorescence intensity measurements of vitrinite to questions of coal formation. Proc. Macerals 89, CSIRO Conf. May 10-11, 10p.

Dillinger, L., (1981) Polishing. "Met-Tips" information brochure no. 13, Leco Corporation 30000 Lakeview Ave., St. Joseph, Michigan, 49085, USA, 5p.

Dow, W. G., (1977) Kerogen studies and geological interpretations. Jour. Geochem. Exploration. 7:79-99

Dulhunty, J. A., (1954) Geologic factors in the metamorphic development of coal. Fuel, 33:145-152

Durie, R. A., (1961) The inorganic constituents in Australian coals III Morwell and Yallourn brown coals. Fuel, 40:407-422

Edwards, A. B., and Baker, G., (1951) Some occurrences of supergene iron sulfides in relation to their environments of deposition. J. Sed. Petrol., no. 1, 21:34-46

Edwards, I A. S., (1989) Structure in carbons and carbon forms In: H. Marsh (ed.) Introduction to Carbon Science. Butterworth & Co., London, pp. 1-36

Esterle, J. S., and Ferm, J. C., (1986) Relationship between petrographic and chemical properties and coal seam geometry, Hance seam, Breathitt Formation southeastern Kentucky. Int. J. Coal Geol., 6:199-214

Falcon, R.M.S. and Snyman, C. P., (1987) An introduction to coal petrography: Atlas of petrographic constituents in the bituminous coals of Southern Africa. Review paper no. 2, Geol. Soc. of South Africa, 27p.

Fermont, W. J. J., (1988) Possible causes of abnormal vitrinite reflectance values in paralic deposits of the Carboniferous in the Achterhoek area, the Netherlands. Org. Geochem., 12:401-411

Finkelman, R. B., (1980) Modes of occurrence of trace elements in coal. U.S. Geol. Surv., Open-File Report OF-83-99, 301p.

Francis, W., (1961) Coal, Its Formation and Composition: 2nd. edition, Edward Arnold, London, 806p.

Fredericks, P. M., Warbrooke, P., and Wilson, M. A., (1983) Chemical changes during natural oxidation of a high volatile bituminous coal. Org. Geochem., no.3, 5:89-97

Fromm, E., and Achert, O., (1903) Uber schwefelhaltige benzyldervate und deren zersetzung durch trockene destillation. Berichte Deutsche Chemische Gesellschaft, 36:534-547

Fujii, K., Sumic, Y., Shoda, K., and Miki, K., (1982) Effect of degradinite on coal properties and its conversion at Ikeshima coal mine. A.A.P.G. Bull., 66:968

Fujii, K., and Kiyo, O., (1985) Some problems on the relationship between vitrinite reflectance and burial depth. Bull. Geol. Surv. Japan, 36:103-110

Fujita, H., Hijiriyama, M., and Nishida, S., (1983) Gasification reactivities of optical textures of metallurgical cokes. Fuel, 62:875-879

Galehouse, J. S., (1971) Point counting. In: R. E. Carver (ed) Procedures in Sedimentary Petrology. Wiley Interscience, New York, p.385-407

George, G. N., Gorbaty, M. L., Kelemen, S. R., and Sansone, M., (1991) Direct determination of sulfur forms in coal from the Argonne Premium Sample Program. Energy and Fuels, 5:93-97

Gill, W. W., Brown, N. A., Coin, C. D. A., and Mahoney, M. R., (1985) The influence of ash on the weakening of coke. ISS-AIME Ironmaking Conf. Proc., Detroit 44:233-238

Given, P. H., Davis, A., Kuehn, D., Painter, P. C., and Spackman, W., (1985) A multi-facetted study of a Cretaceous coal with algal affinities. I. Provenance of the coal samples and basic compositional data. Int. J. Coal Geol., 5:247-260

Given, P. H., and Yarzab, R. F., (1975) Problems and Solutions in the Use of Coal Analyses. Penn State University, Coal Research Section, Tech. Rept. 1, prepared for the U.S. Dept. of Energy, FE-0390-1, 40p.

Given, P. H., and Yarzab, R. F., (1978) Analysis of the organic substance of coals: problems posed by the presence of mineral matter. In: C. Karr (ed) Analytical Methods For Coal and Coal Products, volume II. Academic Press, New York, p.3-41

Given, P. H., Spackman, W., Davis, A., and Jenkins, R. G., (1980) Some proved and unproved effects of coal geochemistry on liquefaction behavior with emphasis on U.S. coals. In: D. D. Whitehurst (ed) Coal Liquefaction Fundamentals, ACS symposium series No. 139, p.1-34

Given, P. H., Weldon, D., and Zoeller, J. H., (1986) Calculation of calorific values of coals from ultimate analyses: theoretical basis and geochemical implications. Fuel, 65:849-854

Gluskoter, H. J., (1965) Electronic low-temperature ashing of bituminous coal. Fuel, 44:285-291

Gluskoter, H. J., (1967) Clay minerals in Illinois coals. Jour. of Sed. Petrol., no.1, 37:205-214

Gluskoter, H. J., (1975) Inorganic sulfur in coal. Am. Chem. Soc. Div. Fuel Chem. Preprints, no.2, 20:94-98

Goodarzi, F., and Murchison, D. G., (1972) Optical properties of carbonized vitrinites. Fuel, 51:322-328

Goodarzi, F., Gentzis, T., Feinstein, S., and Snowdon, L., (1988) Effect of maceral subtypes and mineral matrix on measured reflectance of subbituminous coals and dispersed organic matter. Int. J. Coal Geol., 10:383-398

Goscinski, J. S., Gray, R. J., and Robinson, R. W., (1985) A review of American coal quality and its effect on coke reactivity and after reaction strength of cokes. J. Coal Qual., part 1, 4:3:35-43, part 2, 4:4:21-29,

Gray, R. J., (1982) A petrologic method of analysis of non-maceral microstructures in coal. Int. J. Coal Geol., 2:79-97

Gray, R. J., (1989) Coal to coke conversion, In: H. Marsh (ed) Introduction to Carbon Science. Butterworth, London, p.286-321

Gray, R. J., Goscinski, J. S., and Shoenberger, R. W., (1978) Selection of coals for cokemaking. paper presented at ISS-AIME conference, October 3, Pittsburgh, In: Text to complement lectures, short course in the theory and practice of organic petrology, May 22-25 1984, University park PA. 27p. plus figures.

Gray, R. J., Rhoads A. H., and King D. T., (1976) Detection of oxidized coal and the effect of oxidation on the technological properties. Transactions of the Society of Mining Engineers, 260:334-340

Gray, R. J., and Devanney, K. F., (1983) Coke carbon forms: microscopic classification and industrial applications. Int. J. Coal Geol., 6:277-297

Gray, R. J., and Lowenhaupt, D. E., (1989) Aging and weathering, In: R. Klein and R. Wellek (eds) Sample Selection Aging, and Reactivity of Coal. John Wiley and Sons, New York, p.255-336

Gray, V. R., (1983) Coal Analysis in New Zealand. N.Z. Energy Research and Development Committee Rept. No. 97, ISSN 0110-11692, 75p.

Grint, A., Mehani, S., Trewhella, M., and Crook, M. J., (1985) Role and composition of the mobile phase in coal. Fuel, 64:1355-1361

Habermehl, D., Orywal, F., and Beyer, H., (1981) Plastic properties of coal. In: M. A. Elliot (ed.) Chemistry of Coal Utilization, 2nd suppl. vol., p.319-368

Harris, L. A., Cavin, B. O., Crouse, R. S., and Yust, C. S., (1980) Scanning electron microscopical observations and energy dispersive X-ray analysis of secondary mineralization in a bituminous coal. Microscopica Acta, no.4, 82:343-349

Harrison, C. H., (1990) A method for electron microprobe examination of coal macerals. Laboratory Notes, TSOP Newsletter, 7:6

Harrison, J. A., Jackman, H. W., and Simon, J. A., (1964) Predicting Coke Stability from Petrographic Analysis of Illinios Coals. Ill. State Geol. Surv. Circular 366, 20p.

Harrison, J. A., (1965) Effect of moisture content on the reflectance values of coal. Fuel, 44:225-228

Harrison, J. A. and Thomas, J. Jr., (1966) Relation between moisture content, reflectance values and internal surface area of coal. Fuel, 45:501-503

Hatcher, P. G., Breger, I. A., Szeverenyi, N., and Maciel, G. E., (1982) Nuclear magnetic resonance studies of ancient buried wood - II. Observations on the origin of coal from lignite to bituminous coal. Org. Geochem., 4:9-18

Horvath, Z. A., (1983) Study on maturation process of huminitic organic matter by means of high-pressure experiments. Acta Geologica Hungarica, 26:137-148

Hower, J. C., and Lineberry, G. T., (1988) The interaction of coal lithology and coal cutting characteristics on the breakage characteristics of selected Kentucky coals. J. Coal Qual., 7:88-95

Hower, J. C., Wild, G. D., and Pollock J. D., (1988) Maceral composition of single-lithotype coal samples from Kentucky. The Society for Organic Petrology Newsletter, no.2, 5:4

Hower, J. C., Wild, G. D., and Pollock J. D., (1989) Further comments on coal lithotypes. The Society for Organic Petrology Newsletter, no.1, 6:4-5

Huggins, F. E., Huffman, G. P., and Lin, M. C., (1983) Observations on low temperature oxidation of minerals in bituminous coals. Int. J. Coal Geol., 3:157-182

Huggins, F. E., and Huffman, G. P., (1989) Coal weathering and oxidation: The early stages, In: C. R. Nelson (ed) Chemistry of Coal Weathering, Coal Science and Technology 14, Elsevier, Amsterdam p.33-60

Hunt, J. M., (1979) Petroleum Geochemistry and Geology. W. H. Freeman and Co., San Francisco, 617p.

Hutton, A. C., and Cook, A. C., (1980) Influence of alginite on the reflectance of vitrinite from Joadja, NSW, and some other coals and oil shales containing alginite. Fuel 59:711-714

ICCP, (1963) International Committee for Coal Petrology, Handbook of Coal Petrography, 2nd edition. Centre National de la Recherch Scientifique, Paris

Ignasiak, B. S., Szladow, A. J., and Montgomery, D. S., (1974) Oxidation studies on coking coal related to weathering. 3. The influence of acidic hydroxyl groups, created during oxidation, on the plasticity and dialation of the weathered coking coal. Fuel 53:12-15

Illing, V. C., (1933) The migration of oil and natural gas. J. Inst. Petrol., 19:229-274

Ingram G. R., and Rimstidt, D. J., (1984) Natural weathering of coal. Fuel, 63:292-296

Ishikawa, Y., Kase, M., Abe, Y., Ono, K., Sugata, M., and Nishi, T., (1983) Influence of post reaction strength of coke on blast furnace operation. Ironmaking Proceedings, 42:357-368

ISO International Organization for Standardization, Technical Committee. ISO/TC 27 Solid Mineral Fuels

------ 562-1981(e) Hard coal and coke - Determination of volatile matter content. 5p.

------ 1171-1981(e) Solid mineral fuels- Determiantion of ash. 2p.

------ 7404/3-1984(e) Methods for the petrographic analysis of bituminous coal and anthracite- Part 3: Method of determining maceral group composition. 4p.

------ 7404/5-1984(e) Methods for the petrographic analysis of bituminous coal and anthracite- Part 5: Method of determining microscopically the reflectance of vitrinite. 11p.

Jacob, H., and Hiltmann, W., (1985) Disperse bitumen solids as an indicator for migration and maturity within the scope of prospecting for petroleum and natural gas A model for NW Germany. final report, Deutsche Gesellschaft Fur Mineralolwissenschaft und Kohlechemie, Project 267, Hamburg, 54p. (in german with english abstract and summary).

Jenkins R. J., and Walker, P. L., (1978) Analysis of mineral matter in coal. In: C. Karr (ed) Analytical methods for coal and coal products, volume 2. Academic Press, p.265-292

Jones, J. M., Murchison, D. G., and Saleh, S. E., (1972) Variation of vitrinite reflectivity in relation to lithology. Advances in Organic Geochemistry, p.601-612

Jones, J. M., Davis, A., Cook, A., Murchison D. G., and Scott, E., (1984) Provincialism and correlations between some properties of vitrinite. Int. J. Coal Geol., 3:315-331

Kalkreuth, W. D., (1982) Rank and petrographic composition of selected Jurassic - Lower Cretaceous coals of British Columbia. Bull. Can. Petrol. Geol., 30:112-139

Kalkreuth, W., Steller, M., Wieschenkamper, I., and Ganz, S., (1991) Petrographic and chemical characterization of Canadian and German coals in relation to utilization potential, 1. Petrographic and chemical characterization of feedcoals. Fuel 70:683-694

Kaegi, D. D., (1985) On the identification and origin of pseudovitrinite. Int. J. Coal Geol., 4:309-319

Kelemen S. R., Gorbaty, M. L., George, G. N., Kwiatek, P. J., and Sansone, M., (1991) Thermal reactivity of sulphur forms in coal. Fuel, 70:396-402

Kemezys, M., and Taylor, G. H., (1964) Occurrence and distribution of minerals in some Australian Coals. J. Inst. Fuel, 37:389-397

Kilby, W. E., (1988) Recognition of vitrinite with non-uniaxial negative reflectance characteristics. Int. J. Coal Geol., 9:267-285

King, H. M., and Renton, J. J., (1979) The mode of occurrence and distribution of sulfur in West Virginia coals. In: A. Donaldson, M. Presley, W., and J. Renton (eds) Carboniferous Coal Guidebook, volume 1. West Virginia Geological and Economic Survey, Bulletin B-37-1, p.278-301

King, J. G., Maries, M. B., and Crossley, H. E., (1936) Formulae for the calculation of coal analyses to a basis of coal substance free from mineral matter. J. Soc. of Chem. Ind., 55:T277-281

Kirov, N, Y., and Stephens, J. N., (1967) Physical Aspects of Coal Carbonisation. Kingsway Printers, Caringbah NSW, 221p.

Kisch, H. J., (1968) Coal rank and burial metamorphic mineral facies. In: P. A. Schenck and I. Havenaar (eds) Advances in Organic Geochemistry 1968. Pergamon Press, Oxford, p.407-425

Kiss, L. T., and King, T. N., (1977) The expression of results of coal analysis: the case for brown coals. Fuel, 56:340-341

Lapo, A. V., (1978) Comparative characteristics of vitrinites of Carboniferous coals of the Ukraine and Jurassic coals of Siberia. Fuel 57:179-183

Larsen, J. W., Lee, D., Schmidt, T., and Grint, A., (1986) Multiple mechanisms for the loss of coking properties caused by mild air oxidation. Fuel, 65:595-596

Lavill, D. R., (1987) New Zealand's high fluidity bituminous coals. J. Coal Qual., no. 4, 6:129-132

Law, B. E., Nuccio, V. F., and Barker, C. E., (1989) Kinky reflectance well profiles: Evidence of paleopore pressure in low-permiability gas-bearing sequences in Rocky Mountain foreland basins. A.A.P.G. Bull., 73:999-1010

Levine, J., (1989) note in product information section of TSOP newsletter. 7:10

Levine, J. R., and Davis A., (1984) Optical anisotropy of coals as an indicator of tectonic deformation, Broad Top Coal Field, Pennsylvania. Geol. Soc., Am., Bull., 95:100-108

Lin R., (1988) The Chemistry of Coal Maceral Fluorescence: With Special Reference to the Huminite/Vitrinite Group. unpublished Ph.D. thesis, The Pennsylvania State University, Dept. of Geosciences, 273p.

Lin, R., Davis, A., Bensley, D. F., and Derbyshire, F. J., (1986) Vitrinite secondary fluorescence: Its chemistry and relationship to the development of a mobile phase and thermoplasticity in coal. Int. J. Coal Geol., 6:215-228

Lin, R., Davis, A., Bensley, D. F., and Derbyshire, F. J., (1987) The chemistry of vitrinite fluorescence. Org. Geochem., 11:393-399

Liotta, R., Brons, G., and Isaacs, J., (1983) Oxidative weathering of Illinois No. 6 coal. Fuel, 62:781-791

Loison, R., Peytavy, A., Boyer, A. F., and Grillot, R., (1963) The plastic properties of coal, In: H. H. Lowry (ed) Chemistry of Coal Utilization, suppl. volume., J. Wiley and Sons, New York, p.150-201

Loison, R., Foch, P., and Boyer, A., (1989) Coke Quality and Production, 2nd edition. Buttersworth & Co. Ltd., London, 555p.

Lowenhaupt D. E., and Gray R. J., (1980) The alkali-extraction test as a reliable method of detecting oxidized metallurgical coal. Int. J. Coal Geol., 1:63-73

Mackowsky, M.-Th., (1968) Mineral matter in coal. In: D. Murchison and T. S. Stanley (eds) Coal and Coal Bearing Strata. Oliver and Boyd, London, p.309-321

Mackowsky, M.-Th., (1982) Minerals and trace elements occurring in coal. In: E. Stach, G. H. Taylor, M-Th. Mackowsky, D. Chandra, M. Teichmüller, and R. Teichmüller (eds) Stach's Textbook of Coal Petrology, 3rd edition. Gebruder Borntraeger, Berlin and Stuttgart, p.153-171

Marchioni, D. L., (1983) The detection of weathering in coal by petrographic, rheologic and chemical methods. Int. J. Coal Geol., 2:231-259

Marsh, H., (1982) Metallurgical coke: formation structure and properties. ISS-AIME Ironmaking Conf. Proc., Pittsburgh, 41:2-11

Marsh, H., and Smith, J., (1978) The formation and properties of anisotropic cokes from coals and coal derivatives studied by optical and scanning electron microscopy. In: C. Karr (ed) Analytical Methods for Coal and Coal Products, Volume II, Academic Press Inc., New York, p.371-414

Marsh, H., and Kuo, K., (1989) Kinetics and catalysis of carbon gasification. In: H. Marsh (ed) Introduction to Carbon Science. Butterworth, London, p.108-151

Mastalerz, M., (1991) Variation of vitrinite reflectance in vertical seam section, An example from the Intrasudetic basin, SW Poland. Bull. Soc. Geol. France, t 162, no 2, p.175-182

Mathews, W. H., and Bustin, R. M., (1984) Changes associated with natural in situ weathering of a coking coal from southeastern British Columbia. Fuel 63:548-550

McCartney, J. T., and Teichmüller, M., (1972) Classification of coals according to degree of coalification by reflectance of the vitrinite component. Fuel, 51:64-68

McClung, J. D., and Greer, M. R., (1979) Properties of coal and coal impurtities. In: J. W. Leonard (ed) Coal Preparation 4th ed., American Inst. of Mining, Metallurgical and Petroleum Engineers Inc., New York, Chapter 1, 79p.

Mc Hugh, E. A., (1986) The influence of oxidation on the fluorescence properties of coking coals. Adv. Stud. Sydney Basin, 20th Newcastle Symp. Proc. p.66-70.

McHugh, E. A., Diessel, C. F. K., and Kutzner, R., (1991) Use of fluorescence microscopy in the detection of low level oxidation in bituminous coals. Fuel, 70:647-653

McTavish, R. A., (1978) Pressure retardation of vitrinite diagenesis, offshore north-west Europe. Nature, 271:648-650

Mikula, R. J., and Mikhail, M. W., (1987) A ΔP technique for the prediction and monitoring of coal oxidation. Coal Preparation, 5:57-69

Miller R. N., Yarzab, R. F., and Given, P. H., (1979) Determination of the mineral matter contents of coals by low temperature ashing. Fuel, 58:4-10

Miller, R. N., and Given, P. H., (1987) The association of major, minor and trace inorganic elements with lignites. II Minerals and major and minor element profiles in four seams. Geochim. et Cosmochim. Acta, v.51:1311-1322

Millott, J. O'N., (1958) Mineral matter in coal the water of constitution of the silicate constituents. Fuel 37:71-85

Mitchell, G. D., Davis, A., and Rathbone, R. F., (1991) The use of vitrinite fluorescence as a measure of changes in coal thermoplasticity and weathering. Ironmaking Conference Proceedings, 50:199-206

Moreland, A., Patrick, J. W., and Walker, A., (1988) Optical anisotropy in cokes from high-rank coals. Fuel, 67:730-732

Mott, R. A., and Spooner, C. E., (1940) The calorific value of coal: The Dulong relationship. Fuel 19:226-231 and 242-251

Moxon, N. T., McLellan, J., Warbrooke, P. R., (1987) The effect of time on the laboratory carbonization properties of simulated coal borecoles. J. Coal Qual., no. 1, 6:8-15

Murchison, D. G., (1978) Optical properties of carbonized vitrinites. In: C. Karr (ed) Analytical Methods for Coal and Coal Products, Volume II, Academic Press Inc., New York, p.415-464

Murchison D. G., (1991) Petrographic aspects of coal structure: reactivity of macerals in laboratory and natural environments. Fuel 70:296-315

Nakamura, N., Togino, Y., and Tateoka, M., (1978) Behavior of coke in large blast furnaces. Ironmaking and Steelmaking, 5:1:1-17

Nandi, B. N., and Montgomery, D. S., (1975) Nature and thermal behavior of semifusinite in Cretaceous coals from western Canada. Fuel. 54:193-196

Neavel, R. C., (1981) Origin, petrography, and classification of coal. In: M. A. Elliot (ed) Chemistry of Coal Utilization, 2nd suppl. vol., p.91-158

Neavel, R. C., (1982) Coal plasticity mechanism: Inferences from liquefaction studies. In: M. Gorbaty, J. Larsen and I. Wender (eds) Coal Science volume 1, Academic Press, New York, p.1-19.

Neavel, R. C., (1986) Coal Science: an idiosyncratic view. Fuel, 65:1632-1637

Neavel, R. C., Smith, S. E., Hippo, E. J., and Miller, R. N., (1986) Interrelationships between coal compositional parameters. Fuel, 65:312-320

Newman, J., (1985) Paleoenvironments, coal properties, and their interrelationships in Paparoa and selected Brunner coal measures on the west coast of the South Island. unpublished Ph.D thesis, University of Canterbury, Department of Geology, 269p.

Newman, J., (1985b) Relationships between reflectance and volatile matter in west coals bituminous coals: 1. The effect of isorank type variations on coal properties. Proc. Coal Research Conf., Wellington, paper 2.2, 10p.

Newman, J., (1986) Coal type, rank & paleoenvironments in the Upper Waimangaroa sector, Buller coalfield. Report prepared for New Zealand Mines Division, Coal resources Survey, 49p.

Newman, J., (1987) Coal type, rank & paleoenvironments in the Upper Waimangaroa sector, Buller coalfield. Volume 1, Proc. Coal Research Conf., 2-4 Nov., Wellington, paper R 2.1, 12p.

Newman, J., (1988) Oxidative etching of high rank New Zealand coals. Geological Society of New Zealand Conference, abstract for poster, 28 Nov. - 1 Dec., Hamilton

Newman, J., (1989a) Coal Geology of the West Kawhia Coalfield, New Zealand. Coal Geology Report 17, ISSN 0113-1826, Market Information and Analysis, Ministry of Energy, New Zealand, 33p.

Newman J., (1989b) Why are some high rank Tertiary coals more peculiar than others? Some thoughts on climate and floral assemblage. Volume 1, Proc. Coal Research Conf., 9-11 Oct., Wellington, p.182-186

Newman, J., (1991) Controls on the distribution, timing, and effects of diagenetic sulphur enrichment in some New Zealand coals. Proceeding vol 2., Fourth New Zealand Coal Conference, 14-16 Oct., Wellington p.301-315

Newman, J., and Newman, N. A., (1982) Reflectance anomalies in Pike River coals: evidence of variability in vitrinite type, with implications for maturation studies and "Suggate rank". N. Z. J. Geol. Geophys., 25:233-243

Newman, J., and Newman, N. A., (in press) Tectonic and paleoenvironmental controls on the distribution and properties of upper Cretaceous coals on the west coast of the South Island, New Zealand. In: Controls on the Distribution and Quality of Cretaceous Coals. GSA special paper 267.

Newman, N. A, (1988) Mineral Matter in Coals of the West Coast, South Island, New Zealand. unpublished Ph.D. thesis, University of Canterbury, Department of Geology, 293p.

Newman, N, (1990) Notes for University of Canterbury computer assisted reflectance data aquisition program, unpublished memorandum 2p.

Nordstrom, D. K., (1982) Aqueous pyrite oxidation and the consequent formation of secondary iron minerals. In: Acid Sulfate Weathering. SSSA special publ. no. 10., Symp. Proc., Soil Science Society of America, Fort Collins CO, 5-10 Aug., 1979, p.37-56.

Ode, W. H., and Gibson, F. H., (1960) International system for classifying brown coals and lignites and its application to American Coals. U. S. Bur. Mines, Rept. of Invest. 5695, 20p.

Okuyama, Y., Miyazu, T., Sugimura, H., and Kumagai, M., (1970) Prediction of the coking property of coal by microscopic analysis. J. Fuel Soc. Japan, 49:736-743 (in japanese with english synopsis and captions)

Omega Optical Inc. (1986) There's no end in light. Omega Optical Inc. Catalogue, 3 Grove Street, PO Box 573, Brattleboro Vermont 05301 USA, 16p.

Ottenjann, K., (1986) Calibration of microphotometric system. Notes from the petrology laboratory, TSOP Newsletter, 3:7

Ottenjann, K., (1989) untitled. Notes from the lab, TSOP Newsletter, 6:2

Ourisson G., Albrecht, P., and Rohmer, M., (1984) The microbial origin of fossil fuels. Scientific American, 251:2:34-37

Painter, P. C., Snyder, R. W., Pearson, D. E., and Kwong, J., (1980) Fourier transform infrared study of the variation in the oxidation of a coking coal. Fuel, 59:282-286

Pankhurst, Q. A., McCann, V. H., and Newman, N. A., (1986) Identification of the iron bearing minerals in some bituminous coals using Mossbauer spectroscopy. Fuel, 65:880-883

Parham, W. E., (1966) Lateral variation of clay mineral assemblages in modern and ancient sediments. Volume 1, Proceedings of the International Clay Conference, Jerusalem, Israel, p.135-145

Patrick J. W., Reynolds, M. J., and Shaw, F. H., (1973) Development of optical anisotropy in vitrains during carbonization. Fuel, 52:198-204

Patrick J. W., Reynolds, M. J., and Shaw, F. H., (1979) Optical anisotropy of carbonized coking- and caking-coal vitrains. Fuel, 58:501-509

Peacey, J. G., and Davenport, W. G., (1979) The Iron Blast Furnace Theory and Practice. Pergamon Press, Oxford, 251p.

Pearson, D. E., and Kwong, J., (1979) Mineral matter as a measure of oxidation of a coking coal. Fuel, 58:63-66

Pearson, D. E., (1984) An indirect evaluation of the reactivity of inertinites in western Canadian coking coals. Report to CANMET DSS File No. Energy Mines and Resouces Canada, June 1984

Perch, M., (1981) Solid products of pyrolysis. In: M. A. Elliot (ed) Chemistry of Coal Utilization, 2nd suppl. vol., p.919-981

Peters, K. E., (1986) Guidelines for evaluating petroleum source rock using programmed pyrolysis. A.P.P.G. Bull., 70:318-329

Piller, H., (1977) Microscope Photometry. Springer-Verlag, Berlin, 253p

Potonie, R., (1954) The morphographical and morphological classification in coal microscopy. Reprint, Proceedings of the International Committee for Coal Petrology, Nr. 1, E. Van Aelst Maastricht, the Netherlands. p.9-10

Prado, J. G., (1977) Optical properties of oxidized vitrinite and exinite. Journal of Microscopy, 109:85-92

Price J. T., Grandsen, J. F., and Khan, M. A., (1988) Effect of the properties of western Canadian coals on their coking behaviour. ISS-AIME Ironmaking Conf. Proc., Toronto 17-20 April (1988) 47:39-55

Price, L. C., and Barker, C. E., (1985) Suppression of vitrinite reflectance - a major unrecognized problem. Jour. of Petrol. Geol. 8:59-84

Pye, K., Dickson, J. A. D., Schiavon, N., Coleman, M. L., and Cox, M., (1989)

Querol, X., Chinchon, S., and Lopez-Soler, A., (1989) Iron sulfide precipitation sequence in Albian coals from the Maestrazgo Basin, southeastern Iberian Range, northeastern Spain. Int. J. Coal Geol., 11:171-189

Quick, J. C., and Kneller, W. A., (1987) The use of dyes as an aid to coal petrography. Int. J. Coal Geol., 7:51-68

Quick, J. C., Davis, A., and Lin, R., (1988) Recognition of reactive maceral types by combined fluorescence and reflectance microscopy. ISS-AIME Ironmaking Conf. Proc., Toronto 17-20 April 47:331-337

Quick, J. C., Davis, A., and Glick, D., (1989) Coal oxidation: detection, measurement and effect on thermoplastic behavior. Abst. Prog. 19th Conf on Carbon., Univ. Park PA., 25-30 June, p.232-233

Quick, J., and Moore, T., (1991) Petrographic analysis of some bituminous New Zealand coals: methods and uses. Proc. Fourth New Zealand Coal Conference, 14-16 Oct. Wellington, 13p.

Raymond A. C., and Murchison, D. G., (1991) Influence of exinitic macerals on the reflectance of vitrinite in Carboniferous sediments of the Midland Valley of Scotland. Fuel, 70:155-160

Rees, O. W., Coolican, F. C., Pierron, E. D., and Beeler, C. W., (1961) Effects of Outdoor Storage on Illinois Steam Coal. Illinois State Geol. Surv., Circular 313, 10p.

Rees, O. W., (1966) Chemistry Uses and Limitations of Coal Analyses. Illinois State Geol. Surv., Rept of Invest. 220, 55p.

Reidenouer, D., Williams, E. G., and Dutcher, R. R., (1967) The relationship between paleotopography and sulfur distribution in some coals of western Pennsylvania. Econ. Geol., 62:632-647

Renton, J. J., (1982) Mineral matter in coal. In: R. A. Meyers (ed) Coal Structure. Academic Press, p.283-326

Renton, J. J., and Cecil, C. B., (1979) The origin of mineral matter in coal. In: A. Donaldson, M. Presley and J. Renton (eds) Carboniferous Coal Guidebook, volume 1. West Virginia Geological and Economic Survey, Bulletin B-37-1, p.206-223

Renton, J. J., and Cecil, C. B., (1980) Coal compositional relationships in support of a chemical coal model. In: A. Donaldson, M. Presley, and J. Renton (eds) Carboniferous Coal Guidebook, volume 3. West Virginia Geological and Economic Survey, Bulletin B-37-3, p.103-128

Renton, J. J., Cecil, C. B., Stanton, R., and Dulong, (1980) Compositional relationships of plants and peats from modern peat swamps in support of a chemical coal model. In: A. Donaldson, M. Presley and J. Renton (eds) Carboniferous Coal Guidebook, volume 3. West Virginia Geological and Economic Survey, Bulletin B-37-3, p.57-102

Rhoades, A. H., Gray, R. J., and Huntington, H. D., (1981) Application of microscopic techniques in the evaluation of coal - coke and related products. In: D. M. Hausen and W. C. Park (eds) Process Mineralogy, Proc. of a Symposium, TSM-AIME Process Mineralogy Committee 110th AIME ann. mtg., Chicago., Ill, p.453-470

Rimmer, S. M., and Davis, A., (1984) Geologic controls on the inorganic composition of Lower Kittanning coal. In: K. S. Vorres (ed) Mineral Matter and Ash In Coal. A.C.S. symposium series no. 301, p.41-52

Robinson, J. M., (1990) Lignin, land plants and fungi: Biological evolution affecting Phanerozoic oxygen balance. Geology, 15:607-610

Ruppert, L. F., Cecil, C. B., and Stanton, R. W., (1987) Sources of quartz in Upper Freeport coal. Geol. Soc. of Am. 1987 ann. mtg., Phoenix, October 26-29, Abstr. with Prog., no.7, 19:827

Sanyal, A., (1983) The role of coal macerals in combustion. J. Inst. Energy, 56:92-95.

Sasaki, M., Takahashi, R, and Mochida, I., (1990) Relation between the fluorescence intensity of vitrinites and the fluidity of coals. Fuel, 69:529-532

Schapiro, N., Gray, R. J., and Eusner, G. R., (1961) Recent developments in coal petrography. AIME Blast Furnace Coke Oven and Raw Materials Proceedings, 20:89-112

Schapiro, N., and Gray, R. J., (1963) Relation of coke structure to reactivity. Blast Furnace and Steel Plant, 51:273-280

Schapiro, N., and Gray, R. J., (1964) The use of coal petrography in coke-making. J. Inst. Fuel, June, p.234-242

Schopf, J. M., (1956) A definition of coal. Econ. Geol., 51:521-527

Selvig, W. A., and Ode, W. H., (1953) Determination of Moisture-Holding Capacity (Bed-Moisture) of Coal for Classification by Rank. U. S. Bureau of Mines, Rept. of Invest. 4968, 10p.

Sharp P.A., (1986) Storage of 8 mesh sub-bituminous coal. Jour. Coal Qual., 5:131-132

Sheat, A. W., (1984) Relationships between coking and other properties of Webb-Baynes coal. unpublished report, Coal Research Association of New Zealand, 46p.

Shibaoka, M., Ueda, S., and Russell. N. J., (1980) Some aspects of the behavior of tin (II)-chloride during coal hydrogenation in the absence of a solvent. Fuel 59:11-18

Sinninghe Damste, J. S., Rijpstra, W. I. C., Kock-Van Dalen, A. C., de Leeuw J. W., and Schenck, P. A., (1989a) Quenching of labile functionalised lipids by inorganic sulphur species: evidence for the formation of sedimentaty organic sulphur compounds at the early stages of diagenesis. Geochim. et Cosmochim. Acta., 53:143-155

Sinninghe Damste, J. S., Rijpstra, W. I. C., de Leeuw J. W., and Schenck, P. A., (1989b) The occurrence and identification of a series of organic sulphur compounds in oils and sediment extracts: II. Their presence in samples from hypersaline and non-hypersaline paleoenvironments and possible application as source, paleoenvironmental and maturity indicators. Geochim. et Cosmochim. Acta., 53:123-141

Sinninghe Damste, J. S., Eglington, T. I., de Leeuw J. W., and Schenck, P. A., (1989c) Organic sulphur in macromolecular sedimentary organic matter: I. Structure and origin of sulphur containing moieties in kerogen, asphaltenes and coal as revealed by flash pyrolysis. Geochim. et Cosmochim. Acta., 53:873-889

Spears, D. A., and Kanaris-Sotiriou, R, (1979) A geochemical and mineralogical investigation of some British and other European tonsteins. Sedimentology, no.3, 26:407-425

Staub, J. R., and Cohen, A. D., (1978) Kaolinite-enrichment beneath coals: A modern analog, Snuggedy swamp, South Carolina. Jour. Sed. Petrol., 48:203-210

Staub, J. R., and Cohen, A. D., (1979) The Snuggedy swamp of South Carolina: A back-barrier estuarine coal-forming environment. Jour. Sed. Petrol., 49:133-144

Stone, I. J., and Cook, A. C., (1979) The influence of some tectonic structures upon vitrinite reflectance. J. Geol., 87:497-508

Stout, S. A., Spackman, W., Boon, J. J., Kistemaker, P. G., and Bensley, D. F., (1989) Correlations between the microscopic and chemical changes in wood during peatification and early coalification: a canonical variant study. Int. J. Coal Geol., 13:41-64

Strauss, P. G., Russell, N. J., Bennet, A. J. R., and Atkinson M. C., (1976) Coal petrography as an exploration aid in the West Circum-Pacific. In: W. L. G. Muir (ed.), Coal Exploration, Proc. 1rst Internat. Coal Exploration symposium. Miller-Freeman, San Francisco, p.401-443

Suggate, R. P., (1956a) Air drying of coal. New Zealand J. Sci. Tech., B38:139-148

Suggate, R. P., (1956) New Zealand coals. Nature, 178:757

Suggate, R. P., (1959) New Zealand Coals. New Zealand Department of Scientific and Industrial Research, Bull. 134, 113p.

Suggate, R. P., (1974) Coal ranks in relation to depth and temperature in Australian and New Zealand oil and gas wells. N.Z. Jour. Geol. Geophys. 17:149-167

Suggate. R. P., (1982) Low rank sequences and scales of organic metamorphism. Jour. of Petrol. Geol., 4:377-392

Suggate, R. P., (1990) Variability in type III organic matter at the initiation of diagenesis. In: V. F. Nuccio and C. E. Barker (eds) Application of Thermal Maturity Studies to Energy Exploration. Rocky Mountain Section, SEPM, p.45-52

Suggate, R. P., and Lowery, J. H., (1982) The influence of moisture content on vitrinite reflectance and the assessment of maturation of coal. N.Z. Jour. Geol. Geophys., 25:227-231

Suhr, N. H., and Gong, H., (1983) A data base for the analysis of compositional characteristics of coal seams and macerals, Final report - Part 3, Some procedures for the chemical and mineralogical analysis of coals. (DOE-30013-F3), document prepared for the U.S. Dept. of Energy, Contract DE-AC22-80PC30013, 42p.

Sykes, R., Suggate, R. P., and King, P. R., (1991) Timing and depth of maturation in southern Taranaki basin from reflectance and Rank (S). NZ Oil Exploration Conf. 15-18 September, Christchurch. preprint, 35p.

Tateoka, M., (1990) Recent trends in and future outlook for cokemaking technology in the Japanese steel industry. Proc., Sixth International Iron and Steel Congress. 21-26 October, Nagoya, Japan., vol. 2, p.186-194

Taylor, E., and McKenzie, (1926) Base exchange and its bearing on the origin of coal. Fuel, 5:195-202

Taylor, G. H., and Liu, S. Y., (1987) Biodegradation in coals and other organic rich rocks. Fuel, 66:1269-1273

Taylor, G. H., (1991) Reflections on reflectance. 25th Newcastle Symposium, Advances in the Study of the Sydney Basin, 12-14 April, Newcastle NSW, p.222-229

Tegelaar, E. W., de Leeuw, J. W., Derenne, S., and Largeau, C., (1989) A reappraisal of kerogen formation. Geochim. Cosmochim. Acta., 53:3103-3106

Teichmüller, M., (1974) Generation of petroleum-like substances in coal seams as seen under the microscope. In: B. Tissot and F. Bienner (eds) Advances in Organic Chemistry 1973, Editions Technip, Paris, p.379-407

Teichmüller, M., (1982) Origin of the petrographic constituents of coal. In: E. Stach, M.-Th. Mackowsky, M. Teichmüller, G. H. Taylor, D. Chandra, and R. Teichmüller (eds), Stachs Textbook of Coal Petrology, 3rd edition., Gebruder Borntraeger, Stuttgart, p.219-294

Teichmüller, M., (1982b) Fluoreszenzmikroskopische Anderungen von Liptiniten und Vitriniten mit zunehmendem Inkohlungsgrad und ihre Beziehungen zu Bitumenbildung und Verkokungsverhalten. Geologisches Landesamt Nordhein-Westfalen, Krefeld 119p. (in german, english translation by N. Bostic, special TSOP publication 1)

Teichmüller, M., (1989) The genesis of coal from the viewpoint of coal petrology. Int. J. Coal Geol., 12: 1-87

Teichmüller, M., and Teichmüller, R., (1982) Fundamentals of coal petrology. In: E. Stach, M.-Th. Mackowsky, M. Teichmüller, G. H. Taylor, D. Chandra, and R. Teichmüller (eds) Stachs Textbook of Coal Petrology, 3rd edition. Gebruder Borntraeger, Stuttgart, p.5-82

Teichmüller, M., and Teichmüller, R., (1982b) Relations between coalificationb and paleogeothermics in Variscan and Alpidic foredeeps of Western Europe. In: G. Buntebarth and L. Stenega (eds) Paleogeothermics - Evaluation of Geothermal Conditions in the Geological Past. Springer-Verlag, Berlin, p.53.

Teichmüller, M., and Durand, B., (1983) Fluorescence microscopical rank studies on liptinites and vitrinites in peat and coals, and comparisons with results of the rock-eval pyrolysis. Int. J. Coal Geol., 2:197-230

Thomas, J. Jr. and Damberger, H. H., (1976) Internal surface area, moisture content and porosity of Illinois coals: variations with coal rank. Illinois Geol. Surv. Circ. no.493, 38p.

Thompson, D., (1986) ISO/ASTM differences. unpubl. manuscript, accompanying presentation, Int. Coal Testing Conf., 11-13, Feb., Lexington, Kentucky, 20p.

Thompson, R. R., and Benedict, L. G., (1974) Vitrinite reflectance as an indicator of coal metamorphism for cokemaking. In: R. R. Dutcher, P.A. Hacquebard, J. M. Schopf, and J. A. Simon (eds) Carbonaceous materials as indicators of metamorphism. GSA special paper 153, p.95-108

Tilley, B. J., Nesbitt, B. E., and Longstaffe, F. J., (1989) Thermal history of Alberta Deep Basin: Comparative study of fluid inclusion and vitrinite reflectance data. A.A.P.G. Bull., no.10, 73:1206-1222

Ting, F. T. C., and Spackman, W., (1975) The coal lithotype concept and seam profile. Compte Rendue, 7th International Congress on Carboniferous Stratigraphy and Geology, Krefeld, Germany, 4:279-283

Ting, F. T. C., (1988) Letter to the editor., The Society for Organic Petrology Newsletter, no.4, 5:4-5

Triplehorn, D., and Bohor, B., (1986) Volcanic ash layers in coal: Origin, distribution, composition, and significance. In: K. S. Vorres (ed), Mineral Matter and Ash in Coal. A.C.S. symposium series no. 301, p.90-99

Valia, H. S., (1989) Prediction of coke strength after reaction with CO_2 from coal analyses at Inland Steel Company. Transactions ISS (Iron and Steelmaker), May:77-89

Valia, H. S., (1990) Effects of coal oxidation on cokemaking. paper presented at 49th Ironmaking Conference, 26-28 March, Detroit, 11p.

Van Gijzel, P., (1979) Manual of the Techniques and Some Geological Applications of Fluorescence Microscopy. Am Assoc. of Stratigraphic Palynologists, 12th annual meeting, Oct. 29 - Nov. 2, Core Laboraratories Inc., Dallas TX, 55p.

Van Krevelen, D. W., (1950) Graphical-statistical method for the study of structure and reaction processes of coal. Fuel, 39:269-284

Van Krevelen, D. W., (1961) Coal. Elsevier, New York, 514p.

Veto, I., and Dovenyi, P., (1986) Methods for Paleotemperature estimation using vitrinite reflectance data: a critical evaluation. In: G. Buntebarth and L. Stenega (eds) Paleogeothermics - Evaluation of Geothermal Conditions in the Geological Past. Springer-Verlag, Berlin, p.105-118

Waddell, C., Davis, A., Spackman, W., and Griffiths, W. C., (1978) Study of the Interrelationships Among Chemical and Petrographic Variables of United States Coals. Penn State Univ., Coal Research Section, Tech. Rept 9, prepared for U.S. Dept. of Energy, contract EX76-C-01-2030, 239p.

Walker, A. L., McCulloch, T. H., Petersen, N. F., and Stewert, R. J., (1983) Discrepancies between anomalously low reflectance of vitrinite and other maturation indicators from an Upper Miocene oil source rock, Los Angeles Basin, California. A.A.P.G. Bull., 67:565

Ward, C. R., (1978) Mineral matter in Australian bituminous coals. Proc. Austalas. Inst. Min. Metall., 267:7-25

Ward, C. R., (1984) Coal Geology and Coal Technology, Chapter 2, Chemical analysis and classification of coal, Blackwell Scientific, Melbourne, p.40-73

Ward, C. R., (1986) Review of mineral matter in coal. Australian Coal Geology, 6:87-110

Ward, C. R., (1991) Mineral matter in low rank coals and associated strata of the Mae Moh basin, northern Thailand. Int. J. Coal Geol., 17:69-93

Weaver, S. D., (1987) The preparation of fusion beads. unpublished laboratory method, X-ray Spectrometry Laboratory - Department of Geology, University of Canterbury) 5p.

Wellman, H. W., (1952) Interpretation and discussion of analyses (ch.12) In. Gage (ed) The Greymouth Coalfield, N.Z.G.S. Bull. 45, 232p.

Wenger, L. M., and Baker, D. R., (1987) Variations in vitrinite reflectance with organic facies - examples from Pennsylvanian cyclothems of the midcontinent, USA. Org. Geochem., 11:411-416

Williams, E. G., and Keith, M. L., (1963) Relationship between sulfur in coals and the occurrence of marine roof beds. Econ. Geol., 58:720-729

Winegartner, E. C., and Rhodes, B. T., (1975) An empirical study of the relation of chemical properties to ash fusion temperatures. Journal of Engineering for Power, Trans. ASME, series A, 97:395-406

Wolf, M., Wolff-Fischer, E., Ottenjann K, Hagemann H. W., (1983) Fluorescence properties of vitrinites of selected Sarr and Ruhr coals. Minutes of the 36th ICCP meeting Comm. 3, Oviedo Spain, 14p.

Zeiss Publication (A41-825.8-e) Reflection Microscope Photometry, Application, Measurements on Coal Samples. Carl Zeiss, D-7082 Oberkochen, Germany 36p.

Zodrow, E. L., and McCandlish, K., (1978) Hydrated sulfates in the Sydney coalfield, Cape Breton, Nova Scotia. Canadian Mineralogist, 16:17-22

APPENDIX A
PREPARATION OF POLISHED SPECIMENS

A.1 PELLET PREPARATION

A 500 g split of coal at ~3 mm topsize was stage ground to pass a BS 16 mesh (1 mm) sieve using a mortar and pestle, hand operated coffee grinder, or a micro hammer mill. Where less than 500 g was available the entire sample was ground. Removal of the screens from the micro hammer mill and a slow speed setting minimized the generation of fines. After several passes through the mill with the screens removed, a 3 mm screen was inserted and the remaining hard fraction was efficiently reduced to minus 1 mm. Samples from drillhole 7, drillhole 1494 and the stockpile weathering series were frozen prior to sample preparation. Freezing allowed damp samples to be processed without drying. A micro riffle was used to split about 50 g of -1 mm coal for preparation of polished coal specimens. To allow splitting some samples were dried by spreading the coal in a thin (~2 mm) layer on trays that were placed in a 35-40°C gravity oven for about 1 hour.

Two or more polished, 32 mm diameter coal specimens (pellets) were prepared from each 50 g sample in general accordance with ASTM method D2797-85. Deviations from the standard include:

(1) a minus 1mm particle size,

(2) 7 pressure cycles followed by a 350 kgf/cm2 briquetting pressure, and,

(3) the use of 1 micron diamond grinding compound for rough polishing and colloidal silica final polishing.

The metal molds and pellet press were made to specification. Araldite K-146 epoxy (Ciba-Geigy) was used a binder. Dry film teflon spray (Rocol Ltd. RC-3202) was use as a mold release agent.

A.2 GRINDING AND POLISHING THE PELLET SURFACE

The polishing method used was modified from methods described by ASTM D2797-85, Harrison (1990) and Levine (1989). A LECO Corp. AP-50 with a VP-

150 polishing attachment was used for grinding and polishing the specimens. The lack of success with alumina polishing agents described in ASTM method D2797-85 is thought to be due to the inability of the polishing machine to meet specifications (35 lbs force at 150 rpm).

Four or six pellets were secured in the specimen holder. Care was taken to ensure that the pellets were flush with the pressure plate. Optimum results were obtained where only four pellets were polished at a time. Except where noted all grinding and polishing steps were accomplished with the instrument settings adjusted to 150 rpm and 15 lbs of force; the duration of each grinding and polishing step was about two minutes. A fast flow of water was directed to the lap during grinding and a slow drip during polishing. Because a single machine was used for all polishing and grinding steps the polishing attachment and basin were cleaned (with a damp cloth) between the grinding and polishing stages.

The platens were prepared for grinding and polishing as follows. The brass wheel was dried to ensure that the adhesive backed paper disks adhered. Air bubbles trapped under the paper disks were avoided by pressing from the centre of the disk outward when these adhesive disks were fixed to the platen. The 180 and 320 grit papers were used several times but 400 and 600 grit papers were replaced after every use. Adhesive paper disks (Pan K) used for rough polishing were used 10 or more times and replaced when rough to the touch. Silk fabric used for final polishing was stretched over the metal platen and secured with a metal retaining band. Where specimens were prepared for fluorometric analysis no detergent was added to the ultrasonic cleaning bath; otherwise one or two drops of "Sunlight" dish-washing detergent was added to the bath.

A.2.1 Rough Grinding

The purpose of rough grinding is to produce a relatively undeformed flat surface and ensure that all of the specimens are co-planer. With machine polishing, every time the pellets are releveled in the holder the rough grinding step must be repeated to ensure that the specimens are co-planer. Rough grinding

was accomplished using 400 grit paper. In situations where more than 1 mm of the specimen surface was to be removed, preliminary grinding was accomplished with 180 to 320 grit paper followed by releveling and 400 grit rough grinding. Grinding times were adjusted according to the nature of the coal; relatively friable (high hardgrove index) Stockton/Webb coals ground quickly and rough grinding times of 30 to 60 seconds were common. The sample holder and specimens were rinsed under a strong flow of tap water prior to fine grinding.

A.2.2 Fine Grinding

The purpose of fine grinding is to produce a relief-free surface with a minimum amount of deformation. Fine grinding was accomplished on a 600 grit (~17 micron nominal size) silicon carbide paper with a fast flow of water directed to the lap. Because the 600 grit papers rapidly wore and clogged they were used once and discarded. The sample holder and specimens were ultrasonically cleaned prior to polishing.

A.2.3 Rough Polishing

The purpose of rough polishing is to remove surface deformation caused by fine grinding and to prepare the surface for final polishing. Loose grits rotate under the specimen and remove material by fracturing rather than direct abrasion. Consequently, polishing causes relief to develop and excessive polishing should be avoided (Dillinger, 1981). Furthermore, Bostic (1986) observed more numerous "wild scratches" upon prolonged polishing.

Rough polishing was accomplished using LECO Pan-K paper impregnated by a 2 second burst of 1 micron, medium concentration aerosol diamond (Leco part no. 810-504). A slow water drip was directed to the lap during polishing and a fast flow of water was directed to the lap during the final 5 seconds of polishing. The sample holder and specimens were ultrasonically cleaned prior to final polishing.

A.2.4 Final Polishing

The purpose of final polishing is to remove the deformation caused by rough polishing and to provide a scratch free surface. About 5 ml of colloidal silica (Leco part no. 812-110-300) was poured on the damp silk lap prior to polishing. During the course of final polishing about five additional ml of colloidal silica were incrementally added to lap and a slow water drip was maintained. The lap was flushed with water during the last 5 seconds of polishing. After polishing the sample holder and specimens were immediately plunged into the ultrasonic bath to disperse any remaining colloidal silica. Finally, the specimens were rinsed with tap water and dried by blotting with tissue paper or with a blast of filtered compressed air.

APPENDIX B
REFLECTANCE ANALYSIS

This appendix describes the instrument and calibration method used for reflectance analysis of coals and carbonized coals examined in this thesis. In addition to recording the reflectance values from the coal specimens, reflectance values determined on the calibration standards were routinely recorded every time the microscope was calibrated over a six month period. These data are used to assess the precision of the reflectance calibration.

B.1 INSTRUMENT SET-UP

Reflectance analyses on coal specimens were undertaken in general accordance with ISO 7404/5 using a Zeiss UMSP 50 microscope. The microscope was set-up to measure the mean maximum reflectance of vitrinite. A coated, 40X/0.85NA Pol objective (Zeiss part no. 46-20-09-9901) with Zeiss immersion oil (n_e=1.518 at 23 °C) was used for all measurements. Room temperature was maintained near 19 °C. The temperature of the oil under the objective was not measured but was probably close to 23 °C (Alpern, 1971). Instrumental settings included a polariser set to 45°, a 2.8 um diameter measuring spot (.16 mm setting on turret), and a 7.7 um diameter luminous field stop (.16 mm pinhole) adjusted to be parfocal with the image plane. The tungsten-halogen lamp was set to 12V and a heat reflection filter placed in the incident light path. The grating monochrometer was disengaged and an interference filter with a centre wavelength of 546 nm and a 25 nm half band width was used to isolate the measurement wavelengths. Because this filter was inserted below the oculars the room lights were turned off to avoid stray light contributing to the measured signal. The photometer amplification was adjusted to about 380 on the index dial and the time constant step set at 7 (0.16 seconds). The 100 point adjustment (1, 10, 100, and 1000 selectable settings) was set to the 100 position. At these settings the dark current was about 014.1 or 7% of the full scale (100% = 199.9). Data acquisition was accomplished using an IBM compatible computer, custom built computer interface, and custom software. A computer integration time of

1.5 seconds and a computer multiplication factor of 0.01 were selected. The raw data were recorded on a floppy disk.

B.2 CALIBRATION

A yittrium aluminium garnet standard (YAG, Figure B.1) was used for primary calibration. Calibration on the YAG was undertaken by manual adjustment of the gain to obtain a photometer signal to equal 0.921% reflectance; the dark current signal was simultaneously suppressed to equal zero. The manufacturer reports that the reflectance of the YAG is 0.9213% (where $\lambda = 546$ nm, and $n_{oil} = 1.518$). The instrumental set-up allowed reflectance values to be recorded to three decimal places of significant precision (0.001). Although this level of recorded precision is not required for routine analysis of coal specimens it was necessary for the meticulous examination of the calibration standards described below.

After calibration three areas on the YAG standard were measured and the values recorded mechanically. To validate the calibration the reflectance of the Zeiss sapphire standard as well as one of the glasses in the Zeiss 5-glass standard were recorded (see Figure B.1). Three readings from the centre region of the sapphire and three reading from the centre region of a selected glass were recorded. The calibration was discarded where the average reflectance of the sapphire, glass 3, or glass 4 deviated by more than .005 from the current average values determined (in this study) for these standards. In these rare instances the deviation was usually due to bubbles or dirt in the immersion oil (usually visible in the back image plane of the berek prism upon removal of the ocular) and was corrected by wiping with lens tissue. Less commonly the problem was remedied by re-leveling of the standard. Whatever the cause, where this problem occurred the microscope was recalibrated using the YAG standard until the sapphire and selected glass standard agreed within the prescribed (±0.005) limit. After recording the reflectance values from the standards the coal specimen was analysed. Calibration was accomplished at the beginning of the analysis, and

near 33 and 66 cumulative readings. Multiple specimens were used where significantly more than 100 readings were recorded

The standards were oriented as shown in Figure B.1 with the front of the standard towards the operator during calibration. The front of the standards also faced the operator on the leveling press used to fix the standards to glass slides with plasticine. None of the standards were rotated during calibration.

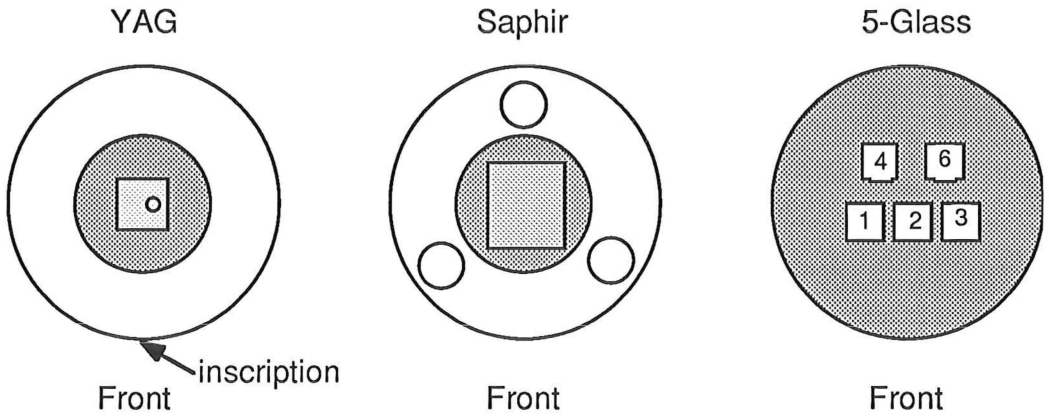

Figure B.1 Illustration of the reflectance standards used in this study: YAG, yittrium aluminium garnet standard (McCrone Research); Saphir, sapphire standard (Zeiss part no. 47-42-54); and 5-glass standard, (Zeiss part no. 41-42-50)

The standards were cleaned every week by gentle repeated wiping with cotton balls saturated with a fresh, dilute solution (about 1 ml detergent to 100 ml water) of "photoflow" detergent and rinsing under flowing water. The standards were stored in a desiccator when not in use.

B.3 Reflectance of Calibration Standards

Table B.1 shows the average reflectance values determined for the primary standard (YAG) and five secondary standards. Also shown are the number and standard deviations of the data that these averages are based on. The readings were routinely recorded upon calibration for reflectance analyses of coal specimens over a six month period. Table B.1 also lists some calculated and determined reflectance values reported by the manufacturer. All of the measurements determined in this study that are reported in Table B.1 were undertaken using polarized light.

TABLE B.1

REFLECTANCE VALUES FOR STANDARDS USED IN THIS STUDY

Standard	Determined, Relative to YAG, (this study)	Standard Deviation (this study)	Number of Readings (this study)	Calculated Value (provided by manufacturer)	Determined Value (provided by manufacturer)
YAG	(0.921)	0.001	563		0.9213
Sapphire	0.599	0.002	560		0.579
glass #2	0.498	0.003	23	0.4958	0.506
glass #3	0.939	0.004	269	0.9207	0.940
glass #4	1.020	0.004	167	1.0085	1.025
glass #6	1.692	0.006	119	1.6618	1.672

Table B.1 shows that the sapphire standard reported the lowest standard deviation (0.002). The low standard deviation for this standard was obtained by measuring in the centre area of the gem and indicates the homogeneous nature of the sapphire surface in this region. The reported value for this standard is lower (-0.02) than the value determined in this study.

Based on 23 readings, the reflectance of glass 2 is shown in Table B.1 to be close to both the calculated and determined values reported by the manufacturer. Glass 2 is badly scratched. The reflectance values of glass 3 and glass 4 determined in this study are close to the determined values provided by the manufacturer. Glass 6 showed a comparatively high standard deviation of 0.006. In addition, the determined reflectance of glass 6 relative to the YAG standard is higher than both the calculated and determined reflectance values reported by the manufacturer.

B.3.1 Discussion

The results reported here are valid only for the microscope set-up that has been described and may have been different had the analyses been undertaken in non-polarized light. For example, after primary calibration on the YAG standard. the mean random reflectance of the sapphire standard (n=12) was found to be 0.007% lower than the mean maximum reflectance value determined with polarized light. Conversely, based on the same set of 12 readings the mean random reflectance of glass 3 was the same as the mean maximum reflectance of glass 3 reported in Table B.1.

The relatively large standard deviations observed for the glass standards compared to the Zeiss sapphire suggests that the surfaces of the glass standards are more heterogeneous than the sapphire mineral standard. Accordingly, Newman (pers. comm. 1990) advises calibration on the same area of a given glass surface where diagnostic surface scratches enable precise location of the measurement area. This approach should improve the precision of calibration since variation due to the heterogeneity of the glass surface is minimized.

The manufacturer of the glass standards provides both calculated and determined reflectance values. With respect to these values Zeiss Publication (A41-825.8 p.13) states;

> "With glass- prism standards one must accept the fact that : (a) the actual reflectances differ from the values calculated ... because the reflecting surface has to be worked (cut, ground, and polished) so that it has another refractive index than the bulk material ... "

Furthermore glasses are easily tarnished especially in the presence of moisture. The reflectance values of the glasses determined in this study are closer to the manufacture's determined values than the generally lower calculated values.

B.3.2 Precision

As expected, the average reflectance of the YAG was 0.921 since an effort was made to calibrate the system to this value. The YAG standard deviation of 0.001 is a fair approximation of the "instrumental" precision attained under the conditions used in this study; instrumental precision is considered here to be errors due to inherent optical and electronic aberrations of the microscope. If the sapphire is considered to present an absolutely homogeneous reflecting surface then the standard deviation of the sapphire (0.002) is a fair approximation of the precision of calibration; The precision of calibration is considered here to include both the instrumental variability as well as additional errors associated with the measurement process (i.e., focus, temperature). The "analytical" precision (repeatability) will include additional errors associated with the measurement of the specimen and cannot be estimated by the data presented in this study.

A good approach to improve the precision of calibration is described by Ottenjann (1986). Rather than using a single, manually adjusted photometer setting for primary calibration Ottenjann's laboratory uses the average of three readings to calculate a calibration factor for the analysis. This mathematical approach eliminates the error associated with manual adjustment of the photomultiplier and the use of three readings rather than a single measurement for calibration reduces error due to instrumental aberrations. Another advantage of a mathematical rather than manual calibration is that it potentially allows the full working range of the photomultiplier to be used. For example, the YAG calibration standard is reported to four significant digits (0.9213) but with direct calibration, as done in this study, only three digits are considered (i.e., the system is calibrated directly to 0.921). If the gain is increased a small amount to provide an output signal with four digits, for example 1.116, multiplication of the raw recorded values by a correction factor (in this instance 0.82554) will allow the precision to be expressed to four significant digits rather than three.

Precision can also be improved by reducing instrumental noise. This can be accomplished (as was done in this thesis) by using an interference filter rather than a grating monochrometer that typically provides a lower light throughput. Provided a high quality transmission filter is used the signal to noise ratio will improve for weakly reflecting materials. It is worth noting here that blocking outside the bandpass is a more important filter characteristic than transmission to reduce the signal to noise ratio for spectral fluorescence microscopy. Alternately a modulated (chopped) light source in conjunction with an amplifier tuned to the frequency of the modulated light will reduce instrumental noise. Attention should also be given to the size of the measuring spot. The 2.7 micron diameter spot size used in this thesis is smaller than the 5 to 10 micron diameter spot size recommended in various standards. The small spot size is useful for many New Zealand coals which lack telovitrinite but has the disadvantage of reducing the light reaching the photomultiplier.

As noted above, the results of this study are only valid for the instrumental conditions that were used and can not be validly used to assess the accuracy of the reflectance values provided by the manufacturers for the various standards. Although the data do provide a means to assess the precision of calibration attained they do not provide a measure of the analytical precision or accuracy of the reflectance analyses undertaken in this thesis. A summary of some reported repeatability and reproducibility values are listed in Table B.2 and provide an indication of the precision and accuracy of reflectance analysis.

TABLE B.2
REPEATABILITY AND REPRODUCIBILITY VALUES REPORTED FOR REFLECTANCE ANALYSIS

Repeatability [1]	Reproducibility [2]	Number of Readings	Standard Method
0.03% [3]		30	AS 2486-1981
0.015% [3]		100	AS 2486-1981
	0.07 (Ro max) [3]	not stated	AS 2486-1981
	0.09 (Ro rand) [3]	not stated	AS 2486-1981
not stated	not clearly stated [4]	100	ASTM D 2798-85
0.06%	0.08 (Ro max & rand)	100 or more	ISO 7404/5-1984E

Notes: 1) Repeatability is the maximum difference between two analyses performed by the same operator on the same specimen using the same apparatus below which 95% of such differences are expected to lie.

2) The reproducibility is the maximum difference between two analyses performed by different operators on different subsamples using different apparatus below which 95% of such differences are expected to lie.

3) Calculated from an inter-laboratory exercise involving 10 Australian laboratories for a single seam coal.

4) The ASTM standard expresses the precision of reflectance analysis as: "[analyses] shall be reproducible within ±0.02 actual reflectance in percent." The standard also notes that the method is not a compliance or referee test.

It seems likely that the calibration standards themselves are responsible for much of the variation between laboratories indicated in Table B.2. As shown in Table B.1 after calibration with the YAG standard the measured reflectance values of the secondary standards do not precisely agree with the values provided by the manufacturers and typically differ by about ±0.02. This observation suggests that

the relative accuracy of calibration standards used in different laboratories limits the reproducibility of reflectance analysis.

B.4 REFLECTANCE ANALYSIS OF CARBONIZED COALS

Calibration for reflectance analyses on the carbonized coals was undertaken in the same manner as for reflectance analysis of vitrinite except that a double grating monochrometer was used to isolate the measurement wavelengths (546 nm centre wavelength and 20 nm half bandwidth) rather than an interference filter. This was done to help reduce the light flux from the highly reflective carbons. For reasons discussed in section 4.4.1, a 5.5 um diameter measurement spot was used rather than the 2.8 um diameter spot used for reflectance analysis of the coals.

B.4.1 Neutral Density Filters

The reflectance values of the carbonized coals were about ten times greater than the available standards. To account for this difference a calibrated, coated neutral density filter with a transmission of 11.15% in the measurement bandpass was placed in the light path after calibration. This filter reduced the light flux from the specimen to a level comparable with that of the standard. The raw measurement values obtained on the carbon specimens were then multiplied by a correction factor of 8.9686.

B.4.2 The Effect of Temperature

Because the actual reflectance of the standard and the specimen are not similar the effect of temperature variation on the refractive index of the immersion oil may be significant. The Fresnel relationship for a non-absorbing substrate can be used to show that a 4 °C increase in the immersion oil temperature will increase the reflectance (at 546 nm) of the non absorbing YAG standard (n_S = 1.8403) by 0.008% absolute given an immersion oil with a refractive index of 1.5180 at 23 °C where dn/dt of the oil is 0.00033 °C. The Fresnel equation for non-absorbing substances is shown below.

$$R\%_{oil} = 100 \left(\frac{(ns-nm)}{(ns+nm)}\right)^2$$

where:
- $R\%_{oil}$ is the percent reflectance in oil of the specimen
- n_s is the refractive index of the specimen at specified wavelength, and;
- n_m is the refractive index of the immersion oil at the same wavelength and a specified temperature.

For measurement of vitrinite reflectance the effect of temperature variation of the immersion oil on the accuracy of the analysis is small since the reflectance of vitrinite (where absorption is negligible) will change in the same way as that of the standard. In the above example calibration to 0.921 on a standard with a reflectance of 0.929 will be compensated by an equivalent increase in the reflectance of non-absorbing vitrinite specimen. Problems arise where the absorbence of the specimen is significant as in the case of coals with more than 89% C or, of concern here, thermally altered coal. Beer's equation (shown below) can be used to calculate the effect of temperature variation in where absorption is significant.

$$R\%_{oil} = 100 \frac{(ns-nm)^2+ns^2k^2}{(ns+nm)^2+ns^2k^2}$$

where:
- $R\%_{oil}$ is the percent reflectance in oil of the specimen;
- n_s is the refractive index of the specimen at a specified wavelength;
- n_m is the refractive index of the immersion oil at the specified wavelength and temperature, and;
- k is the absorption index of the specimen at the specified wavelength.

With nominal values of $k = 1.975$ and $n_S = 0.44$ (obtained by Goodarzi and Murchison 1972, for a 900 °C carbonized bituminous vitrinite concentrate, a heating rate of 2.45 °C/hr and a 1 hour soak) the reflectance of the carbon will increase from 7.44 to 7.45 (0.0144% absolute) as the temperature of the immersion oil increases from 23 °C (n_m=1.5180) to 27 °C (n_m=1.5167). If the microscope is calibrated to a value of 0.921 (YAG reflectance at 23 °C) and an 11.15% transmission neutral density filter used to reduce the signal from the carbon, then the determined reflectance of the carbon at 27 °C will be about

0.06% (absolute) too low. This value is arrived at by multiplying the error of the calibration on the YAG (0.008) times the neutral density correction factor (8.9686) and then subtracting the compensating error (0.0144) due to the related increase in actual reflectance of the carbon.

B.4.3 Discussion

The calibration method used for the carbonized coal specimens illustrates the advantage of calibrated neutral density filters to extend the calibration range of available standards. Coated neutral density filters are recommended for this purpose because they provide a flat spectral transmission but tinted glass filters are also acceptable where the measurement bandwidth is small. Importantly, these filters must be individually calibrated over the wavelength region of interest, and must be kept scrupulously clean. Finally, if neutral density filters are used during calibration for measurement of specimens that have significant absorbance then the effect of temperature should be considered. However, based on the example given above, the effect of temperature variation is probably not a significant source of error in this study.

APPENDIX C
FLUOROMETRIC ANALYSIS

This section provides a general description of the microscope used for fluorometric analysis followed by discussion of specific instrumental and procedural details. The fluorometric analyses were accomplished with the Zeiss UMSP 50 microscope and in-house data acquisition system used for reflectance analyses (Appendix B). The instrument is shown in Plate C.1 where various components are numerically annotated; these components correspond to bracketed numbers that appear the text.

C.1 GENERAL DESCRIPTION

A lateral illuminator [1] was used to position the arc lamp close to the specimen. Excitation energy from a 100 watt Hg arc lamp [2] passed through a BG-38 heat filter and a 395-485 nm interference bandpass filter and was reflected to the specimen with a 520 nm dichroic reflector. The fluorescence emission was filtered through a 550-650 nm interference bandpass filter that functioned as both a barrier and measurement filter. Calibration was accomplished using a Wild Leitz masked uranyl glass standard that was arbitrarily assigned an intensity value of 100. Calibration was checked after every 50 readings. The measuring spot diameter was 9.4 um (0.63 mm on turret [3]) and the illuminated field diameter set at ~15 um (0.4 mm pinhole aperture). These diameters were measured using a Leitz, incident-light stage micrometer (part no. 335-563011). Individually calibrated neutral density filters were used to reduce the fluorescence intensity of the standard to levels comparable to those in coal. The photomultiplier gain [4] was adjusted according to the fluorescence characteristics of the specimen but usually was between 0.66 and 0.74 kV (300 and 400 settings on the index dial). The time constant [5] was maintained at 7 (0.16 seconds) and the 100 point adjustment [6] (adjustable to 1, 10, 100 and 1000 X settings) set to the 100 position. An integration time of 1.5 seconds and an appropriate calibration factor were entered into the data acquisition program. The specimen surface was continuously swept with nitrogen gas at a rate of 1.7 litres per minute

PLATE C.1 Microscope Used in Study

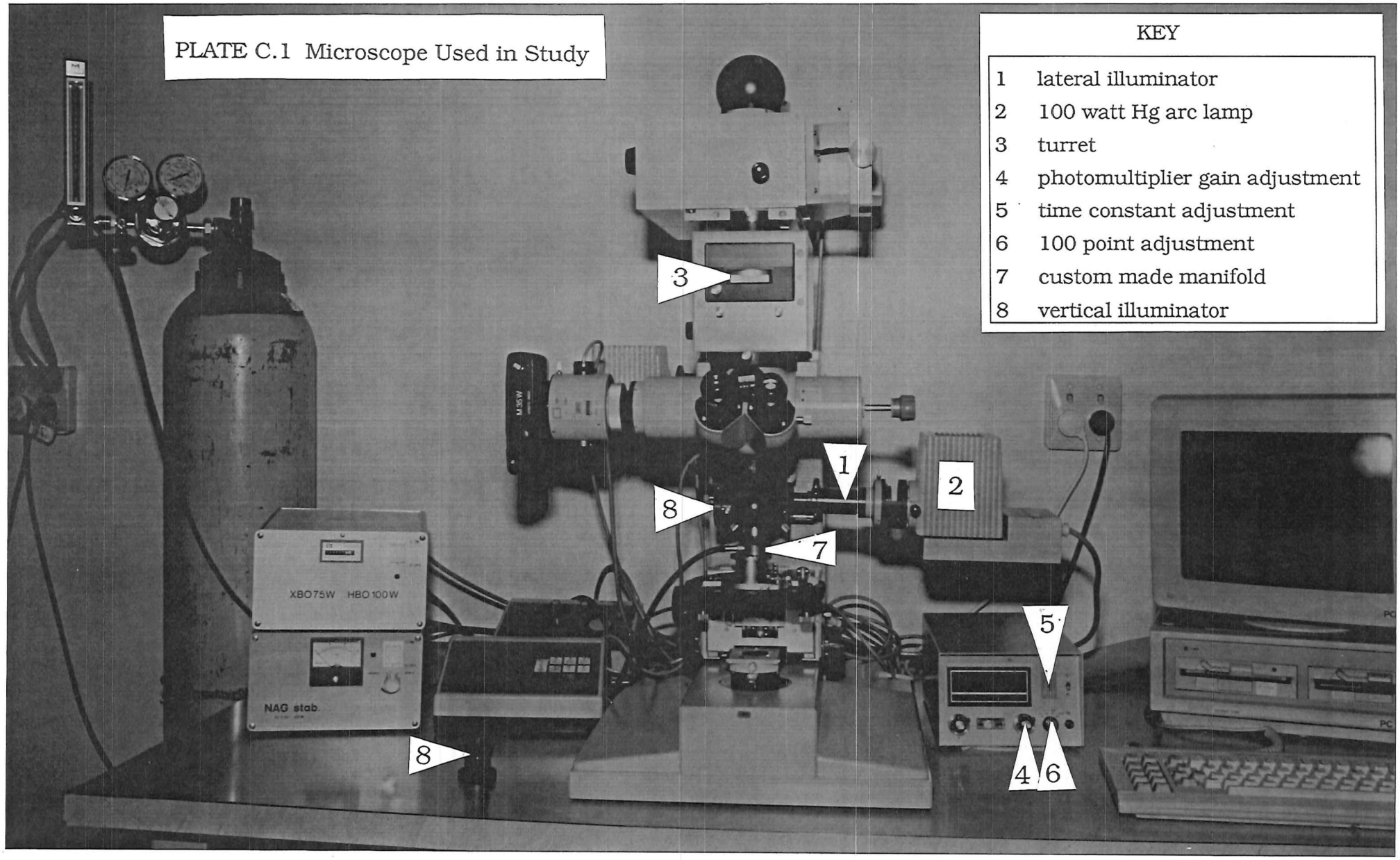

during the analysis. A custom made manifold [7] fitted to the dry, 40X/0.85NA Epiplan Pol objective was used to deliver nitrogen gas to the specimen surface. One hundred or more measurements were recorded for each analysis.

C.2 THE HG ARC LAMP

The nominal spectral intensity distribution of a 100 W Hg arc lamp is shown in Figure C.1 and compared with the nominal spectral emission of a 100 watt tungsten-halogen lamp. The comparison shows the relatively high intensity and characteristic emission lines of the Hg arc lamp (note the distinctive 365 nm Hg line is off the figure scale). More importantly it shows strong Hg emission peaks at 405 and 436 nm within the 395-485 nm excitation filter bandpass. Thus the character of the excitation energy varies according to both the spectral intensity distribution of the arc lamp and the selected bandpass filter.

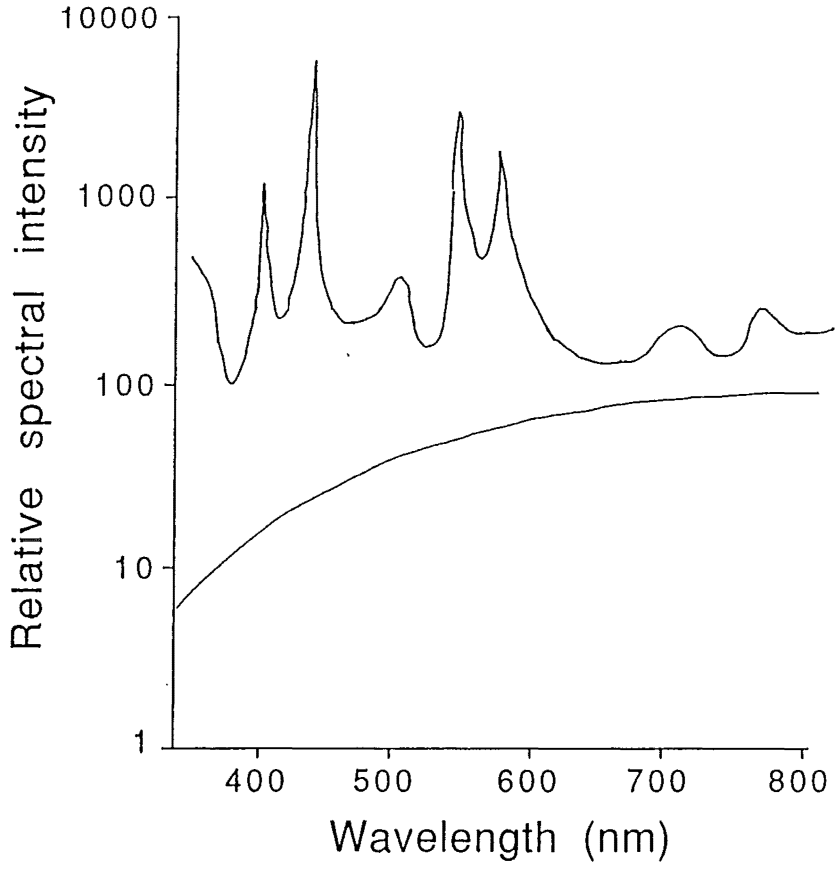

Figure C.1 Comparison of the spectral fluorescence intensity of a 100 watt mercury arc lamp and a 100 watt tungsten-halogen lamp (modified from Zeiss Instruction Manual A41-825.8-e).

The popularity of the 100 watt Hg arc lamp for fluorescence microscopy is due to the high luminous density provided by this lamp. Luminous density is not solely a function of the total luminosity of a lamp, but also varies according to the size of the arc. The small (.25 x.25 mm) arc of the 100 watt Hg lamp allows a larger luminous flux to be transmitted through the illumination side optics of the microscope than is possible with brighter lamps that have larger arcs.

Although the high luminous density of the 100 watt Hg arc lamp is advantageous, the emission of arc lamps is not as steady as that from filament type lamps. The tendency of the arc to switch paths between the anode and the cathode causes the energy reaching the sample to fluctuate. This situation (lamp flicker) hinders precise calibration and can result in substantial variation in the fluorescence intensity from a specimen. Qualitative observations showed flickering to occur more frequently as the lamps approached their rated life (~200 hours). During the first 50 hours of operation flickering was rare. Thereafter it occurred more frequently and typically was first observed after about 6 hours of continuous burning. As the lamps aged the time between ignition at the beginning of a days work and the onset of flickering decreased. These are general observations; some lamps provided 150 hours of useful service and others became troublesome after 80 hours of use.

General rules for safe and efficient operation of arc lamps are provided by the manufacturer. Four important rules are: 1) never re-ignite a lamp until it has cooled, 2) never switch off a lamp until it has burned for more than 30 minutes, 3) never overlap the primary and mirror image of the arc, and 4) ensure that the mirror image and the primary image are in the same focal plane. Installation of the arc lamp in accordance with the manufacture's instructions assures solid electrical contacts and the absence of physical stress on the lamp. These precautions minimize the risk of an explosion and release of mercury vapour.

Procedures recommended by the microscope manufacturer for alignment of the lamp should be followed to maximize the optical flux reaching the specimen. Sacrificing even field illumination in order to focus more energy on the

measurement spot can significantly increase fluorescence emission. This approach should be used with caution since tight focusing of the arc on the measurement area makes the system especially sensitive to the "flickering" condition described above.

C.3 FILTER CHARACTERISTICS

Figure C.2 shows the spectral characteristics of the excitation filter, dichroic reflector and measurement filter used in this study. These filters were made to specification by Omega Optical Inc. The Omega Optical Inc. (1986) catalogue provides a concise, practical discussion of optical filters and filtering strategies for quantitative measurement of light.

The selection of appropriate excitation filters for use in this study was based on early studies that reported fluorescent emission of vitrinite. Early observations of fluorescent vitrinite were accomplished using BG 12 glass excitation filters (Teichmüller 1974, Creaney *et al.*, 1980, Teichmüller, 1982b, Wolf *et al.*, 1983) rather than the shorter wavelength UG glass filters used for spectral fluorescence studies. Diessel (1985) used even longer wavelengths (450-490 nm) isolated with a high performance interference filter to induce measurable fluorescence intensity of both vitrinite and inertinite. The use of longer wavelength, interference type excitation filters was an important step in the development of fluorometric analysis. Interference filters offer three significant advantages compared to coloured glass filters, including: 1) high transmission efficiency in the bandpass region, 2) significantly improved blocking outside the bandpass region, and 3) a wider range of filters with different centre wavelengths and bandpass widths. Most filter sets offered by microscope manufacturers are designed for specific applications in the large biological market. Rather than select a filter set designed for a biological application the filters used in this study were custom made to specification. The excitation filter selected for use has a centre wavelength of 440 nm and a 90 nm half band pass. The 90 nm excitation bandpass is wider than those used for most biological applications and greatly increases the amount of energy directed to the specimen. The higher energy is

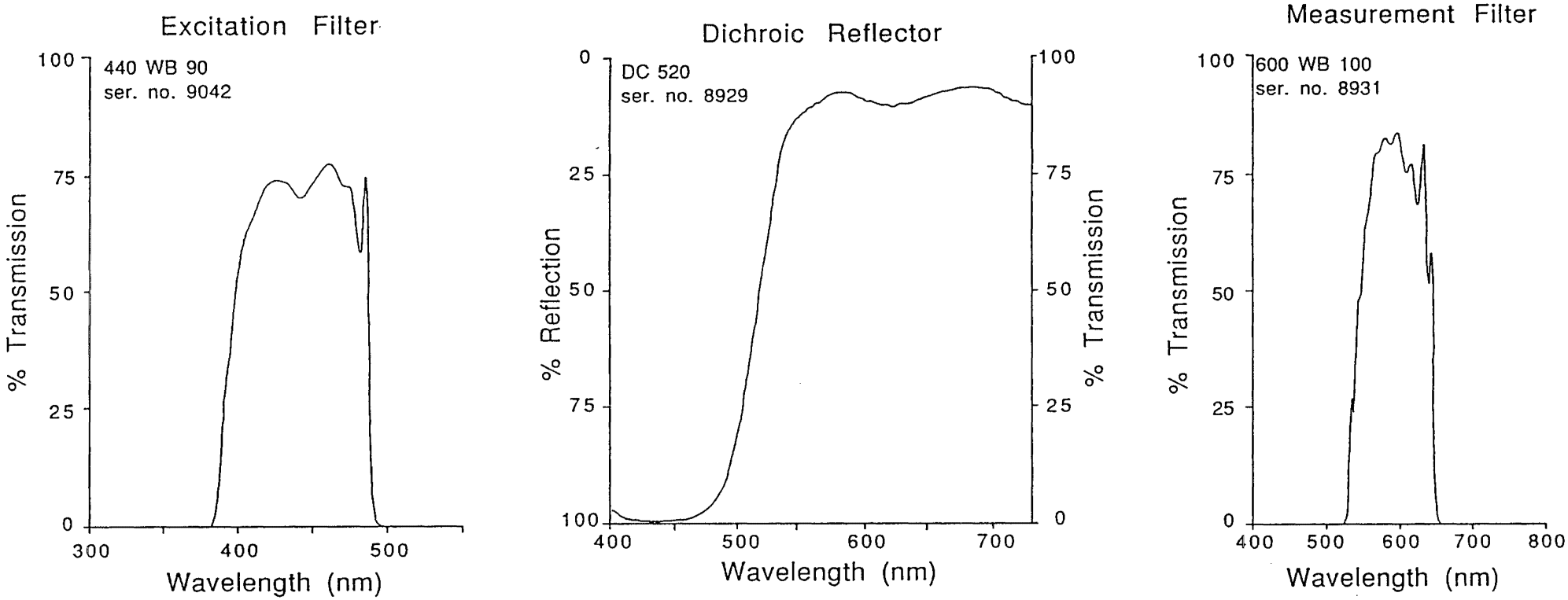

Figure C.2 Spectral characteristics of the filter set used for fluorometric analysis. The figures were constructed from individual calibration charts provided with each filter by Omega Optical Inc.

desirable to induce measurable fluorescence in weakly fluorescent macerals such as vitrinite and inertinite. The 90 nm bandwidth approaches the maximum width for dichroic filters where good blocking outside the bandpass region is required.

The use of a dichroic illuminator is essential for fluorometric analysis because it efficiently reflects the excitation wavelengths and transmits the longer wavelength fluorescence emission. These filters more than triple fluorescence emission compared to conventional (50% reflection - 50% transmission) half silvered reflectors. Dichroic reflectors also help to block excitation light reflected from the specimen but are not 100% efficient. A small amount of shortwave light reflected from the specimen leaks though the dichroic reflector into the emission side of the optical train. Although the amount of leaked excitation light is comparatively small, it is sufficient to overwhelm the weaker fluorescence emission. For this reason a barrier filter must be used to block the leaked excitation wavelengths. The wavelengths to be measured are usually isolated by a second filter or monochrometer placed in front of the photomultiplier detector. In this study the barrier filter was replaced with a 600 nm, wide band (100 nm bandpass) measurement filter and all of the light passing through this filter was directed to the detector.

The use of a single filter to function as both a barrier and a measurement filter has some advantages and disadvantages. To avoid eye damage due to leaked short-wave light the filter must be placed below the oculars. This placement requires the analysis to be conducted in a darkened room to prevent stray light from entering the oculars and contributing to the measured signal. Another disadvantage is that the visible fluorescence is less than would be obtained where a conventional long-pass barrier filter is used. This filtering strategy is also less aesthetically pleasing where the pinhole field stop is removed for observation of the whole field of view. Here, vignetting due to refraction within the dichroic reflector is enhanced. This effect was not investigated but where the field stop was inserted no vignetting was noted. However, the advantages of using a single filter as both a barrier and a measurement filter outweigh the

disadvantages for measurement of fluorescence intensity. Since the emitted light passes through only one filter about 20% more light reaches the detector. More importantly, with this filter placement, no correction for background fluorescence was required. Although the reason for this fortunate circumstance was not investigated it may have been due, in part, to the lack of a barrier filter. The absorption glasses used in long-pass barrier filters are usually slightly fluorescent and emit a weak, but measurable, fluorescence signal. With the microscope set-up described here the background correction was found to be less than 0.01. For example, the measured fluorescence intensity of the coating on the uranyl standard as well as sulphide minerals encountered in coal specimens were 0.00 (at 550-650 nm relative to the uranyl standard set to equal 100). It is worth noting that the threshold of visible fluorescence in this study was near a measured intensity of 1.5 and that visibly non-fluorescent inertinite macerals always reported a measurable fluorescence where the instrument was calibrated for maximum sensitivity. Although the background correction has also been attributed to fluorescence of the glass lenses in the objective (Ottenjann, 1989) autofluorescence of these components must have been insignificant within the measurement bandpass used in this study.

C.4 THE URANYL GLASS STANDARD

A Wild Leitz masked uranyl glass standard was used for calibration and is illustrated in Figure C.3. The Wild Leitz standard incorporates a uranyl glass disk that has been coated with an opaque, vapour-deposited mask. An un-coated 14 um diameter circle in the centre of the standard is used for calibration. Coloured concentric circles and guide lines serve to help locate this spot in reflected light. After locating the measurement spot in the reflected light mode it is necessary to switch microscope illuminators [8] for calibration in the fluorescence mode. Upon inserting the blue light illuminator the position of the illuminated field sometimes shifted slightly; this resulted in only part of the bare uranyl glass being irradiated and a measurably lower, but visibly unchanged, fluorescence signal. Since the

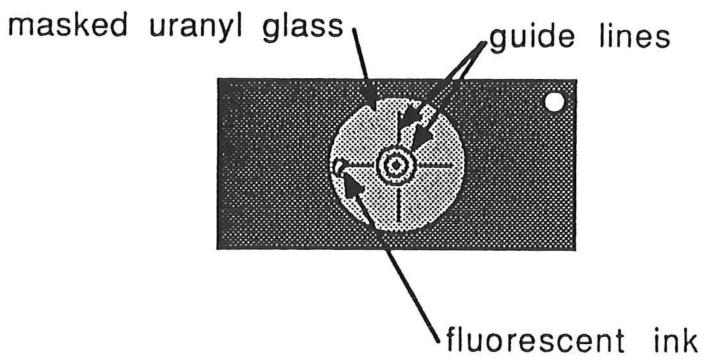

Figure C.3 Illustration of the masked uranyl glass standard used in this study (Wild Leitz part no. 621-059)

illuminated field diameter was ~15 um and the uncoated uranyl glass diameter was 14 um precise centring of the field diaphragm was required. To assure repeatable calibration the following procedure was adopted. A fluorescent marking pen was used to deposit a small amount of pigment at the edge of the standard (Figure C.3). After locating the unmasked measuring spot in the reflected light mode the standard was move laterally until this pigment was encountered. The fluorescence illuminator was inserted and the illuminated field critically centred with respect to the measuring spot. The standard was then moved laterally back to the unmasked spot for calibration. During this lateral traverse the guide lines and standard surface were not visible but the fluorescent green unmasked spot appeared as the centre of the standard passed under the objective.

C.4.1 Calibration With Neutral Density Filters

Neutral density filters were used during calibration to improve the precision of the analysis and extend the useful range of the photomultiplier output. The following example illustrates the value of neutral density filters for fluorometric calibration. A neutral density filter with a transmission (T) of 26.83% in the measurement bandpass is placed below the detector and the uranyl glass standard is critically focused. The photomultiplier gain is adjusted to provide an output signal (Po) of 160.0 (±0.5). The filter is removed from the light path prior to

analysis of the specimen. Each raw fluorescence intensity value obtained from the specimen is multiplied by a calibration factor (F) of 0.16769 and the corrected value is recorded. In this example raw values of 160.0, 42.3, 5.2 and 0.2 correspond to corrected fluorescence intensities of 26.83, 7.09, 0.87 and 0.03 respectively. The raw values provide an extra digit of precision compared to those that would have been obtained if the system had been calibrated directly to 100 without using the neutral density filter. This technique also allows measurement of fluorescence intensity values less than 0.1 relative to the standard = 100.0. The calibration factor (F) is calculated based on the transmission of the neutral density filter (T) and the selected photomultiplier output (Po) according to the equation:

$$\frac{T}{Po} = F$$

The selection of appropriate neutral density filters and photomultiplier gain depends on the nature of the coal and the calibration factor will vary according to these selections. Although the use of neutral density filters to improve the precision and sensitivity of fluorometric analysis is independent of the actual level of maceral fluorescence intensity it can only marginally improve a weak or noisy fluorescence signal. Furthermore, the system should be calibrated to avoid raw intensity values above 180.0 (a-non linear region) which is slightly less than the instrumental limit of 199.9.

Individually calibrated neutral density filters were used in this study. Metallic coated filters were selected since they provide an exceptionally flat spectral response; the spectral characteristics of the neutral density filters used in this study are shown in Figure C.4. Filter ND 0.1 was used for weakly fluorescent specimens and filter ND 0.6 was used where the mean fluorescence intensity was greater than about 12 relative to the uranyl glass standard = 100. The plots shown in Figure C.4 allow the light transmission at a given wavelength (T_λ) to be calculated from the corresponding optical density at the specified wavelength (od_λ) according to:

$$T_\lambda = 10^{(2 - od_\lambda)}$$

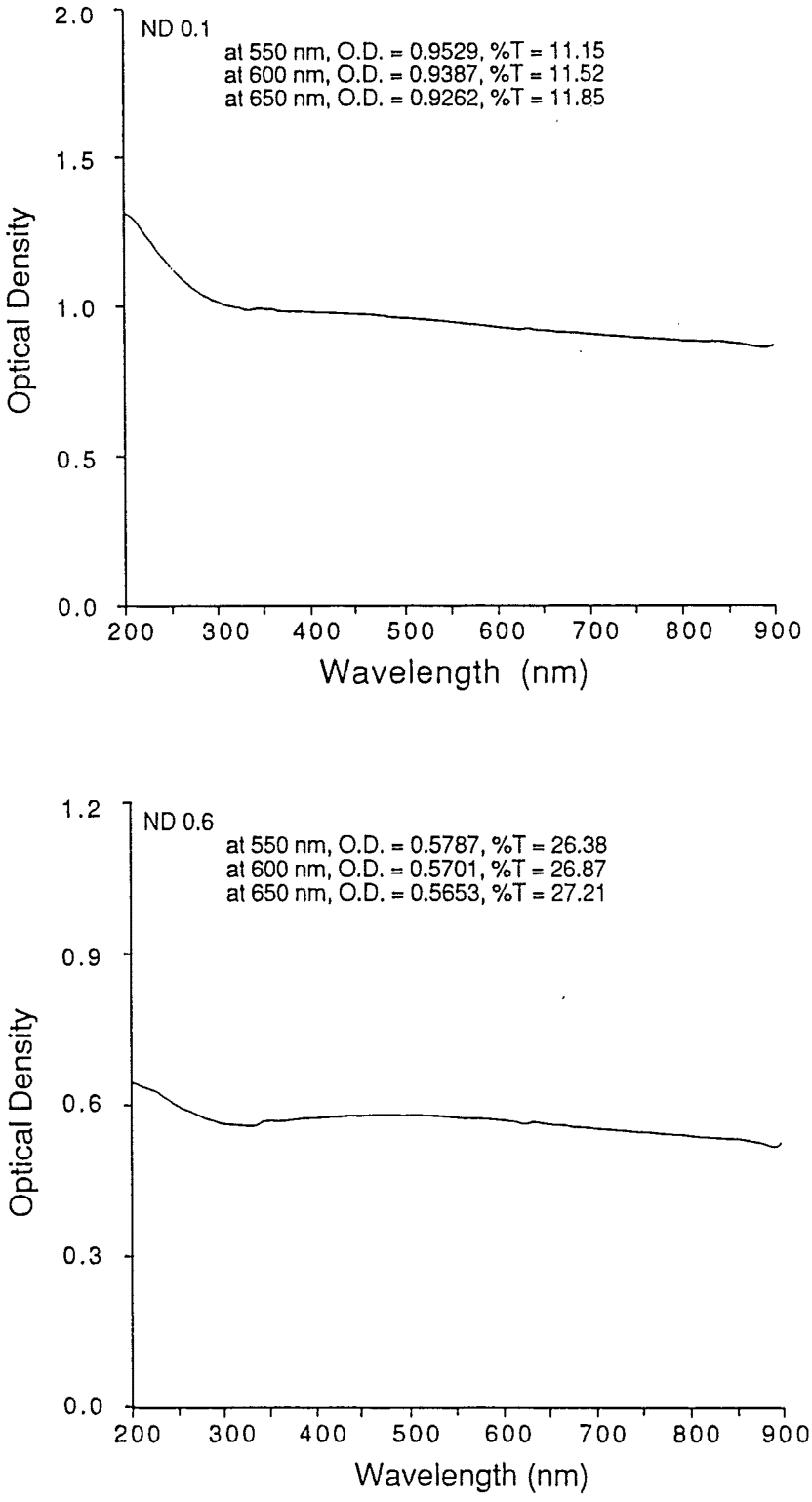

Figure C.4 Spectral absorbence of the neutral density filters used in this study. The figures were constructed from individual calibration charts provided with each filter by Omega Optical Co.

The specific transmission values used for calculation of the calibration factor were calculated according to:

$$T_{550\text{-}650} = \frac{T_{550} + 2T_{600} + T_{650}}{4}$$

C.5 THE OBJECTIVE AND THE ADVANTAGE OF NITROGEN

For incident light fluorescence microscopy the objective serves as both a collector and a condenser. Hence fluorescence intensity increases exponentially with the numerical aperture.

A diagnostic characteristic of thermoplastic coal is the rapid loss of fluorescence intensity upon exposure to the excitation energy. This phenomenon complicates measurement of fluorescence intensity and has required that intensity measurements be obtained immediately upon irradiation. Until recently (Davis *et al.*, 1990, Mitchell *et al.*, 1991, Quick and Moore, 1991), this was accomplished by selecting an area of interest in white light and then switching to the blue light mode for measurement. Because a hundred or more measurements may be required for a single fluorometric analysis the repeated switching between modes of illumination increases the time required for analysis. Davis *et al.*, (1990) have shown that fading can be prevented by maintaining a nitrogen flow over the irradiated area. In the present study a nitrogen gas flow was maintained over the irradiated coal surface to circumvent the need for frequent switching between white and blue light.

The device used to deliver the nitrogen gas to the specimen surface is shown in Figure C.5. Nitrogen gas is introduced through a hole in a custom made manifold near the front lens of the objective. During analysis the flat bottom of the manifold is separated from the specimen surface by less than 0.23 mm (the free working distance of the objective); this narrow gap serves to confine the nitrogen gas and prevent oxygen from migrating to the irradiated specimen surface. The rim on the pellet holder is flush with the specimen surface and serves to confine the nitrogen gas and allow measurement at the edge of the pellet. Using the device shown in Figure C.5 a nitrogen gas flow of 1.7 litres per minute effectively prevented negative alteration over the entire polished surface of the specimen.

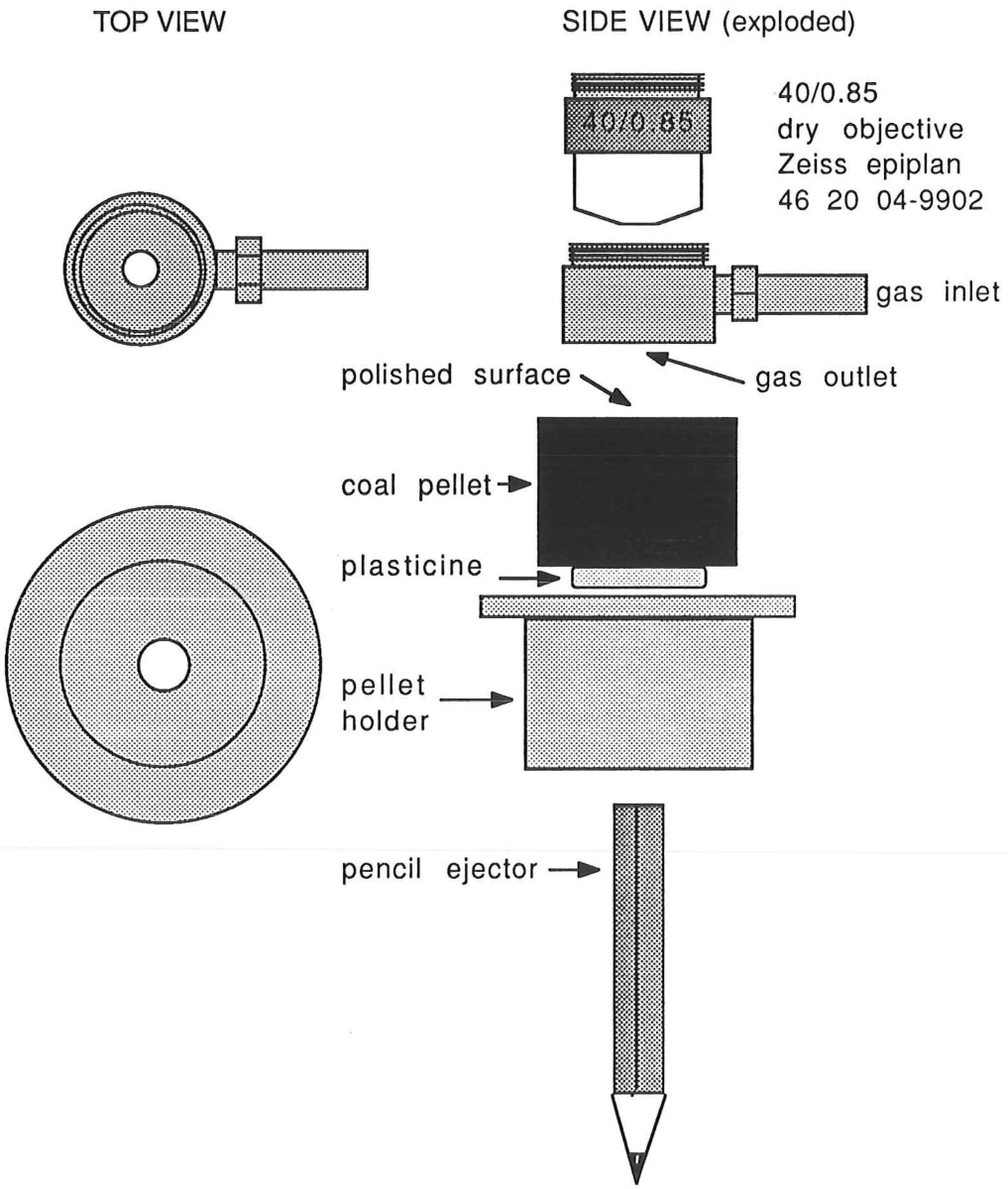

Figure C.5 Illustration of the device used to deliver nitrogen gas to the specimen surface.

APPENDIX D
SUGGATE RANK

This appendix describes a coal classification scheme introduced by Suggate (1959). The method is applied to some coals examined in this thesis and the results discussed.

D.1 SUGGATE RANK IN NEW ZEALAND

Suggate (1959) proposed a geological classification scheme where carbon and hydrogen, or alternatively, specific energy and volatile matter, are used to establish coal rank. In Suggate's classification coals are ranked according to a numerical value ranging from 1 to 24. As originally proposed, these numbers served to indicate the absolute rank of coal that is related to the maximum depth of burial. For example, rank 6.5 corresponds to a coal that had been buried to a depth of 6,500 feet. Later, Suggate (1974) abandoned the idea that absolute rank can be related to burial depth. In this and later work (Suggate, 1982), a geological rank classification of coal by moisture and calorific value was proposed where both calorific value and moisture were graphically corrected to an "average type" basis. Advancing this idea further, Suggate and Lowery (1982) used moisture as a measure of "physical rank" and Suggate rank numbers (Rank S) as a measure of maturation (i.e., "chemical rank") to show that vitrinite reflectance does not provide a definitive measure of maturation. Although agreeing with the idea that vitrinite reflectance needed to be re-examined, Newman and Newman (1982) criticized the use of Rank S to test the validity of vitrinite reflectance as a rank parameter, since the validity of Rank S had not been tested. Accordingly, Newman and Newman examined the theoretical basis of Rank S and concluded that Rank S cannot be justifiably used as a precise index of thermal maturity. Sykes *et al.*, (1991) modified the Rank S classification based on additional but unspecified data. Using the revised Rank S method they report that Rank S vs depth profiles for oil wells in the southern Taranaki basin are less variable than corresponding reflectance vs depth profiles.

D.2 DETERMINATION OF RANK S

Rank S is determined by plotting the position of a coal on a special graph annotated with lines that indicate Rank S numbers. Two different annotated graphs may be used and these are called Suggate plots in this appendix. Figure D.1 shows a Suggate plot of carbon vs hydrogen. Where these data are not available Figure D.2, which shows a specific energy vs volatile matter Suggate plot, may be used. After a coal has been located on a Suggate plot, the Rank S number is graphically estimated by measuring its position perpendicular to the adjacent annotated "isorank" lines. For example, a coal that plots halfway between line 9 and line 10 is assigned a Rank S of 9.5.

To position a coal on a Suggate plot the diagnostic carbon and hydrogen or specific energy and volatile matter values must first be mathematically adjusted according to the following equations (Suggate, 1959):

$$C_{dmmsnf} = \frac{100\ C}{(100 - 1.10\ A - N - S)} \qquad \text{(eq. D.1)}$$

$$H_{dmmsnf} = \frac{100\ (H - 0.009\ A)}{(100 - 1.10\ A - N - S)} \qquad \text{(eq. D.2)}$$

$$VM_{dmmsf} = \frac{100\ (VM - 0.10\ A - S)}{(100 - 1.10\ A - S)} \qquad \text{(eq. D.3)}$$

$$Btu/lb_{dmmsf} = \frac{100\ (Btu/lb - 40\ S)}{(100 - 1.10\ A - S)} \qquad \text{(eq. D.4)}$$

where,

C is the weight percent dry carbon
H is the weight percent dry hydrogen
N is the weight percent dry nitrogen
S is the weight percent dry total sulphur
A is the weight percent dry ash
VM is the dry basis, weight percent volatile matter
Btu/lb is the dry basis, British thermal units per pound

and the subscripts,

dmmsnf specifies a dry mineral matter, sulphur and nitrogen free basis
dmmsf specifies a dry mineral matter and sulphur free basis

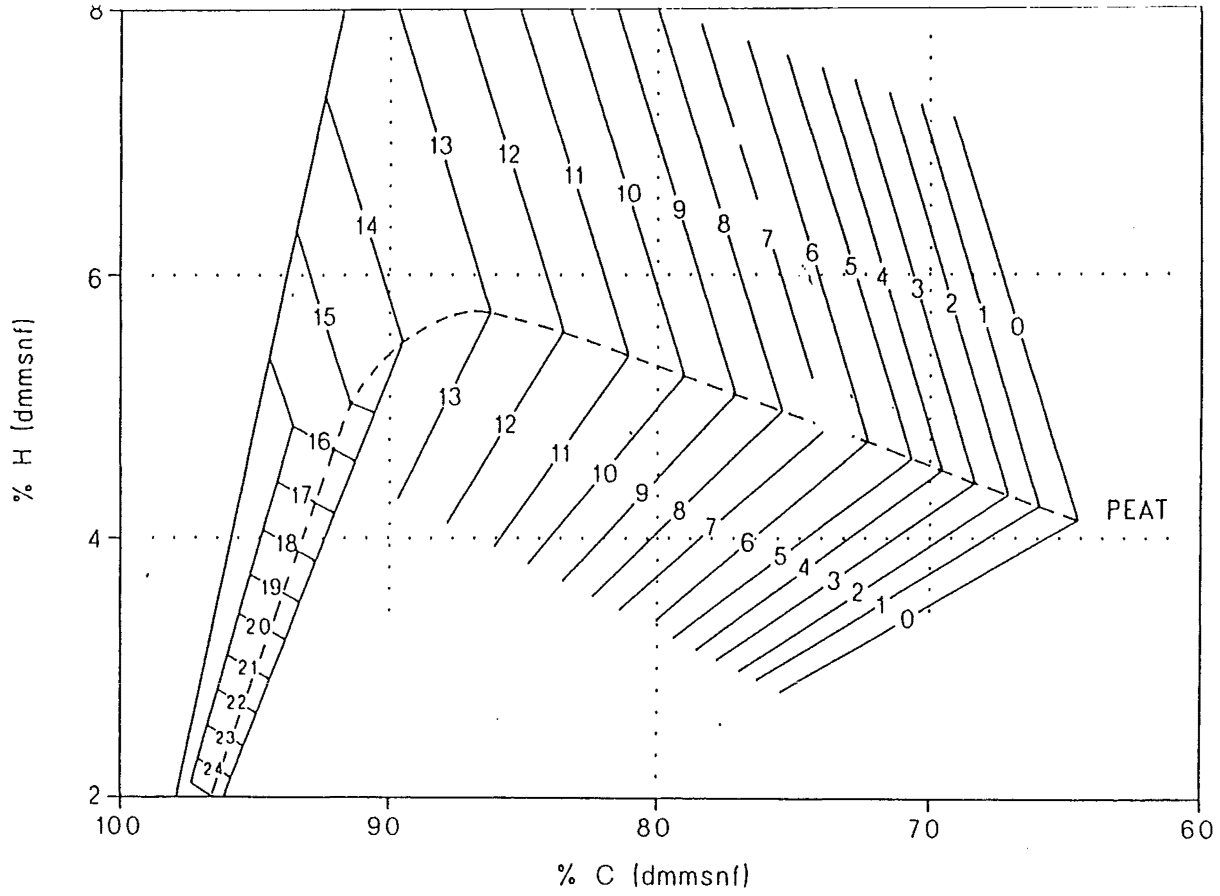

Figure D.1 Carbon vs hydrogen Suggate plot; reproduced from Sykes *et al.*, (1991) after Suggate (1959).

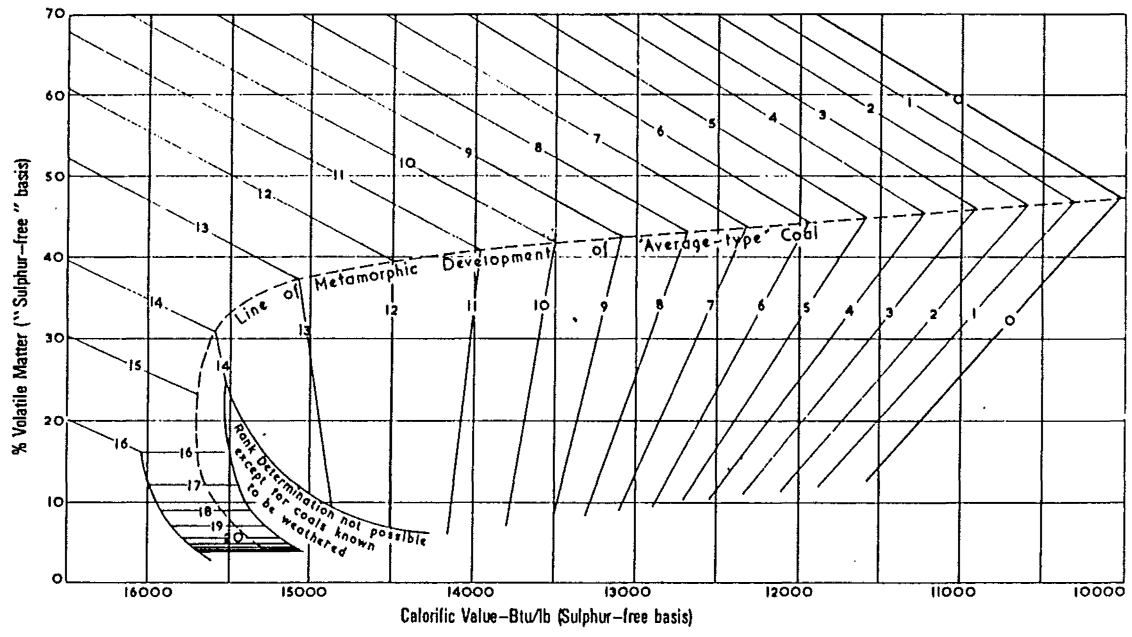

Figure D.2 Specific energy vs volatile matter Suggate plot (from Suggate, 1959).

Equation D.4 subtracts 40 Btu/lb from the determined specific energy for every one percent sulphur in the coal; Gray (1983) notes that this is based on the assumption that organic sulphur in coal has the same heat of combustion as elemental sulphur. Gray further argues that the calculation of BTU/lb to a sulphur free basis is not rational since the [organic] sulphur in coal is (p. 70) "just as much a part of the coal substance as the carbon, hydrogen oxygen and nitrogen." The same logic can be used to question the sulphur correction in Equations D.1, D.2, and D.3. The reason that Suggate (1959) adopted this adjustment for sulphur can be understood given the geological context of his classification, and his restrictive definition of coal type. Suggate correctly surmised that the bulk of the sulphur in New Zealand coals did not originate from the accumulated plant material and stated (p.31): "Since the greater part of the sulphur is not an original constituent of the coal substance, it is essential in comparing coals to adjust for the sulphur, for otherwise differences in coal type and rank will be obscured." Note that Suggate defined coal type as being determined by the "state of the vegetation before its burial" (p.17) and that sulphur in New Zealand coals was considered to be introduced after burial. Thus correction for sulphur might be explained for two reasons. Firstly, because sulphur was introduced after burial it could not be attributed to coal type since type was narrowly defined as a function of the nature of the vegetation prior to burial. Secondly, the notion that sulphur is a diluent implies that the introduction of sulphur into a seam did not change the relative carbon and hydrogen abundances that were inherited from the original vegetation prior to burial.

In this thesis coal type is considered to be determined by multiple processes that include biologically mediated changes which may occur after burial (section 2.4). Furthermore, the idea that (organic) sulphur can be considered as a diluent is rejected since the biologically mediated origin of organic sulphur may alter the organic matter (section 2.4.2). Finally, (organic) sulphur is not

considered as diluent in this thesis because, as explained above, it is as much a part of the organic fraction of coal as carbon, hydrogen, nitrogen or oxygen.

D.3 APPLICATION OF RANK S

Figure D.3 shows an enlarged portion of a specific energy vs volatile matter Suggate plot and Figure D.4 shows an enlarged portion of a carbon vs hydrogen Suggate plot; serial ply samples from two New Zealand coal seams have been plotted on both figures. Note that two high ash ply samples (46/750 and 46/945) have been omitted. Both plots indicate generally higher Rank S values for the serial ply samples from the Pike River coalfield compared to those from drillhole 1494 in the Buller coalfield.

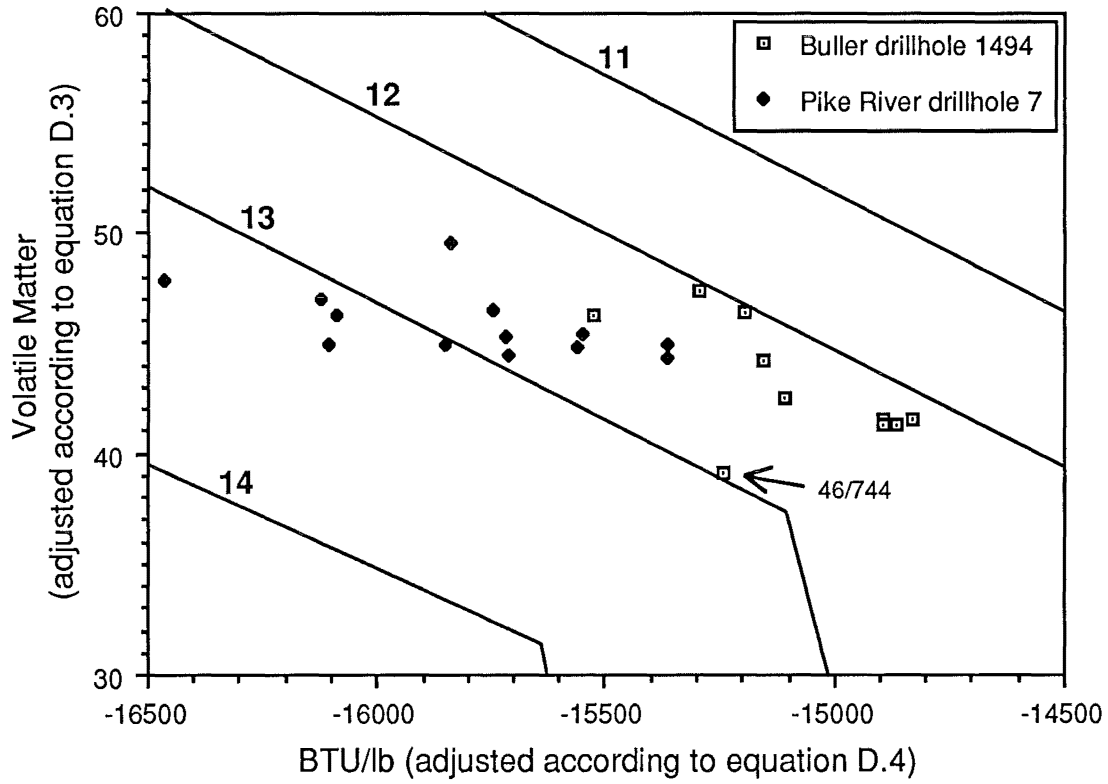

Figure D.3 Expanded view of Btu/lb vs Volatile Matter Suggate plot. The plotted coal samples are from serial ply samples encountered in Brunner coal measures from the Buller Coalfield (drillhole 1494) and the Pike River Coalfield (drillhole 7).

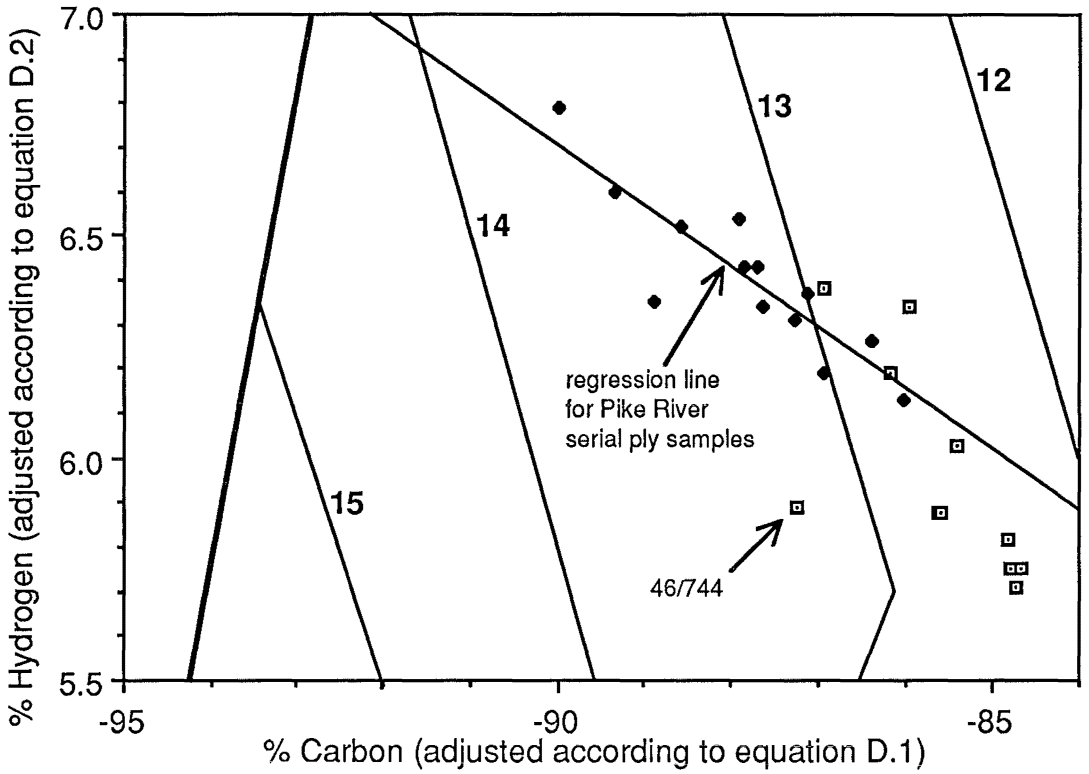

Figure D.4 Expanded view of a carbon vs hydrogen Suggate plot. The plotted coal samples are from serial ply samples encountered in Brunner coal measures from the Buller Coalfield (drillhole 1494) and the Pike River Coalfield (drillhole 7). Linear regression on the Pike River coal samples showed a coefficient of determination (r^2) of 0.78.

According to Figure D.3 the indicated Rank S of the Buller coals varies between 12 and 13 whereas according to Figure D.4 Rank S is shown to vary between 12.5 and 13.2. The Pike River coals show the same amount of scatter in both figures but a slightly higher indicated Rank S according to Figure D.4. Linear regression on the individual seam samples plotted in both figures showed no significant correlations except for the Pike River coals in Figure D.4 where the regression line is shown to diverge from the Rank S lines.

The lack of correlation for serial ply samples from drillhole 1494 can be attributed to sample 46/744. If this sample is removed from the data set regression analysis on the remaining ply samples from drillhole 1494 shown in Figures D.3 and D.4 report coefficients of determination of 0.81 and 0.83 respectively. In both cases the resulting regression lines (not shown) generally correspond to the Rank S ("isorank") lines. Because sample 46/744 is similarly displaced in both Figures D.3 and D.4 it is unlikely that the reason for the

anomalous behaviour of this coal can be attributed to analytical error in either the determination of specific energy and volatile matter or carbon and hydrogen. Although the direction of the displacement is consistent with elevated inertinite content (discussed in section D.4) this is unlikely to have caused the displacement since sample 46/744 reports less than 1% inertinite. A possible explanation for the deviation of sample 46/744 is a relatively high pyritic sulphur content (3.1% dry basis). Where only organic sulphur (1.6% dry basis) is considered in equations D.1, D.2, D.3, and D.4 the plotted position of sample 46/744 falls near the other ply samples in this seam. Table D.1 shows how the calculated hydrogen, carbon, volatile matter, and BTU/lb values vary according to whether total or organic sulphur is considered.

TABLE D.1
THE EFFECT OF PYRITIC SULPHUR PRESENT IN SAMPLE 46/744
ON THE DIAGNOSTIC VALUES USED TO ESTABLISH RANK S

Calculated Value	Calculated using total S (4.5% S)	Calculated using organic sulphur (1.6% S)
% Carbon (eq. D.1)	87.3	84.4
% Hydrogen (eq.D.2)	5.88	5.69
% Volatile Matter (eq.D.3)	39.2	41.2
BTU/lb (eq. D.4)	15,239	14,868

D.4 RANK S AND MACERAL ABUNDANCE

Rank S is best used where the maceral assemblage is dominated by one or two maceral groups (Newman 1989). Problems can be expected where all three maceral groups vary in abundance in a single sample of coal. To explain this problem it is worth considering how the Rank S lines shown in Figure D.1 were established. The composition of vitrain (vitrinite rich) dry durain (inertinite rich) and wet durain (liptinite rich) lithotypes that were hand-picked from individual (largely Carboniferous age) seams were plotted on an H/C graph and lines connecting these points were drawn on the graph. The collective lines were used as guides to position the Rank S (isorank) lines on the graph. Much of the scatter

shown in the original data used by Suggate to establish the classification scheme was probably a consequence of the heterogeneous composition of the individual lithotypes. Recently, density gradient centrifugation of demineralized coal specimens have allowed the isolation of relatively pure maceral concentrates from a single coal. Figure D.5 shows how the vitrinite, liptinite and inertinite group maceral fractions isolated from a single coal compare to the composition of the coal that the macerals were isolated from. The solid lines connecting the maceral groups are analogous to the Rank S lines shown in Figure D.1. Note that the parent coal plots in a triangular area defined by the three component group macerals. Thus the position of a coal on an H/C plot will vary within an area rather than along a line or a band in accordance with the relative amount of the component maceral groups. The maceral composition of the whole coal plotted on Figure D.5 is 73% vitrinite, 12% liptinite and 15% inertinite.

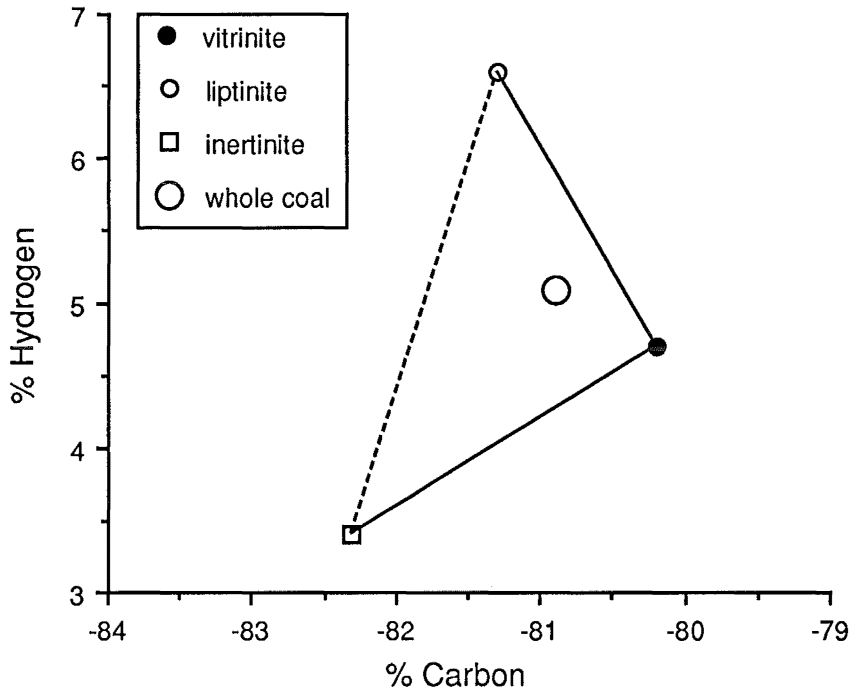

Figure D.5 Carbon vs Hydrogen plot showing the position of macerals separated from demineralized coal relative to the position of the parent coal. Data for Argonne Premium Coal Sample 7, reported by Choi *et al.*, (1989).

D.5 CONCLUSIONS

Some conclusions of this brief examination of Rank S are :

1) Rank S is misleading where pyritic sulphur is high.
2) Rank S will vary depending upon whether a C vs H or a CV vs VM Suggate plot is used.
3) Serial ply samples from a seam encountered in drillhole 7 from the Pike River coalfield diverge from the Rank S lines.
4) Rank S is likely to vary according to maceral composition where both inertinite and liptinite are present in increasing amounts.

These problems may be minimized where only New Zealand coals (excluding certain coals from the Pike River coalfield) that are rich in vitrinite and contain little pyrite are considered. However, consideration of New Zealand coals according to a classification that cannot accommodate more variable internationally traded coals hinders comparisons of these coals. Admittedly, all methods used to asses rank are problematic. However, based on this review it is suggested that Rank S offers no advantage for industrial characterization and a disadvantage in that it is seldom used outside of New Zealand. For example, Gray (1983) has shown that Rank S is linearly correlated with oxygen content. Oxygen content, like Rank S, is an imprecise measure of coal rank but has an advantage in that it is readily understood and easily calculated. Rank S is not considered further in this thesis.

APPENDIX E
ANALYTICAL DATA

This appendix lists analytical data for coal samples examined in this thesis. Most of the coal samples are serial ply samples and are listed here according to drillhole number. Two other groups of data are listed and include coals from the CRANZ mine sampling programme (run-of-mine samples) as well as samples taken at monthly intervals from two stockpiles (weathering series).

E.1 COMPOSITIONAL DATA

Compositional data include (where available) results from proximate analysis, ultimate analysis, forms of sulphur, CO_2, Gieseler thermoplastic indices and Rock-Eval analyses. Where serial ply samples are listed the depth of the ply intervals are also provided. Unless specified analytical data are on an air-dried basis.

TABLE E.1
COMPOSITIONAL DATA FOR SAMPLES FROM DRILLHOLE 1480

Buller coalfield DH-1480, Stockton area, Brunner coal measures								
Lab No	depth to top (m)	depth to bottom (m)	thickness	air-dried Moisture	Ash	Volatiles	Sulphur	Swelling
a90-85	13.6	13.8	0.2	1.2	0.94	35.7	0.88	8.5
a90-86	13.8	14.3	0.5	1.3	0.27	35.5	0.76	9.0
a90-87	14.3	14.8	0.5	1.3	0.35	35.2	0.67	8.5
a90-88	14.8	15.3	0.5	1.6	0.22	35.8	0.49	8.5
a90-89	15.3	15.8	0.5	1.7	0.09	34.4	0.50	9.5
a90-90	15.8	16.3	0.5	1.5	0.22	34.6	0.53	9.0
a90-92	16.3	16.8	0.5	1.5	0.12	34.9	0.60	9.5
a90-93	16.8	17.3	0.5	1.5	0.22	34.8	0.70	9.0
a90-94	17.3	17.8	0.5	1.3	0.15	35.4	0.84	9.0
a90-95	17.8	18.3	0.5	1.3	0.14	34.1	1.22	9.0
a90-96	18.3	18.8	0.5	1.6	0.18	34.1	1.82	9.0
a90-97	18.8	19.3	0.5	1.5	0.18	33.4	2.41	9.0
a90-98	19.3	19.8	0.5	1.4	0.27	33.8	3.02	9.0
a90-99	19.8	20.3	0.5	1.0	0.45	33.8	3.46	9.0
a90-100	20.3	20.8	0.5	0.7	0.74	35.7	3.96	9.5
a90-102	20.8	21.3	0.5	0.6	1.20	39.5	4.24	10.5
a90-103	21.3	21.8	0.5	0.6	5.60	34.1	4.40	8.5
			(composite samples)					
a90-251	13.6	18.3	4.7	1.1	0.12	34.8	0.72	9.0
a90-252	18.3	21.8	3.5	0.7	1.30	34.3	3.46	9.5

Gieseler plastometer:	°C initial softening	°C maximum fluidity	°C solidification	°C plastic range	ddpm
a90-251	404	440	493	89	8,960
a90-252	382	447	498	116	23,138
whole seam	392	439	493	101	10,862

TABLE E.2
COMPOSITIONAL DATA FOR SAMPLES FROM DRILLHOLE 1481

Buller coalfield DH-1481, Stockton area, Brunner coal measures								
Lab No	depth to top (m)	depth to bottom (m)	thickness	air-dried Moisture	Ash	Volatiles	Sulphur	Swelling
a90-134	33.72	34.0	0.28	0.7	7.60	36.5	6.36	9.0
a90-135	34.0	34.3	0.3	0.8	3.30	36.0	4.08	9.0
a90-136	34.3	34.8	0.5	0.9	2.50	36.0	3.54	9.0
a90-137	34.8	35.3	0.5	1.0	1.70	36.2	2.67	9.0
a90-138	35.3	35.8	0.5	1.1	0.11	35.6	1.11	9.0
a90-139	35.8	36.3	0.5	1.2	0.16	34.2	0.83	9.0
a90-140	36.3	36.8	0.5	1.3	0.12	33.2	0.72	9.0
a90-141	36.8	37.3	0.5	1.2	0.16	33.6	0.75	8.5
a90-142	37.3	37.8	0.5	1.2	0.18	33.2	0.80	9.0
a90-143	37.8	38.3	0.5	1.1	0.14	34.6	0.83	9.0
a90-146	38.3	38.8	0.5	1.0	0.24	35.6	0.85	9.0
a90-147	38.8	39.3	0.5	1.2	0.39	32.6	0.97	8.5
a90-148	39.3	39.8	0.5	1.3	0.21	33.1	1.07	9.0
a90-149	39.8	40.0	0.2	1.2	0.25	31.6	1.20	9.0
a90-150	40.0	40.5	0.5	1.0	1.10	32.7	1.74	9.0
a90-151	40.5	41.0	0.5	0.8	5.20	31.5	4.41	9.0
a90-152	41.0	41.5	0.5	0.7	10.80	29.6	2.70	8.5
				(composite samples)				
a90-215	33.72	35.3	1.58	0.7	3.1	36.8	3.78	9.0
a90-216	35.3	40.5	5.2	1.1	0.23	33.7	0.94	8.5

Gieseler plastometer:	°C initial softening	°C maximum fluidity	°C solidification	°C plastic range	ddpm
a90-215	371	442	492	121	42,719
a90-216	399	443	493	94	6,268
whole seam	396	448	495	99	7,383

TABLE E.3
COMPOSITIONAL DATA FOR SAMPLES FROM DRILLHOLE 1489

Buller coalfield DH-1489, Webb area, Brunner coal measures								
Lab No	depth to top (m)	depth to bottom (m)	thickness	air-dried Moisture	Ash	Volatiles	Sulphur	Swelling
a90-596	13.05	13.50	0.45	0.9	6.70	30.10	0.81	8.0
a90-597	13.50	13.80	0.30	0.9	2.00	30.20	0.81	8.5
a90-598	13.80	14.30	0.50	0.9	0.62	30.90	0.88	8.5
a90-599	14.30	14.80	0.50	0.8	0.14	31.10	0.77	8.5
a90-600	14.80	15.30	0.50	1.0	0.09	30.20	0.74	9.0
a90-601	15.30	15.80	0.50	0.8	0.10	30.50	0.70	9.0
a90-602	15.80	16.30	0.50	1.0	0.06	30.60	0.67	9.0
a90-603	16.30	16.80	0.50	0.9	0.16	30.00	0.65	8.5
a90-604	16.80	17.30	0.50	0.8	0.22	30.50	0.62	8.5
a90-605	17.30	17.80	0.50	0.8	0.23	30.40	0.68	8.5
a90-611	17.80	18.30	0.50	1.0	0.21	30.20	0.66	8.5
a90-612	18.30	18.80	0.50	1.0	0.21	30.40	0.71	9.0
a90-613	18.80	19.30	0.50	0.9	0.26	30.00	0.76	9.0
a90-614	19.30	19.80	0.50	0.9	0.62	29.40	1.18	9.0
a90-615	19.80	20.30	0.50	0.8	0.23	29.80	1.31	9.5
a90-616	20.30	20.80	0.50	0.8	0.54	29.60	2.08	9.0
a90-617	20.80	21.30	0.50	0.8	0.36	29.50	2.55	9.5
a90-618	21.30	21.80	0.50	0.7	0.14	29.50	3.00	9.0
a90-620	21.80	22.30	0.50	0.7	0.72	29.90	3.74	9.0
a90-621	22.30	22.80	0.50	0.6	1.30	29.60	4.74	9.0
a90-622	22.80	23.30	0.50	0.6	1.20	29.60	4.26	9.5
a90-623	23.30	23.80	0.50	0.8	3.50	29.50	4.20	9.0
a90-624	23.80	24.05	0.25	0.9	7.80	29.10	4.01	9.0

TABLE E.4
COMPOSITIONAL DATA FOR SAMPLES FROM DRILLHOLE 1490

Buller coalfield DH-1490, Webb area, Brunner coal measures								
Lab No	depth to top (m)	depth to bottom (m)	thickness	air-dried Moisture	Ash	Volatiles	Sulphur	Swelling
a90-628	7.13	7.40	0.27	2.4	4.20	30.20	1.49	1.5
a90-629	7.40	7.60	0.20	2.4	1.30	29.70	1.25	1.0
a90-630	7.60	8.00	0.40	2.7	0.30	29.70	1.16	1.0
a90-631	8.00	8.50	0.50	2.1	0.30	30.20	0.99	0.5
a90-635	8.50	9.00	0.50	3.0	0.22	29.10	0.84	0.0
a90-636	9.00	9.50	0.50	2.5	0.17	29.60	0.80	0.5
a90-637	9.50	10.00	0.50	2.5	0.10	30.00	0.76	1.0
a90-638	10.00	10.50	0.50	2.6	0.16	30.00	0.76	0.5
a90-639	10.50	11.00	0.50	2.3	0.11	29.80	0.77	0.5
a90-640	11.00	11.50	0.50	2.6	0.13	29.30	0.77	0.0
a90-641	11.50	12.50	1.00	3.1	0.13	29.30	0.85	0.0
a90-645	12.50	12.50	0.00	4.2	0.25	28.60	0.93	0.0
a90-646	12.50	13.00	0.50	3.6	0.21	29.00	1.01	0.0
a90-647	13.00	13.50	0.50	2.7	0.16	29.00	1.09	0.5
a90-648	13.50	14.00	0.50	2.1	0.24	28.80	1.25	1.0
a90-649	14.00	14.50	0.50	2.6	0.11	28.50	1.41	1.0
a90-650	14.50	15.00	0.50	2.1	0.15	28.70	1.71	1.0
a90-651	15.00	15.50	0.50	2.4	0.56	28.40	2.17	0.5
a90-652	15.50	16.00	0.50	2.9	0.68	28.10	2.54	0.5
a90-653	16.00	16.50	0.50	2.0	0.67	28.50	2.78	2.0
a90-654	16.50	17.00	0.50	2.1	0.60	28.40	3.24	1.0
a90-659	17.00	17.50	0.50	2.3	0.42	28.20	2.42	1.0
a90-660	17.50	18.00	0.50	2.5	0.61	28.10	3.26	0.5
a90-661	18.00	18.50	0.50	2.1	0.59	28.30	3.76	0.5
a90-662	18.50	19.00	0.50	2.1	1.00	28.70	3.84	1.0
a90-663	19.00	19.25	0.25	1.6	2.70	28.60	3.82	3.5
a90-664	19.25	19.50	0.25	0.9	7.70	28.70	3.86	7.5

TABLE E.5
COMPOSITIONAL DATA FOR SAMPLES FROM DRILLHOLE 1492

Buller coalfield DH-1492, Webb area, Brunner coal measures								
Lab No	depth to top (m)	depth to bottom (m)	thickness	air-dried Moisture	Ash	Volatiles	Sulphur	Swelling
a90-3482	26.05	28.3	2.25	5.3	0.78	34.3	3.33	0
a90-3484	28.3	37.6	9.3	0.9	0.05	33.0	1.19	9
a90-3486	37.6	39.6	2.0	0.6	3.3	32.5	4.25	9

E.2 MACERAL COMPOSITION DATA

Tables E.10 and E.11 show the results of maceral analyses expressed on a volume percent, mineral free basis. Mineral identifications are expressed on a counted, mineral matter containing basis. Volume percent mineral matter are calculated according to ASTM-2799. Maceral analyses calculated from the results of point count analyses undertaken in both the reflected white light mode and the fluorescence mode (2 scans).

TABLE E.6

COMPOSITIONAL DATA FOR SAMPLES FROM DRILLHOLE 1494

Buller coalfield drillhole 1494, Upper Waimangaroa sector, Brunner coal measures

Lab No	rider 46/750	ply 1 46/739	ply 2 46/740	ply 3 46/741	ply 4 46/742	ply 5 46/743	core not recovered	ply 6 46/744	ply 7 46/745	ply 8 46/746	ply 9 46/747	ply 10 46/748	ply 11 46/749
depth to top (m)	244.51	255.63	255.90	256.50	257.10	258.20	259.40	259.85	261.29	262.45	263.04	263.97	264.75
depth to bottom (m)	244.70	255.90	256.50	257.10	258.20	259.40	259.85	261.29	262.45	263.04	263.97	264.75	265.36
thickness (m)	0.19	0.27	0.60	0.60	1.10	1.20	0.45	1.44	1.16	0.59	0.93	0.78	0.61
% recovery	100	100	100	100	53	100	0	27	100	49	93	78	61
total moisture	4.7	13.0	8.4	7.2	9.3	10.7		9.3	10.4	9.7	11.1	10.5	11.4
air-dried moisture	3.1	3.0	3.0	2.9	3.8	4.2		4.7	4.9	4.8	4.8	4.6	4.7
ash	31.4	2.4	1.8	4.2	1.2	1.2		4.1	0.42	0.16	0.55	0.26	2.6
volatiles	31.4	47.2	46.7	46.6	44.2	42.2		38.7	40.0	40.0	39.9	40.2	39.2
MJ/kg	21.78	32.42	32.40	31.73	32.44	32.36		31.01	32.42	32.56	32.38	32.54	31.77
CO_2	0.08	0.04	0.02	0.02	0.02	0.01		0.02	0.02	0.03	0.03	0.02	0.02
total sulphur	1.18	4.39	4.53	6.25	3.88	3.26		4.50	1.42	1.18	1.33	1.08	1.02
sulphate	0.02	0.00	0.00	0.00	0.00	0.01		0.02	0.00	0.00	0.00	0.03	0.03
pyritic	0.38	1.37	1.36	3.16	0.76	0.71		2.93	0.18	0.03	0.20	0.04	0.04
organic	0.78	3.02	3.17	3.09	3.12	2.54		1.55	1.24	1.15	1.13	1.01	0.95
dry carbon	53.7	78.8	79.3	76.3	79.9	80.6		78.1	82.2	82.5	82.1	82.6	81.2
dry hydrogen	4.4	5.8	5.7	5.6	5.7	5.6		5.3	5.6	5.6	5.6	5.6	5.6
dry nitrogen	0.9	1.1	1.3	1.0	1.0	1.1		1.1	1.2	1.1	1.2	1.1	1.1
crucible swelling	3.5	4.0	5.5	4.5	5.0	5.5		4.0	4.0	4.0	4.0	4.0	4.0
Gieseler													
initial softening °C	397	382	383	382	380	386		396	395	397	396	396	397
maximum fluidity °C	432	424	421	419	424	425		438	438	438	440	438	441
solidification °C	458	473	470	471	462	462		462	466	464	462	460	464
fluid range °C	61	91	87	89	82	76		66	71	67	66	64	67
ddpm	320	41,706	44,346	39,887	24,524	1,224		106	130	140	135	130	191
Rock-Eval													
Tmax °C	429	428	426	425	425	429		434	433	431	436	428	436
S1 mg HC/g coal	5.77	8.90	9.54	8.22	7.73	7.86		6.02	5.75	5.58	5.33	6.82	7.17
S2 mg HC/g coal	218	311	286	322	269	273		237	228	258	226	267	258
S3 mg HC/g coal	0.97	1.50	1.18	1.29	1.28	1.09		1.68	0.90	2.00	1.22	1.41	1.19

TABLE E.7

COMPOSITIONAL DATA FOR SERIAL PLY SAMPLES FROM DRILLHOLE 7

Pike River coalfield drillhole 7, Brunner coal measures

Lab No	rider 46/847	ply 1 46/835	ply 2 46/836	ply 3 46/837	ply 4 46/838	ply 5 46/839	ply 6 46/840	ply 7 46/841	ply 8 46/842	ply 9 46/843	ply 9a 46/945	ply 10 46/844	ply 11 46/845	ply 12 46/846
depth to top (m)	112.30	118.63	119.10	119.70	120.90	122.10	123.30	124.50	125.70	126.90	128.64	128.84	129.90	130.50
depth to bottom (m)	112.52	119.10	119.70	120.90	122.10	123.30	124.50	125.70	126.90	128.64	128.84	129.90	130.50	131.15
thickness (m)	0.22	0.47	0.60	1.20	1.20	1.20	1.20	1.20	1.20	1.74	0.12	1.06	0.60	0.65
% recovery	100	100	100	100	100	100	100	100	100	89	100	100	100	100
total moisture	n.d.	n.d.	n.d.	n.d.	n.d.	n.d.	n.d.	n.d.	n.d.	n.d.	n.d.	n.d.	n.d.	n.d.
air-dried moisture	1.0	0.5	0.7	0.8	0.9	0.9	1.0	0.9	0.8	0.6	0.3	0.5	0.5	0.5
ash	7.2	8.0	2.2	2.4	0.84	1.1	2.7	1.9	4.0	1.6	30.0	1.6	2.6	11.7
volatiles	44.6	47.9	47.2	45.8	45.1	45.3	43.4	44.4	44.2	45.7	43.8	47.5	47.8	44.7
MJ/kg	32.63	32.24	34.52	34.10	35.21	35.35	34.04	34.73	33.32	35.19	17.28	35.46	35.09	32.05
CO_2	0.07	2.90	0.73	1.40	0.35	0.69	2.00	1.20	2.90	1.00	22.90	0.65	0.90	0.22
total sulphur	5.33	4.22	3.54	3.06	2.44	1.62	1.07	1.38	2.12	2.96	1.84	3.95	4.08	3.94
sulphate	0.02	0.02	0.00	0.00	0.00	0.00	0.02	0.01	0.01	0.01	0.02	0.01	0.01	0.03
pyritic	2.52	1.58	0.36	0.14	0.06	0.02	0.01	0.01	0.06	0.07	0.13	0.20	0.28	0.78
organic	2.79	2.62	3.18	2.92	2.38	1.60	1.04	1.36	2.05	2.88	1.69	3.74	3.79	3.13
dry carbon	76.1	75.6	81.7	81.3	83.3	84.4	82.5	82.5	79.5	82.7	48.8	82.7	82.3	74.2
dry hydrogen	5.5	5.7	6.0	5.9	6.1	6.2	5.9	6.0	5.7	6.0	3.2	6.1	6.1	5.7
dry nitrogen	1.0	0.9	1.0	1.1	1.0	0.9	1.0	1.0	1.0	0.9	0.5	0.9	0.9	0.7
crucible swelling	6.0	7.0	7.0	8.5	9.0	8.5	8.5	8.5	9.0	8.5	6.5	8.0	7.0	7.5
Gieseler														
initial softening °C	368	376	371	382	386	396	395	398	392	385	n.d.	385	364	376
maximum fluidity °C	429	444	442	442	440	434	437	435	442	446	n.d.	447	443	447
		436-451	432-452							440-452		435-458	426-460	431-462
solidification °C	475	480	482	478	478	482	480	482	480	482	n.d.	484	488	490
fluid range °C	107	104	111	96	92	86	85	84	88	97	n.d.	99	124	114
ddpm	44,704	+50,000	+50,000	49,538	32,936	47,783	48,581	49,374	44,393	+50,000	n.d.	+50,000	+50,000	+50,000
Rock-Eval														
Tmax °C	n.d.	438	435	433	438	439	440	439	437	439	438	438	435	436
S1 mg HC/g coal	n.d.	19.3	19.8	13.8	13.9	11.9	11.2	5.58	8.62	11.9	14.9	16.3	18.4	21.3
S2 mg HC/g coal	n.d.	346	351	301	324	327	298	318	324	344	177	329	380	373
S3 mg HC/g coal	n.d.	0.97	2.06	1.11	1.00	1.00	1.34	1.02	1.30	3.07	1.54	0.75	1.89	1.62

TABLE E.8

COMPOSITIONAL DATA FOR SAMPLES FROM DRILLHOLE 712, AND DRILLHOLE 7 PAPAROA SEAM COALS

	Greymouth coalfield drillhole 712, Rapahoe sector						Pike River Drillhole 7, Paproa coal measures					
	ply 1	ply 2	ply 3	ply 4	ply 5	ply 6	seam 1	seam 2	seam 3	seam 4	seam 5	seam 6
Lab No	50/639	50/640	50/641	50/642	50/643	50/644	46/919	46/920	46/921	46/922	46/923	46/924
depth to top (m)	386.35	389.35	392.35	394.80	395.65	399.15	264.11	305.48	310.36	329.45	338.10	341.35
depth to bottom (m)	389.35	392.35	394.80	395.65	399.15	403.00	264.53	305.68	310.63	329.65	338.85	343.20
thickness (m)	3.00	3.00	2.45	0.85	3.50	3.85	0.42	0.20	0.27	0.20	0.75	1.85
% recovery							100	100	100	100	100	36
total moisture	9.3	8.8	8.1	7.7	8.4	7.0	6.4	2.2	4.9	4.4	3.6	5.2
air-dried moisture	3.3*	3.1*	2.9*	2.5*	2.9*	2.8*	1.4	1.0	1.1	1.1	0.84	1.2
ash	7.1	1.2	1.0	20.1	3.3	6.1	13.0	20.7	20.4	17.2	19.4	11.6
volatiles	38.0	44.0	45.2	35.0	42.8	40.8	33.0	32.0	31.6	34.0	33.8	35.2
MJ/kg	29.62	32.14	32.31	25.87	31.61	30.72	30.23	27.85	27.75	28.70	28.60	31.26
CO_2							0.17	0.19	0.10	0.06	1.10	1.10
total sulphur	0.34	0.30	0.28	0.24	0.33	0.46	0.61	0.49	0.53	0.73	0.32	0.32
sulphate							0.00	0.00	0.00	0.00	0.00	0.00
pyritic							0.05	0.02	0.02	0.01	0.02	0.04
organic							0.56	0.47	0.51	0.72	0.30	0.28
dry carbon	76.4	79.7	79.8		78.1	75.5	74.5	67.8	67.8	70.0	69.3	76.8
dry hydrogen	5.2	5.6	5.8		5.6	5.4	5.0	4.7	4.7	5.0	4.9	5.3
dry nitrogen	1.1	1.1	1.2		1.3	1.1	0.9	0.9	1.0	0.9	1.1	1.2
crucible swelling index	1.5	3.5	3.5	2.0	3.5	3.0	8.0	8.5	8.5	8.0	8.5	8.0
Gieseler												
initial softening °C	411	405	391		398	409	406	402	404	392	392	397
maximum fluidity °C							438	441	433	438	442	440
solidification °C	422	453	450		448	446	474	478	474	478	480	479
fluid range °C	31	48	59		50	37	68	76	70	86	88	82
ddpm	1	2	4		3	2	2,320	3,490	2,150	27,545	8,782	7,807
Rock-Eval												
Tmax °C	426	422	422	422	423	422						
S1 mg HC/g coal	1.32	3.02	2.63	1.29	2.33	2.02						
S2 mg HC/g coal	185	220	267	174	239	230						
S3 mg HC/g coal	4.19	4.30	4.66	3.67	4.17	3.91						

*note: these anomalously low moisture values resulted from conditioning the specimens at higher temperature and lower humidity than normally used to determine air-dried moisture (J Newman pers. comm.)

TABLE E.9

COMPOSITIONAL DATA FOR SAMPLES FROM RUN OF MINE (B) SAMPLES

Lab No	46/068	64/064	45/963	45/978	45/965	46/296	45/971	46/426
mine name	Kiwi	Strongman	Island Block	Cascade	Echo	Stockton	Sullivan	Roa
total moisture	11.2	10.7	7.9	13.4	7.6	8.1	8.0	n.d.
air-dried moisture	7.4	6.0	3.3	4.5	3.1	2.3	0.6	1.0
ash	5.5	2.2	1.1	3.8	4.2	1.0	4.0	3.3
volatiles	38.5	39.9	40.4	37.1	39.3	31.4	30.8	21.8
MJ/kg	29.31	31.43	30.88	31.52	30.25	n.d.	34.61	n.d.
CO_2	0.48	0.42	0.04	0.03	0.03	0.03	0.03	0.06
total sulphur	0.21	0.20	1.42	0.42	0.48	0.71	0.81	0.34
sulphate	0.00	0.00	0.02	0.01	0.01	0.01	0.03	0.01
pyritic	0.10	0.06	0.16	0.13	0.06	0.06	0.06	0.04
organic	1.10	0.14	1.24	0.28	0.41	0.64	0.72	0.29
dry carbon	76.1	80.2	79.9	79.6	77.9	85.6	84.2	86.6
dry hydrogen	5.3	5.7	5.4	5.3	5.3	5.3	5.3	4.8
dry nitrogen	1.0	1.2	1.2	1.4	1.3	1.2	1.6	1.5
crucible swelling	1.5	3.0	4.0	5.5	4.0	8.0	9.5	10.0
Gieseler								
initial softening °C	404	400	417	409	416	417	400	444
maximum fluidity °C		433		439		458	453	477
solidification °C	440	450	445	459	451	484	492	503
fluid range °C	36	50	28	50	35	67	92	59
ddpm	2	6	2	5	2	114	1,862	62

TABLE E.10

MACERAL DATA FOR SAMPLES FROM DRILLHOLE 712 AND DRILLHOLE1494

	Greymouth coalfield Drillhole 712, Rapahoe sector						Buller coalfield Drillhole 1494, Upper Waimangaroa sector, Brunner coal measures											
Sample ID	ply 1 50/639	ply 2 50/640	ply 3 50/641	ply 4 50/642	ply 5 50/643	ply 6 50/644	rider 46/750	ply 1 46/739	ply 2 46/740	ply 3 46/741	ply 4 46/742	ply 5 46/743	ply 6 46/744	ply 7 46/745	ply 8 46/746	ply 9 46/747	ply 10 46/748	ply 11 46/749
Vitrinite	87.1	90.8	91.5	91.9	92.5	90.0	94.3	93.7	94.1	95.2	96.6	97.0	96.3	95.0	94.5	94.0	93.4	96.4
Liptinite	4.0	4.0	3.0	3.6	3.1	3.7	5.1	4.3	3.9	3.5	2.6	2.2	3.1	3.0	1.8	2.8	3.8	2.0
Inertinite	9.0	4.5	5.4	4.5	4.5	6.3	0.6	2.0	2.0	1.2	0.8	0.8	0.6	2.0	3.7	3.2	2.8	1.6
Telovitrinite	35.9	25.7	22.8	28.1	23.5	26.2	27.5	8.2	5.7	9.8	5.9	13.7	10.1	7.2	5.1	8.0	6.0	7.9
Detrovitrinite	50.0	65.8	68.8	63.4	68.6	63.8	66.8	84.9	87.0	84.8	89.9	82.9	86.1	86.9	88.8	85.4	87.2	88.4
Eugelinite	0.8	0.0	0.0	0.0	0.2	0.0	0.0	0.0	0.2	0.0	0.0	0.0	0.0	0.2	0.2	0.2	0.0	0.0
Corpogelinite	0.4	0.0	0.0	0.4	0.2	0.0	0.0	0.6	1.2	0.6	0.8	0.4	0.0	0.6	0.4	0.4	0.2	0.0
Sporinite	1.0	0.4	0.6	0.9	0.8	0.0	0.0	0.2	0.6	0.2	0.2	0.4	0.0	0.0	0.0	0.4	0.6	0.6
Cutinite	0.0	0.6	0.2	0.5	0.2	0.4	1.8	0.0	0.0	0.0	0.0	0.0	0.0	0.0	0.0	0.0	0.0	0.0
Suberinite	0.8	0.2	0.0	0.5	0.4	0.4	0.3	0.6	0.0	0.8	0.4	0.0	0.0	0.0	0.0	0.2	0.0	0.0
Resinite	0.6	0.2	0.2	0.2	0.2	0.0	1.0	0.4	0.4	0.8	0.4	0.4	0.2	0.8	0.2	0.8	0.8	0.4
Liptodetrinite	1.3	2.2	1.8	1.6	1.4	2.9	1.3	2.5	2.5	1.5	1.2	1.0	2.5	1.2	1.0	1.2	1.0	1.0
Alginite	0.0	0.2	0.0	0.0	0.0	0.0	0.0	0.0	0.0	0.0	0.0	0.0	0.2	0.4	0.2	0.0	0.0	0.0
Bituminite	0.0	0.0	0.0	0.0	0.0	0.0	0.0	0.0	0.0	0.0	0.0	0.0	0.0	0.0	0.0	0.0	0.0	0.0
Exudatinite	0.0	0.0	0.0	0.0	0.0	0.0	0.0	0.2	0.0	0.0	0.2	0.0	0.0	0.0	0.0	0.0	0.0	0.0
Fluorinite	0.2	0.2	0.2	0.0	0.0	0.0	0.8	0.4	0.4	0.2	0.2	0.4	0.2	0.6	0.4	0.2	1.4	0.0
Fusinite	2.4	0.8	1.6	1.0	1.8	1.4	0.0	0.0	0.0	0.0	0.0	0.0	0.0	0.0	0.0	0.0	0.0	0.0
Semifusinite	3.8	2.4	2.0	2.4	1.2	1.4	0.0	0.8	1.2	0.2	0.2	0.2	0.2	1.2	2.2	2.0	0.6	0.4
Sclerotinite	0.0	0.0	0.0	0.0	0.0	0.2	0.2	0.4	0.2	0.6	0.4	0.4	0.2	0.6	1.2	0.4	1.0	1.0
Inertodetrinite	2.4	0.8	1.4	1.0	1.4	3.0	0.4	0.2	0.2	0.4	0.2	0.2	0.2	0.0	0.2	0.6	0.8	0.2
Macrinite	0.0	0.0	0.0	0.0	0.0	0.2	0.0	0.6	0.4	0.0	0.0	0.0	0.0	0.2	0.0	0.2	0.4	0.0
Micrinite	0.4	0.6	0.4	0.0	0.0	0.0	0.0	0.0	0.0	0.0	0.0	0.0	0.0	0.0	0.0	0.0	0.0	0.0
sulfide	0.4	0.0	0.0	0.2	0.0	0.0	0.4	0.6	1.0	0.8	0.6	0.0	1.2	0.2	0.0	0.0	0.0	0.2
clay	0.2	0.2	0.2	0.8	0.2	0.2	9.6	0.0	0.0	0.0	0.0	0.0	0.0	0.0	0.0	0.0	0.0	0.0
carbonate	0.0	0.0	0.0	0.0	0.0	0.0	0.0	0.0	0.0	0.0	0.0	0.0	0.0	0.0	0.0	0.0	0.0	0.0
quartz	0.6	0.0	0.0	1.9	0.2	0.6	0.6	0.0	0.0	0.0	0.0	0.0	0.0	0.0	0.0	0.0	0.0	0.0
other	0.4	0.0	0.0	0.8	0.2	0.8	2.2	0.0	0.0	0.0	0.4	0.0	0.0	0.0	0.0	0.0	0.0	0.0
MM counted	1.6	0.2	0.2	3.6	0.6	1.6	12.8	0.6	1.0	0.8	1.0	0.0	1.2	0.2	0.0	0.0	0.0	0.2
MM calculated	4.1	0.7	0.6	12.2	1.9	3.5	21.1	2.6	2.3	4.1	1.8	1.6	3.6	0.6	0.4	0.7	0.4	1.7

TABLE E.11

MACERAL DATA FOR SAMPLES FROM DRILLHOLE 7

Drillhole	Brunner coal measures														Paproa coal measures					
Sample ID	rider 46/847	ply 1 46/835	ply 2 46/836	ply 3 46/837	ply 4 46/838	ply 5 46/839	ply 6 46/840	ply 7 46/841	ply 8 46/842	ply 9 46/843	ply 9a 46/945	ply 10 46/844	ply 11 46/845	ply 12 45/846	seam 1 46/919	seam 2 46/220	seam 3 46/921	seam 4 46/922	seam 5 46/923	seam 6 46/924
Vitrinite	96.3	94.2	92.8	95.3	92.9	91.3	94.2	90.7	91.2	92.2	96.9	95.9	94.7	94.8	93.8	94.1	93.1	96.7	94.7	93.8
Liptinite	1.9	3.6	4.5	3.1	5.9	6.3	3.3	7.3	5.8	6.3	2.2	3.7	4.7	5.0	5.2	3.7	2.5	2.9	2.0	2.1
Inertinite	1.8	2.2	2.7	1.6	1.3	2.4	2.6	2.0	3.0	1.5	0.8	0.4	0.6	0.2	1.0	2.3	4.4	0.4	3.2	4.1
Telovitrinite	24.6	15.4	10.7	13.2	15.9	12.1	13.6	9.9	18.5	15.9	17.6	13.2	9.4	6.3	21.4	26.7	23.8	31.9	16.8	14.2
Pseudovitrinite															33.3	18.9	13.9	16.8	11.5	9.1
Detrovitrinite	71.7	77.5	81.5	81.1	75.1	76.8	78.8	78.2	71.7	74.9	78.5	82.3	82.3	87.3	39.1	48.3	55.5	48.0	66.4	70.2
Eugelinite	0.0	0.2	0.2	0.2	1.7	0.8	0.2	0.8	0.0	0.2	0.4	0.2	0.8	0.6	0.0	0.2	0.0	0.0	0.0	0.0
Corpogelinite	0.0	1.1	0.4	0.8	0.2	1.6	1.5	1.8	1.0	1.3	0.4	0.2	2.1	0.6	0.0	0.0	0.0	0.0	0.0	0.2
Sporinite	0.0	0.4	0.2	0.6	0.8	0.4	0.4	0.4	0.0	0.4	0.0	0.2	0.2	0.0	0.4	1.1	0.7	0.2	0.2	0.2
Cutinite	0.0	0.0	0.0	0.0	0.2	0.0	0.0	0.0	0.0	0.0	0.0	0.0	0.6	0.0	0.0	0.0	0.0	0.4	0.2	0.2
Suberinite	0.2	0.4	0.4	0.4	2.0	1.0	0.4	0.4	1.0	1.2	1.5	0.8	0.0	0.7	2.4	0.7	0.7	1.3	0.0	0.2
Resinite	0.0	0.6	1.2	0.2	0.6	0.8	0.4	1.8	0.4	1.0	0.0	0.4	0.4	0.4	0.0	0.2	0.2	0.2	0.5	0.0
Liptodetrinite	1.5	2.1	2.7	1.8	2.2	3.8	2.0	4.5	4.3	3.7	0.7	2.2	3.5	3.7	2.4	1.6	0.9	0.7	1.1	1.5
Alginite	0.0	0.0	0.0	0.0	0.0	0.0	0.0	0.0	0.0	0.0	0.0	0.0	0.0	0.0	0.0	0.0	0.0	0.0	0.0	0.0
Bituminite	0.0	0.0	0.0	0.0	0.0	0.0	0.0	0.0	0.0	0.0	0.0	0.0	0.0	0.0	0.0	0.0	0.0	0.0	0.0	0.0
Exudatinite	0.0	0.0	0.0	0.0	0.0	0.2	0.0	0.0	0.0	0.0	0.0	0.0	0.0	0.2	0.0	0.0	0.0	0.0	0.0	0.0
Fluorinite	0.2	0.0	0.0	0.0	0.0	0.0	0.0	0.2	0.0	0.0	0.0	0.0	0.0	0.0	0.0	0.0	0.0	0.0	0.0	0.0
Fusinite	0.0	0.0	0.8	0.0	0.0	0.0	0.0	0.0	0.0	0.0	0.0	0.0	0.0	0.0	0.0	0.8	1.2	0.0	0.4	0.6
Semifusinite	1.0	1.5	0.0	1.0	0.4	1.4	1.3	1.2	2.0	1.0	0.8	0.4	0.0	0.0	0.2	0.6	1.4	0.2	2.0	1.8
Sclerotinite	0.2	0.2	0.0	0.0	0.0	0.0	0.2	0.2	0.2	0.0	0.0	0.0	0.0	0.0	0.0	0.0	0.0	0.0	0.2	0.0
Inertodetrinite	0.6	0.4	1.6	0.4	0.8	1.0	0.4	0.2	0.4	0.4	0.0	0.0	0.6	0.0	0.8	0.6	1.6	0.2	0.6	1.6
Macrinite	0.0	0.0	0.2	0.2	0.0	0.0	0.6	0.4	0.4	0.0	0.0	0.0	0.0	0.2	0.0	0.2	0.2	0.0	0.0	0.0
Micrinite	0.0	0.0	0.0	0.0	0.0	0.0	0.0	0.0	0.0	0.0	0.0	0.0	0.0	0.0	0.0	0.0	0.0	0.0	0.0	0.0
sulfide	4.4	1.2	0.2	0.0	0.0	0.2	0.0	0.0	0.0	0.2	0.1	0.0	0.4	0.6	0.0	0.0	0.0	0.0	0.2	0.0
clay	0.4	0.0	0.6	0.2	0.0	0.0	0.0	0.0	0.2	0.0	0.5	0.0	0.0	1.0	1.7	0.2	2.8	8.2	1.5	1.4
carbonate	0.0	2.7	0.0	0.4	0.0	1.0	1.6	0.6	2.9	0.6	30.9	0.6	0.8	0.0	0.2	0.0	0.0	0.0	0.4	1.0
quartz	0.0	0.0	0.0	0.0	0.0	0.0	0.0	0.0	0.0	0.0	0.0	0.0	0.0	0.2	1.2	4.0	2.0	0.5	2.5	0.2
other	0.0	0.0	0.0	0.0	0.0	0.0	0.0	0.0	0.0	0.0	0.0	0.0	0.0	0.0	0.0	0.0	0.0	0.0	0.0	0.8
MM counted	4.8	3.8	0.8	0.6	0.0	1.2	1.6	0.6	3.1	0.8	31.6	0.6	1.2	1.8	3.1	4.2	4.8	8.7	4.5	3.3
MM calculated	5.52	5.63	2.15	2.12	1.11	1.02	1.74	1.39	2.74	1.66	19.6	1.93	2.51	7.77	7.60	12.5	12.3	10.3	11.5	6.62

E.3 REFLECTANCE, FLUORESCENCE AND SAFRANIN O STAINING DATA

Table E.12 to E.21 report the mean maximum reflectance of vitrinite, the mean fluorescence intensity of vitrinite and inertinite, and the volume % stained particles. Some notations used in Tables E.12 to E.21 are described below.

$R_{o\ max}$	mean maximum reflectance of vitrinite
FLI	mean fluorescence intensity of vitrinite and inertinite at 600 nm, 550-650 nm HBW, masked uranyl glass standard = 100
σ^2	sample standard deviation
n	number of measurements
*	raw data lost, statistics not determined
% stained	mineral matter free, volume percent particles stained with Safranin O (% weathered coal)
counts	total number of observations
n.d.	not determined

TABLE E.12

REFLECTANCE AND FLUOROMETRIC DATA: DRILLHOLE 1480

Buller coalfield DH-1480, Stockton area, Brunner coal measures						
Lab No	$R_{o\ max}$	σ^2	n	FLI	σ^2	n
a90-85	1.10	.042	50	6.3	0.82	105
a90-86	1.08	.042	50	6.6	1.18	103
a90-87	1.07	.059	50	6.8	1.45	107
a90-88	1.08	.078	50	6.7	1.81	108
a90-89	1.10	.059	50	n.d.	n.d.	n.d.
a90-90	1.09	.045	50	6.4	1.06	137
a90-92	1.10	.048	50	6.6	1.23	102
a90-93	1.10	.055	50	7.1	1.42	107
a90-94	1.10	.053	50	7.2	1.68	209
a90-95	1.14	.047	50	6.8	1.60	102
a90-96	1.11	.054	50	8.0	1.35	107
a90-97	1.12	.052	50	9.0	1.43	108
a90-98	1.08	.049	50	10.0	1.59	102
a90-99	1.10	.044	50	10.2	1.67	131
a90-100	1.12	.053	50	12.3	2.02	128
a90-102	1.09	.045	50	14.9	4.24	103
a90-103	1.07	.048	50	14.1	3.32	143

TABLE E.13

REFLECTANCE AND FLUOROMETRIC DATA: DRILLHOLE 1481

Buller coalfield DH-1481, Stockton area, Brunner coal measures						
Lab No	$R_{o\ max}$	σ^2	n	FLI	σ^2	n
a90-134	0.98	.074	100	22.3	5.30	200
a90-135	0.97	.071	60	19.1	4.79	109
a90-136	0.98	.069	100	16.2	4.29	200
a90-137	1.03	.081	60	11.8	4.05	105
a90-138	1.07	.072	100	8.3	2.66	200
a90-139	1.10	.065	50	6.6	1.49	107
a90-140	1.17	.063	50	6.4	1.57	107
a90-141	1.15	.053	50	6.6	1.20	107
a90-142	1.12	.038	50	6.9	1.51	107
a90-143	1.10	.061	100	7.7	1.89	200
a90-146	1.06	.072	50	8.8	3.52	110
a90-147	1.08	.069	50	6.8	1.05	108
a90-148	1.11	.073	100	6.8	1.32	207
a90-149	1.13	.067	50	5.8	1.43	106
a90-150	1.16	.071	50	7.4	1.29	107
a90-151	1.13	.045	100	7.9	1.66	200
a90-152	1.14	.054	100	8.2	1.60	200

TABLE E.14

REFLECTANCE AND FLUOROMETRIC DATA: DRILLHOLE 1489

Buller coalfield DH-1489, Webb area, Brunner coal measures						
Lab No	$R_{o\ max}$	σ^2	n	FLI	σ^2	n
a90-596	1.15	.074	50	6.2	1.06	105
a90-597	1.22	.045	50	5.4	1.02	107
a90-598	1.22	.062	50	5.3	1.22	107
a90-599	1.24	.043	50	5.3	0.89	107
a90-600	1.25	.056	50	5.6	1.09	107
a90-601	1.24	.054	50	5.8	1.11	107
a90-602	1.22	.054	50	5.7	1.09	109
a90-603	1.26	.054	50	5.4	0.96	107
a90-604	1.25	.060	50	5.7	1.38	109
a90-605	1.25	.047	50	6.0	1.03	107
a90-611	1.28	.054	50	5.8	1.04	110
a90-612	1.30	.037	50	6.3	0.79	107
a90-613	1.29	.039	50	5.4	0.85	112
a90-614	1.31	.047	50	5.5	1.23	108
a90-615	1.32	.045	50	6.2	0.96	107
a90-616	1.33	.047	50	5.8	0.94	108
a90-617	1.31	.042	50	6.7	0.99	110
a90-618	1.32	.067	50	7.8	1.37	102
a90-620	1.30	.057	50	9.6	1.11	107
a90-621	1.31	.038	50	9.8	1.09	107
a90-622	1.31	.056	50	9.6	1.36	107
a90-623	1.30	.044	50	8.5	2.79	110
a90-624	1.26	.041	50	8.8	3.19	102

TABLE E.15
REFLECTANCE AND STAINING DATA: DRILLHOLE 1490

Buller coalfield DH-1490, Stockton area, Brunner coal measures					
Lab No	$R_{o\ max}$	σ^2	n	% stained	counts
a90-628	1.18	.059	50	35.4	500
a90-629	1.21	.073	50	23.8	1009
a90-630	1.23	.054	50	30.2	500
a90-631	1.22	.039	50	9.4	500
a90-635	1.26	.047	50	24.7	1000
a90-636	1.22	.041	50	18.2	500
a90-637	1.23	.028	50	14.8	500
a90-638	1.25	.030	50	23.6	500
a90-639	1.25	.045	50	20.4	500
a90-640	1.25	.057	50	21.4	500
a90-641	1.25	.035	50	32.4	500
a90-645	1.28	.042	50	44.4	500
a90-646	1.27	.034	50	45.7	1000
a90-647	1.28	.032	50	25.8	500
a90-648	1.29	.045	50	10.4	500
a90-649	1.31	.028	50	21.0	500
a90-650	1.31	.037	50	22.2	500
a90-651	1.30	.038	50	24.8	500
a90-652	1.35	.033	50	46.2	500
a90-653	1.32	.044	50	25.8	500
a90-654	1.31	.037	50	28.4	1000
a90-659	1.33	.043	50	26.6	500
a90-660	1.32	.041	50	44.8	500
a90-661	1.32	.049	50	18.0	500
a90-662	1.30	.039	50	28.6	500
a90-663	1.30	.051	50	18.8	500
a90-664	1.21	.047	50	3.0	500

TABLE E.16
REFLECTANCE AND STAINING DATA: DRILLHOLE 1492

Buller coalfield DH-1492, Webb area, Brunner coal measures					
Lab No	$R_{o\ max}$	σ^2	n	% stained	counts
a90-3482	0.98	.094	100	78.8	500
a90-3484	1.15	.068	100	0.6	500
a90-3486	1.14	.059	100	0.5	500

TABLE E.17
REFLECTANCE AND FLUOROMETRIC DATA: DRILLHOLE 1494

Buller coalfield DH-1494, U. Waimangaroa sector, Brunner coal measures						
Lab No	$R_{o\ max}$	σ^2	n	FLI	σ^2	n
46/750	0.66	.063	50	11.5	3.26	100
46/739	0.56	.046	50	31.4	6.38	100
46/740	0.57	.040	50	30.3	6.32	99
46/741	0.56	.046	50	29.9	6.40	100
46/742	0.62	.063	50	20.6	4.08	100
46/743	0.67	.046	50	14.9	3.11	102
46/744	0.70	.058	50	11.0	1.97	100
46/745	0.71	.070	50	10.5	1.84	100
46/746	0.71	.050	50	10.1	1.78	100
46/747	0.69	.058	50	11.5	2.39	103
46/748	0.72	.052	50	10.2	2.30	100
46/749	0.71	.053	50	11.0	1.98	100

TABLE E.18
REFLECTANCE AND FLUOROMETRIC DATA: DRILLHOLE 712

Greymouth coalfield DH-712, Rapahoe sector, Paparoa coal measures						
Lab No	$R_{o\ max}$	σ^2	n	FLI	σ^2	n
50/639	0.56	.053	50	6.7	2.35	200
50/640	0.53	.055	50	8.5	3.64	200
50/641	0.51	.039	50	10.2	4.50	300
50/642	0.52	.038	50	7.9	2.52	200
50/643	0.52	.031	50	9.0	2.88	200
50/644	0.57	.056	50	7.4	2.75	200

TABLE E.19
REFLECTANCE AND FLUOROMETRIC DATA: DRILLHOLE 7

Pike River coalfield DH-7, Brunner coal measures						
Lab No	$R_{o\ max}$	σ^2	n	FLI	σ^2	n
46/847	0.65	.055	50	39.4	8.83	99
46/835	0.63	.059	50	56.7	13.91	100
46/836	0.66	.029	50	39.4	*	*
46/837	0.71	*	*	30.8	7.98	100
46/838	0.73	.058	50	23.8	5.35	100
46/839	0.73	.050	50	20.7	5.07	100
46/840	0.77	.035	50	18.4	3.60	100
46/841	0.74	.063	50	21.1	4.54	100
46/842	0.76	.040	50	24.7	5.25	100
46/843	0.71	.052	50	32.1	7.27	100
46/945	0.74	.042	50	34.1	6.83	100
46/844	0.68	.042	50	43.6	8.58	100
46/845	0.67	.038	50	51.3	8.22	100
46/846	0.66	.066	50	54.7	11.21	100
Pike River coalfield DH-7, Paparoa coal measures, whole seam						
Lab No	$R_{o\ max}$	σ^2	n	FLI	σ^2	n
46/919	0.93	.084	50	10.0	3.41	200
46/920	0.88	.067	50	11.9	2.86	200
46/921	0.88	.075	50	11.9	3.64	200
46/922	0.89	.073	50	14.0	3.58	200
46/923	0.83	.058	50	11.3	2.77	200
46/924	0.88	.054	50	9.7	2.60	200

TABLE E.20
REFLECTANCE AND FLUOROMETRIC DATA: STOCKPILE SAMPLES

Stockpile samples						
Lab No	$R_{o\ max}$	σ^2	n	FLI	σ^2	n
46/068	0.60	.051	50	6.3	2.45	200
64/064	0.62	.054	100	6.9	3.48	200
45/963	0.73	.064	50	6.1	2.69	200
45/978	0.74	.047	50	6.5	2.36	200
45/965	0.75	.047	50	6.1	1.97	200
46/296	1.15	.070	50	n.d.	n.d.	n.d.
45/971	1.20	.074	50	7.1	1.53	200
46/426	1.60	.055	50	2.7	0.81	200

TABLE E.21

REFLECTANCE AND FLUOROMETRIC DATA: WEATHERING SERIES

Stockpile weathering, monthly samples, Stockton coal							
Lab No		$R_{o\ max}$	σ^2	n	FLI	σ^2	n
45/483	0 mo	1.11	.078	50	8.5	2.61	200
45/626	1.mo	1.11	.063	50	8.4	2.61	200
45/751	2.mo	1.08	.086	50	7.9	2.70	200
45/926	3.mo	1.09	.054	50	7.7	2.06	200
46/075	4.mo	1.11	.075	50	7.6	2.74	200
46/220	5.mo	1.10	.067	50	7.4	2.08	200
46/525	7.mo	1.09	.070	50	7.6	2.44	200
46/714	8.mo	1.11	.060	100	7.3	2.28	200
46/874	9.mo	1.10	.068	50	7.3	2.43	200
47/053	11.mo	1.10	.085	100	7.1	2.50	200
47/923	12.mo	1.08	.091	100	7.2	2.49	200
Stockpile weathering, monthly samples, Sullivan coal							
Lab No		$R_{o\ max}$	σ^2	n	FLI	σ^2	n
45/481	0 mo	1.17	.061	50	7.8	1.39	300
45/624	1 mo	1.16	.069	50	7.4	1.69	200
45/749	2 mo	1.15	.073	50	7.2	1.64	200
45/924	3 mo	1.18	.073	50	7.1	1.37	200
46/073	4 mo	1.15	*	*	6.9	1.59	200
46/218	5 mo	1.16	.065	50	7.1	1.56	300
46/523	7 mo	1.15	.061	50	6.7	1.50	200
46/712	8 mo	1.14	.075	50	6.8	1.36	200
46/872	9 mo	1.16	.067	50	6.6	1.37	200
47/051	11 mo	1.16	.066	100	6.7	1.43	200
47/921	12 mo	1.16	.070	100	6.7	1.50	200

E.4 RAW CARBON MICROTEXTURE DATA

Table E.22 lists the raw carbon microtexture data for selected carbonized coal samples. The data are on a volume percent mineral free basis.

E.5 COAL ASH OXIDE COMPOSITION

Table E.23 lists the raw ash composition data for selected coal samples.

TABLE E.22

VOLUME PERCENT MICROTEXTURES IN SOME CARBONIZED COALS

Sample ID	isotropic	fine mosaic	medium mosaic	coarse mosaic	coarse flow	lamellar	basic anisotropy
46/836	0.8	0.0	99.2	0.0	0.0	0.0	0.0
46/841	0.8	0.0	71.2	27.6	0.4	0.0	0.0
46/845	0.0	14.4	79.6	6.0	0.0	0.0	0.0
46/919	1.2	72.4	24.8	1.6	0.0	0.0	0.0
46/922	0.4	30.0	61.6	1.6	6.4	0.0	0.0
46/923	3.2	0.0	80.0	12.8	4.0	0.0	0.0
46/924	1.6	4.4	87.2	6.8	0.0	0.0	0.0
46/741	3.2	46.0	49.2	1.6	0.0	0.0	0.0
46/743	13.6	85.6	0.8	0.0	0.0	0.0	0.0
46/747	42.4	57.6	0.0	0.0	0.0	0.0	0.0
45/963	99.2	0.8	0.0	0.0	0.0	0.0	0.0
45/965	98.0	2.0	0.0	0.0	0.0	0.0	0.0
45/971	2.8	0.4	28.0	64.0	4.4	0.4	0.0
45/978	87.2	12.8	0.0	0.0	0.0	0.0	0.0
46/064	100.0	0.0	0.0	0.0	0.0	0.0	0.0
46/068	99.6	0.4	0.0	0.0	0.0	0.0	0.0
46/426	1.6	0.0	0.4	26.4	31.2	32.8	7.6
a90-93	4.0	1.6	68.0	26.0	0.4	0.0	0.0
a90-102	0.8	2.4	82.0	14.8	0.0	0.0	0.0
a90-136	3.2	3.2	76.0	17.2	0.4	0.0	0.0
a90-140	2.4	2.4	78.4	16.0	0.8	0.0	0.0
a90-151	1.6	0.8	77.2	19.2	1.2	0.0	0.0
a90-636	5.2	2.8	4.4	3.6	2.4	0.4	81.2
a90-646	7.6	0.0	0.0	0.0	0.0	0.0	92.4
a90-599	2.0	0.8	32.0	59.2	6.0	0.0	0.0
a90-621	3.2	3.2	50.0	43.2	0.4	0.0	0.0
50/639	100.0	0.0	0.0	0.0	0.0	0.0	0.0
50/641	99.6	0.0	0.4	0.0	0.0	0.0	0.0

TABLE E.23

ASH OXIDE COMPOSITION OF SOME SELECTED COALS

Buller coalfield drillhole 1494 Upper Waimangaroa sector Brunner coal measures

Lab No	SiO2	TiO_2	Al_2O_3	Fe_2O_3	MnO	MgO	CaO	Na_2O	K_2O	P_2O_5	SO_3	LOI	sum
46/750	42.00	1.10	32.95	2.65	0.00	0.66	8.66	0.47	3.24	5.54	0.94	0.91	99.12
46/739	20.94	0.22	11.63	62.91	0.06	0.15	0.55	0.99	0.30	0.05	0.09	-0.35	97.54
46/740	2.70	0.12	1.37	93.03	0.07	0.22	0.36	0.44	0.08	0.04	0.14	-0.18	98.39
46/741	1.50	0.09	1.01	94.98	0.02	0.29	0.16	0.37	0.04	0.03	0.05	0.51	99.05
46/742	4.79	0.31	2.96	86.16	0.11	0.29	0.76	1.18	0.12	0.04	0.72	-0.04	97.40
46/743	5.57	0.24	4.91	86.42	0.03	0.26	0.55	0.84	0.08	0.03	0.10	-0.23	98.80
46/744	2.21	0.25	1.44	95.81	0.00	0.17	0.13	0.34	0.00	0.03	0.09	-0.19	100.3
46/745	34.79	1.39	26.72	29.97	0.02	0.30	2.21	1.26	0.27	0.05	0.45	0.39	97.82
46/746	26.85	3.15	23.27	30.44	0.07	0.49	3.05	2.98	0.25	.22	2.89	1.28	94.94
46/747	11.83	0.39	10.61	73.75	0.00	0.08	0.35	0.34	0.05	0.03	0.07	0.43	97.93
46/748	41.88	1.98	36.84	12.91	0.02	0.06	2.52	1.14	0.31	0.06	0.17	0.13	98.02
46/749	60.20	2.93	25.51	2.05	0.00	0.00	3.43	0.40	0.27	2.30	0.02	1.15	98.26

Pike River coalfield drillhole 7 Brunner coal measures

Lab No	SiO2	TiO_2	Al_2O_3	Fe_2O_3	MnO	MgO	CaO	Na_2O	K_2O	P_2O_5	SO_3	LOI	sum
46/847	20.50	0.39	11.99	56.85	0.07	0.85	3.94	0.47	0.50	0.06	3.21	0.45	99.28
46/835	12.93	0.12	2.34	23.74	0.12	13.45	18.98	0.43	0.27	0.02	27.51	-0.33	99.58
46/836	4.41	0.14	1.61	16.55	0.16	6.56	28.19	1.15	0.20	0.01	39.34	0.00	98.32
46/837	3.99	0.12	1.05	5.93	0.21	13.34	31.64	0.89	0.09	0.02	41.32	0.46	99.06
46/838	12.22	.24	3.26	8.51	0.10	17.33	25.74	3.55	0.55	0.02	16.45	7.30	95.27
46/839	4.17	0.14	1.55	3.47	0.08	16.70	28.15	1.40	0.28	0.00	40.82	0.29	97.05
46/840	2.22	0.06	0.78	0.90	0.05	24.35	36.13	0.19	0.05	0.01	29.81	4.57	99.12
46/841	1.61	0.13	1.07	0.84	0.06	17.57	34.44	0.58	0.12	0.00	42.20	0.40	99.02
46/842	1.30	0.05	1.07	1.41	0.06	23.74	37.29	0.15	0.04	0.02	26.99	8.08	100.2
46/843	1.51	0.09	1.68	4.50	0.10	15.25	34.60	0.85	0.27	0.01	39.33	0.24	98.43
46/945	0.41	0.06	0.36	0.58	0.16	19.97	52.26	0.00	0.02	0.00	11.72	12.85	98.39
46/844	3.81	0.08	1.00	13.27	0.18	12.76	27.30	0.71	0.21	0.00	39.56	0.52	99.40
46/845	20.73	0.64	6.56	16.35	0.17	12.78	18.87	3.01	0.44	0.04	13.58	4.80	97.97
46/846	64.86	0.62	12.81	8.54	0.03	0.78	3.48	1.07	1.71	0.03	4.12	0.15	98.20

Pike River coalfield drillhole 7 Paparoa coal measures

Lab No	SiO2	TiO_2	Al_2O_3	Fe_2O_3	MnO	MgO	CaO	Na_2O	K_2O	P_2O_5	SO_3	LOI	sum
46/919	66.74	1.36	22.83	3.34	0.02	0.60	0.68	0.43	2.40	0.06	0.54	0.60	99.60
46/920	84.06	0.76	9.57	1.79	0.01	0.23	0.58	0.34	0.68	0.06	0.71	-0.17	98.62
46/921	67.62	1.41	24.52	1.36	0.01	0.20	0.39	0.30	2.05	0.31	0.32	0.59	99.08
46/922	54.03	1.23	38.27	1.14	0.00	0.06	0.75	0.34	1.50	1.26	0.17	0.74	99.49
46/923	62.97	1.89	15.34	2.58	0.01	2.00	6.12	1.09	1.52	1.21	4.47	0.20	99.40
46/924	42.55	3.82	21.94	4.07	0.01	2.26	10.86	1.06	0.61	3.68	5.95	2.10	98.91

Greymouth coalfield drillhole 712 Rapahoe sector Paparoa coal measures

Lab No	SiO2	TiO_2	Al_2O_3	Fe_2O_3	MnO	MgO	CaO	Na_2O	K_2O	P_2O_5	SO_3	LOI	sum
50/639	74.26	1.11	15.76	3.42	0.00	0.62	0.28	0.72	2.79	0.14	0.12	0.51	99.73
50/640	70.00	1.32	15.87	4.57	0.02	0.38	1.53	2.51	0.81	0.06	0.35	0.79	98.21
50/641	64.85	1.32	18.48	3.85	0.01	0.62	2.13	3.47	1.37	0.11	0.59	0.76	97.56
50/642	71.55	0.93	18.59	1.38	0.00	0.80	0.74	0.48	3.57	0.86	0.20	0.10	99.20
50/643	75.27	1.53	16.45	2.16	0.01	0.22	0.96	1.18	0.77	0.14	0.24	0.60	99.53
50/644	78.48	1.99	13.47	3.24	0.00	0.09	0.45	0.77	0.36	0.12	0.11	0.22	99.30

APPENDIX F
PHOTOGRAPHS OF CARBONIZED COAL SPECIMENS

Plate F.1
Carbonized Coals

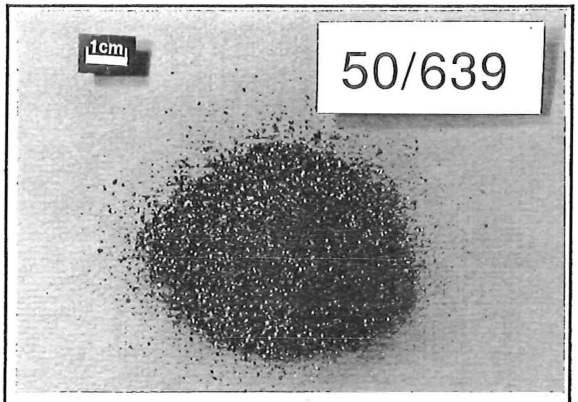

Greymouth, DH-712, ply

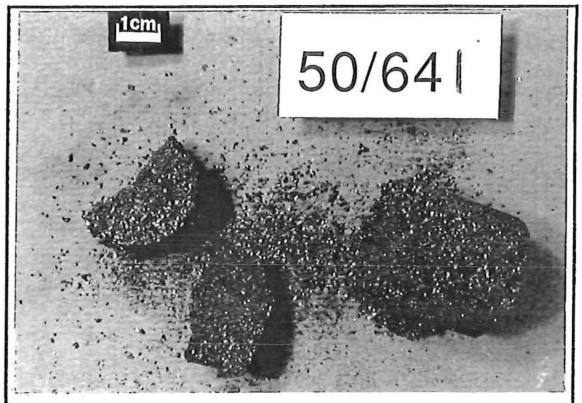

Greymouth, DH-712, ply

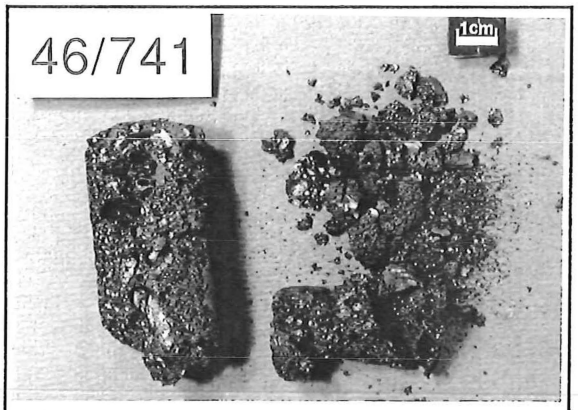

U. Waimangaroa, DH-1494, ply

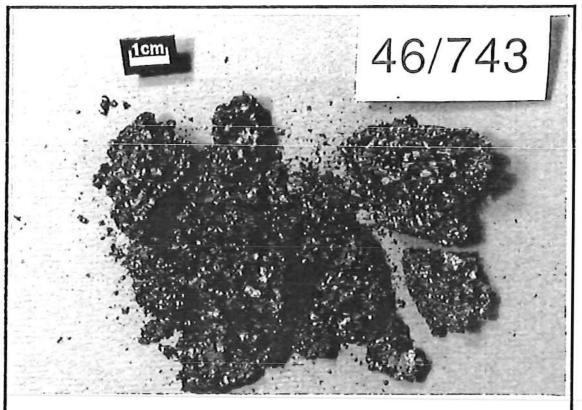

U. Waimangaroa, DH-1494, ply

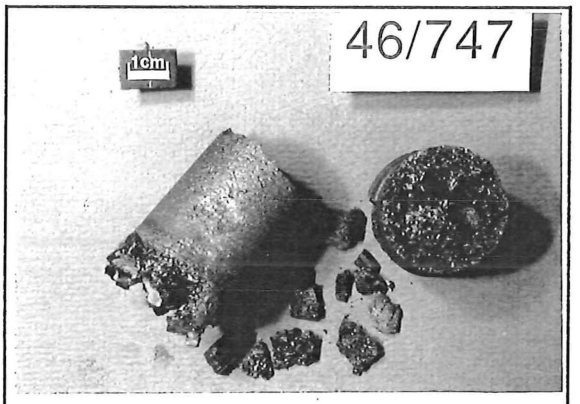

U. Waimangaroa, DH-1494, ply

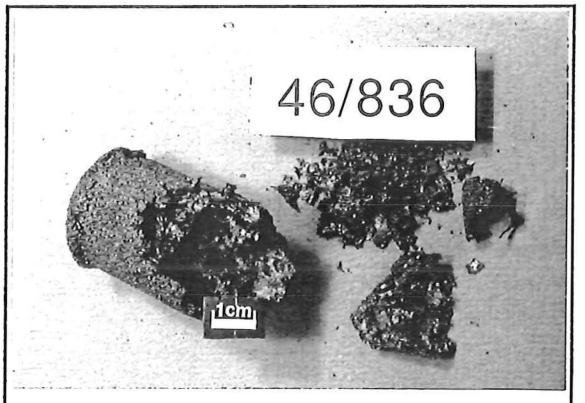

Pike River, Brunner, DH-7, ply

Notes to Plates F.1, F.2, F.3, and F.4,

Photographs of carbonized coals are one half actual size.

The carbonized coals are identified according to the ID number of the parent coal.

Plate F.2 -Carbonized Coals

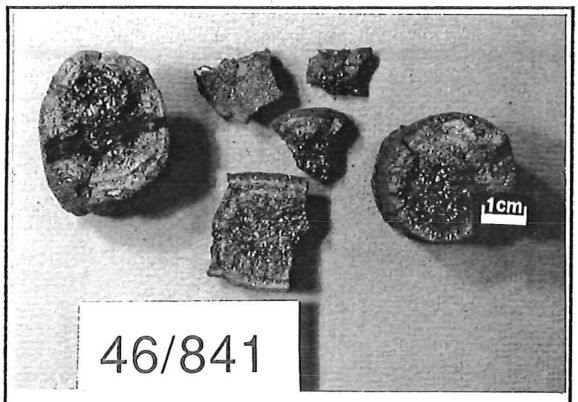

Pike River, Brunner, DH-7, ply

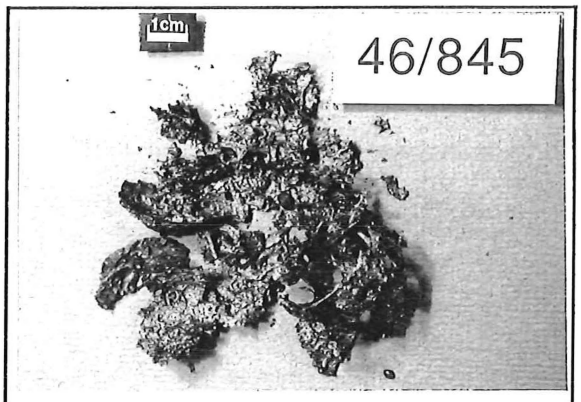

Pike River, Brunner, DH-7, ply

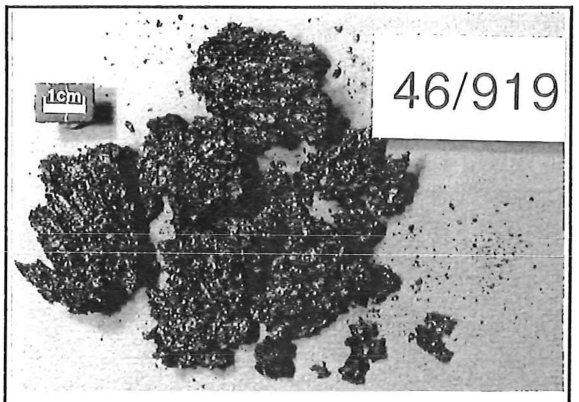

Pike River, Paparoa, DH-7, seam 1

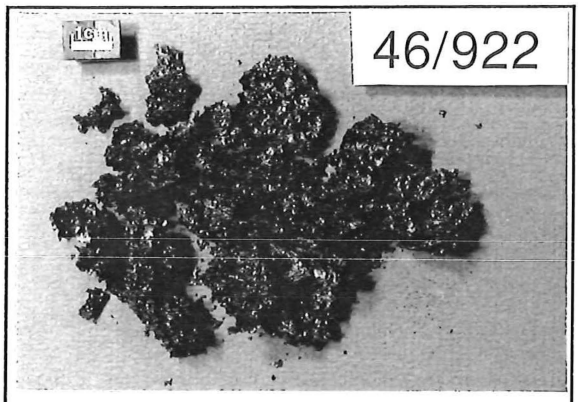

Pike River, Paparoa, DH-7, seam 3

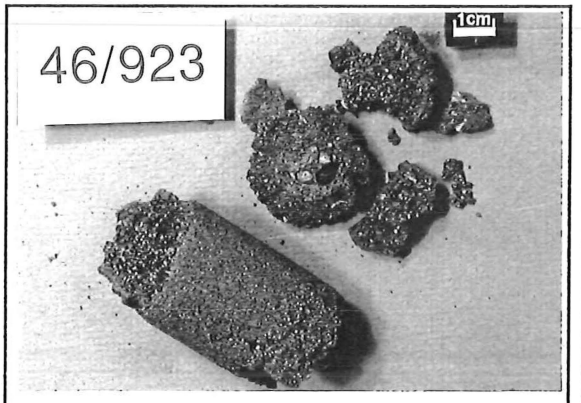

Pike River, Paparoa, DH-7, seam 4

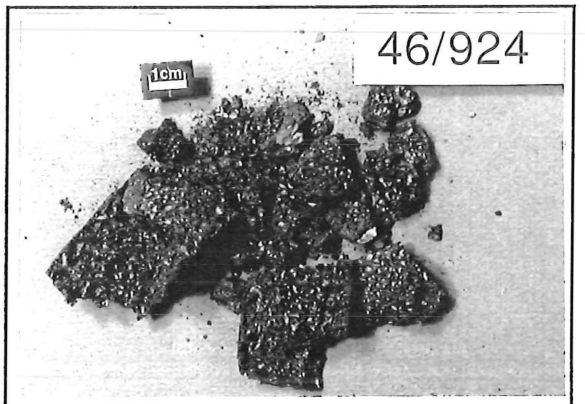

Pike River, Paparoa, DH-7, seam 5

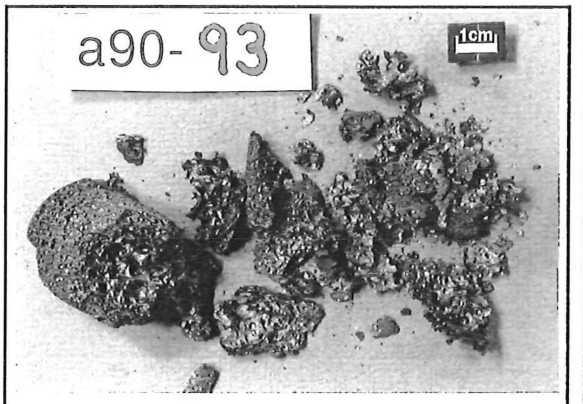

Stockton, DH-1480, ply

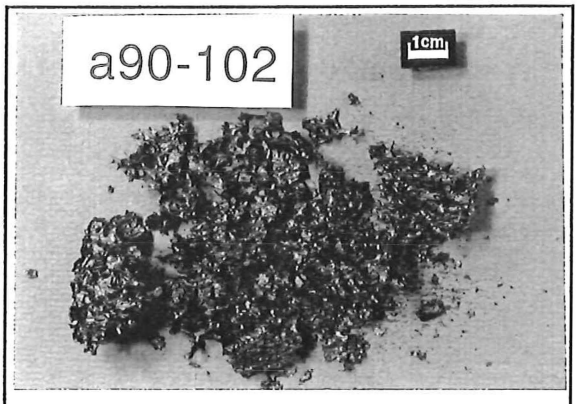

Stockton, DH-1480, ply

Plate F.3 - Carbonized Coals

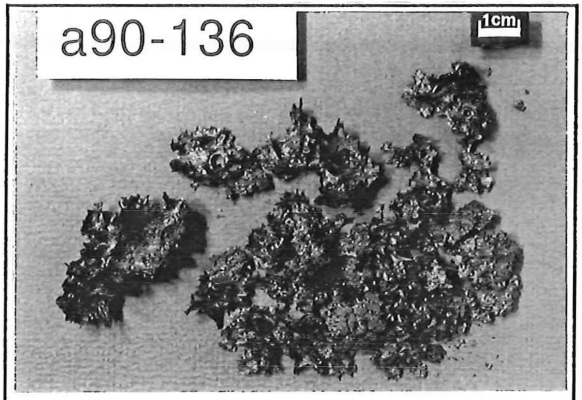

Stockton, DH-1481, ply

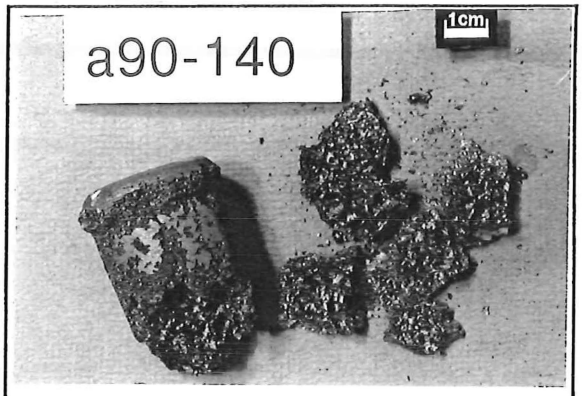

Stockton, DH-1481, ply

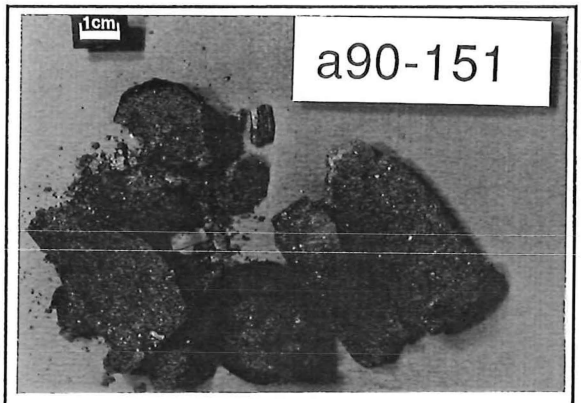

Stockton, DH-1481, ply

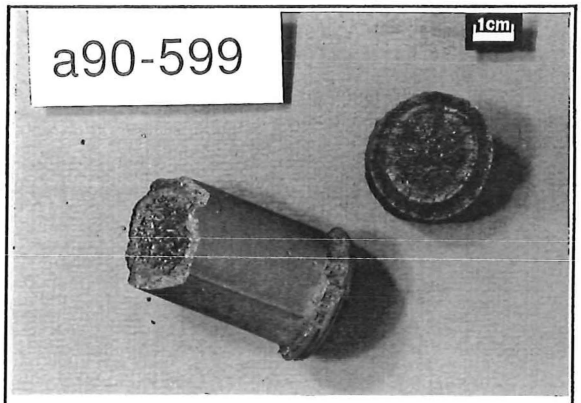

Webb, DH-1489, ply

Webb, DH-1489, ply

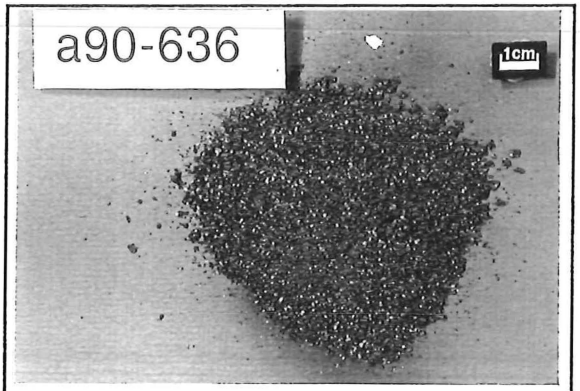

Webb, DH-1490, weathered ply

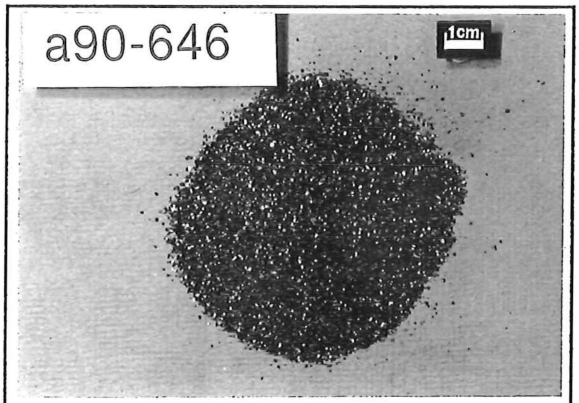

Webb, DH-1490, weathered ply

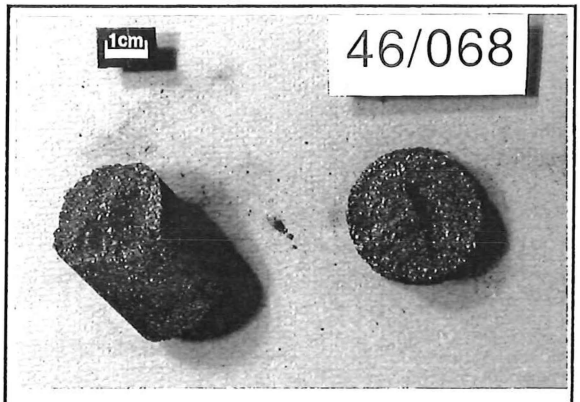

Greymouth, Kiwi run of mine

Plate F.4
Carbonized Coals

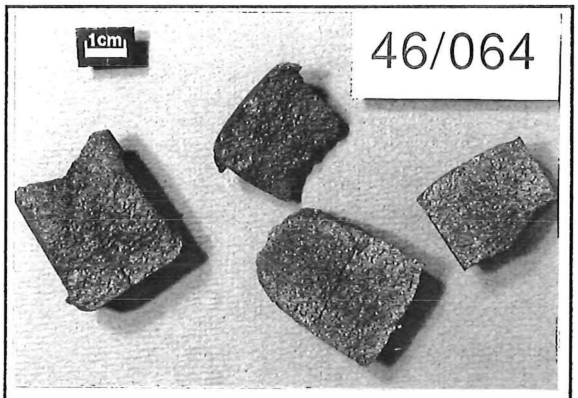

Greymouth, Strongman, run of mine

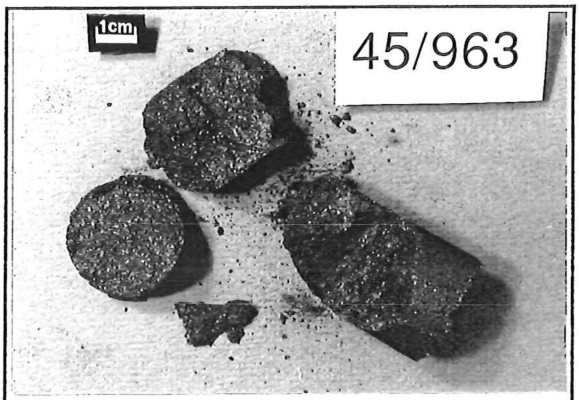

Reefton, Island Block, run of mine

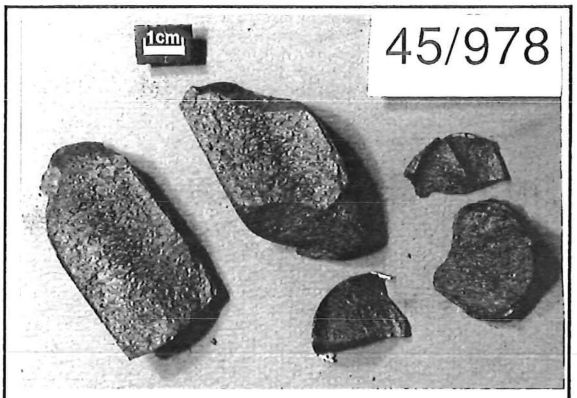

Buller, Cascade, run of mine

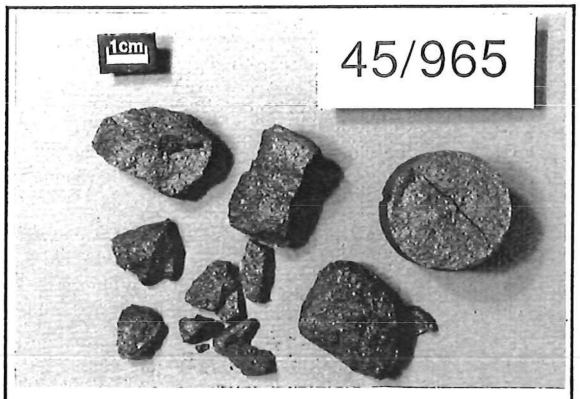

Greymouth, Echo, run of mine

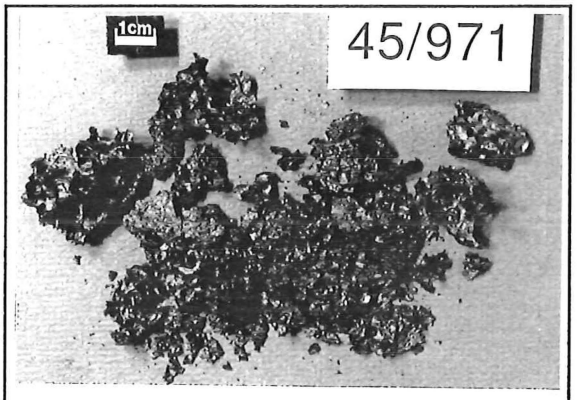

Buller, Sullivan, run of mine

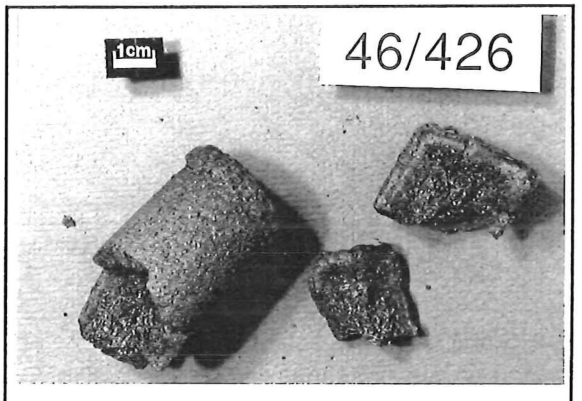

Greymouth, Roa, run of mine